Distribution Category:
General, Miscellaneous, and
Progress Reports (Nonnuclear)
(UC-13)

ANL-81-38

ARGONNE NATIONAL LABORATORY
9700 South Cass Avenue
Argonne, Illinois 60439

CHEMICAL ENGINEERING DIVISION
ANNUAL TECHNICAL REPORT
1980

L. Burris — Division Director
D. S. Webster — Deputy Division Director
D. L. Barney — Associate Division Director
F. A. Cafasso — Associate Division Director
M. J. Steindler — Associate Division Director

June 1981

Previous reports in this series

ANL-80-66 January-December 1979
ANL-79-22 January-December 1978
ANL-78-70 January-December 1977

TABLE OF CONTENTS

		Page
I.	OVERVIEW	1
	A. Introduction	1
	B. Current Programs	3
	1. Development of Advanced Batteries	3
	2. Office for Electrochemical Project Management	5
	3. Advanced Fuel Cell Development	6
	4. Utilization of Coal	8
	5. Magnetohydrodynamics	9
	6. Solar Energy	10
	7. Fast Reactor Chemistry	10
	8. Nuclear Fuel Cycle Studies	12
	9. Magnetic Fusion Energy Research	13
	10. Basic Energy Science	14
	11. Analytical Chemistry Laboratory	17
	12. Computer Applications	17
II.	ADVANCED BATTERY PROJECT	18
	A. Overview	18
	B. Electrode Chemistry	20
	1. Agglomeration Effects in the LiAl Electrode	21
	2. FeS Electrode Studies	22
	3. Electrochemical Studies of Electrode Processes	23
	C. Materials Engineering	24
	D. Cell Development	25
	1. Modeling Studies	25
	2. Capacity Stabilization Studies	26
	E. Cell and Battery Testing	28
	1. ANL Cells	28
	2. Subcontractor Cells	29
	3. Cell Failure Mechanisms	32
	4. Battery Module Tests	33

TABLE OF CONTENTS (contd)

		Page
F.	Battery and Auxiliary Components Development	34
	1. Thermal Management	34
	2. Charger Development	36
G.	Commercialization Studies	36
H.	Calcium/Metal Sulfide Battery	37
III.	OFFICE FOR ELECTROCHEMICAL PROJECT MANAGEMENT	38
A.	Introd[illegible]	38
B.	Near-Term Battery Contracts	38
	1. Lead-Acid Batteries	38
	2. Nickel/Iron Batteries	40
	3. Nickel/Zinc Batteries	40
C.	National Battery Test Laboratory	41
	1. Facility Operation	41
	2. Post-Test Analysis	43
D.	Battery Support Research	46
	1. Experimental and Mathematical Modeling	46
	2. Electrochemical Studies	48
	3. Chemical and Physical Analysis	51
	4. Component Evaluation	52
	5. Battery/Vehicle Integration	52
E.	Electrochemical Technology for Energy and Resource Savings	53
	1. Review of Industrial Technology	53
	2. ANL Research	54
F.	Load-Leveling Battery for Electric Utilities	57
IV.	ADVANCED FUEL CELL DEVELOPMENT	60
A.	Overview	60
B.	Sintered Electrolyte Structures	62
C.	Cathode Development	64
D.	Cell Testing	66
E.	Fuels Processing	67
F.	Future Direction	67

TABLE OF CONTENTS (contd)

		Page
V.	UTILIZATION OF COAL	68
	A. Overview	68
	B. Limestone Utilization in Fluidized-Bed Combustion	69
	1. Sorbent-Utilization Prediction Methodology	69
	2. Hydration-Enhanced Limestone Utilization	74
	C. Flue Gas Cleaning for Pressurized FBCs	76
	1. Removal of Alkali Metal Compounds from Hot Flue Gas	76
	2. Development of Na_2SO_4 Dew Point Meter	77
	3. Cyclone Evaluation for Particulate Removal	78
	D. Fluidized-Bed Combustion Program Evaluation and Analysis	79
	1. Program Planning Assistance for METC	79
	2. Instrumentation Needs for FBCs	80
	3. Project Management Support	80
	4. International Energy Technology Assessment Program	81
	5. Atmospheric Fluidized-Bed Boiler Installation at ANL	81
	6. Systems Engineering	81
	7. Design of Advanced Fossil Fuel Systems	81
	E. Sampling and Analysis of Fluidized-Bed Combustion Gases	82
	1. Analytical Protocol for PAHs	82
	2. On-Line Instrumentation for Monitoring PAHs	83
	F. Fossil Fuel Conversion and Utilization	84
	1. Gas Cleanup for Fuel Cell Use	84
	2. Environmental Control for Coal Utilization	85
	3. Technical Management of Synfuel Utilization Project	85
VI.	MAGNETOHYDRODYNAMICS HEAT AND SEED RECOVERY TECHNOLOGY	87
	A. Overview	87
	B. Argonne MHD Process Engineering Laboratory	87

TABLE OF CONTENTS (contd)

		Page
	C. Thermochemical Support Studies	89
	D. Seed-Reprocessing Studies	92
VII.	SOLAR ENERGY	93
	A. Solar Collector Development	93
	1. Introduction	93
	2. FY-80 Work Highlights and Significance	94
	3. Status and Direction	95
	B. Ice Storage	96
	1. Objectives	96
	2. Accomplishments	96
	C. Thermal Energy Storage	97
	1. Stratified Storage Measurement	97
	2. Testing Latent Heat Storage	97
	3. Development of a Thermal Energy Storage Device Using Cross-Linked High-Density Polyethylene	98
VIII.	FAST REACTOR CHEMISTRY	99
	A. Reactor Fuels Chemistry	99
	1. Oxygen Solid-State Thermomigration and Its Heat of Transport	99
	2. Oxygen Heat of Transport at Stoichiometry	101
	3. Oxygen Heat of Transport at Off-Stoichiometry	102
	B. High-Temperature Physical Properties Studies for Reactor Safety Analysis	104
	1. Compilation and Extrapolation of Thermophysical Data to Very High Temperatures	104
	2. Thermodynamic Functions of Fuel-Vapor Species at Very High Temperatures	107
	3. Enthalpy of Thoria/Urania Fuels	109
	C. Sodium Technology	111
	1. Cold-Trap Optimization	111
	2. Sodium Purification by Distillation	112
	3. Sodium Waste Technology Program	114

TABLE OF CONTENTS (contd)

		Page
IX.	NUCLEAR FUEL CYCLE STUDIES	115
	A. Nuclear Waste Management Studies	115
	1. Waste Form Characterization	115
	2. Metal-Matrix Encapsulation of Waste	120
	3. Geochemical Studies	121
	B. Nuclear Fuel Reprocessing	124
	C. LWBR Proof-of-Breeding Analytical Support Project	127
	1. Full-Scale Shear	128
	2. Single-Unit Dissolver	129
	3. Multiple Dissolver System	129
	4. Scrap and Waste Equipment	129
	5. Computer System	130
X.	MAGNETIC FUSION ENERGY RESEARCH	132
	A. Introduction	132
	B. Systems Analysis and Engineering Experimentation	132
	1. Liquid Breeder Processing Research	132
	2. Tritium Systems Analyses	134
	C. Fusion Materials Research and Development	134
	D. Solid Breeder-Blanket Technology	136
	E. Recent Advances in Neutron Dosimetry and Damage Analysis	137
XI.	BASIC ENERGY SCIENCE	140
	A. Homogeneous Catalysis	140
	1. Experimental and Theoretical Studies of Mechanisms in the Homogeneous Catalytic Activation of Carbon Monoxide	140
	2. Ethanol Synthesis	143
	B. Thermodynamics	145
	1. Theory	145
	2. Alloy Thermodynamics	150

TABLE OF CONTENTS (contd)

		Page
	3. Thermochemistry	153
	4. Gas-Condensed Phase Equilibria	157
	5. Impurity Interactions in Liquid Metals	158
C.	Environmental Chemistry	159
	1. Overview	159
	2. Characterization of Atmospheric Aerosols	159
	3. Chemistry of Atmospheric Sulfate Formation	160
	4. Nitrogen Chemistry	162
D.	Electrochemistry	162
	1. Investigations in Electrocatalysis	162
	2. Studies in Corrosion	163
	3. Structural Ordering and Complex Ions in Chloraluminate Melts	164
	4. Spectroscopic Investigations of Species in Molten-Salt Electrolytes	166
E.	Physical Properties of Salt Vapors	166
	1. Spectroscopic Studies of High-Temperature Molten-Salt Vapors and Vapor Complexes	166
	2. *Ab Initio* Molecular Orbital Calculations of High-Temperature Vapor Complexes	167
	3. Dimensional Model for Entropies and Free-Energy Functions	169
XII.	ANALYTICAL CHEMISTRY LABORATORY	171
A.	Overview	171
B.	Organic Analysis Facility	172
C.	Support to Major R&D Programs	172
D.	New Capabilities	173
E.	Future Plans	174
XIII.	COMPUTER APPLICATIONS	175
A.	Accomplishments	175
B.	Present and Future Plans	175
XIV.	ADDENDUM. CHEMICAL ENGINEERING DIVISION PUBLICATIONS--1980	177

CHEMICAL ENGINEERING DIVISION
ANNUAL TECHNICAL REPORT
1980

ABSTRACT

Highlights of the Chemical Engineering (CEN) Division's activities during 1980 are presented. In this period, CEN conducted research and development in the following areas: (1) rechargeable lithium-aluminum/iron sulfide batteries for electric vehicles and other applications; (2) ambient-temperature batteries--improved lead-acid, nickel/zinc, and nickel/iron--for electric vehicles; (3) energy-efficient industrial electrochemical processes; (4) molten carbonate fuel cells for use by electric utilities; (5) coal technology, mainly fluidized-bed combustion of coal in the presence of SO_2 sorbent of limestone; (6) heat- and seed-recovery technology for open-cycle magnetohydrodynamic systems; (7) solar energy collectors and thermal energy storage; (8) fast breeder reactor chemistry research--chemical support of reactor safety studies, chemistry of irradiated fuels, and sodium technology; (9) fuel cycle technology--management of nuclear wastes, reprocessing of nuclear fuels, and proof-of-breeding studies for the Light Water Breeder Reactor; and (10) magnetic fusion research--systems analysis and engineering experimentation, materials research, and neutron dosimetry and damage analysis. The CEN Division also has a basic energy sciences program, which includes experimental and theoretical research on (1) the catalytic hydrogenation of carbon monoxide and methanol homologation, (2) the thermodynamic properties of a wide variety of inorganic and organic materials, (3) significant mechanisms for the formation of atmospheric sulfate and nitrogen-bearing aerosols, (4) processes occurring at electrodes and in electrolytes, and (5) the physical properties of salt vapors. In addition, the Division operated the Central Analytical Chemistry Laboratory.

I. OVERVIEW

A. Introduction

The Chemical Engineering Division (CEN) is a multidisciplinary research and development organization in which work is performed on a wide variety of programs related to the nation's energy and environmental needs. Following its single-purpose mission in the 1940's and early 1950's, namely, development of processes for recovering spent nuclear fuels, the Division diversified its programs through two major stages of expansion: first, expansion into other nuclear areas and, second, expansion into nonnuclear areas when, with formation of the Energy Research and Development Administration (ERDA), national laboratories were encouraged to undertake work on the development of all types of energy sources. The Division's work comprises three major activities: (1) process and equipment development through engineering-scale demonstrations, (2) applied chemistry, and (3) basic research in many different areas, some of which are related to the Division's applied technology programs. While the Division has kept the name "Chemical Engineering" since it was formed in 1947, its work is best characterized by the term "Chemical Technology."

In 1980, there were no major changes in the Division's programs. The following list illustrates the breadth of CEN's efforts:

- Development of near-term and advanced batteries for electric vehicles.
- Fluidized-bed coal combustion research.
- Development of energy-efficient industrial electrochemical processes.
- Support for the national breeder reactor research program.
- Studies of reactor-fuel reprocessing and radioactive waste management.
- Dosimetry and radiation damage studies.
- Tokamak fusion reactor research.
- Research and development of fuel cells for use by electrical utilities.
- Environmental chemistry studies.
- Thermodynamics studies, including thermochemistry.
- Electrochemical research.
- Catalysis research.
- Various theoretical studies.
- Operation of Argonne's Analytical Chemistry Laboratory.

Management of industrial contracts for research and development continued to occupy a substantial portion of CEN's manpower during the past year. The management responsibilities are in line with the policy of the Department of Energy (DOE) to place programmatic management "in the field." The programs for which CEN has been assigned management responsibilities are the near-term (lead-acid, nickel-iron, nickel-zinc) and advanced (lithium-aluminum/iron sulfide) battery programs and the advanced fuel cell program. In these programs, we also perform R&D work, thereby enabling us to maintain a high level of expertise and to be sensitive to programmatic needs and problems. In the programs on battery development, Argonne National Laboratory (ANL) has been designated by DOE as having the "lead mission" assignment; that is, ANL has the major responsibility for planning and managing the programs within the policy guidelines and funding established by DOE.

The total funding for CEN for FY 1981 (October 1, 1980 through September 30, 1981) is about $29.2 million, which compares with $30.1 million in FY 1980. In the programs that the Division manages for DOE, a considerable amount of work is contracted to organizations outside CEN--industrial firms, universities, and other ANL divisions. The dollar value of outside contracts is about $10 million, which is 34% of the total funding for the Division. Percentages of this total funding in the Division's major programs are as follows: electrochemical technology (development of batteries and fuel cells), 62%; fission-related programs, 15%; coal technology, 10%; basic energy sciences, 8%; and other small programs (solar, fusion, special contracts), 5%. At the end of 1980, about 308 people were employed in CEN, 221 of whom are staff, the remainder being various types of support personnel that round out the Division's capabilities.

The Division's scientific staff consists principally of chemists and chemical engineers, but includes other types of engineers as well as scientists of other disciplines, e.g., physicists and metallurgists. In addition to its permanent members, CEN also employs some personnel on a temporary basis--post-doctoral appointees, research associates, visiting scientists, and students. In general, there may be 10 to 20 such people working in the Division at any given time; however, in the summer, there may be as many as 50--mainly students and professors. For FY 1981, the Division has one appointee from the Faculty Leave Research Appointment (FLRA) Program, in which university professors spend their sabbatical year at Argonne on a shared-cost basis. We expect that the FLRA program will grow substantially in future years. In addition, CEN also has contractual relations with consultants from universities and industry.

With regard to publications, 1980 was an unusually productive year for CEN. The list of publications at the end of this report (Section XIV) shows 138 open-literature publications and 65 ANL reports during this period.

In recent years, the diversity of the Division's programs and the capability to perform a wide variety of work have produced growth and helped to assure growth. However, with the recent change in administrations and impending cuts in the funding of many programs, it is unlikely that the Division's programs will emerge unscathed. At this time, the identity of programs affected and the magnitude of funding restrictions are unknown. Certainly, every effort will be made to mitigate the effects of any cutbacks in present programs by seeking new programs and funding sources.

B. Current Programs

Current programs within CEN are briefly summarized below. These programs are discussed in greater detail in the remainder of the report.

1. Development of Advanced Batteries

Advanced batteries, which have four to five times the energy densities of state-of-the-art lead-acid batteries, are being developed for vehicle-propulsion and stationary energy-storage applications. Nearly all of the effort at the present time is directed toward the electric-vehicle application, with an emphasis on passenger automobiles. Widespread use of electric vehicles would conserve petroleum fuels by shifting the demand to other sources such as coal, nuclear, hydroelectric, and solar. A secondary benefit would be decreased air pollution in congested urban areas.

The Division's work on advanced batteries is concentrated on the lithium-aluminum/iron sulfide (FeS or FeS_2) system, although exploratory studies have continued on the potentially less-expensive calcium-alloy/iron sulfide system. The Li-Al/iron sulfide cells have LiCl-based molten-salt electrolytes, which require operating temperatures in the range of 400-500°C. Porous BN felt or MgO powder separators provide electronic insulation of the electrodes and permit the transport of lithium ions between the electrodes.

A major objective of this program is to transfer the technology to industry for commercialization. Thus, for a number of years, industrial organizations have sent people to ANL as industrial participants in advanced battery development, and subcontracts have been let with industrial firms involved in battery development. At present, about 60% of the funding for this program is expended through such contracts. Two major cell and battery development contracts are with battery manufacturing companies, Eagle-Picher Industries, Inc. and Gould Inc. Other contracts are with the Carborundum Division of the Kennecott Copper Corp., General Motors Research Laboratories, Rockwell International, the Institute of Gas Technology, and the University of Florida.

The electric-vehicle battery program consists of three stages, designated Mark IA, Mark II, and Mark III. The purpose of the Mark IA program, which ended in 1979, was to evaluate the overall technical feasibility of the lithium/iron sulfide system for electric-vehicle propulsion and to identify problem areas. The program is currently in the Mark II stage, the objective of which is to develop a commercially viable battery for passenger automobiles. The first phase of the Mark II program, which is nearing completion, stresses the development of high-reliability cells and includes the fabrication and testing of small (up to 10 cells) modules. In addition, a "status cell" program has been instituted in which groups of cells of an identical design are fabricated and tested to monitor progress in the state of the art. The second phase of the Mark II program, which is scheduled to begin early in 1981 and to reach completion in 1984, involves the development of improved cells, the testing of interconnected modules, and the fabrication and testing of full-scale electric-automobile batteries. The Mark III battery, scheduled for testing in 1986, will be a high-performance prototype to be demonstrated and evaluated in a passenger automobile; it is expected

to be able to sustain 1000 deep discharge cycles, which is equivalent to a driving distance of 200,000 km (120,000 miles).

CEN maintains a base technology program aimed at advancing the technology of the lithium/iron sulfide system. During the past year, this research and development work has included studies of cell capacity loss and swelling, cell modeling, materials engineering, fabrication and testing of status cells, battery component and auxiliary systems development, and potential applications and cost studies. In addition, CEN has continued to test contractors' cells and conduct post-test examinations to identify causes of failure. Highlights of this CEN work during the past year are as follows:

1. Studies were conducted on agglomeration effects in lithium-aluminum electrodes, which lead to loss of cell capacity under certain conditions. Effects of electrolyte composition, current density, and additives on the degree of agglomeration were investigated.

2. Data were obtained on the emf values associated with the six electrochemical reactions involved in the discharge of an FeS electrode. This additional information has permitted an essentially complete characterization of the thermodynamics of the FeS electrode.

3. Current-interruption studies with a micro-reference electrode have provided data on electrode relaxation potentials at different states of charge and discharge. These results indicate that the specific energy and power of the Li-Al/FeS cell are limited by the ohmic resistance.

4. In the materials engineering studies, the addition of fine iron powder to FeS electrodes resulted in greatly reduced corrosion rates of nickel and low-carbon steel current collectors. In other materials studies, protective coatings on low-cost substrate materials have shown promise for current collector applications in FeS and Li-Al electrodes.

5. Engineering modeling studies have provided empirical equations that predict the specific energies of cells as a function of design variables such as electrode thickness, electrode loading densities, and electrode capacity ratios. The results of this study are being used to assist the contractors in developing cell designs for the Mark II program.

6. Reference electrodes were used to investigate the factors that affect the rate of capacity loss of a cell during cycling. The cause of capacity fading was traced to the negative electrode, and the resulting recommendations on cell design changes have resulted in a significant improvement in capacity retention of the Mark II cells.

7. Twelve identical cells fabricated at ANL were designated as "status cells" and were subjected to cycle-life tests. These cells were operated for an average of 287 cycles with an average capacity loss of 7%.

8. Thermal management studies during the past year included an analysis of the heat generated in Li-Al/FeS cells during constant-current cycling. The heat-generation rate was found to be substantially higher during discharge than during charge and to increase markedly near the end of discharge and the end of charge.

2. Office for Electrochemical Project Management

The Office for Electrochemical Project Management (OEPM) assists DOE in the planning, management, and implementation of certain electrochemical programs. These are (1) management of a project on research, development, and demonstration of near-term batteries--improved lead-acid, nickel/iron, and nickel/zinc--for electric vehicles, (2) operation of the National Battery Test Laboratory (NBTL), (3) research studies in support of the effort to develop near-term electric-vehicle batteries, (4) studies and research on industrial electrolytic technology to conserve energy and improve utilization of resources, and (5) the research, development, and demonstration of advanced lead-acid batteries for electric-utility load-leveling applications.

During 1980, the development of the three near-term battery systems for electric vehicles was continued by the eight industrial firms under contract with ANL. The R&D efforts of these contractors were directed toward the development of individual cells and multicell modules that would meet performance and lifetime objectives set forth for FY 1980. During the past year, 43 modules consisting of 180 cells were delivered to NBTL for performance-verification testing. Results of NBTL tests to date showed that (1) all three battery systems exceeded or nearly achieved the FY 1980 objectives for specific energy and power and (2), although only the nickel/iron system demonstrated the FY 1980 objective for cycle life, all three systems showed improvement over the cycle life demonstrated in 1979.

The National Battery Test Laboratory is the principal facility within the DOE Electric and Hybrid Vehicle Program for the independent testing and evaluation of batteries as they are developed. In 1980, the testing capability of the laboratory was expanded from 18 to 32 test stations, of which 29 are for cells and modules and three are for full-size batteries. Recently, three environmental chambers were installed for testing batteries at temperatures above and below normal operating temperatures. The NBTL has the capability of cycling battery modules under an urban driving schedule (SAE J227a/D), with and without regenerative braking. At NBTL, this cycling procedure is now routinely incorporated into the characterization and testing of modules. In tests of modules cycled with the SAE J227 urban driving schedule, it was found that the use of regenerative braking can increase the projected mileage (range) that a vehicle would traverse in one complete battery discharge by 20 to 30%.

Post-test analyses of contractor-fabricated modules tested at NBTL were carried out to identify and characterize failure mechanisms. Post-test analyses of nickel/zinc modules have, for example, identified the major problems with this system to be shape change, zinc dendritic growth, and mossy zinc deposits on the negative electrode.

The in-house support research consists of basic and applied research in areas identified as important to the progress of the near-term battery technologies. Currently, studies are under way to develop mathematical models describing the mass-transfer and electrochemical behavior of electrodes and cells. A mathematical model of the current distribution in a porous zinc electrode suggested that the conductance of zincate-supersaturated KOH electrolyte

within the electrode pores has a strong influence on the zinc-electrode performance. Therefore, an experimental study was undertaken to measure the conductivity of KOH electrolyte solutions at various levels of zincate concentrations (<1.5M). Other work has shown that the β-PbO_2 lattice in the positive electrodes of lead-acid batteries is lead deficient, rather than containing lead in excess of stoichiometric as had been previously assumed.

The goal of the electrolytic technology program is to increase the energy efficiency of industrial electrolytic processes. In 1980, two studies were conducted by contracted industrial firms: (1) a survey of alternative processes for the electrochemical production of inorganic compounds and (2) an engineering and economic evaluation of diaphragm-type and membrane-type chlorine cells. In-house experimental work was focused on a study of a process for the production of aluminum by the electrolysis of aluminum sulfide. Experiments demonstrated that the reaction of -300 mesh aluminum sulfate particles with carbon disulfide in a fluidized bed at 700°C will yield 55% aluminum sulfide. The solubility of aluminum sulfide in a $MgCl_2$-NaCl-KCl eutectic at 750°C was found to be 3 wt %, which is acceptable for practical electrolysis cells. Preliminary data indicated that the electrolysis of Al_2S_3 can be carried out at a voltage of 1.4 to 1.6 V, which is significantly less than the 4.5 V used in conventional Hall-Heroult cells.

In the load-leveling battery program, efforts are under way to advance the lead-acid battery technology to a state where the cycle life is 3000 cycles, the initial cost is \$37-50/kW-h, and the area energy density is >75 kW-h/m^2. In FY 1980, contracts were awarded to C&D Batteries, Inc. and Exide Management and Technology Co. for the research and development of advanced lead-acid cells and modules. Under another contract, VARTA Batterie in Germany has designed, constructed, and tested an H_2/O_2 recombination device for lead-acid batteries that provides safe operation of the battery and removes stibine and arsine from the battery off-gases.

3. Advanced Fuel Cell Development

Within DOE's fuel cell development program, CEN has two responsibilities. These are (1) to provide technical management of all DOE contracts on advanced fuel cell development and (2) to conduct R&D on alternative component concepts for molten carbonate fuel cells.

The management responsibility is carried out by the Advanced Fuel Cell Program Office at CEN. Nearly all of the management activities conducted by this office are related to the DOE Molten Carbonate Fuel Cell Program. The major thrust of this program is centered in parallel contracts at General Electric Co and United Technologies Corp. The objective of these contracts is to advance fuel-cell technology to a state of readiness for fabrication of full-scale stacks of cells. In FY 1980, CEN also provided technical management to DOE's program on processing of liquid fuels for fuel cells. The limited FY 1981 budget includes no funds for the fuels processing program and only about half that required to maintain the planned schedule for the overall molten carbonate fuel cell program. Argonne received about 12% of the FY 1981 budget for the molten carbonate fuel cell program; these funds are divided about evenly between research and management activities.

Recently, Argonne's fuel cell research has been concentrated on the development of alternative design concepts, primarily sintered $LiAlO_2$ electrolyte supports and improved cathodes of lithiated nickel oxide, for molten carbonate fuel cells.

In the molten carbonate fuel cell, the electrolyte structure is a composite of solid $LiAlO_2$ particles and a mixture of lithium and potassium carbonates that is liquid at the cell operating temperature of about 925 K. Sintered $LiAlO_2$ structures are under investigation because they are expected to be more stable than the current paste-type structures. In the past year, synthesis procedures and specifications for $LiAlO_2$ particles for sintering were developed, and acceptable sinters were prepared by cold-pressing and firing any one of the three allotropic forms of $LiAlO_2$ (α, β, or γ). The best results were obtained with α-$LiAlO_2$ powders, but work is continuing on sintering of β-$LiAlO_2$ because of its ease of synthesis. Tape-casting (rather than cold-pressing) has been found to be a promising process for preparing green bodies for sintering, and work is under way on producing tapes of good quality.

The cathode used in the molten carbonate fuel cell is lithiated nickel oxide, which is a semiconductor. These cathodes are normally produced by the in-cell reaction of a porous nickel plate. However, this in situ oxidation and impregnation with lithium results in cathode swelling and yields a structure with many individual crystallites having many point contacts. In conjunction with the Materials Science Division at ANL, CEN is working on the preparation of cathode plates of sintered $Li_{0.05}Ni_{0.95}O$ for assembly into fuel cells. The effect of sintering conditions on pore structure, electrical resistivity, and lithium vaporization of this cathode is under study. Cathodes have been produced with a bimodal pore-size distribution; this pore distribution was selected because it is expected that the large pores will permit gas passage while the small pores will retain electrolyte and provide electrochemical-reaction surface. One such sintered cathode was tested in a cell. As expected, no dimensional change of the cathode occurred; furthermore, the large pores remained open and the small pores filled with carbonates. However, the cell showed relatively poor electrochemical performance, which indicates that the structure must be improved further.

Another alternative component under investigation is a cathode/electrolyte support composite. During the past year, composites were prepared by bonding thin sintered cathode layers to the surface of sintered $LiAlO_2$ disks; this promising new technology will be investigated further.

As in the past, tile (paste structure) electrolytes are being used in cell tests to assess other components. Motion monitors are now used to detect cell-thickness change during cell tests; this has been valuable in assessing cell sealing and cathode dimensional changes. A new test-cell design was prepared to increase experimental flexibility and more closely approximate a commercially viable design. The first cell employing this design is being fabricated.

4. Utilization of Coal

The Division's major program in coal technology continues to be fluidized-bed combustion (FBC), a process in which coal is burned in a fluidized bed of limestone ($CaCO_3$) or dolomite [$CaMg(CO_3)_2$] particles. The limestone bed retains most of the SO_2 liberated when the coal is burned, and the process is expected to offer potentially higher efficiencies and lower capital costs than those for alternative combustion processes.

Small (50,000 to 100,000 lb steam per hour) atmospheric-pressure fluidized-bed combustors (AFBCs) are now available from several different companies and appear to be competitive with pulverized-coal boilers equipped with flue-gas desulfurization units. The future of FBC will depend very much on the performance of these first units in the field.

The development of FBC for electricity production is proceeding along two paths--the development of AFBC power plants by the Tennessee Valley Authority and the development of pressurized fluidized-bed combustor (PFBC) plants by DOE and the American Electric Power Co. The CEN program in FBC provides base technology for both atmospheric and pressurized FBC. Work is under way in the following areas: enhancement of limestone utilization, flue gas cleaning for PFBCs, evaluation and analysis of the fluidized-bed combustion program, and sampling and analysis of fluidized-bed combustion gases.

The limestone-utilization studies have been concentrated in two areas: the development of a sorbent-utilization prediction methodology and studies of the ANL hydration process for enhanced limestone utilization (hydration-dehydration of partially sulfated limestone). A new mathematical model of the sulfation process in FBC was developed as a part of the prediction methodology. In addition, an attrition model is under development to account for disintegration of limestone particles in FBC. For both models, standard laboratory tests are used to determine sorbent-specific parameters. These models have been used as the basis for ranking a selection of typical limestones and dolomites in terms of calcium sulfation and elutriation. In the other activity on limestone utilization, (1) basic studies have been conducted that have resulted in a more complete understanding of the ANL hydration process, and (2) engineering studies are under way to ascertain the kinetics of the hydration process and to develop methods of utilizing the water in a commercially suitable manner.

The studies of flue gas cleaning for PFBCs involve (1) the development of granular bed sorbents (e.g., activated bauxite) for the removal of gaseous alkali metal chlorides from high-temperature, high-pressure flue gas, (2) the investigation of a new concept for the determination of the Na_2SO_4 dew-point temperature, and (3) the analysis of data obtained in the operation of cyclones. The data obtained from cyclone operation are being compared with predictions of theoretical models and are being used to design a full-sized cyclone system that will achieve the particulate removals required to protect downstream gas turbines from excessive erosion.

The FBC program evaluation and analysis effort consisted of (1) program planning assistance for Morgantown Energy Technology Center (METC);

(2) a review of the state of the art of instrumentation needed for the operation of fluidized-bed combustors; (3) project management support for METC; (4) assessment of the status of foreign work in PFBC technology; (5) a review of the technical performance, environmental impacts, and economic factors of AFBCs and PFBCs, which will be used in an extensive, up-to-date review of fossil-energy combustion systems; and (6) assistance to the Energy and Environmental Systems Division of ANL in a program on the design of advanced fossil fuel systems.

The hot off-gas from FBC contains polycyclic organic material which could be biologically hazardous. In work on the sampling and analysis of hydrocarbons in flue gases, a protocol is under development for the assay of the gases from fluidized-bed combustors to determine the quantities and types of organic compounds present. A preliminary version of the analytical protocol has been developed, and its validity is being tested.

The CEN Division is also furnishing support for studies of advanced methods of gas cleanup for fuel cell use, support to the DOE Office of Environment in its efforts to ensure that adequate technology is developed for mitigating the environmental impacts of increased coal utilization, and technical support to DOE in the management of a broad alternative-fuels effort.

5. Magnetohydrodynamics

The Chemical Engineering Division is participating in a multidivisional program at ANL on the development of open-cycle magnetohydrodynamics (MHD) for the generation of electricity from coal combustion. In the MHD open-cycle system, hot (2900 K) combustion gases containing potassium salts, which are added as "seed" materials to enhance the electrical conductivity of the gases, flow through an MHD channel surrounded by a magnetic field to produce electricity directly. The emerging gases, still at a high temperature (2300 K), are processed in a downstream system to separate molten slag, recover the seed materials, and recover heat in a combustion air preheater and steam generator. The CEN Division has responsibility for the development of the technical support base for designing and operating the downstream gas system and for the seed-recycle process. The work consists of an engineering program, thermochemical support studies, and development of a process for recovering the potassium seed materials.

The engineering program is carried out primarily at the Argonne MHD Process Engineering Laboratory (AMPEL), which is a versatile, 2-MWt facility for testing components under prototype MHD conditions. This facility was used to obtain experimental data on the formation of NO during the final oxidation of the fuel-rich gases leaving the MHD channel and to determine the heat-transfer rate to air-cooled tubes exposed to seed- and slag-laden gas streams. In 1982, the many design problems related to the radiant boiler will be investigated in AMPEL.

The thermochemical support studies are directed toward understanding the interactions between coal-slag and potassium seed materials in gaseous and condensed phases. During this past year, the MHD80 computer code, which

describes thermodynamic equilibria in the gas-slag-seed system, was used to predict (1) the extent of the interaction between slag and seed and (2) the condensation of potassium salts over a wide range of plant operating conditions. In other thermochemical studies, the seed-slag deposit that formed on an air-cooled tube during AMPEL experiments was examined with an electron microprobe to establish the distribution of potassium, aluminum, sulfur, iron, calcium, and silicon. With the slag distribution determined by this electron probe analysis, it was calculated that about 75% of the slag-seed layer on the tube was K_2SO_4 and K_2CO_3.

A major step in the seed recovery process is the conversion of the K_2SO_4 recovered from MHD combustion gases to a sulfur-free potassium compound suitable for reuse. During 1980, CEN assisted DOE in managing seed-reprocessing studies and in evaluating the results of these studies. Because of a lack of funding, work in this area is at a low level.

6. Solar Energy

The solar energy activities in CEN, which are part of an overall Applied Solar Energy Program at ANL, include solar collector development and thermal energy storage.

In the area of solar collector development, the following activities were undertaken: (1) review and evaluation of seven first-generation collector designs--six from industry and one from a joint industry/university effort; (2) study of four second-generation optical designs developed at ANL; (3) measurement of the optical/thermal performance of nine collector modules--three first-generation ANL prototypes, three first-generation industrial collectors, and three second-generation prototypes; (4) initiation of long-term performance tests of first- and second-generation nonimaging collectors; (5) measurement of the optical properties of two new absorber materials and a new reflector material; and (6) participation in various committees for standards organizations.

In the area of thermal energy storage, work has continued on the use of ice produced and stored in an underground tank during the winter for year-long cooling. Water in the buried tank is converted to ice by means of Freon-containing heat pipes that act as passive refrigeration units; the heat pipe is designed so that ice formed along its submersed portion will break off periodically and float to the top of the storage tank. Under investigation as heat pipes are indoors heat-pipe evaporator and condenser units made from Roll-bond panels. Other CEN efforts related to thermal heat storage include (1) a study of the thermal stratification in thermal storage tanks, (2) development of a procedure for testing latent heat storage units, and (3) development of a thermal energy storage device using polyethylene as a latent heat storage material.

7. Fast Reactor Chemistry

Reactor Fuels Chemistry. In support of gas-cooled fast-reactor (GCFR) technology, CEN is investigating the transport and reaction of oxygen and fission products in irradiated fuels. Because GCFRs and LMFBRs both use

mixed uranium-plutonium oxide fuel, GCFR technology relies heavily on LMFBR base technology but requires investigation of features that are unique to GCFRs--namely, the use of vented fuel pins, roughened cladding, helium coolant, and direct contact between the primary coolant and the steam generator. Studies in progress show that successful utilization of the unique features of the GCFR requires an understanding of the complex chemistry and transport phenomena occurring under the large temperature gradients that exist within the fuel pin. The chemical elements whose behavior dominates fuel-pin chemistry are oxygen and fission-product cesium.

Under the strong axial temperature gradient within the fast-reactor fuel pin, solid-state thermomigration is primarily responsible for oxygen (as well as actinide) redistribution within the fuel. A mathematical model that describes this oxygen redistribution during irradiation has been developed. The model utilizes a defect structure for urania-plutonia fuel involving oxygen vacancies and electronic disorder. The model relates a thermodynamic factor, $1 + \partial \ln \gamma_V / \partial \ln C_V$ (where γ_V is the oxygen-vacancy activity coefficient, and C_V is the vacancy concentration), to the oxygen potential of the fuel, a quantity for which extensive data as well as accurate models exist. In the present analysis only one quantity, the heat of transport for oxygen vacancy, is required (together with the reactor operating conditions) to obtain profiles of the steady-state oxygen redistribution.

Reactor Safety. The Division's program in fast reactor safety has as its objective the measurement, assessment, and compilation of high-temperature (up to 6000 K) physical-property data that are needed in fast reactor safety analysis. Recently, this effort has focused on (1) review and assessment of physical-property data for sodium and uranium dioxide, (2) spectroscopic investigations of gaseous species of uranium oxides, and (3) enthalpy measurements for thoria/urania fuels. After a review and assessment of the available information on sodium and uranium dioxide, we prepared reports in which updated thermodynamic and transport properties of these materials are given. Experimental studies using the infrared spectra of gaseous uranium oxide species yielded improved values for thermodynamic functions, which are being used in the calculation of vapor pressures. Measurements of the enthalpy of thoria and thoria-urania mixtures at temperatures up to 3400 K have produced new enthalpy data and have revealed a transformation of a type previously observed in other fluorite and anti-fluorite crystals.

Sodium Technology. The Division has considerable experience and expertise in the technology of sodium, the coolant in LMFBRs, and has carried out a number of programs in sodium chemistry and sodium purification. Our recent efforts have concentrated on (1) purification of sodium by removal of both radioactive and nonradioactive impurities and (2) the disposal of radioactive sodium waste. For the first effort, removal of nonradioactive impurities by low-temperature precipitation in cold traps was studied in impurity-precipitation experiments and with computer modeling, and a low-pressure distillation method was developed for separating radioactive contaminants from sodium. For the second effort, methods of disposal of radioactive sodium waste, including evaporation of sodium residue from waste components and conversion of sodium metal to sodium oxide, were studied to determine the optimum parameters for these processes.

8. Nuclear Fuel Cycle Studies

Management of Nuclear Waste. The CEN Waste Management Program provides support to the national program on management of high-level waste. As part of this program, CEN is conducting studies on the use of radiochemistry in determining leach rates of candidate waste forms, with particular emphasis being given to the determination of leach rates from neutron-activated samples of simulated waste glasses. The high sensitivity of this neutron activation analysis was found to permit detection of waste elements (e.g., ^{141}Ce, ^{134}Cs, ^{152}Eu, ^{95}Zr, and ^{65}Zn) at concentrations normally undetected by other workers.

An important waste-form property is resistance to dispersion from mechanical impacts received during processing, handling, interim storage, or transportation. As a result, CEN is undertaking studies on the fracture characteristics of brittle waste forms. During the past year, further refinements have been made to our model based on the observation that particle size distributions of various types of brittle materials (vitreous, crystalline, ceramic, and conglomerate) which have undergone mechanical impacts can be fitted to a lognormal distribution. This model has been extended to allow determination of the fraction of particles within the respirable particle-size range (<10 μm) as well as new surface areas formed by the impact.

In FY 1980, studies were continued on the advantages of high-level waste encapsulated in a metallic matrix as an alternative to glass-monolith waste forms. This effort included assessment of the impact fracture and leach-rate characteristics as well as cost of solid waste form. The CEN metal-matrix encapsulation program was terminated at the end of FY 1980; the only remaining DOE-sponsored work on this waste form will be done by another laboratory.

The role of geologic formations in retarding migration of radionuclides from a nuclear-waste repository is an important factor in safe disposal of waste. In 1980, CEN conducted an applied program to evaluate radionuclide migration from a breached repository and a basic energy science program to study fundamental mechanisms of transport of trace elements through geologic media. The applied program (terminated at the end of FY 1980) involved leach-migration experiments under conditions that closely simulate those in repositories now under consideration. In the basic program, geochemical studies are under way on the mechanisms of mobilization of trace elements and the hydraulic properties of massive crystalline rock.

Nuclear Fuel Reprocessing. Work continued on the development of the ANL centrifugal contactor for application in solvent extraction processes. The near-term objective of this program is to develop a contactor design for a multistage extraction bank that would be tested in ORNL's Integrated Equipment Test Facility. Our experience from earlier work with contactors was used to design a 12-cm-dia unit capable of processing 0.5 Mg of fuel per day. This unit performed well in vibrational, hydraulic, and mass-transfer tests. A multistage 4-cm-dia unit was also built and will be tested to gain insight into the possible operating problems of a multistage 12-cm-dia contactor. In addition, the 4-cm-dia unit will be tested with three liquid phases under a variety of operating conditions.

LWBR Proof-of-Breeding Analytical Support Project. After the light water breeder reactor (LWBR) at Shippingport, PA, has been operated for a little more than four years at full power, proof-of-breeding will be determined by nondestructively assaying a sampling of the fuel rods with an irradiated-fuel assay gauge (IFAG). In this effort, ANL will provide calibration of the IFAG and independent verification of its measurements by physical, chemical, and radiometric analyses of irradiated LWBR fuel rods and fuel-rod segments. For this analytical project, process requirements include high-precision shearing of the fuel rods to obtain segments for dissolution, high fuel recovery, and minimal cross-contamination between segments. Under way now are the design and procurement of full-scale equipment to accommodate full-size fuel rods that will be analyzed in an end-of-life campaign. This includes a high-precision shear, multiple dissolvers, and equipment for disposal of scrap and waste generated during the process work. Testing of the shear and a prototype single-unit dissolver and design of the waste and scrap equipment are now in progress. In addition, a computer system is being developed that will provide (1) data collection and data processing and (2) control of the operational sequences for the shear, dissolver, and waste calciner. The end-of-life campaign is scheduled for CY 1983 but may be extended beyond this period.

9. Magnetic Fusion Energy Research

The program on fusion energy research at CEN embodies a family of research topics covering a variety of interrelated areas of fusion reactor technology. The CEN work includes (1) systems analysis and tritium breeder-blanket processing, (2) materials research and development, and (3) neutron dosimetry and damage analysis. Over the past year, several significant changes have taken place in the CEN fusion activities. These changes are (1) a redirection of both the engineering experimentation and the materials research to provide greater emphasis on the development of solid, rather than liquid, tritium-breeder materials, (2) a broader role in major national and international design activities, (3) an expansion of the dosimetry and damage analysis project to permit additional emphasis on the development of advanced damage analysis methodology, and (4) increased participation in joint research projects involving other ANL divisions, other laboratories, and industry. These changes have resulted in a discontinuation (presumably temporary) of work on liquid lithium processing and hydrogen isotope permeation. In particular, operation of the Lithium Processing Test Loop has been curtailed pending DOE's decision on its future role in the development of liquid lithium technology.

During the past year, the work on tritium-blanket processing research focused on (1) a comprehensive analysis of solid breeder-blanket performance and (2) planning and conceptual design of an experiment to test continuous in-pile recovery of tritium from a miniaturized solid breeder assembly. Since the physical and chemical data base for candidate solid breeder materials is extremely limited, modeling and extrapolation from known property data of similar ceramic materials have been used to make performance predictions. Also, examination of a variety of tritium recovery methods indicated that the most attractive method is continuous, in situ tritium recovery from a stationary compact of solid pellets by means of low-pressure ($\leq$1 atm) helium purging. The results of assessments conducted to date indicate that

the most promising breeder materials are lithium-bearing ceramics, e.g., $LiAlO_2$, Li_2ZrO_3, Li_2O, Li_2SiO_3, and Li_2TiO_3.

Design work on fusion-reactor tritium and blanket systems has continued during the past year. In this period, CEN personnel participated in several major DOE-sponsored design studies for tokamak fusion reactors, including the STARFIRE Commercial Reactor, the Engineering Test Facility (ETF), and the International Tokamak Reactor (INTOR).

Studies in materials chemistry and compatibility in first-wall and blanket environments for fusion reactors have been in progress at ANL since the early 1970's. Much of the past work has focused on hydrogen dissolution and permeation characteristics of various classes of structural alloys (austenitic steels, nickel-base alloys, refractory alloys, composite materials, and titanium alloys). In recent years, the scope of work was broadened to include other chemistry/compatibility aspects of materials behavior in fusion systems. During 1980, efforts were directed toward studies of (1) hydrogen permeation characteristics of ferritic steels and (2) corrosion of structural alloys by candidate ceramic solid-breeder materials.

The purpose of the CEN program on neutron dosimetry and damage analysis is to characterize irradiation facilities used by the magnetic fusion materials program at ANL and other laboratories. Neutron fluxes and energy spectra for reactors and accelerators are measured, and these data are used to compute fundamental displacement damage, gas production, and transmutation in fusion materials. Experimenters are provided with these basic exposure parameters in order to correlate property changes between facilities or predict the behavior of materials in fusion reactors. Experiments are conducted to test nuclear data and techniques. Damage parameters have been calculated from basic nuclear interactions for 23 elements to 20 MeV, and some calculations have been extended to 50 MeV.

10. Basic Energy Science

Homogeneous Catalysis. Research in this area deals with two topics: (1) the catalytic hydrogenation of carbon monoxide and (2) methanol homologation. With regard to the first topic, experimental studies of the mechanism by which $HCo(CO)_4$ catalyzes CO hydrogenation have been completed. A reaction mechanism involving hydrogen migration to a carbonyl in $HCo(CO)_4$ to give a formyl complex followed by addition of hydrogen to form a coordinated formaldehyde complex has been proposed and appears to be consistent with all current observations.

The methanol homologation reaction under study constitutes a new catalytic system. Research on this system has involved (1) exploring the steps which might occur in the catalytic sequence, (2) determining which other amines (or other bases) also have chemical properties necessary for the reaction, and (3) establishing the temperature, pressure, and solvent conditions required for the reaction to occur. Considerable knowledge has been gained about the overall catalytic mechanism. The new chemistry demonstrated by the reaction is not due to any unprecedented reaction, but rather to a series of precedented reactions proceeding in an unprecedented sequence.

Thermodynamics. Recently, several advancements have been made in our work on fundamental solution theories. First, a priori computations of the ternary phase diagram of AlF_3-CaF_3-NaF and AlF_3-CaF_2-LiF by the conformal ionic solution theory yielded predicted phase diagrams consistent with reliable thermodynamic information. The applicability of this theory to handle the thermodynamic properties of multicomponent ionic reciprocal systems is highlighted by this accomplishment. Second, relations based on the coordination cluster theory have been derived for molten salts, aqueous solutions, and slag equilibria. In addition, measured activity coefficients for dilute solutions of lithium in Li-Al-Bi, a system which exhibits a miscibility gap and has large deviations with ideality, have been found to be in good agreement with calculations based on this theory.

Study of the solution behavior of hydrogen in $CaAl_2$ has shown that this alloy can serve as a high-temperature hydrogen storage medium with an absorptive capacity which is as good as that of $LaNi_5$ or FeTi, two well-known hydrogen storage systems.

The enthalpies of formation, heat capacity (5 to 350 K), and enthalpy increments (198.15 to 625 K) of analcime as well as the heats of formation of dehydrated analcime and natrolite have been measured. These measurements constitute the first part of a program to study zeolite thermodynamics as a function of composition and structure-type.

Fluorine-bomb calorimetry is being used to improve the confidence level of the data base for the thermochemistry of inorganic sulfides. In this connection, measurements have started on $CuFeS_2$ (chalcopyrite) and K_2S.

In studies of gas-condensed phase equilibria, a sophisticated computer program has been developed and has been used to calculate the complex chemistry of the condensation of sulfates from combustion gases. It has been found that, in comparison with pure Na_2SO_4, Na_2SO_4-K_2SO_4 solutions condense at somewhat higher temperatures but have a much lower liquidus temperature. This suggests that, under typical burner conditions, a much larger fraction of the alkali sulfates condense to corrosive liquids rather than to less corrosive solids. To improve the computer program, reciprocal molten-salt solution theories will be incorporated into it; this may make possible the treatment of the complicated multicomponent solutions that occur in hot corrosion.

Environmental Chemistry. Research in this area is concerned with (1) establishing the significant mechanisms for the formation of atmospheric sulfate and nitrogen-bearing aerosols and (2) developing the instrumental capability to conduct these studies.

With regard to the first activity, oxygen isotopy is being used as a means for differentiating between likely sulfate formation mechanisms; the evidence accumulated thus far has indicated that a reaction involving the conversion of SO_2 to H_2SO_3 followed by oxidation, heterogeneously and catalytically, to H_2SO_4 may be a dominant SO_2-conversion process in the Chicago area during late autumn, winter, and early spring. Further, it has been suggested that some of the atmospheric sulfate may be primary in origin.

The Fourier Transform IR-Impactor instrument has been demonstrated to be sensitive to submicrogram levels of sulfates and nitrates and to rapid changes in aerosol chemistry. The sensitivity and capability of this instrument were demonstrated when it was used for sampling and analysis of the aerosol formed in a power-plant plume. Even on one pass through the plume, sufficient aerosol was collected for analysis. The potential of this device for atmospheric sampling and analysis appears high.

Electrochemistry. This program is concerned with experimental and theoretical investigations of processes occurring at electrodes and in electrolytes. The subjects under study include (1) the electroreduction of oxygen on carbon-supported iron phthalocyanine electrodes, (2) the anodic corrosion and passivation of metals in molten-salt and aqueous environments, (3) the structure of dissolved sulfur species in a variety of electrolytes associated with some high-temperature electrochemical systems, and (4) ordering and complex-ion formation in chloraluminate electrolytes.

To gain an understanding of these electrode and electrolyte processes at the microscopic level, a strong emphasis is placed on the use of spectroscopic and theoretical methods as well as electrochemical techniques. During the past year, there have been numerous interesting findings. Among these are the following:

1. The structure of oxygen complexes formed with an electrocatalyst such as iron phthalocyanine was calculated from theory to be different from that formed with an oxygen carrier such as iron porphyrin; the implications of this result are being explored.

2. The corrosion-passivation behavior of several metals (e.g., Fe, Co, Cu, Ta) in molten LiCl-KCl containing Li_2O at temperatures up to 450°C appears similar to that found in aqueous systems.

3. Analysis of data on the NaCl-$AlCl_3$ system has indicated an unusual degree of ordering near the 50-50 composition and has highlighted conditions where the concept of pCl in chloraluminates can be related to a thermodynamic quantity, viz., $-\ln a_{NaCl}$.

4. The predominant sulfur species in CsCl-$AlCl_3$ melts is S_3^-, and it tends to form adduct-type molecular ions such as $AlCl_3{:}S_3^-$ in the melt.

Physical Properties of Salt Vapors. Spectroscopic, thermodynamic, and theoretical studies on a wide variety of inorganic vapors and vapor complexes are being conducted. Spectrophotometric investigations were performed on the reactions involving $FeCl_2$ and $ErCl_3$ with the complexing gases $AlCl_3$, $InCl_3$, and $GaCl_3$. The laser-induced fluorescence spectra of one of the complexes so formed, $ErCl_3 \cdot AlCl_3$, was examined. It was found that the fluroescence proceeded through dissociation of the vapor complex. Further, the structures and energies of the complexes $BeF_2 \cdot AlF_3$, $MgF_2 \cdot AlF_3$, and $AlF_3 \cdot BeF_2 \cdot AlF_3$ were studied by ab initio molecular orbital methods. The most stable forms for these complexes as well as metal-halide complexes in general appear to possess edge-bridged structures.

A general relation (dimensional model) for the nonelectronic entropy and free energy function of gaseous molecules has been shown to predict values for molecules of the type MX_n (where $3 \leq n \leq 6$) that are in good agreement with data in the JANAF tables. This lends confidence that this method may be useful for calculating entropies and free energy functions of unmeasured systems and thus for extending the JANAF tables.

11. Analytical Chemistry Laboratory

The CEN Division operates Argonne's central Analytical Chemistry Laboratory (ACL) on a full-cost recovery basis. With a staff of 30 people, the ACL supports ANL's scientific and engineering programs by performing chemical analyses, developing analytical methods and instrumentation, and consulting with experimenters. The Organic Analysis Group (six ACL staff) has recently acquired new facilities for the preparation and analysis of samples requiring the characterization of organic constituents. This group is developing a computerized gas chromatograph/mass spectrometry (GC/MS) system, based on time-of-flight MS, to perform rapid analysis of complex organic mixtures; commercial GC/MS instrumentation is on order. During the past year, the capability of the ACL has been expanded with the addition of (1) a microanalysis apparatus for the determination of hydrogen, oxygen, and nitrogen by inert gas fusion, (2) an apparatus that measures the fluorescence of uranium produced by a pulsed nitrogen laser, and (3) the preparation of isotopic standards for lithium. Furthermore, an Inductively Coupled Plasma-Atomic Emission Spectrometer (ICP-AES), which will provide rapid and accurate multielement analytical capability, is on order. The ACL has worked hard to develop a close collaborative role with the R&D programs it serves and views with satisfaction the relationships that have evolved with the Proof-of-Breeding Project, the Coal Toxicology Program, and the OEPM Group engaged in analysis of stibine and arsine generated from lead-acid batteries.

12. Computer Applications

The Computer Applications Group assists CEN staff in many aspects of computer-related activities--laboratory data acquisition and control, computer modeling and simulation, data-base development, and consulting. To meet the growing needs of the Division, this group has procured a 32-bit minicomputer system (VAX 11/780), which will be integrated into a laboratory-wide computer network. This system will provide a significant improvement in local computing capacity, data management, word processing, and graphics capabilities.

II. ADVANCED BATTERY PROJECT

A. Overview

The objectives of the advanced battery project at ANL are to develop high-performance, electrically rechargeable batteries and to transfer this technology to industry for commercialization. Although the major emphasis is currently on batteries for electric automobiles, a small effort is aimed toward development of stationary energy-storage batteries for load leveling on electric-utility systems and for systems utilizing solar, wind, or other cyclic or intermittent energy sources.

The battery cells that are under development consist of Li-Al negative electrodes, FeS or FeS_2 positive electrodes, BN felt or MgO powder separators, and a molten salt electrolyte. Although LiCl-KCl eutectic was used as the electrolyte in most of the earlier cells, those now under development generally utilize other electrolyte compositions such as "LiCl-rich" LiCl-KCl (typically 67 mol % LiCl-KCl), LiF-LiCl-KCl, or LiF-LiCl-LiBr. To ensure that the electrolyte is fully molten, the cells are normally operated within a temperature range of about 430-500°C. The overall reaction for a Li-Al/FeS cell can be written as follows:

$$2LiAl + FeS \underset{}{\overset{2e^-}{\rightleftharpoons}} Li_2S + Fe + 2Al \qquad (1)$$

The theoretical specific energy for reaction 1 is about 460 W-h/kg, and the voltage vs. capacity (charge and discharge) curves have a single open-circuit voltage plateau at about 1.3 V. The reaction is actually more complex than shown and involves intermediate products such as $LiK_6Fe_{24}S_{26}Cl$, which is formed by a reaction with KCl in the electrolyte. A Li-Al/FeS_2 cell exhibits the same voltage plateau as reaction 1 and an additional plateau at about 1.7 V, which results from the reaction

$$2LiAl + FeS_2 \underset{}{\overset{2e^-}{\rightleftharpoons}} Li_2S + FeS + 2Al \qquad (2)$$

The total theoretical specific energy for reactions 1 and 2 is approximately 650 W-h/kg. Reaction 2 also involves several complex intermediate compounds.

The cell designs currently being developed have a prismatic configuration, with one or more positive electrodes and facing negative electrodes. The cells can be fabricated in a charged, uncharged, or partially charged state by using various combinations of reactants and products in the electrodes. Both the positive and negative electrodes are normally fabricated by cold- or hot-pressing methods. A key cell component is the electrode separator, a porous material that provides electrical isolation of the electrodes but permits the migration of lithium ions between the electrodes. In most cell designs, it is also necessary to use screens or other structures to retain particulate material within the electrodes. To enhance the electronic conductivity of

the electrodes, metallic current collectors are used to provide a low-resistance current path between the active material and the electrode terminal.

As reported last year, the Mark IA electric-vehicle battery, which consisted of two 20 kW-h modules, was fabricated by Eagle-Picher Industries, Inc. and delivered in May 1979 to ANL for road-testing in a van. During startup heating prior to testing, one of the modules developed a short circuit, which resulted in complete failure of the module. As a result of the Mark IA experience, the original strategy for the development of the Mark II was revised into two phases. The first phase, which is nearing completion, stresses the development of high-reliability cells and involves the fabrication and testing of small (up to 10 cells) modules. In addition, groups of cells of identical design (referred to as "status cells") are periodically fabricated and tested to monitor progress in the state of the art. The second phase, which is expected to begin early in 1981, will consist of the development of interconnected modules and full-scale batteries for passenger automobiles. Completion of the Mark II program is currently scheduled for 1984. The performance and lifetime goals for the Mark II cell and battery are listed in Table II-1, along with achieved values for contractor-fabricated cells recently tested. To meet the requirements for an electric automobile, the power goal has been increased substantially above that given in last year's report. The Mark III battery, scheduled for testing in 1986, will be a higher performance

Table II-1. Performance and Cycle Life for the Mark II Electric-Vehicle Battery

	Achieved[a]		
	Developmental Cells	Status Cells	Goal
Specific Energy,[b] W-h/kg			
Battery	--	--	100
Cell	70	81	125
Energy Density,[b] W-h/L			
Battery	--	--	150
Cell	188	217	300
Peak Specific Power,[c] W/kg			
Battery	--	--	150
Cell	60	60	185
Lifetime (deep cycles)			
Battery	--	--	500
Cell	399	239	500

[a] Cells fabricated by Eagle-Picher as part of phase I of Mark II program; data obtained at end of CY 1980.

[b] Calculated at the 4-h discharge rate.

[c] Peak power sustainable for 15-s pulse at 0 to 50% state of discharge.

prototype to be demonstrated in a passenger automobile; it is expected to be able to sustain 1000 deep discharges.

Eagle-Picher Industries, Inc. and Gould Inc. are both under subcontracts with ANL for Mark II battery development. As part of the Mark II cell development effort, both contractors are fabricating and testing Li-Al/FeS multiplate cells* of a prismatic design. All of the Eagle-Picher cells have BN felt separators; whereas Gould has recently reoriented its program toward the development of cells with MgO powder separators, which have the potential for lower cost in the near future.

In addition to the major cell and battery development programs at Gould and Eagle-Picher, the Carborundum Company† is developing a process for the production of BN felt separator material. Furthermore, smaller subcontracted programs are being carried out at General Motors Research Laboratories, the Institute of Gas Technology, Rockwell International, Illinois Institute of Technology, and the University of Florida.

The research and development work at ANL during the past year has included cell capacity-loss studies, cell-swelling studies, cell modeling, materials engineering, cell and battery testing, post-test examinations of cells, fabrication and testing of status cells, battery component and auxiliary systems development, and potential applications and cost studies.

A major objective of the program at ANL is to transfer the technology to industry for commercialization. Technology transfer is implemented by various means, including the temporary assignment of engineers and scientists from industry to ANL and the subcontracting of development work on cells, batteries, and auxiliary items to industrial firms. Cost, design, and marketing studies are also conducted with the assistance of subcontractors and consultants. During the past year, foreign institutions in Germany, France, Japan, and Korea have sent industrial participants to ANL. Various academic institutions are also involved in the program through temporary student and faculty assignments, subcontracts, and consultants.

Although the major portion of the effort in 1980 has been focused on the Li-Al/FeS Mark II cells, work has also been in progress on lithium-alloy/FeS_2 cells and cells having calcium-alloy negative electrodes. The FeS_2 positive electrode offers the possibility of higher cell capacity and power, but it poses corrosion and long-term stability problems that require further work. The calcium-alloy negative electrodes offer a lower cost substitute for the lithium used in the present cells.

B. Electrode Chemistry

The electrode-chemistry studies are directed toward (1) understanding and solving the chemical and electrochemical problems that arise with electrodes during the development work on cells and batteries, (2) acquiring an

---

*A multiplate cell has two or more positive electrodes and facing negative electrodes.

†A subsidiary of the Kennecott Copper Corp.

understanding of the processes that occur within the electrodes during cell operation, and (3) identifying new electrodes and electrolytes that may improve cell performance and life. Recently, the electrode studies have been concentrated on the chemistry and the performance characteristics of the LiAl and FeS electrodes.

1. Agglomeration Effects in the LiAl Electrode

In the normal operation of the LiAl negative electrode, the active material forms an open, skeletal, three-dimensional structure that persists during extended charge-discharge cycling. Under certain conditions, however, there is a tendency toward agglomeration of the active material which is believed to be a possible cause of capacity decline. A new experimental technique has been developed to determine the effects of several variables on the degree of agglomeration in the negative electrode.

For the comparative agglomeration experiments, a LiAl(α + β) electrode* and a pure aluminum electrode were immersed in electrolyte to form a small cell. This cell was cycled for a selected period, and then the electrodes were sectioned and examined microscopically.

Comparative agglomeration experiments were conducted to determine the effects of electrolyte composition, current density, and additives on the agglomeration process. The electrolytes were LiCl-KCl eutectic (59 mol % LiCl), LiCl-rich (67 mol %) LiCl-KCl, and an all-lithium cation system, LiF-LiCl-LiBr; the current densities were 25, 50, and 75 mA/cm^2; and the electrode additives were magnesium and cadmium.

Although electrolyte composition and current density both affected the degree of agglomeration in the electrodes, neither was a dominant factor. When agglomeration developed after cycling of the cell, it usually did so in the electrode that was originally pure aluminum. A striated structure that was parallel to the current flow in the electrode was frequently associated with the agglomeration; this structure is believed to be a stage in the agglomeration process. It was hypothesized that the agglomeration phenomenon may be related to the unusually high concentration of vacancies in β-LiAl (lithium-rich alloy), and that the agglomeration process might be controlled through modification of the vacancy concentration by additives. Magnesium and cadmium, however, did not appear to be effective in this capacity.

The results of these studies showed that agglomeration is a mechanism for capacity decline in the negative electrode and that it is affected by electrolyte composition and current density. This mechanism, however, is not necessarily the only cause of capacity decline in Li-Al/FeS cells.

---

*The Li-Al alloy used for the electrode consists of two co-existing solid phases, α-Al and β-LiAl. The α-Al phase is a solid solution of aluminum saturated with lithium, and the β-LiAl phase is basically the intermetallic compound LiAl.

2. FeS Electrode Studies

The FeS electrode, when discharged in the LiCl-KCl electrolyte, is known to undergo six electrochemical reactions:

$$FeS \rightarrow J \text{ phase } (LiK_6Fe_{24}S_{26}Cl) \quad (3)$$

$$J \rightarrow X \text{ phase } (Li_2FeS_2) \quad (4)$$

$$J \rightarrow Li_2S \quad (5)$$

$$FeS \rightarrow X \quad (6)$$

$$FeS \rightarrow Li_2S \quad (7)$$

$$X \rightarrow Li_2S \quad (8)$$

In earlier studies (see last year's report), emf expressions for reactions 4, 5, and 8 were derived from experimental measurements made with small (about 1 A-h) Li-Al/FeS cells having LiCl-KCl electrolyte. Efforts to measure emf's of reaction 3 were unsuccessful because of its irreversibility, and emf values for reactions 6 and 7 could not be measured because these two transitions do not occur under equilibrium conditions in the LiCl-KCl electrolyte.

The first three transitions, reactions 3 to 5, involve J phase, which is formed by a reaction with the KCl in the electrolyte. Consequently, the emf's for reactions 6 and 8 at various temperatures were measured in two small Li-Al/FeS cells having an electrolyte free of potassium ions, LiF-LiCl-LiBr. A linear regression analysis of the emf data obtained from the two cells, which were in excellent agreement (±0.6 mV), resulted in the following expressions:

$$\text{Reaction 6:} \quad E_{FeS \rightarrow X} = 1335.24 + 0.0217T \quad (9)$$

$$\text{Reaction 8:} \quad E_{X \rightarrow Li_2S} = 1425.23 - 0.1375T \quad (10)$$

where E is in millivolts and T is in degrees Kelvin. These data were then used to calculate the emf expression for reaction 7, which is equal to one half the sum of these two emf expressions. Thus,

$$E_{FeS \rightarrow Li_2S} = 1380.24 - 0.058T \quad (11)$$

The emf values for reaction 8 differ slightly from those previously measured in cells with LiCl-KCl electrolyte. However, this difference is quite small (<2 mV) in the temperature region measured. The emf values for reaction 6 also differ from those reported previously (about 4 mV at 400°C, and about 1 mV at 500°C).[1] This difference is largely due to the fact that the earlier

[1] D. L. Barney et al., High Performance Batteries for Electric-Vehicle Propulsion and Stationary Energy Storage: Progress Report for the Period October 1978-September 1979, Argonne National Laboratory Report ANL-79-94, p. 146 (1980).

emf values had been calculated rather than measured. A significant point, however, is that the slope of the emf vs. temperature curve for Reaction 6 was positive when measured but negative when calculated.

The free energies of formation of Li_2S at 700 and 800 K were calculated from the emf data for reaction 7 and literature values for the free energies of formation for FeS[2] and LiAl[3]. In these calculations, the diatomic gas was chosen as the standard state for sulfur; and the values for the free energy of formation of Li_2S at 700 and 800 K were found to be -102.5 and -99.9 kcal/mol, respectively.

With the addition of the above information, the thermodynamics of the FeS electrode appears to be fairly well characterized.

3. Electrochemical Studies of Electrode Processes

The objective of this work is to develop a better understanding of the voltage-loss processes (primarily electrode polarization) which limit the performance of the Li-Al/FeS cell. In this work, electrode potential measurements were made on several 100 A-h cells to investigate their electrode polarization characteristics. The measurements were made with a current-interruption technique in which the potentials of the working electrodes in the cell were monitored against a $Ni/Ni_3S_2/S^{2-}$ reference electrode before and after current interruption. The instrumentation developed for this work has a long-term stability of 1 mV and a resolution capability of 1 mV. With this experimental setup, curves for electrode potential (η) vs. relaxation time (t) can be derived.

Typical curves of the electrode relaxation potentials for two states of charge and discharge (A-h) are shown in Fig. II-1 for a bicell* (G-RE-1) constructed with electrodes of the type that Gould uses in its Mark II cells. The polarization in the electrodes is indicated in this figure by the potential change during the relaxation period; the zero value of the relaxation corresponds to the potentials of the electrodes prior to current interruption. It is interesting that the polarization of the positive electrode is much greater than that of the negative electrode during both the charge and the discharge of the cell. An examination of the relaxation potentials observed within microseconds of current interruption indicated that these values change markedly with state of discharge; this potential shift is usually associated with the ohmic resistance of the cell system under investigation. The relaxation values observed after this ohmic step, which are believed to be principally electrochemical and chemical in nature, change very little during discharge. These observations suggest that the specific energy and power of the cell system are limited by the ohmic resistance. This ohmic

---

[2] K. C. Mills, Thermodynamics Data for Inorganic Sulfides, Selinides, and Tellrites, Butterworth, London (1974).

[3] N. P. Yao, L. Heredy, and R. C Saunders, J. Electrochem. Soc. 118, 1039 (1971).

* A bicell consists of one positive and two negative electrodes.

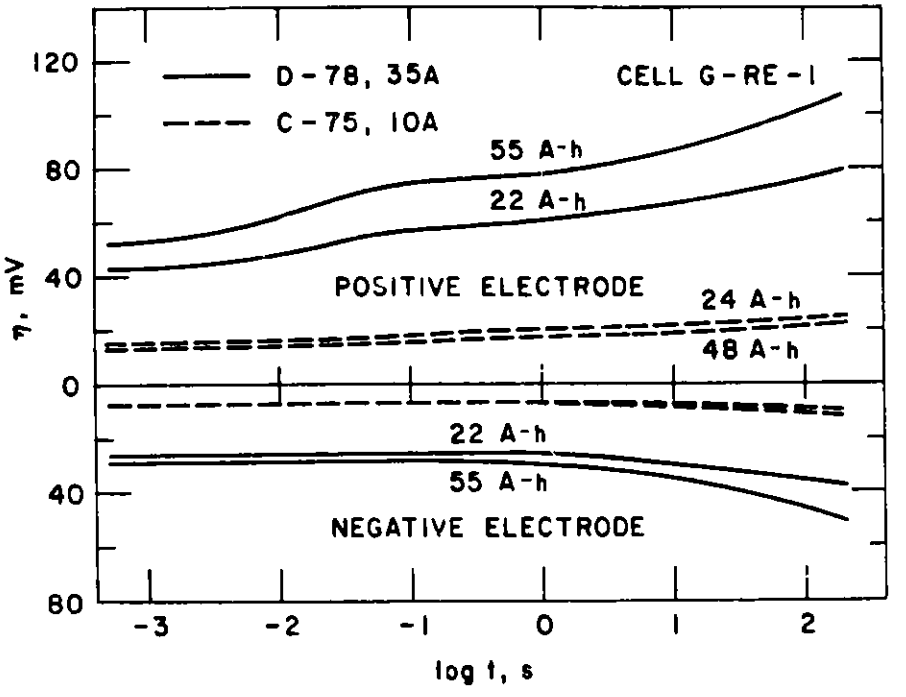

Fig. II-1. Electrode Potential vs. Relaxation Time after Current Interruption for a Mark II-Type Bicell with Gould Electrodes (negative-to-positive capacity ratio of 1.27)

limitation generates a polarization in the electrodes at any given state of charge or discharge that is nearly a linear function of the applied current density. Studies of electrode polarization will be continued in 1981.

C. Materials Engineering

Efforts in this program are directed toward the development of materials for cell components (current collectors, cans, feedthroughs, electrode retainers, etc.). The corrosive conditions within the electrodes at the cell operating temperature severely restrict the materials available which will satisfy the criteria of long life, low cost, high electronic conductivity, and ease of fabrication. Candidate cell materials are evaluated for chemical compatibility and mechanical stability by two methods: static immersion tests in mixtures that simulate positive and negative electrodes (i.e., FeS/LiCl-KCl and LiAl/LiCl-KCl) and tests in 50 A-h cells.

The corrosion resistance of nickel was found to be very good in static immersion tests in an equal-volume mixture of FeS and electrolyte (simulating a charged electrode); however, in-cell tests showed the corrosion behavior of nickel to be very dependent on the state of charge of the as-fabricated electrode. For cells assembled in the fully charged state, the corrosion behavior of nickel was the same as that observed in the static immersion tests; whereas cells assembled semi-charged and uncharged showed localized areas of severe

intergranular corrosion in the nickel components. Additional tests showed that the use of fine iron powder (75- to 100-μm dia) in the electrode mix prevents corrosion of nickel; the reason for this behavior is not yet fully understood.

Previous static immersion tests had shown that low-carbon steel was severely corroded in the FeS-electrolyte mixture. Also, post-test examinations of numerous engineering cells showed substantial corrosion (75-150 μm/yr) of low-carbon steel current collectors; the corrosion rate was very rapid for the first 200 days, with a sharp decline to a low rate thereafter. The corrosion reaction resulted in a dispersion of fine iron particles throughout the positive electrode. Based on this observation, it was reasoned that the addition of fine iron powder to the electrode mix should reduce the corrosion of low-carbon steel current collectors. This has now been confirmed by static immersion tests and in-cell tests. These results indicate that FeS positive electrodes with low-carbon steel current collectors and fine-iron powder additives should give adequate cycle life to meet the Mark II goals.

Protective coatings on low-cost substrate materials are being investigated for current-collector applications in FeS and LiAl electrodes. ' ating processes for the test samples included chemical-vapor, electrochemical, and electroless deposition and RF sputtering. The coating materials included TiC, TiN, TiN-TiC, Cr, Ni, $MoSi_2$, Mo, Mo-TiN, and Mo-Ni; the substrate material was low-carbon steel in most cases. Preliminary results indicate that Ni, Ni-Mo, Cr, and TiN-TiC coatings on substrates have adequate chemical compatibility with the FeS electrode. In addition, the results indicate no chemical reaction of the LiAl electrode with the TiC, TiN and TiN-TiC coatings. No further work on protective coatings is planned at this time.

D. Cell Development

The objective of this work is to identify and test cell and electrode designs that provide improved performance and lifetime. Results from these tests are incorporated into the cell-development programs of the contractors.

1. Modeling Studies

Engineering modeling studies are being conducted to obtain mathematical correlations of performance and lifetime with cell design parameters and operating variables. In this effort, empirical equations have been developed by multiple regression analysis of test data from previously operated cells. These empirical equations were used to predict the specific energy for up to 800 cycles of eighty-four Li-Al/FeS multiplate cell designs. The following design variables were investigated: positive-electrode thickness (0.28 to 0.52 cm), volume fraction of salt in the positive electrode (0.38 to 0.67), positive-electrode loading density (0.7 to 1.6 A-h/cm^3), negative-electrode thickness (0.28 to 1.14 cm), and negative-to-positive capacity ratio (1.0 to 1.3).

This study was designed to identify the most likely cell designs to meet the Mark II cycle-life goals for the Mark II battery: less than 20% decline in specific energy over 500 cycles. The following conclusions were

drawn: (1) a 50% decrease in the negative-electrode thickness results in a 50% decrease in the specific-energy decline by 200 cycles of operation and a 25% decrease in the specific-energy decline by 800 cycles; (2) changes in the positive-electrode loading density ($A\text{-}h/cm^3$) have little effect on the rate of specific-energy decline; (3) negative electrodes with 30% excess lithium capacity show a lower rate of specific-energy decline than those with no excess lithium capacity; and (4) a 40°C temperature increase, from 440 to 480°C, results in a 50% decrease in the rate of specific-energy decline per cycle at less than 200 cycles of operation.

In other efforts, a model of the electrochemical process occurring within cells is being developed.

2. Capacity Stabilization Studies

In general, the Mark IA cells showed significant capacity decline during cycling (typically 20% within 80 cycles). The objective of this work is to provide design recommendations that will reduce the rate of capacity loss in Li-Al/FeS cells.

In an earlier study (see last year's report), a reference electrode was inserted into an engineering-scale Li-Al/FeS bicell with Mark IA electrodes (designated EPRE-1); the negative-to-positive capacity ratio of the cell was 1.11. Measurements made with the reference electrode indicated that the capacity of the cell was limited by the positive electrode during charge and by the negative electrode during discharge; furthermore, the power of the cell was limited by the positive electrode. In a subsequent test, reference electrodes were implanted in a Li-Al/FeS bicell identical in design to EPRE-1, except that the theoretical capacity of the negative electrode was doubled (negative-to-positive capacity ratio of 2.22). As shown in Fig. II-2, this cell (EPRE-2) exhibited very little capacity decline over 55 cycles. (Operation of Cell EPRE-2 was terminated after 55 cycles because of a temperature-controller malfunction.) The positive electrode utilization for this cell was 95%. Measurements with the reference electrode indicated (1) that the negative electrode was essentially unpolarized during cycling and (2) that essentially all the polarization developed by the cell was present in the positive electrode. Therefore, the cell capacity was limited on both charge and discharge by the positive electrode. The observations made concerning this cell indicate that the capacity fading observed in EPRE-1, as well as in the previous Mark IA cells, was caused by the capacity decline of the negative electrode (see also Section II.B.1 of this report).

An analysis of performance data from various cells suggested a correlation between capacity stability and initial utilization of the negative electrode. Figure 1I-3 shows the rate of capacity decline for three cells as a function of initial negative-electrode utilization. The Mark IA cell (negative-to-positive capacity ratio, 1.0) and the Matrix D cell (capacity ratio, 1.1) are both Li-Al/FeS multiplate cells fabricated by Eagle-Picher as part of the Mark IA program. As shown in Fig. II-3, the rate of capacity decline decreased as the initial negative utilization was decreased, and reached a very low value below about 60% utilization of the negative electrode. In addition, lowering the depth of discharge of the Matrix D cell

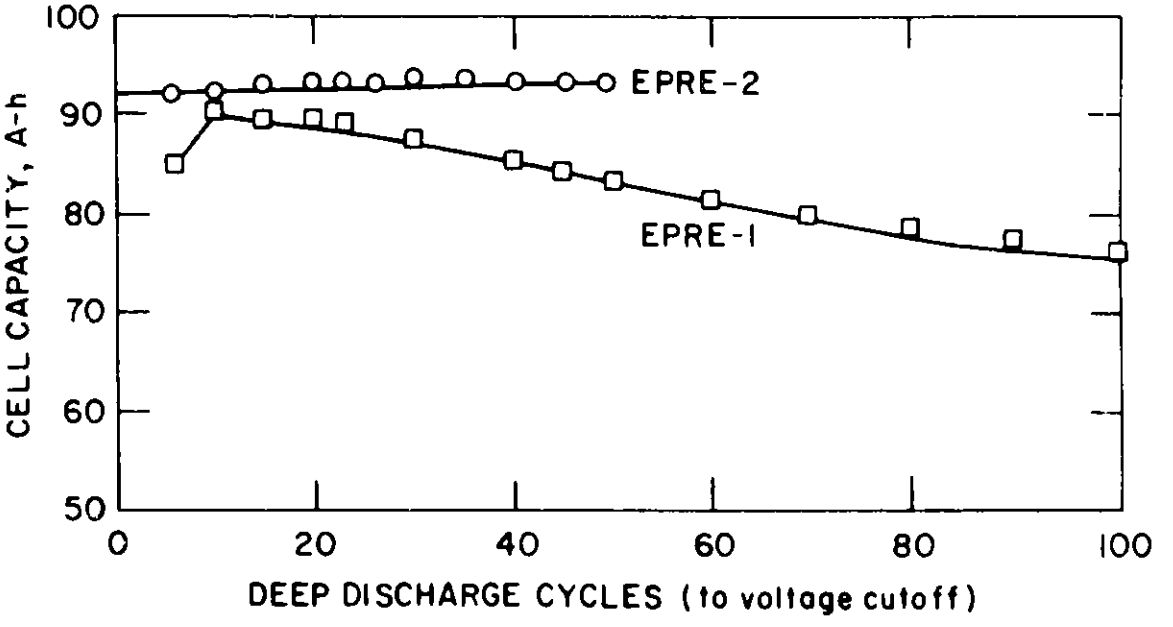

Fig. II-2. Cell Capacity as Function of Cycle Life for Cells with Different Negative-to-Positive Capacity Ratios

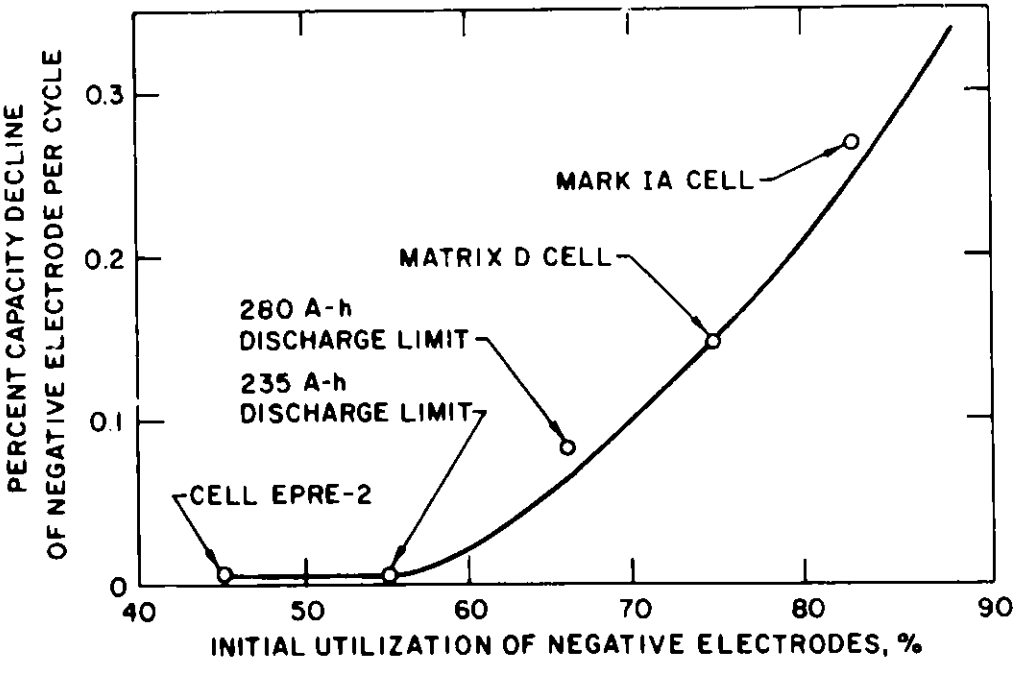

Fig. II-3. Capacity Decline in Negative Electrode as Function of Initial Negative Electrode (46 at. % Li-Al) Utilization

from 320 A-h to 280 and 235 A-h resulted in a significant decrease in the capacity-decline rate. It should be noted that all three of the cells shown in the figure were fabricated with 46 at. % Li-Al alloy in the negative electrode and LiCl-KCl eutectic electrolyte and were operated at 465°C. Past studies at ANL have already indicated that more stable capacity can be achieved in cells with LiCl-rich electrolyte, with operating temperatures above 460°C, and probably with an initial lithium content higher than 46 at. % in the negative-electrode alloy.

As reported below, the capacity-loss studies conducted over the past year have resulted in design recommendations that have significantly improved the capacity retention of the Li-Al/FeS cell.

E. Cell and Battery Testing

The performance and lifetime of engineering-scale Li-Al/FeS cells fabricated by ANL and its contractors are determined by tests conducted by both ANL and the contractors. In these cells, the separator material was normally BN felt, which has the advantage of lower potential cost than the BN fabric used in the Mark IA cells. Post-test examinations of these cells are used to identify failure mechanisms; recommendations for design improvements can then be formulated.

Status cell tests are periodically conducted to monitor the overall technical progress of the program. In these tests, groups of cells of an identical design are fabricated and subjected to cycle-life tests to obtain statistical data on cell lifetime. The criterion for the end of life of a cell is a 20% loss of the initial (stable) capacity or a decrease of the coulombic efficiency to 95%.

1. ANL Cells

In total, sixty Li-Al/FeS bicells were fabricated and tested at ANL to investigate the effects of LiCl-rich electrolyte, negative-to-positive capacity ratios greater than one, and current-limited, constant-voltage charging on the rate of capacity decline during cycling. The average rate of capacity decline was less than 0.03% per cycle over an average of about 290 cycles, which is a significant improvement over that achieved with the Mark IA cell. This improved capacity-decline rate has also been demonstrated in multiplate cells fabricated by the contractors in the Mark II program.

Twelve status bicells were fabricated and tested at ANL to obtain reliable cycle-life data. These cells had a negative-to-positive capacity ratio of 1.4, LiCl-rich LiCl-KCl electrolyte, and an operating temperature of 460°C, all measures which had been previously shown to reduce the rate of capacity decline with cycling. The 12 status cells were operated for an average of 287 cycles and showed an average capacity loss of only 7% (less than 0.03% per cycle). The average specific energy of these cells was 69 W-h/kg at the 4-h rate, and the average specific power was 72 W/kg at 50% depth of discharge. Performance data for the individual cells are presented

in Table II-2. In addition, measurements were made which showed that the capacity loss at the standard 4-h discharge rate (74 mA/cm^2) and 8-h charge rate (37 mA/cm^2) was recovered when a lower charge rate (18 mA/cm^2) was used.

Table II-2. Performance of the ANL Status Bicells

Cell	Peak Performance[a]		Performance Decline, %		Cycles	Capacity Decline per Cycle, %
	Capacity, A-h	Energy, W-h	Capacity	Energy		
SM8F01	82	95	11	8	129	0.085
SM8F02	83	97	2	2	241	0.008
SM8F03	83	100	4	5	433	0.009
SM8F04	82	95	12	10	101	0.119
SM8F05	81	97	20	23	82	0.244
SM8F06	81	95	4	3	355	0.011
SM8F07	78	93	1	1	400	0.002
SM8F08	82	96	2	2	363	0.006
SM8F09	82	98	4	6	268	0.015
SM8F10	82	96	4	4	600	0.007
SM8F11	81	96	2	2	400	0.005
SM8F12	84	99	20	20	75	0.267
Average	82	96	7	7	287	0.02

[a]Recorded at a discharge current density of 74 mA/cm^2 (4-h discharge rate).

2. Subcontractor Cells

As part of the first phase of the Mark II program, the two subcontractors--Eagle-Picher and Gould--are striving to build reliable Li-Al/FeS multiplate cells. After fabricating and testing developmental cells of various designs, each subcontractor produced a group of 12 status cells that were tested at ANL. The goal was for these cells to maintain stable capacity over extended cycling (>200 cycles) and to attain a peak specific energy of 90 W-h/kg at the 4-h rate.

In early 1980, Eagle-Picher fabricated fifteen Li-Al/FeS multiplate cells, which were tested at ANL. The specific energy of these cells at the 4-h discharge rate was 69 W-h/kg, and the peak power at 50% discharge was

50 W/kg. These somewhat low values were the result of the use of very heavy components in the electrode structures; these components have since been eliminated. These cells showed very stable capacity, with an average decline rate of 0.03% per cycle over an average of 322 cycles.

Subsequently, twelve multiplate status cells were fabricated by Eagle-Picher and then tested at ANL. As shown in Table II-3, the average specific energy for these cells is about 80 W-h/kg, with an average capacity-decline rate of less than 0.03% per cycle. The cycle life to date for the eight cells that are still on test is between 116 and 218 cycles. Testing of four of the 12 cells was terminated because of electrical short circuits brought about by problems involved in the cell assembly and fabrication. These problems have now been largely eliminated by major modifications of the cell-assembly procedure at Eagle-Picher.

Table II-3. Performance of Eagle-Picher Status Cells[a]

Cell No.	Cycle Life		Initial Capacity,[b] A-h	% Capacity Loss per Cycle	Peak Specific Energy,[b] W-h/kg
	Terminated Cells	Operating Cells			
55	149	--	325	c	91.1
60	185	--	295	0.015	81.8
67	102	--	262	0.061	72.0
68	23	--	272	--	74.0
Average	115	--	285	0.038	79.7
54	--	187	292	0.027	81.2
61	--	154	201	0	81.7
62	--	212	320	0.022	88.9
63	--	218	302	0.020	82.5
65	--	191	300	0.024	82.7
66	--	200	300	0.033	82.2
69	--	116	305	0.079	84.2
71	--	179	262	0.030	70.2
Average	--	160	298	0.029	81.7

[a]Data obtained at end of FY 1980.

[b]Measured at a 4-h (70-A) discharge rate.

[c]Electrolyte solidified after 69 cycles, and significant capacity loss ensued.

The developmental cells now being fabricated by Eagle-Picher are demonstrating specific energies in the range of 95-100 W-h/kg; however, insufficient testing time has elapsed to obtain meaningful data on their cycle life or rate of capacity loss.

In its cell development effort for the Mark II program, Gould initially fabricated eleven multiplate Li-Al/FeS cells. In tests at ANL, these cells achieved a specific energy of 86 W-h/kg at the 4-h rate and a specific power of 100 W/kg at 50% discharge. The average decline in capacity for these cells was acceptable, 0.07% per cycle over 114 cycles, but the cycle life was poor (<150 cycles). The performance of 12 multiplate status cells fabricated by Gould is given in Table II-4. The average specific energy of these status cells was 93.2 W-h/kg at the 5-h rate and the average rate of capacity loss was 0.08% per cycle. Testing of five of these cells was terminated after less than 80 cycles because of short circuits. These short circuits appear to have been caused by extrusion of active material from the positive electrode near the positive terminal rod. To eliminate this problem, a modified electrode design was recommended to Gould by CEN.

Table II-4. Performance of Gould Status Cells[a]

Cell No.	Cycle Life		Initial Capacity,[b] A-h	% Capacity Loss per Cycle	Peak Specific Energy,[b] W-h/kg
	Terminated Cells	Operating Cells			
76	75	--	199.0	0.070	94.1
78	42	--	193.0	0.049	89.6
79	80	--	197.5	0.123	93.5
85	66	--	198.0	0.084	94.0
87	50	--	198.0	0.091	95.4
Average	63	--	197.1	0.083	93.3
77	--	64	196.0	0.035	92.2
80	--	57	194.0	0.099	94.0
81	--	49	202.0	0.133	93.0
83	--	78	198.0	0.073	93.1
84	--	68	197.5	0.083	93.2
86	--	50	196.0	0.085	92.2
82	--	20	201	0.025	94.4
Average	--	58	197.8	0.076	93.2

[a]Data obtained at end of FY 1980.

[b]Measured at a 5-h (40-A) discharge rate.

During the past year, the Gould effort has been reoriented toward the development of cells having MgO powder, rather than BN felt, separators. The principal motivation for this change is the potentially lower cost of the MgO separators in the near term. Although an insufficient number of cells of this type have been tested to provide meaningful cycle-life data, the preliminary results appear promising.

3. Cell Failure Mechanisms

Post-test examinations of cells fabricated by ANL and the contractors have continued to provide valuable information on cell failure mechanisms, in-cell corrosion reactions, and electrode morphology (i.e., microstructure, active-material distribution and utilization, reaction uniformity, impurities, and cross-contamination of electrodes). The results from these examinations are evaluated and used as a basis for recommendations on improvements in cell design. A total of 93 cells--46 multiplate cells and 47 bicells--were examined during the past year.

Post-test data on the multiplate cells are listed in Table II-5. The two major causes of short circuits were extrusion of active material from the positive electrode and localized Li-Al protrusions through the separator. Both of these problems appear to have been solved by changes in the cell and electrode designs. Short circuits in the electrical feedthroughs were caused by metallic bridges that formed across the upper insulator as a result of electrolyte leakage through the BN powder seal and subsequent corrosion at the top of the feedthrough. The metallic aluminum deposits across the separators were caused by an excess application of $LiAlCl_4$ wetting agent in localized areas of the separator. Corrective measures for these two failure mechanisms are under investigation.

Post-test examinations of the 47 bicells showed that the causes of failure were generally similar to those identified for the multiplate cells.

Table II-5. Failure Mechanisms for Multiplate Cells

Cause of Failure	Number of Cells
Extrusion of active material from positive electrode	19
Localized Li-Al protrusions through separator	10
Unidentified short circuits	5
Short circuit in electrical feedthrough	4
Metallic deposits in separator	4
Other	4
Total	46

Nine of the ANL status bicells were included in this group. Of these status cells, four failed because of extrusion of active material from the electrodes, two because of Li-Al protrusions in the separators, and two because of iron deposits in the separator; the cause of the short circuit could not be identified in one cell.

As in previous years, the major reason for cell failure was short circuits caused by the extrusion of active material from one electrode as the other electrode expanded. Two earlier major causes of cell failure, copper deposits in the separator and cutting of the separator by the electrode structures, have been eliminated.

4. Battery Module Tests

The battery development work performed by the contractors provides design information on the following: (1) type and selection of materials, (2) choice of electrical components, (3) provisions for cell restraint to prevent swelling, (4) methods of coping with possible electrolyte leakage from cells, (5) methods for electrical insulation of cells and cell stacks, (6) design of flexible, low-resistance intercell connectors, bus bars, and leads, (7) provisions for thermal management, and (8) effects of cell equalization. These aspects of battery development are investigated by assembling and operating small modules consisting of several cells.

During 1980, a module consisting of nine Mark IA cells was assembled and tested at Eagle-Picher; the cells were encased in a Min-K* insulated housing that was available from earlier tests. Based upon the failure analysis of the Mark IA battery, several new design features were incorporated into this unit, including a redesigned cell tray, flexible rather than rigid intercell connectors, and a different type of electrical insulation (Raybestos plus Vitrabond mica) between the cells. The module was operated through 72 deep cycles (4-h discharge and 8-h charge); the relatively short cycle life of this module is consistent with earlier cycle-life data for other Mark IA cells. The results of this test showed that the design changes instituted by Eagle-Picher as a result of the Mark IA failure analysis were effective. In the next year, Eagle-Picher will complete fabrication of a 10-cell Mark II module, which is scheduled for testing at ANL in February 1981.

A three-cell (500 W-h) module was assembled by Gould to examine the feasibility of its module casing. The cells were of a Mark II multiplate design with BN felt separators and were encased in a cylindrical insulated housing with a vacuum jacket. This module was successfully operated through 134 deep cycles. Gould has now assembled a 10-cell (1.5 kW-h) module, which was placed on test near the end of the year to obtain additional information on battery hardware and thermal management.

Further testing of contractor-fabricated small modules will be continued in 1981. The information obtained from these tests will be incorporated into a Failure Modes and Effects Analysis, which will be used to identify the potential sources and consequences of failure in a Mark II-type battery.

---

*A product of the Johns-Manville Co.

F. Battery and Auxiliary Components Development

1. Thermal Management

An analysis of the heat generated in Li-Al/FeS cells during constant current cycling has been completed. The instantaneous and average heating rates determined for a Mark IA cell during a 70-A discharge and a 40-A charge are given in Fig. II-4. From this figure, it was concluded that the heat generation rate (1) is substantially higher during discharge than during charge and (2) increases substantially near the end of discharge and the end of charge. The instantaneous heat generation for a Mark IA cell discharged at currents of 30 to 100 A is given in Fig. II-5. In this discharge current range, the average heat generation rate was found to be 5 to 30 W. Based upon these results, the following simple correlation between average heat-generation rate ($\dot{Q}$) and discharge current (I) was derived:

$$\dot{Q} = 0.33\ I - 5$$

where Q is in watts and I is in amperes.

The procedure for calculating heat generation during discharge of a cell was used to estimate the internal temperature during a 70-A (4-h) discharge of a five-cell (6-V) module. As shown in Fig. II-6, the estimated and measured temperatures were in reasonable agreement.

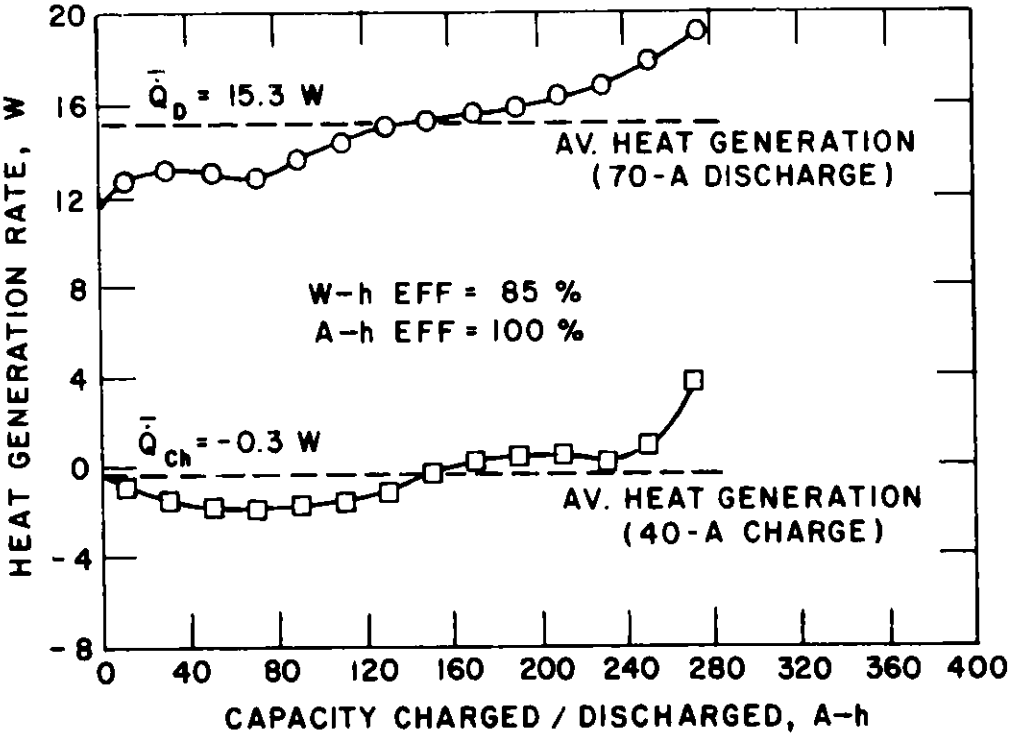

Fig. II-4. Heat-Generation Rate as a Function of the State of Charge and Discharge

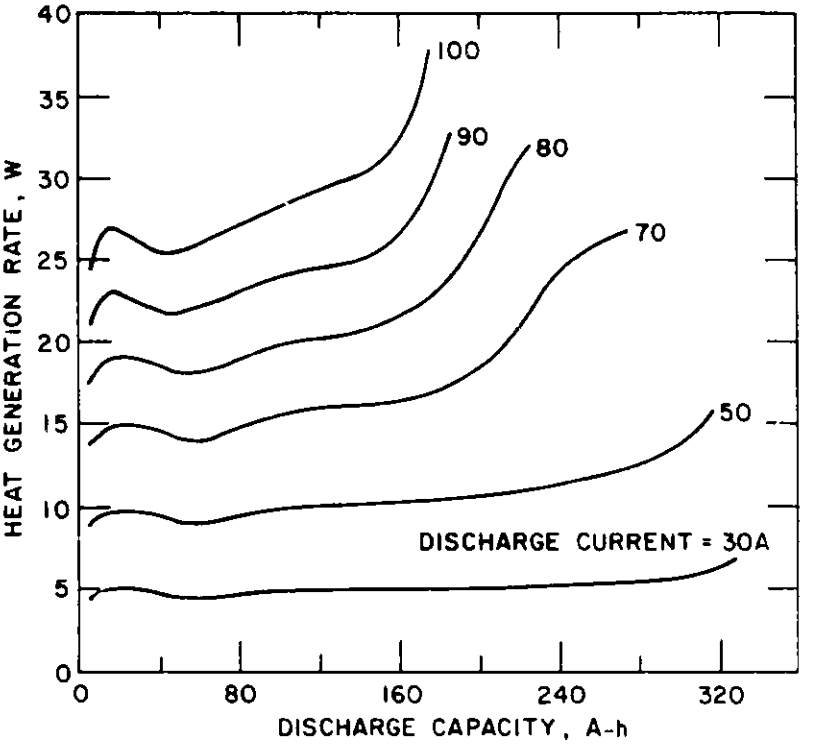

Fig. II-5. Heat-Generation Rate for a Cell Discharged at Currents of 30-100 A

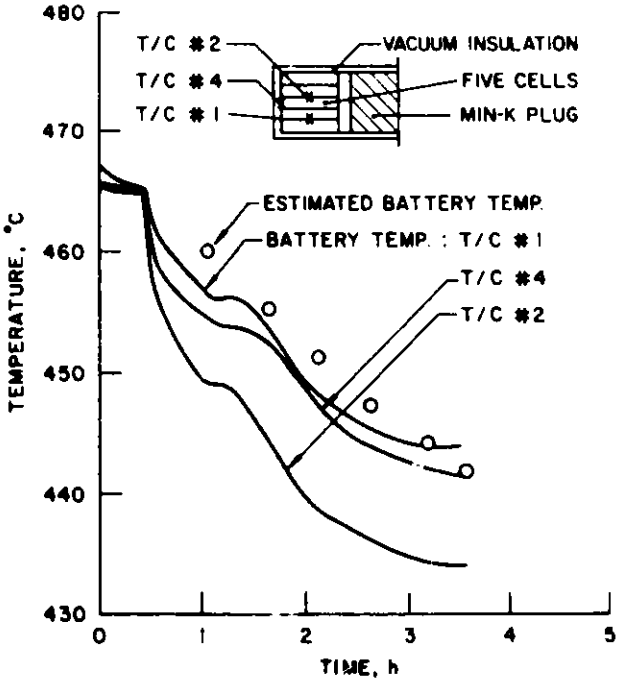

Fig. II-6. Estimated and Measured Temperatures of 6-Volt Module (T/C = thermocouple)

2. Charger Development

An important factor in the successful application of lithium/iron sulfide batteries in vehicle propulsion is proper charging. The charging system must charge all of the cells in the battery system to full capacity, yet prevent detrimental overcharging of the more efficient cells. A charging scheme has been developed at ANL which employs (1) a current-controlled main charger for replacement of the bulk charge to the battery and (2) current bypass circuits for shunting charge current around individual cells to achieve charge equalization. In late 1978, a proof-of-concept charging system for batteries of up to six cells was built and used successfully to demonstrate operating principles and capabilities of the concept. A full-size charging system has since been designed, and a prototype unit built for applications with batteries of up to 16 cells. Six units, each capable of charging a 16-cell battery, are being fabricated. Both the Li/FeS system and near-term batteries (lead-acid, Ni/Zn, and Ni/Fe) will be tested using the charger.

G. Commercialization Studies

The objective of the commercialization studies is to identify potential markets for lithium/iron sulfide batteries as a function of cost and timing.

An ANL study, completed in 1977, identified market sectors that could support pilot-plant production of Li-Al/FeS batteries. A recent study examined these markets in more detail, plus several additional ones, to assess support for a first-generation production plant. For a Li-Al/FeS battery priced at $95/kW-h (1979 dollars), the size of the various market sectors, in units of kW-h/yr, was estimated to be as follows: (1) forklift trucks: 265,000-1,450,000; (2) delivery vans: 150,000-1,000,000; (3) transit buses: 0-600,000; (4) mining vehicles: 90,000-240,000; (5) postal vans: 65,000-155,000; (6) school buses: 0-150,000; (7) submersibles: 7,500.

The key element in the analysis was economic viability, which was judged by consideration of many factors, including ease of market capture, existence of subsidies, and timing (or year) of production. An important consideration in all markets except that for submersibles was the existence of time-of-use power rates and the availability of low-cost, off-peak power. An interesting finding from this study was the importance of matching vehicle range to vehicle usage. For a passenger electric automobile, a range greater than 90-100 miles is probably uneconomic as there are insufficient operating savings to pay for the increased battery cost. The conclusion from this study was that commercialization of the Li-Al/FeS battery at $95/kW-h is feasible at pilot-plant and first-generation production-plant levels.

Efforts were continued in establishing working relationships with potential users of the Li-Al/FeS battery in both the institutional and private sectors. A joint effort (with Eagle-Picher) is under way to develop a 30-kW-h fork-lift battery for the U.S. Army. An initiative to establish a development contract with the Department of Transportation for a bus battery is planned and will be based upon the favorable economic analysis derived in the market

assessment described above. Technical exchanges which have been held with Chrysler and General Motors in the past will be continued. Preliminary discussions have been held with personnel from the Ford Motor Co.

H. Calcium/Metal Sulfide Battery

The objective of this program is to develop an inexpensive, high-performance calcium battery for electric vehicles or stationary applications. The ultimate goals for the calcium cells are a specific energy of 160 W-h/kg, a peak specific power of 200 W/kg, a lifetime of 1000 cycles, and a materials cost (in 1979 dollars) of $15/kW-h.

During the past year, effort was concentrated on finding a calcium alloy for the negative electrode that is compatible with BN-felt separator material. The components that have been identified for high-performance cells of reasonably long life are as follows: negative electrodes of $CaAl_{1.2}Si_{0.4}$, positive electrodes of $Fe_{0.93}Co_{0.07}S_2$, BN felt separators, iron (negative) and molybdenum (positive) current collectors, and $LiCl-NaCl-CaCl_2-BaCl_2$ electrolyte. A 154 A-h bicell consisting of these components was operated for 102 cycles (3500 h). The peak specific energy of the cell was 47 W-h/kg at the 5-h discharge rate, and the peak specific power (15-s pulse) was 50 W/kg. These low values are not believed to be representative of the ultimate capability of the system, since the theoretical specific energy of the $CaAl_{1.2}Si_{0.4}/FeS_2$ cell is 610 W-h/kg. The goal for next year is to demonstrate a specific energy of at least 100 W-h/kg at the 5-h rate.

III. OFFICE FOR ELECTROCHEMICAL PROJECT MANAGEMENT (OEPM)

A. Introduction

The OEPM is the DOE field project office responsible for the following activities: (a) management of DOE's programs on research, development, and demonstration of near-term batteries for electric vehicles; (b) operation of the National Battery Test Laboratory (NBTL); (c) research studies in support of electric-vehicle battery development; (d) program planning and research related to electrochemical technology for energy conservation and resource savings in industrial electrolytic processes; and (e) the research, development, and demonstration of advanced lead-acid batteries for load-leveling applications on electric utilities. These five activities are discussed below.

B. Near-Term Battery Contracts

The OEPM effort in the management of industrial contracts for the research, development, and demonstration of near-term batteries for electric vehicles is part of an overall DOE program to implement the Electric and Hybrid Vehicle Research, Development and Demonstration Act of 1976. Studies performed in 1977 identified three near-term battery systems--lead-acid, nickel/iron, and nickel/zinc--that could be developed to meet the performance and cost requirements of electric vehicles and that also offered promise of commercialization by the mid-1980's. The OEPM is now managing eight R&D contracts on a cost-sharing basis with the following firms. Eltra Corp., Exide Management and Technology Co., and Globe Battery Division of Johnson Controls (lead-acid); Westinghouse Electric Corp. and Eagle-Picher Industries, Inc. (nickel/iron); Energy Research Corp., Exide Management and Technology Co., and Gould Inc. (nickel/zinc). These contracts, which were initiated in 1978, are for periods of three to four years. Progress on the contracted work is monitored by technical design reviews, program reviews, and monthly reports, as well as by tests on cells, modules, and full-size batteries at NBTL and the contractors' test facilities. In the research and development efforts, each contractor is encouraged to adopt technical approaches that best utilize its available resources and expertise. Cost sharing by the contractors creates an incentive for the development of approaches leading to early commercialization.

The status of the three near-term battery systems prior to initiation of the above contracts is shown in the first column of data in Table III-1. The next two columns present the performance and lifetime achievements and objectives for cells and modules fabricated by the contractors and tested at the NBTL during 1980. The last column shows the goals set for full-sized electric-vehicle batteries in 1986.

A brief description of the contractors' approaches and accomplishments during 1980 is given below.

1. Lead-Acid Batteries

The industrial contractors for lead-acid batteries (Eltra, Exide, and Globe) are developing improved state-of-the-art (ISOA) batteries as well as batteries of an advanced design. During 1980, the principal emphasis

Table III-1. Performance Objectives and Accomplishments for the Near-Term Battery Project[a]

	Pre-Contract Status (1977)	CY 1980 Accomplishments	FY 1980 Objectives	1986 Projections
Lead-Acid				
Specific Energy,[b] W-h/kg	30	41	42	50
Specific Power,[c] W/kg	70	111	105	110
Cycle Life[d]	250	279	400	800
Nickel/Iron				
Specific Energy,[b] W-h/kg	44	48	54	60
Specific Power,[c] W/kg	100	103	110	120
Cycle Life[d]	1400	>477[e]	300	1200
Nickel/Zinc				
Specific Energy,[b] W-h/kg	55	68	64	70
Specific Power,[c] W/kg	90	131	110	120
Cycle Life[d]	100	179	200	800

[a] Pre-contract status is based on tests of single cells, whereas accomplishments are based on verified results demonstrated at NBTL for multi-cell modules. The 1986 projections are for full-sized EV batteries.

[b] Measured at the 3-h discharge rate.

[c] Peak power (30-s average) measured at 50% state of charge.

[d] Cycling at >80% depth of discharge until 75% of original capacity reached.

[e] Tests are continuing.

was on the construction of ISOA cells and modules for cycle-life testing at NBTL.

In its battery development program, Eltra is developing ISOA lead-acid batteries with electrodes fabricated from expanded metal (lead-calcium) mesh instead of the conventional cast grid. These expanded metal grids are especially lightweight and are expected to reduce battery self-discharge and grid corrosion. Exide's approach to the ISOA battery is based upon modifications of its commercially available EV-106 golf-cart battery. To optimize key design parameters, Exide has carried out factorial experiments in which the effects of four positive-plate compositions, two types of separator material, two electrolyte concentrations, and two cell designs were investigated. In addition, Exide is investigating the use of tubular positive plates. Globe's approach to the ISOA battery emphasizes the development of an optimized cell design (plate size, plate-aspect ratios, number of plates, and acid concentration) and an innovative electrolyte circulation system.

As shown in Table III-1, the cells and modules fabricated by the three contractors essentially achieved the FY 1980 objectives for specific energy and power. However, these performance levels have not been consistently achieved with all modules and cells tested; fabrication of reliable multi-cell modules by the contractors is a major objective for 1981. The FY 1980 objective for cycle life (400 cycles) was not achieved in the tests at NBTL, although modules tested at the contractors' facilities have demonstrated lifetimes well in excess of 400 cycles.

2. Nickel/Iron Batteries

In the Ni/Fe battery, the nickel electrode limits performance and accounts for a large portion of the cost. In its development program, Westinghouse is investigating methods for producing low-cost nickel electrodes that are capable of sustaining the long-life characteristics inherent in the Ni/Fe system. The approach being taken by Westinghouse is to use sintered steel wool as the current collector for both the positive and negative electrodes. For the positive electrode, the steel wool is plated with nickel to avoid undesirable irreversible side reactions within the cell, and then this substrate is impregnated with nickel hydroxide by either an electrochemical or pasting process. Westinghouse has also developed an electrolyte-maintenance and gas-management system that improves electrical performance and minimizes safety problems associated with hydrogen gas evolution during charging.

Eagle-Picher Industries, Inc. (EPI) has concentrated its efforts on the development of a high-performance Ni/Fe battery. To this end, EPI has developed a thick (two or three times normal) sintered nickel plaque for the positive electrode; and the Swedish National Development Co. has developed, under a subcontract with EPI, a sintered iron plaque for the negative electrode. Swedish National also has identified a ribbed, sintered PVC separator that is suitable for Ni/Fe batteries.

As shown in Table III-1, the Ni/Fe cells and modules fabricated by these two contractors have achieved the FY 1980 objective for cycle life; however, demonstrated specific energy and power were 89% and 94%, respectively, of the objectives. Hence, further work is required in improving the performance of the Ni/Fe system.

3. Nickel/Zinc Batteries

The Ni/Zn cells and modules fabricated by the three contractors (ERC, Exide, and Gould) were also evaluated at NBTL during FY 1980. In the tests at NBTL, the FY 1980 performance and lifetime objectives shown in Table III-1 were essentially achieved by the modules of one of the contractors (Gould). Furthermore, selected cells and modules have achieved these objectives in tests at the other contractors' facilities. The cycle life of the Ni/Zn system still remains a problem because the zinc electrode undergoes dendrite formation, shape change, densification, and passivation during cycling.

In its near-term battery program, ERC is emphasizing the development of a Ni/Zn battery with low initial cost. To reduce the cost of the expensive sintered nickel electrode, ERC is developing a low-cost, plastic-bonded nickel

electrode containing graphite as a conductive diluent. Exide is investigating a unique cell design based upon vibrating zinc electrodes; when the zinc electrode is vibrated during charge, the lifetime-limiting problems of zinc dendritic formation and electrode shape change are avoided. Gould is pursuing the development of a high-performance Ni/Zn battery based upon the use of a sintered nickel electrode, a membrane-type separator, and additives to the positive electrode.

The eight near-term battery contracts will extend through FY 1981. The effort during FY 1980 emphasized the construction of improved multi-cell modules for verification testing at NBTL, particularly verification of cycle life. The effort in FY 1981 will focus on evaluation of prototype electric-vehicle battery modules at NBTL.

C. National Battery Test Laboratory

The National Battery Test Laboratory was established to provide a facility for the independent testing and evaluation of various batteries as they are developed. This facility is an integral part of the DOE battery research and development program. Cells and batteries developed within DOE-sponsored programs and those developed by private funds are tested at the NBTL. Applications for these batteries include electric-vehicle propulsion, electric-utility load leveling, and solar and wind energy storage. The laboratory, when fully constructed, will be capable of the simultaneous testing of about 40 cells or modules of 0.3-4.0 kW-h capacity and up to eight batteries of 30-40 kW-h capacity under simulated driving conditions as well as under standard test conditions. The laboratory operates unattended under computer control 24 hours a day, seven days a week. Displays and graphs of present and past battery performance are conveniently and quickly available through the computer.

1. Facility Operation

During 1980, the testing capability of the NBTL was expanded from 18 to 32 test stations, 29 of which are for cells or modules and three are for full-sized batteries. In addition, several test stations were modified to allow cell operation under simulated driving power profiles (SAE J227a/D) as well as the simplified profile developed at CEN (see last year's report). Three walk-in environmental chambers for testing batteries at temperatures above and below the normal operation temperature were procured and installed in a newly constructed annex to the NBTL. Figure III-1 is a photograph of the environmental chambers in the newly constructed NBTL Annex.

As of the end of FY 1980, a total of 226 industrial-fabricated cells have been tested at NBTL (see Table III-2). Table III-1 shows the performance (specific energy and power) and lifetime achieved by the multi-cell modules cycled at constant-current discharge. At NBTL, a number of modules were cycled using the SAE urban driving schedule, with and without regenerative braking. The projected range (i.e., distance that would be traversed by

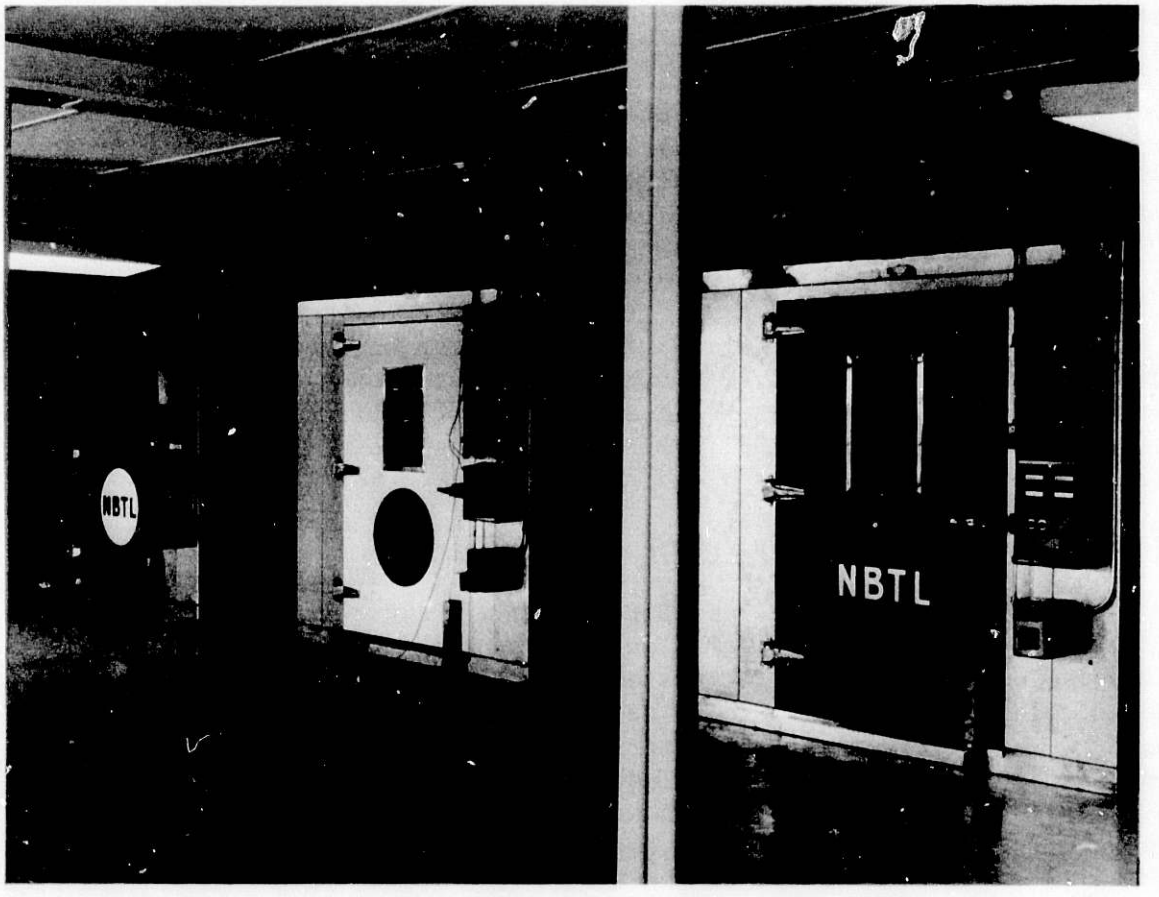

Fig. III-1. Photograph of Walk-in Environmental Chambers (selectable temperature and humidity)

the ETV-1 electric automobile during a single battery discharge) for these modules is given in Fig. III-2. This figure illustrates the greater range available from the developmental near-term batteries in comparison with the state-of-the-art lead-acid battery.

Studies on the effects of regenerative braking have been conducted using simulated driving schedules applied to lead-acid, nickel/iron, and nickel/zinc batteries in the NBTL. Important observations from these studies can be summarized as follows:

1. Significant increases (20-30%) in the range are possible with regenerative braking in urban driving situations (see Fig. III-2).

2. Charge acceptance by batteries to the large pulse of current occurring during regenerative braking is particularly good (about 100%).

3. The use of regenerative braking creates little or no additional thermal burden on the batteries; in fact, in some cases, cooling is slightly enhanced by entropic effects associated with the pulse of current produced by the regenerative braking.

Table III-2. Description of Cells Tested at NBTL from June 1978 to October 1980

Developer	System	Number of Cells	Capacity, A-h
Eltra, C&D Batteries Inc.	Advanced Lead-Acid	6	171
Exide	Advanced Lead-Acid	8	180
Eltra, C&D	Lead-Acid	21	141
Exide	Lead-Acid	27	175
Globe/GE	Lead-Acid	6	174
Globe	Lead-Acid	23	250
Eagle-Picher	Ni/Fe	15	270
NIFE	Ni/Fe	5	245
Westinghouse	Ni/Fe	28	220
Eagle-Picher	Ni/Zn	20	225
ERC	Ni/Zn	42	250
Gould	Ni/Zn	39	400/225
Yardney Electric Co.	Ni/Zn	26	220

2. Post-Test Analysis

Seventeen contractor-fabricated modules have been subjected to post-test analysis. The analysis mainly consisted of visual examination of battery components; analytical techniques and facilities are under development. The three near-term systems under test at NBTL exhibited a variety of failure modes, some of which are discussed below.

In the lead-acid system, post-test inspections have identified the positive electrode as the usual limiting component. Failure occurs by active-material shedding, active-material degradation, and collector-grid corrosion. Figure III-3 shows radiographs of a Pb-Ca expanded-metal grid and a Pb-Sb cast grid from different lead-acid batteries. On the Pb-Ca expanded metal grid, corrosion is typically exhibited on the lines between the nodes of the matrix. In contrast, for the Pb-Sb cast grid, the corrosion is typically located at the nodes or intersections of the grid. This difference may be a manifestation of the way in which the grids are stressed during fabrication. Metallographic

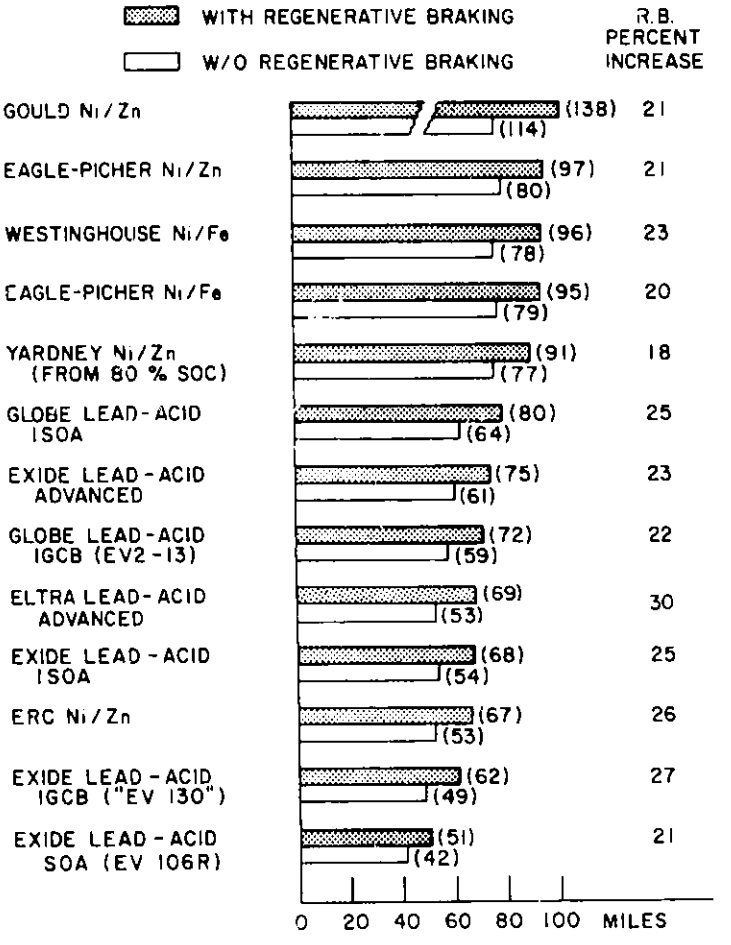

Fig. III-2. Range Projected (miles) for One Complete Discharge of Battery* Powering an Electric Automobile (ETV-1) over the SAE J227a/D Urban Driving Schedule (with and without regenerative braking)

encapsulating and cross-sectioning techniques will be used to correlate corrosion with grid stress levels and active material composition.

Post-test inspections of Ni/Zn modules have shown the major problems to be shape change, dendrite growth, and mossy zinc deposits on the negative electrode. Thickness measurements of a zinc electrode showed variations in thickness of 0.203 to 0.305 cm and indicated that collector potential gradients may be partially responsible for the shape change. Nickel/iron modules examined have exhibited simple hardware failures. One finding of particular interest was cracks in the current collector assemblies, which also were observed in some Ni/Zn modules. Metallographic examination indicated that a common mechanism may be responsible for corrosion in both battery systems.

*In this figure, IGCB refers to an improved golf-cart battery.

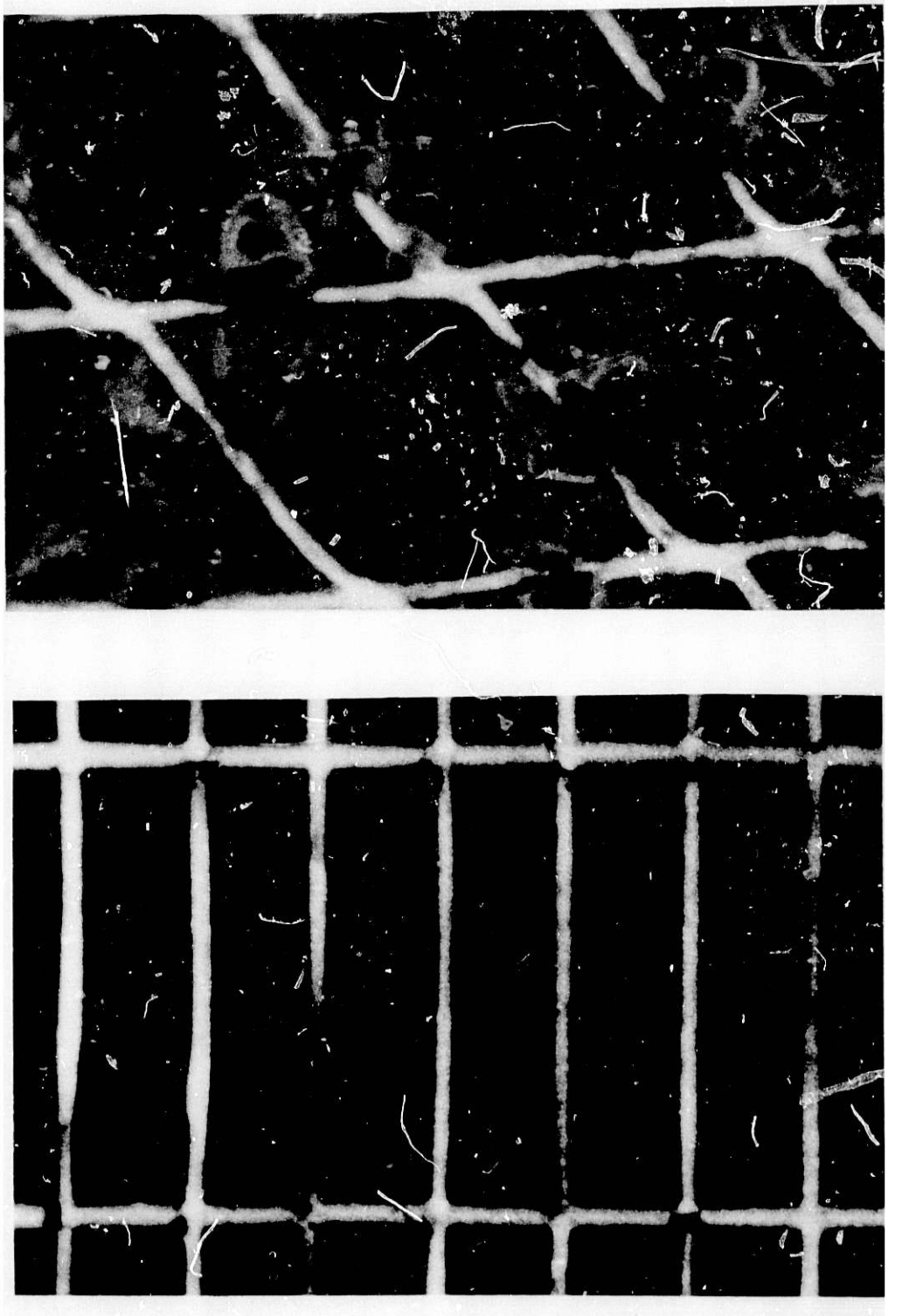

Fig. III-3. Radiographs of a Pb-Ca Expanded-Metal Grid (top) and a Pb-Sb Cast Grid (bottom) Showing Different Locations of Corrosion

Timely reporting of failure results and contractor participation in the post-test analysis enabled the contractors to incorporate appropriate design changes into their next generation of modules. Component analysis and characterization by several analytical methods are being used to build a data base for comparison and correlation of future failures.

D. Battery Support Research

One function of the OEPM is to perform basic and applied research in support of the battery programs. Research is undertaken in areas of significant interest to OEPM contractors and in areas identified by OEPM as essential to the progress of the program. This work presently includes experimental and mathematical modeling of battery systems; electrochemical studies to characterize battery electrode behavior; chemical and physical analysis of battery components and materials; component and accessory evaluation; and studies of battery/vehicle integration.

1. Experimental and Mathematical Modeling

Several studies are being directed toward the development of models of electrodes and cells that will provide a basis for evaluating the effects of design variables upon cell performance.

One such study is an investigation of passive cooling of Ni/Zn cells to control the internal temperature. This effort is being carried out as a subcontract with the University of Illinois and is directed initially toward obtaining thermal data for the positive (Ni, NiO_x) electrode. These data will be used in a mathematical model to define the characteristics of passive cooling.

A second study involved the development of a mathematical model for the mass-transfer and current-density distributions occurring over the surface of the vibrating zinc electrode of Exide. The zinc electrode in this cell has been reported to have an outstanding quality of zinc deposit. It is anticipated that the model will characterize the desirable conditions that occur in the electrode as well as indicate nonuniformities that could cause problems (e.g., shorting) in the future. At the present time, equations for the potential-flow and steady-streaming velocities have been obtained by using conformal mapping techniques.

In a third study, an equivalent electrical circuit model for predicting the voltage-time profile (V-t) of cells was formulated. Using this model, a computer is able to predict V-t profiles for cells undergoing constant-current discharge as well as discharge according to simulated urban driving schedules (with and without regenerative braking). Figure III-4 (top) presents an example of a V-t profile predicted for a cell undergoing a simulated driving schedule (single discharge). For comparison, the V-t profile obtained for a six-cell lead-acid module tested at NBTL under a simulated driving schedule is given in Fig. III-4 (bottom). Not only is the general shape of the two profiles similar, but the individual segments (each segment represents a single driving cycle) are also simila. However, the number of

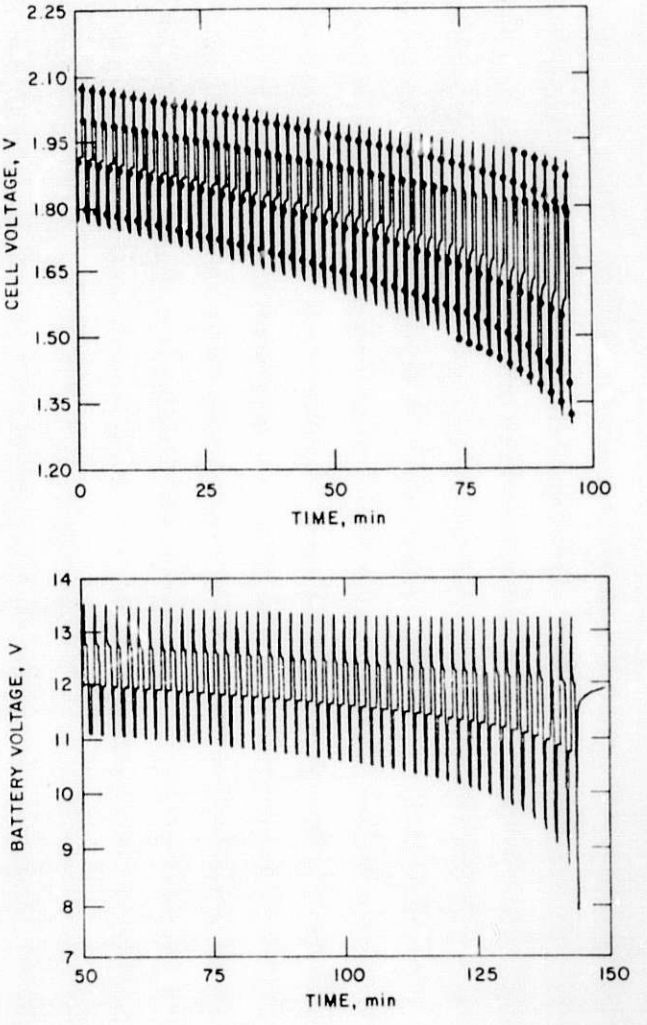

Fig. III-4. Voltage vs. Time Profiles Obtained from Computer Simulation (top) and NBTL Test Data (bottom)

driving cycles completed is not quite the same for the two cases. Future plans involve further refinement of the model to obtain a more pecise simulation of experimental data. In addition, an attempt will be made to relate model parameters with actual battery characteristics.

Another modeling activity, completed during the past year, consisted of the development of a satisfactory mathematical description of the time-dependent current distributions within a porous zinc electrode. Figure III-5 shows experimental data for the current distribution obtained during discharge of a simulated porous zinc electrode (KOH electrolyte saturated with ZnO) divided into five segments. In this figure, the first segment is the one closest to the bulk electrolyte. Predictions derived from our mathematical model showed good agreement with these experimental data when the conductivity of the electrolyte in the electrode pores was assumed to decrease by about

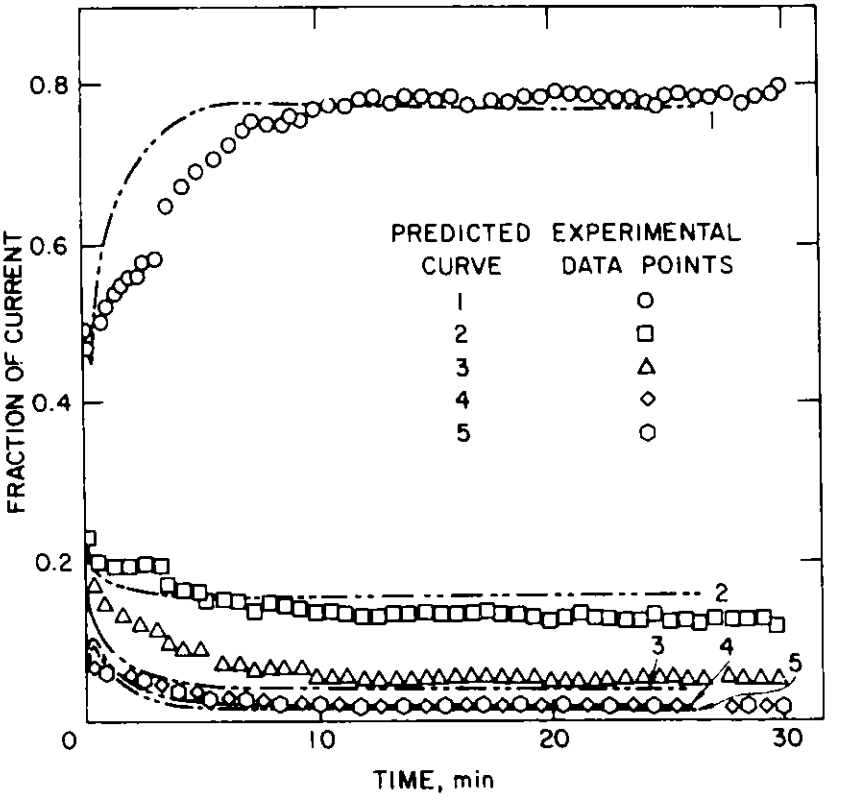

Fig. III-5. Experimental and Predicted Current Distribution with Time for Simulated Porous Electrode

80% of its initial value during discharge. The extent of this reduction in conductivity implies a supersaturation of zincate of four times chemical saturation, which has been observed experimentally. Further calculations indicated that this conductivity reduction contributes to a decrease in the reaction penetration depth for the electrode because of an increased potential gradient.

2. Electrochemical Studies

The above results suggest that the conductance of zincate-supersaturated KOH electrolyte has a strong influence on the zinc electrode performance; therefore, an experimental study was undertaken to extend the range of conductivity measurements from the subsaturated range (<0.7M zincate) reported in the literature into the supersaturated range. In our Ni/Zn experimental cells, additives that would stabilize the supersaturated solution were not used; consequently, precipitation of ZnO occurred and limited the practical range of conductivity measurements to <1.5M zincate. The results of this study, shown in Fig. III-6, indicated that the previously reported linear

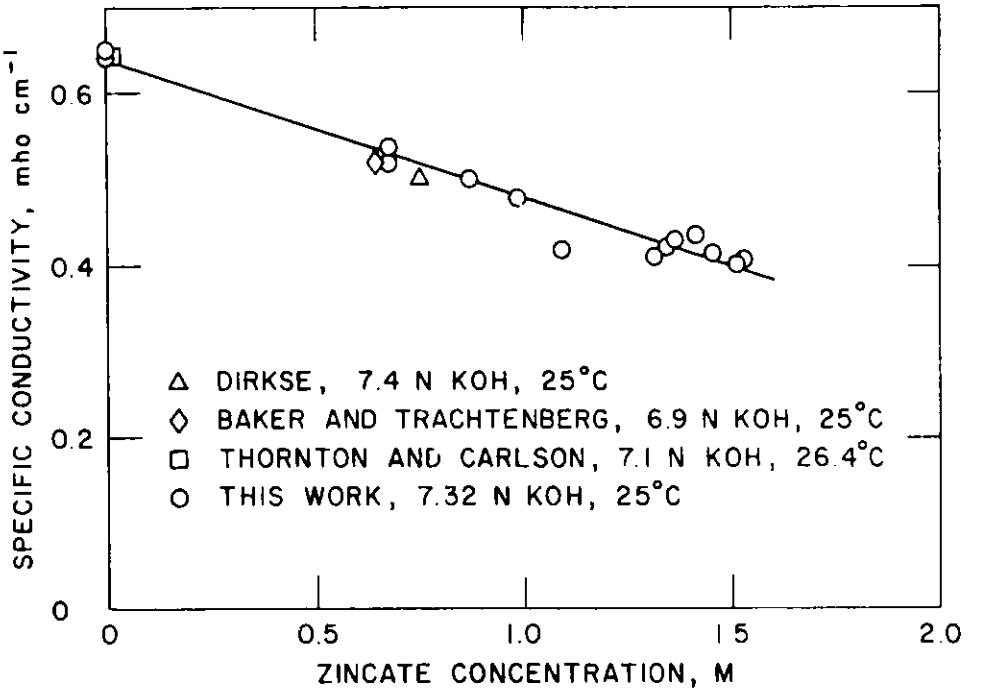

Fig. III-6. Specific Conductivity of KOH Battery Electrolyte as Function of Zincate Concentration

decrease in conductance with increasing zincate concentration[1-3] is valid over the extended concentration range. Therefore, the use of a simple mixture rule to predict conductivities is possible, at least for engineering calculations. (Examination of literature data for KOH-KF[3] and KOH-K_2CO_3[4] systems indicates that a simple mixture rule holds equally as well for these two systems as for the KOH-$K_2Zn(OH)_4$ system).

Galvanostatic polarization studies of the anodic discharge process in the zinc electrode were also carried out in 1980. For these studies, small zinc electrodes were discharged in KOH electrolyte of various concentrations (0.78 to 7.24M) and the passivation time recorded. Based upon both these and literature data, a scheme was proposed to describe the processes occurring in a zinc electrode (in alkaline electrolyte) that eventually becomes passivated. This scheme, shown in Fig. III-7, entails an increasing zincate concentration during the initial stages of discharge (t_a), followed by a time period during which ZnO precipitates as the anodic dissolution process proceeds (t_b). Finally, an anodic oxidation process occurs that produces ZnO directly on the metal surface (t_c). It is this oxide film which results in passivation of the electrode.

---

[1] T. P. Dirske, J. Electrochem. Soc. 106, 154 (1959).

[2] C. T. Baker and I. Trachtenberg, J. Electrochem. Soc. 114, 1045 (1967).

[3] R. F. Thorton and E. J. Carlson, J. Electrochem. Soc. 12 , 1448 (1980).

[4] M. Nitabah, D. Lucesdi, and P. Degobert, Electrochem. Acta 17, 327 (1972).

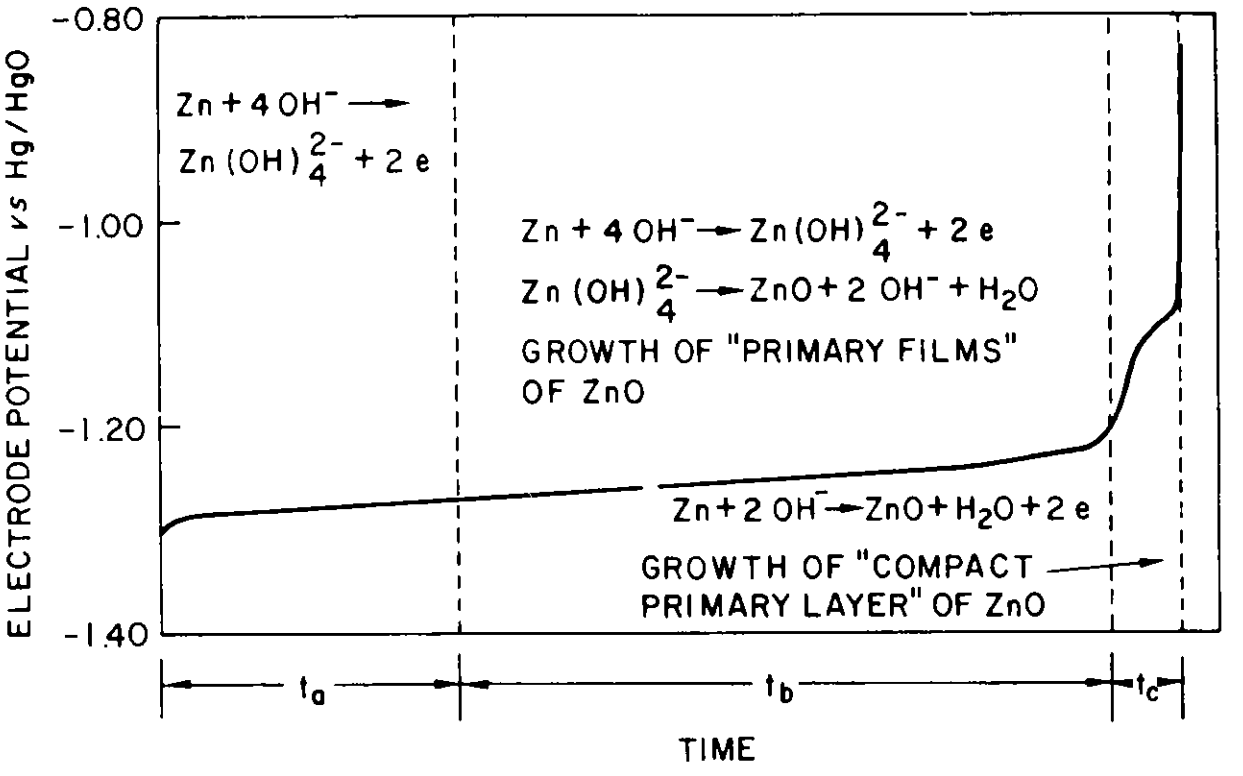

Fig. III-7. Changes in Electrode Reaction Occurring in a Zinc Anode Undergoing Galvanostatic Polarization

Future electrochemical studies of the zinc electrode will include investigations of organic additives and pulse charging to reduce dendrite formation.

Another electrochemical study, recently completed, involved the identification of the variables affecting the available capacity of (Ni, NiO_x) electrodes. The available capacity of (Ni, NiO_x) electrodes at any time after charge was found to depend upon the charge acceptance and a time-dependent capacity loss (self-discharge), the rate of which decreased logarithmically with time. It also was noted that, during charging, the presence of iron in the electrode led to a 50% increase in the rate of O_2 generation at a given electrode potential. These results correlate well with the observed (at the NBTL) performance of near-term alkaline batteries.

In last year's report, preliminary in situ laser Raman spectroscopic studies of lead positive electrodes were described. During the past year, further efforts were extended to examine the use of tetrabasic lead sulfate (TBLS) as the primary component in the fabrication of these electrodes. Figure III-8 illustrates the progressive changes occurring in the complex Raman spectrum during the anodic oxidation of TBLS. Comparison of these spectra with those of well-characterized reference compounds suggested that, in addition to the electrochemical oxidation process, other chemical changes also are occurring in this electrode. A significant amount of $PbSO_4$ forms, as

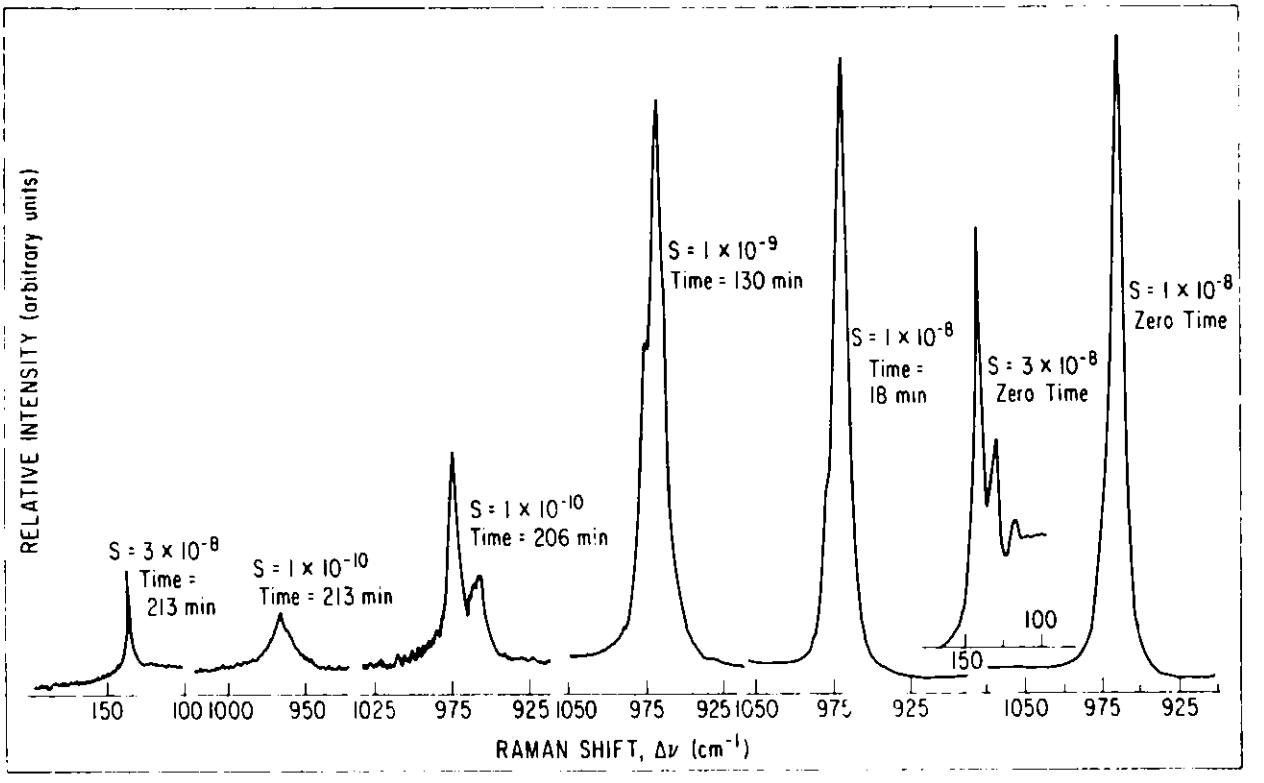

Fig. III-8. In Situ Raman Spectra Obtained for TBLS Electrode Anodized in 0.1N H_2SO_4 at +1.5 V vs. Hg/Hg_2SO_4 and 15 mA/cm^2 ($\overline{Kr}^+$ ion laser; λ = 6470.89 Å)

well as minor amounts of $3PbO \cdot PbSO_4 \cdot H_2O$ and $PbO \cdot PbSO_4$. It also has been possible to tentatively rank the electrochemical oxidation rates of the substances as follows: TBLS > $PbO \cdot PbSO_4$ > $PbSO_4$. Upon discharge of the fully oxidized lead electrode, $PbSO_4$ was observed as the sole product. It appears that the value of using TBLS in the fabrication of these electrodes lies only in the changes occurring in the first formation charge.

3. Chemical and Physical Analysis

In spite of the fact that the near-term battery systems have been in existence for many years, analytic characterization of the active materials is not complete. As a result, the proposed electrochemical reaction schemes are tenuously supported by very limited data. In an effort to develop a better understanding of the electrochemical reaction mechanisms, studies are being carried out on lead and nickel positive electrodes.

In cooperation with the Solid State Science Division of ANL, neutron scattering studies have been done on β-PbO_2 active material formed in small, commercial lead-acid batteries. By using normal and deuterated electrolyte in these batteries, it was determined that hydrogen (or deuterium) is incorporated into the β-PbO_2 lattice. Furthermore, a preliminary analysis of the data indicated that the lattice is lead deficient. Further work using neutron diffraction is in progress. Also, battery active materials, namely, β-PbO_2

and nickel hydroxides, are being analyzed by thermogravimetric and infrared analysis for hydrogen and deuterium incorporation.

In a study of the nickel positive electrode, α- and β-$Ni(OH)_2$ were identified with in situ laser Raman scattering. Examination of the oxidized state, NiOOH, with ex situ laser Raman has resulted in a tentative identification of the γ and β phases. In future work, studies will be undertaken on the effects of impurities upon the phase structure of nickel active material.

4. Component Evaluation

An effort to evaluate separators for Ni/Zn cells was initiated at the end of 1979. The objective of this task is to screen selected separator materials for appropriate physical and electrochemical properties prior to subjecting them to cycle-life testing in full-scale cells. The accomplishment of this objective requires the development of a reliable test apparatus as well as test procedures for obtaining the needed data. In the past year, this effort has been focused on electrical-resistance measurements, transport-properties determination, and zinc-penetration studies of candidate separators. One of the important findings was an apparent decrease in the rate of OH^- transport across cellophane (Du Pont 193 PUDO) with increasing temperature. The reverse had been anticipated based upon the observed behavior of other separator materials. This behavior could adversely affect the high-temperature performance of the electrodes. Testing of candidate separator materials will continue.

5. Battery/Vehicle Integration

The objective of this effort is to assess and characterize battery/vehicle integration so as to ensure (1) compatibility of battery R&D goals with vehicle requirements and (2) availability of application data to electric-vehicle developers.

During FY 1980, OEPM conducted an analysis of available battery and vehicle performance data. Preliminary findings indicated that, for the ETV-1 vehicle, a 488-kg battery would require an energy density (at a 3-h constant-current discharge) of 40-49, 51-62, and 59-75 W-h/kg for a range (J227a/D driving schedule) of 75, 100, and 125 miles, respectively. The energy-density range is a function of the amount of regenerative braking assumed and the battery type. Additional data must be obtained on peak-power requirements and on vehicle costs before the analyses can be completed.

During FY 1980, OEPM also conducted a series of tests to analyze air samples taken during battery charging and during operation of electric vehicles. Tests were made on two electric vehicles at Long Island Lighting Co. and on a vehicle at ANL. The principal concern was to determine the concentrations of the gases stibine (SbH_3) and arsine (AsH_3) in the workplace since these gases are evolved from lead-acid batteries during charging. In 1976, the National Institute for Occupational Safety and Health (NIOSH) set limits on occupational exposure to these gases. Gas samples were taken in the battery compartment, in the vehicle, and in the garage space. The principal findings were: (1) measured concentrations of stibine and arsine in the

vehicle and in the garage never exceeded 20% of the limits set by NIOSH; (2) ventilation of the battery compartment, at air flow rates used to provide adequate dilution of the hydrogen evolved, is sufficient to dilute the stibine and arsine produced during charging of the battery to concentrations less than the NIOSH limits; and (3) not all the stibine, arsine, and hydrogen produced in the battery is released during the charging operation, since delayed release of these gases was observed during operation of the electric vehicle. The third finding indicates the need (1) to ventilate the battery compartment while the vehicle is operated and (2) to isolate the battery compartment from the vehicle interior by proper design.

E. Electrochemical Technology for Energy and Resource Savings

The goal of this program is to reduce the specific energy consumed in electrolytic processes used to produce materials by 30% by the year 2000. Assuming a 5% growth rate in energy consumption, it was estimated that 200 MBOE/yr (millions of barrels of oil equivalent per year) could be saved by the year 2000. The near-term savings in the existing electrolytic processes are expected to be accomplished largely by process improvements. The larger energy savings projected for the year 2000 will require the development of alternative, in some cases nonelectrolytic, processes or major modification of present technology. In 1980, the contractual effort included (1) a survey of alternative processes for the electrochemical production of inorganic compounds and (2) an engineering and economic evaluation of the diaphragm- and membrane-type chlorine cells. The in-house effort involved research at ANL on promising new electrolytic technology.

1. Review of Industrial Technology

In a survey study, Castle Technology Corp. assessed alternative processes for the electrochemical production of inorganic chemicals. Many alternative processes and process modifications were identified that offer significant energy savings over conventional technology. The principal recommendations of this survey are (1) significant energy savings in chlorate production can result from the development of suitable electrocatalysts for lowering the cathodic overpotential, (2) hydrogen peroxide could be made electrolytically by a new process in which anodic oxidation of sulfate is coupled with cathodic reduction of oxygen in alkaline solution, and (3) ozone can be produced efficiently via an electrolytic process using an oxygen-enhanced anodic reaction requiring two instead of six Faradays per mole of ozone.

A survey, conducted in FY 1979 by Versar Inc., identified the new membrane-type cell for the production of chlorine as a promising technology. As a result of this finding, in FY 1980, ABAM Engineering Inc. conducted an engineering and economic evaluation of the membrane cells and membrane cells with advanced cathodes (oxygen-depolarized and hydrogen-catalyzed cathodes), which were compared to the conventional diaphragm cell. The principal conclusions of this study are (1) diaphragm-cell technology is somewhat economically superior to the best membrane-cell plants and will probably maintain its economic position in the short- to mid-term; (2) although not economically

competitive, membrane cells with oxygen cathodes have a potential for saving energy, especially for applications where generated hydrogen can be used for its chemical value; and (3) the opportunity for the most rapid reduction in energy consumption by the chlor-alkali industry lies in tax law changes that would encourage the installation of additional cells in existing plants.

2. ANL Research

For the in-house effort, OEPM is studying the production of aluminum via the electrolysis of aluminum sulfide instead of the conventional electrolysis of aluminum oxide. This effort is focused on verifying the underlying chemical assumptions of the proposed aluminum sulfide concept as a low-energy alternative for the production of aluminum. In this regard, studies were undertaken to demonstrate (1) the feasibility of synthesizing Al_2S_3 and (2) the feasibility of electrolyzing Al_2S_3 with good current efficiency.

Experiments conducted to sulfidize coked alumina using sulfur under equilibrium conditions failed to result in any measurable amounts of Al_2S_3 at temperatures up to 1100°C. Subsequently, preliminary experiments were conducted to sulfidize aluminum sulfate in a fluidized-bed reactor (temperatures of 450-750°C), using carbon disulfide as a reducing and sulfidizing agent. There was an indication that aluminum sulfate converted to Al_2S_3, the conversion efficiency being a function of the $Al_2(SO_4)_3$ particle size. A maximum conversion efficiency of 55% was obtained at a temperature of 700°C and a particle size of -300 mesh. It is believed that the limiting factor to complete conversion is the formation of an inhibiting coating of Al_2S_3 on the $Al_2(SO_4)_3$ particles, which limits the diffusion of gases to and from the reaction front. Further experiments are being carried out to verify the formation of Al_2S_3 and to increase the conversion efficiency.

Three types of experiments were conducted to study the electrolysis of Al_2S_3: solubility measurements, electrochemical characterization of the cathodic and anodic reactions, and electrolysis measurements.

The solubility of aluminum sulfides in chloride melts was studied as a mean of selecting an appropriate melt for the electrolysis of Al_2S_3. The solubility of Al_2S_3 in $MgCl_2$-NaCl-KCl eutectic at 750°C was found to be 3 wt %, which is considered adequate for practical electrolysis cells (e.g., the $AlCl_3$ concentration in Alcoa cells is 2 to 5 wt %). The molar ratio of Al/S in these melts was found to be 1:1 instead of 1:1.5. Extensive thermodynamic calculations indicated that Al_2S_3 is dissolved in the melt via the formation of an aluminum-sulfur-chloride complex $(AlSCl)_x$, where the molar ratio of Al/S is 1.

The electrochemical mechanism for Al_2S_3 electrolysis in the $MgCl_2$-NaCl-KCl eutectic at 750°C was studied in detail. A typical cyclic voltammogram for the electrolysis of Al_2S_3 is shown in Fig. III-9. Both the anodic and cathodic reactions show one peak for the reduction of aluminum ions and another peak for the oxidation of sulfide ions. Analysis of the data

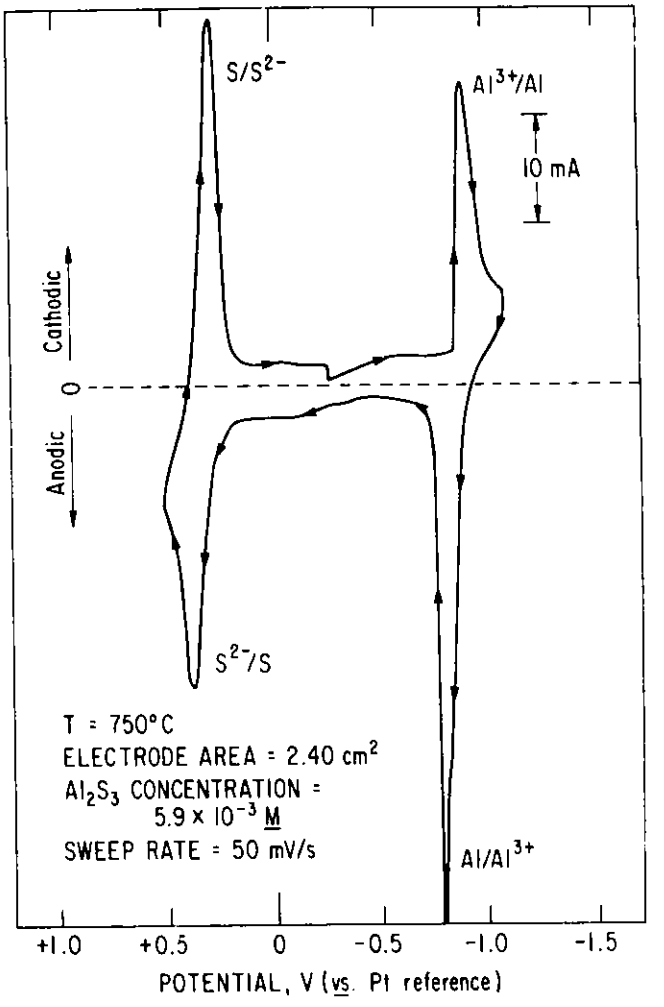

Fig. III-9. Typical Voltammogram of Al_2S_3 in Molten $MgCl_2$-NaCl-KCl Eutectic

obtained from the cyclic voltammetry indicated that the reduction of aluminum ions proceeds via a reversible three-electron transfer step forming aluminum metal and that the oxidation of sulfide proceeds via a two-step process--(1) a reversible two-electron charge transfer forming atomic sulfur followed by (2) a fast chemical reaction in which the atomic sulfur dimerizes to form S_2. Thus, it seems that the electrolysis of Al_2S_3 in this melt proceeds to aluminum and sulfur with little complication.

Electrolysis experiments were conducted with three different Al_2S_3 concentrations (1, 2, and 3 wt % Al_2S_3) at 750°C and various current densities. The current-voltage curves for the anodic and cathodic reactions are shown in Fig. III-10. It can be seen that both the aluminum cathode and sulfur anode show very little polarization with increasing current density at all Al_2S_3 concentrations. The cell voltage for the electrolysis of Al_2S_3 at 200 mA/cm^2 was about 1.4 to 1.6 V. (The cell voltage is typically 3.3 V for $AlCl_3$ electrolysis and 4.5 V for conventional Hall-Heroult cells). In further studies, the current efficiency for Al_2S_3 electrolysis in $MgCl_2$-NaCl-KCl melts was found to increase with increasing current density. As shown in Fig. III-11,

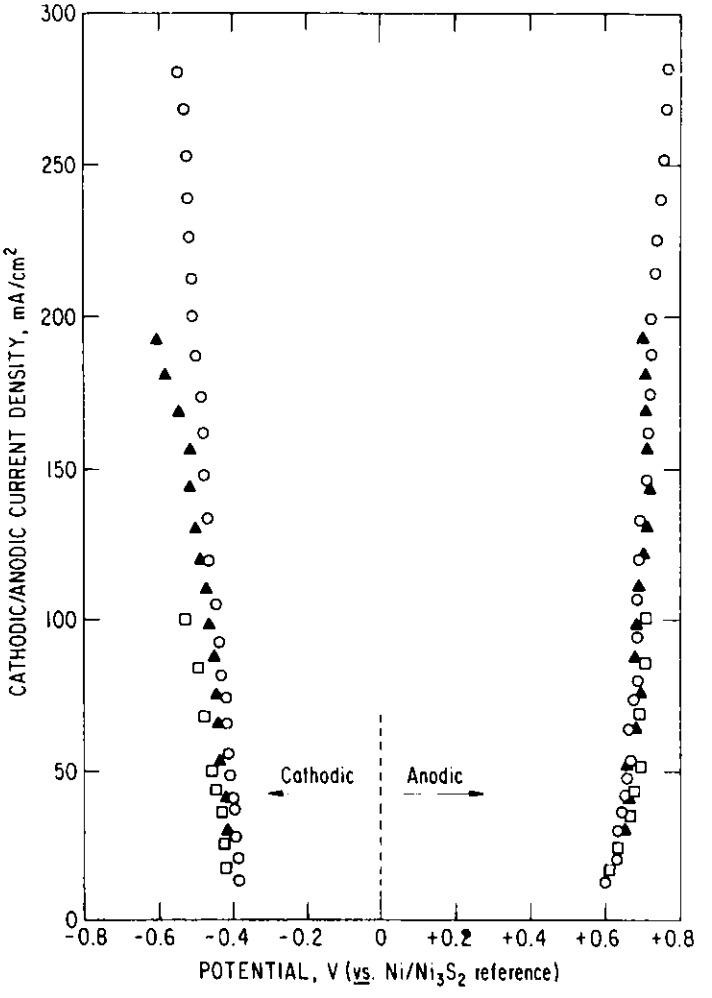

Fig. III-10. Current vs. Voltage Curves for the Electrolysis of Al_2S_3 in $MgCl_2$-NaCl-KCl Eutectic at 750°C (squares, 1 wt % Al_2S_3; triangles, 2 wt % Al_2S_3; circles, 3 wt % Al_2S_3)

a current efficiency of 82% was obtained at a current density of 200 mA/cm^2; this indicates that the electrolysis of Al_2S_3 with good current efficiency is technically feasible. In future efforts, the electrolysis of Al_2S_3 at high current density (>200 mA/cm^2) will be investigated; this electrolysis is expected to be achieved through the use of higher concentrations of Al_2S_3 (>3 wt %) and by the enhancement of mass transfer during electrolysis.

In other activities, OEPM is investigating ways to make the membrane-cell technology more attractive to industry. One way under investigation is the direct production of 50 wt % NaOH, instead of the conventional 29 wt % NaOH, in membrane cells. To this end, an effort was initiated to investigate the kinetics of hydrogen evolution in concentrated caustic soda and to determine the effect of increasing the caustic concentration on the membrane-cell

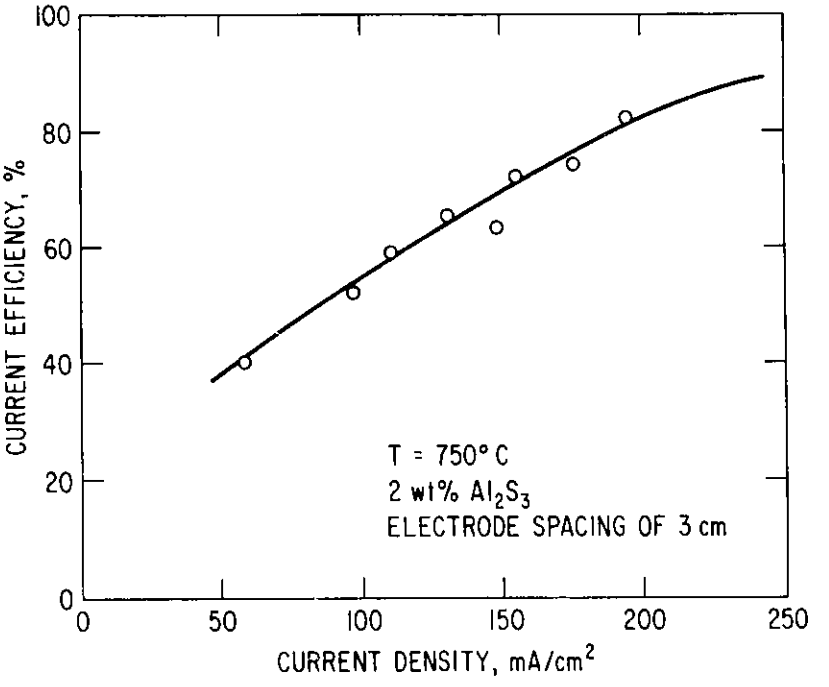

Fig. III-11. Current Efficiency for Electrolysis of Al_2S_3 in $MgCl_2$-NaCl-KCl Eutectic at 750°C

voltage. The results indicated that the membrane, not the electrode polarization or electrolyte conductivity, appears to be the critical element in terms of energy savings and technical feasibility in the direct manufacture of 50 wt % NaOH in membrane cells.

In the area of metal winning, the alkaline electrowinning of zinc was evaluated for energy savings. In this evaluation, a comparison was made between the energy requirement for a typical sulfate plant and that for an equivalent alkaline plant. A 10% energy reduction was estimated for the alkaline process. A technical method, however, needs to be developed for high current-density operation in which zinc powder is produced without increasing cell voltage.

F. Load-Leveling Battery for Electric Utilities

This project involves research, development and demonstration of advanced lead-acid batteries for electric-utility load leveling. In 1979, a cost/design study was made of state-of-the-art (SOA) lead-acid batteries by ESB, Gould, Eltra, and Westinghouse. This study showed that the projected cost ($42-58/kW-h), cycle life (<2000 cycles), and area energy density (43-54 kW-h/m^2) of SOA batteries results in a marginally acceptable system for electric-utility load-leveling applications. The objective of this project is to advance the lead-acid technology to produce a battery that is acceptable to the utility industry; the goals for this battery are a cycle life of ≥3000 cycles, initial costs of $37-50/kW-h, and an area energy density of >75 kW-h/m^2.

In FY 1980, contracts were awarded to C&D Batteries Inc. and Exide Management and Technology Co. The contracts call for a three-phase effort: the first phase will emphasize research and development of advanced lead-acid cells/modules; the second phase will emphasize the demonstration of pilot-line production of advanced modules; and the third phase will be the construction of a 5000 kW-h advanced lead-acid battery to be tested at the Battery Energy Storage Test Facility (BEST). Verification and qualification testing of advanced cells/modules will be conducted at NBTL. The technology and economic feasibility of an advanced lead-acid battery will be demonstrated within 6-7 years.

Exide initiated a program involving the research, development, and testing of advanced cells and modules aimed at increasing cell cycle life from 2000 to 4000 cycles and reducing costs from $100-120/kW-h (present-day value) to $50/kW-h. In this program, Exide is investigating the effects of changing battery design parameters such as plate thickness, active material density, acid volume and density, separator material, and grid alloy. To evaluate the proposed changes as quickly as possible, three types of accelerated lifetime tests are used: overcharge cycling, shallow cycling (i.e., 48 shallow cycles per day), and deep cycling. For the latter test, cells are deep cycled (80% depth of discharge) for two cycles per day; each cycle consists of a 4-h discharge to 80% of the rated 5-h capacity and a 7- to 8-h charge that returns 125% of the previous discharge output. A summary of the equivalent normal load-leveling cycles accumulated by the cells tested at Exide is given in Table III-3.

Table III-3. Test Results of Exide Load-Leveling Cells

No. Cells Tested	Capacity, A-h	Test Designation	Equivalent Normal Cycles Accumulated[a]
36	400	Overcharge	2200
60	200	Shallow	350
60	1800	Deep	900

[a]Testing is continuing.

To improve the cycle life of lead-acid batteries with Pb-Sb grids, C&D is investigating a number of promising concepts, e.g., high paste density, phosphoric acid, additives, and tetrabasic lead sulfate as the positive active material. In addition, C&D is developing a battery with a Pb-Ca metal grid, which holds promise of reduced maintenance costs and less adverse environmental impact. In tests of seventy-five 360 A-h cells, C&D is determining the effects of several battery design parameters, including grid thickness, grid-alloy additives, electrolyte specific gravity, and active-material composition and density. To date, these cells have completed 200 cycles and are still being operated.

Under another contract, VARTA Batterie designed, fabricated, and tested a prototype 435-W H_2/O_2 recombination device (HORD) for lead-acid batteries. In addition to reducing maintenance and providing a safe operation of the battery, this device removes arsine and stibine from the battery off-gases. Three devices are being fabricated by VARTA for tests by the load-leveling battery subcontractors.

In addition to the contractual effort, OEPM is providing support research to characterize the compositional changes of the positive active material as a function of cycle life. Furthermore, testing of 15 kW-h SOA lead-acid modules is being conducted at NBTL to provide baseline data by which the progress of the contrator's advanced modules will be measured.

IV. ADVANCED FUEL CELL DEVELOPMENT

A. Overview

The fuel cell is one of the most promising technologies being developed by DOE to reduce the nation's reliance on petroleum fuels for electrical generation. The CEN Division has two responsibilities within the DOE program to develop fuel-cell power plants. These are (1) to conduct technical management of DOE's program on advanced fuel cell development and (2) to provide supporting research and development to the molten carbonate fuel cell program. The R&D is focused on alternative stack concepts and yields fundamental understanding of fuel cell behavior and fuels-processor performance.

Molten carbonate fuel cells consist of a porous nickel alloy anode, a porous nickel oxide cathode, an electrolyte structure separating the anode and cathode, and appropriate metal separator sheets. The separator sheets isolate reactant gases in adjacent cells, electrically join these cells, and bear upon the electrolyte structure to form a "wet" seal that separates the cell interior from the surroundings. The electrolyte structure, commonly called "tile," is a composite of solid $LiAlO_2$ particles and a mixture of lithium and potassium carbonates that is liquid at the cell operating temperature of about 925 K. At the anode, hydrogen and carbon monoxide in the fuel gas react with carbonate ion from the electrolyte to form carbon dioxide and water, giving up electrons to the external circuit. At the cathode, carbon dioxide and oxygen react and accept electrons from the external circuit to form carbonate ion, which is conducted through the electrolyte to the anode. In practical cell stacks, CO_2 for the cathode will probably be obtained from the anode exhaust.

In a power plant, several hundred cells with parallel gas flows will be assembled in a series electrical connection to form a stack. Depending on plant size, from about ten to more than a thousand stacks will use synthesis gas (H_2 and CO) from a fuel processor to generate electrical output. For large plants, the fuel processor will be a coal gasifier/cleanup subsystem. Heat from the cells and coal gasifier will be used in a bottoming cycle to increase electric output. Alternatively, the heat may be used for industrial processes with cogeneration plants. The advantages of these power plants are (1) use of coal, (2) very low pollutant emissions, and (3) high efficiency (about 50%, coal to bus bar, in a baseload plant).

Smaller dispersed plants are expected to use liquid or gaseous fuels and to have efficiencies near 60%. An objective for these plants is the use of coal-derived liquids or unconventional gases such as from geopressured aquifers and coal mines or from processing of wastes.

Nearly all the technical management activities conducted by the ANL Advanced Fuel Cell Program Office are related to the DOE Molten Carbonate Fuel Cell Program. The major thrust of this program is centered in two parallel contracts, one with General Electric Company (GE) and the other with United Technologies Corporation (UTC). The objectives of these contracts

are (1) to bring the technology to a state of readiness for fabrication and development of full-size (1/2 to 1 MW) stacks of cells and (2) to provide the information DOE needs to decide prudently whether or not to commit itself to stack development, which will require at least a twofold increase in expenditures, mostly from DOE.

The primary output of the contracts will be as follows: (1) demonstration of short (20 to 100 cells) stacks of full-size (area of 1 to 1-1/2 m^2 and thickness of 5 mm) cells; (2) preparation of detailed construction drawings for full-size stacks, a test plan for their initial tests, and layouts of test facilities; (3) operation of smaller single cells of the same type as the full-size ones under plant conditions (pressure, temperature, utilization of fuel and oxidant, thermal-cycle frequency, etc.) and for 10,000 h with economically acceptable performance decay; (4) preparation of a detailed reference design for a coal-fueled fuel-cell plant in which economic and physical parameters of the plant, as well as operating conditions and characteristics of the plant subsystems, are defined and necessary work not directly involving fuel cells is identified; and (5) experimental verification of allowable contaminant levels in the feed gases of the fuel cell stack, including operation of cells on gases from a coal gasifier.

In addition to the major contractors, Energy Research Corp. (ERC) is developing alternative cell technology, mainly with funding from Electric Power Research Institute (EPRI). DOE-funded work at ERC complements this EPRI-funded work. To carry out this task, ERC has formed a team with Westinghouse Electric Corp., and together they represent a third possible vendor. There is considerable incentive for GE and UTC each to focus primarily on one stack design; ERC/Westinghouse and ANL will provide alternative basic stack concepts. Because of limited funding in FY 1981, there is essentially no other technical work in the program.

Upon completion of the above-mentioned activities, the program will be directed mainly toward development of full-scale stacks. This work, of course, will be accompanied by (1) development and testing of components with single cells and small stacks and (2) materials testing. Tests of cell/stack longevity will be an important part of this phase.

At present, DOE plans call for construction of a pilot plant which will be used to test systems integration; this will be followed by demonstration of a commercial-size coal-fueled plant. Planning for these plants is under review in order to provide for a manageable rate of technology introduction. The incentive for initial commercial use of small plants, most likely gas-fueled, is great; and potential users of such plants are being consulted. Involvement of potential users and cost sharing by vendors are expected to increase rapidly after the present phase ends (scheduled for 1983) so that DOE involvement can be decreased.

Thus far, progress under present contracts has been satisfactory. Both contractors have essentially defined their stack concepts and cell sizes, developed economical means of fabricating the critical electrolyte structure,

and identified the major developments required for the anode, cathode, and separator sheets. United Technologies has tested small stacks of cells and has a considerable lead in this area. GE has done an outstanding job of plant- and stack-design analysis and has begun refinement and cost analysis of four design concepts. Work on contaminant levels in feed gases has been nearly stopped for budgetary reasons.

The FY 1981 budget is about half of that required to maintain the planned program schedule for the major contracts. It does not appear that the 1982 budget will allow recovery of this lost time, but it may reestablish the planned technology-development rate. There is almost no hope of reestablishing an adequate supporting research and development program. In the FY 1981 budget, eighty percent of the funding goes into the major contracts. The remaining funds are distributed as follows: ERC/Westinghouse, 3%; ANL, 12% (half for R&D and the other half for program management); and program definition and supporting research, 4%.

Research on solid oxide fuel cells is conducted at Westinghouse, with funding separate from DOE's molten carbonate fuel cell program. Westinghouse has made excellent progress in solving the difficult materials and fabrication problems of fuel cells operating at 1000°C, but has had difficulty with gas manifolding and electrical connections. At ANL instigation, Westinghouse has redirected its work to address these problems and has evolved new design concepts that promise to lead to workable hardware.

During 1980, CEN continued to provide technical management for DOE's program on fuel utilization for fuel cells. The goal of this program has been the development of liquid-fuel processors suitable for integration with fuel cells to form small-scale dispersed electric power generating stations. In the overall program, advances have been made in the development of catalysts and reactor designs for autothermal steam reforming of middle-distillate fuel oils, and progress has been made in the two-year effort (initiated in FY 1979) to identify and model carbon-formation mechanisms in high-temperature reformers. It is becoming increasingly apparent that natural gas will be the preferred fuel for dispersed fuel cell power plants until at least into the middle or late 1990's. Consequently, the development effort for heavy-liquid fuel processors is being deemphasized by DOE in this time of severe budget constraints. For this reason, ANL will not be involved in the DOE fuels processing effort in FY 1981.

B. Sintered Electrolyte Structures

For the past several years, we have been synthesizing mixtures of $LiAlO_2$ particles and carbonate salt, which were then pressed into a paste-like tile for testing. Recently, we have shifted our attention, in collaboration with the Ceramics Group of the Materials Science Division (MSD) at ANL, to the development of electrolyte structures consisting of a sintered $LiAlO_2$ matrix. Sintered electrolyte structures have the following advantages: they can be easily inspected to determine their acceptability, they ought to be relatively stable thermally in operating fuel cells because the cell operating temperature is about 200° below the sintering temperature, and they have the potential of being used to form a composite electrolyte-electrode structure (discussed later).

A sintered electrolyte should have relatively high porosity (about 60%) and be as thin as practical in order to minimize resistance to carbonate ion transfer. The pore size must be small compared to that of the electrodes (5-15 μm) in order to retain the electrolyte effectively, which promotes ion transfer and prevents cross-leakage of reactant gases. Further, the pore size must be small enough to resist blowout of electrolyte under normal and expected abnormal pressure differentials across the cell. A narrow pore-size distribution with a mean of about 0.5 μm is appropriate. The first sinters were prepared by cold-pressing $LiAlO_2$ powders and firing the resultant "green body" at temperatures between 1175 and 1375 K. The powder prepared for sintering must not contain carbonate salts, which would cause the product to undergo excessive particle growth and densification during sintering; the sintered structure can be impregnated easily with the carbonate salts.

Lithium aluminate exists in three allotropic forms. Sintered $LiAlO_2$ structures contain only the γ-allotrope because the sintering temperature is above the temperature at which α- or β-phase transforms to γ-$LiAlO_2$. Differential thermal analysis has been used to determine the temperature at which α- and β-phase transform to γ-$LiAlO_2$. These transition temperatures were found to be highly sensitive to the presence of impurities (e.g., carbonate salt, Al_2O_3) in the $LiAlO_2$. Nevertheless, for the $LiAlO_2$ powder typically used for sintering, the transition temperatures were found to be about 1205 K for the α-phase and 1035 K for the β-phase. (In the presence of Li_2CO_3-K_2CO_3, α- and β-phase transformed to γ-phase at about 1010 K.)

Very little particle growth of $LiAlO_2$ powder has been found to occur during either phase transformation or sintering; therefore, any one of the three $LiAlO_2$ phases can be used as starting material for the preparation of sinters. The α- and β-phases can be easily synthesized. The process we first used for α-$LiAlO_2$ synthesis involved ball-milling Al_2O_3 and Li_2CO_3 in methanol, recovering the solids by centrifuging, drying and screening the powder, and reacting this mixture at 925 K for four days. Currently, we are investigating a much simpler approach that entails blending the Al_2O_3 and Li_2CO_3 in acetic acid solution and spray-drying the resultant slurry to obtain a fine powder mix of Al_2O_3 and $LiC_2H_3O_2$. This mixture is reacted at 925 K to form α-$LiAlO_2$. Our β-$LiAlO_2$ is produced by spray-drying a slurry of aqueous LiOH solution and $Al(OH)_3$ (or Al_2O_3). The resulting mix of LiOH and $Al(OH)_3$ is reacted at 725 to 875 K for about an hour to form β-$LiAlO_2$. The γ-phase can be produced by heat-treating either α- or β-$LiAlO_2$.

Acceptable sinters were prepared with all three allotropes, but a narrower pore-size distribution and finer pores were obtained with the α- and β-materials. Moreover, less particle growth occurred during sintering of α- or β-$LiAlO_2$, which transformed to γ-$LiAlO_2$, than occurred during the heat treatment of α- or β-$LiAlO_2$ prior to sintering of γ-$LiAlO_2$.

At present, the best sinters have been those prepared from α-$LiAlO_2$ powders, but sinters from β-$LiAlO_2$ powders also appear satisfactory for cell testing. We have measured the mechanical properties of α-$LiAlO_2$ sinters,

with and without the pores filled with Li_2CO_3-K_2CO_3, and have made numerous examinations of $LiAlO_2$ particles and sintered material with a scanning electron microscope. These examinations have highlighted the importance of avoiding the use of excess LiOH or Li_2CO_3 reagent, which was found to cause excessive sintering. We did not test any sinters in cells this year but will next year.

We concluded from a literature review that tape-casting is a better procedure than cold-pressing for preparing thin sintered plates to be tested in cells. Accordingly, we obtained the consulting services of a tape-casting expert (R. E. Mistler of Plessey, Inc.) and collected the apparatus and reagents necessary to begin tape-casting. For the tape-casting procedure, thick slurries (slips) are prepared from plasticizer, binder, deflocculating agent, solvent, and the $LiAlO_2$ particles to be sintered; this slip is distributed on a plate and dried to form a pliable sheet (tape), which subsequently is fired to produce the sintered structure. We currently are working on producing a tape of good quality.

C. Cathode Development

The cathode used in a molten carbonate fuel cell is lithiated nickel oxide, which is a semiconductor. These cathodes are normally produced by the in-cell oxidation and lithiation of a sintered porous nickel plate by reaction with the cathode gas (CO_2-air) and Li_2CO_3 in the electrolyte. This *in situ* reaction has several disadvantages. The oxidized nickel breaks up into many small oxide crystallites that are not sintered together; this breakup results in many point contacts and an associated resistance to electron flow. The reaction is accompanied by an expansion of the cathode by as much as 30 or 40%. As a result of the *in situ* oxidation, the porosity and pore-size distribution of the cathode cannot be rigidly controlled. The *in situ* lithiation results in a local perturbation of the electrolyte composition.

The laboratories working on molten carbonate fuel cells are seeking alternative cathodes. We have been working on the preparation of electrode plates of $Li_{0.05}Ni_{0.95}O$ for later assembly into fuel cells. Based on experience with cathodes prepared *in situ*, we estimated that an optimum cathode would have 60-70% porosity, with about 75% of the porosity in relatively large pores (about 15-20 μm) and 25% in relatively fine pores (about 1 μm). The large pores permit gas passage, whereas the fine pores retain electrolyte and provide sufficient reaction surface. We have succeeded in producing flat, sintered cathodic plates with this bimodal pore-size distribution.* The room-temperature resistivity of the lithiated nickel oxide plate is typically about 2 ohm·cm, depending upon sintering time and temperature. The resistivity of the structure decreases by a factor of about 100 when heated from room temperature to 925 K. Figure IV-1 shows the effect of sintering temperature (for a 1-h period) on the room-temperature resistivity, porosity, and composition of the lithiated

*The cathode fabrication development is being conducted by the Materials Science Division of ANL.

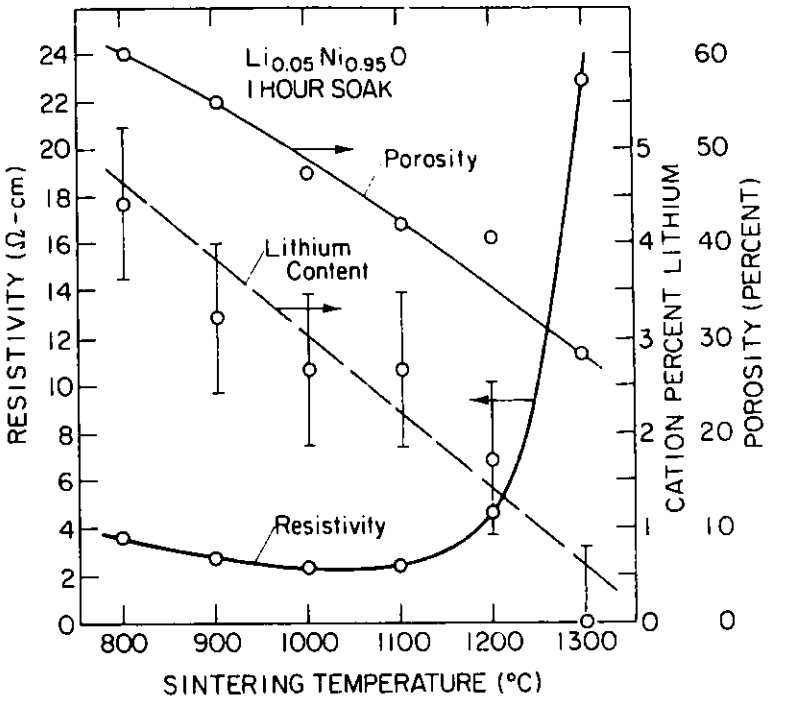

Fig. IV-1. Effect of Sintering Temperature (1-h period) on the Porosity, Room-Temperature Resistivity, and Composition of Lithiated NiO Structure

NiO cathode. The resistivity data in this figure suggest that temperatures below about 900°C (1173 K) produce slow sintering and that temperatures above 1100°C (1373 K) result in rapid lithium loss. The sintering temperature (and time) must be selected to promote particle sintering without significant loss of lithium brought about by vaporization. In the next year, sintering temperatures between 800 and 1200°C (1073 and 1473 K) will be studied further.

One sintered cathode has been tested in a cell. The electrochemical performance of this cell was not as good as that attained with our best previous cells, but sealing problems normally associated with cathode swelling were avoided completely. Post-test examination revealed that electrical contact had not been made with about one-fifth of the cathode surface; this partially explains the poor performance. The bimodal structure functioned as intended: the fine pores were flooded with electrolyte, and the large, coarse pores were open for gas movement. However, we believe that the structure must be improved. The fine pores lie within agglomerates of fine particles, the pore size being controlled by the firing time and temperature; the coarse pore structure is formed by the agglomerates. We will explore the possibility of using smaller agglomerates (to allow better utilization of the interior porosity) combined with pore-forming additives to encourage formation of branched chains of the agglomerates and, hence, long and interconnected coarse pores.

In scouting experiments, we have prepared composites in which a thin sintered cathode was bonded to the surface of a sintered $LiAlO_2$ disk. By varying the green-body properties and firing conditions, we were able to match the shrinkage during sintering for the two materials. Further investigation of this promising new technology will be continued in the forthcoming year.

D. Cell Testing

Although the major emphasis of our electrolyte development effort is on sintered supports, we are continuing to use tiles (paste structures) in cell tests to assess other components, notably cathodes. In the course of preparing tiles for these tests, several materials-handling changes seem to have resulted in a significant improvement in the quality and reliability of the tile itself.

By installing linear motion monitors on the cells used in recent tests, we have been able to better define events pertaining to component deformation. Some deformation after assembly is necessary to ensure adequate surface contact between cell components. Using these monitors, we observed an expected stiffening of the tiles a short time after the electrolyte melted on the first heatup. This stiffening was associated with the redistribution of a portion of the carbonate phase to the electrodes. As initially loaded, the carbonate in the tiles flowed under very low load to form a good edge seal, but this seal was lost when the cathode expanded on oxidation. Several hundred hours under load were required to reestablish the edge seals. Problems associated with cell swelling during in situ cathode oxidation would be compounded for cell stacks.

In a single cell test with a preoxidized and prelithiated cathode, no sealing problem was encountered. However, good contact between the tile and electrode surface was not obtained because (1) the tile, which apparently contained inadequate carbonate salt, did not flow sufficiently and (2) the thickness of the as-fabricated cathode was not uniform. For the next cathode test, a tile with a higher Li_2CO_2-K_2CO_3 content (64 wt % rather than 61 wt %) and a flatter cathode will be used.

Observations made during recent tests indicate that, when cracks are formed in the tile of a cell during a thermal cycle that involves solidification of the electrolyte, the tile will heal if it is under adequate compressive load during reheating. However, if the load is inadequate to seal the crack quickly and the cell is operated, irreversible damage will be done to the crack region; this damage is caused by local overheating as a result of gas cross-leakage and direct chemical combination of the gases. The small-diameter, high-surface-area $LiAlO_2$ particles near the crack will grow into low-surface-area bypyramidal particles, which do not retain electrolyte

A new test-cell design has been devised to increase our experimental flexibility and more closely approximate a commercially viable design. Two particularly important features of the design are that it uses sheet-metal separator plates in place of machined ribs in heavy cell housings and that it permits testing two or more cells assembled in series (a stack). The design allows parallel, countercurrent, or cross flow of the fuel and oxidant streams. The gas manifolding is accomplished through steel frames around the active cell area. Sealing will be provided by gasketing material (ZrO_2 felt) rather than a wet seal.

In the next year, we will study cell characteristics by making potential-relaxation measurements with the current-interruption technique; this effort is part of a cooperative research program with Illinois Institute of Technology. Thus far, we have developed a fast ($<1 \times 10^{-7}$ s) current-interrupt switch that results in voltage signals free from switching and power-supply noise. In the next year, reference electrodes will be incorporated into present cell hardware.

E. Fuels Processing

CEN has been providing technical support for the development of fuels processors for the use of middle- and heavy-liquid fuels of petroleum or coal origin in dispersed fuel cell power plants. The use of heavy oils in steam reformers entails two major processing problems--formation of carbon in the reforming reactors and poisoning of the reforming catalysts by sulfur compounds in the oil.

As part of an ongoing effort to identify carbon-forming mechanisms in high-severity reformers, CEN has been investigating the role of sulfur in the loss of activity of reforming catalysts at very high temperatures characteristic of autothermal or other high-temperature reformers. During the course of these investigations, a narrow range of operating conditions was identified in which catastrophic loss of reforming activity occurs, possibly initiated by the onset of carbon formation on the active sites. This phenomenon was found to be reversible at a temperature about 200°C higher than that for the catastrophic loss, giving the appearance of possible multiple steady states for the reformer. The reforming reactor used in these experiments was modified for operation at high temperatures (up to 1000°C) and pressures of 1400 kPa (200 psi), and a limited amount of data was obtained for sulfur poisoning under these severe operating conditions. Because of the termination of funding for all heavy-oil research for fuel cell application in FY 1981, this work will not be continued.

F. Future Direction

In the future, our component development effort will continue to emphasize alternative components and approaches for molten carbonate fuel cells. Our major effort will be concentrated on sintered electrolyte structures and sintered cathodes. In addition, we plan to continue exploring the sintered cathode-electrolyte laminate, and will investigate incorporation of the anode into this laminate, probably as nickel deposited on a ceramic substrate that is sintered to the electrolyte support structure. Initially, $NiAl_2O_4$ will be considered as a potential substrate for the anode.

V. UTILIZATION OF COAL

A. Overview

The major part of CEN's fossil energy research program involves studies in support of the DOE program for the development of fluidized-bed combustion (FBC) systems. Fluidized-bed coal combustion, a process in which coal is burned in a fluidized bed of limestone, is believed to be a potentially superior method for the use of coal as an energy source. This method is especially useful for the combustion of coals which have high contents of sulfur, since the SO_2 produced in the combustion process is captured by the limestone; a dry, easy-to-dispose-of waste is produced. Probably, the main incentive for the development of FBC is that its combustors are expected to be smaller than comparable pulverized-coal combustors and, hence, less costly to build. A smaller size and lower cost should be especially attainable for pressurized fluidized-bed combustors (PFBCs).

During the past year, development of FBCs has continued along the directions indicated in previous reports. Small industrial boilers (50,000- to 200,000-lb steam per hour) are now available from several different companies. One company has shipped more than eight units from its plant. This suggests that these units are competitive in cost to other coal-combustion systems. The atmospheric fluidized-bed combustor (AFBC) steam boiler at Georgetown University (Washington, DC) has been operated without major problems, and its builder now offers an entire series of AFBC steam boilers for commercial use. The first steps have been taken to procure an AFBC steam boiler for the Argonne heating plant. Although it is too early to claim that FBCs have gained complete acceptance in the marketplace for small steam boilers, a good beginning has been made. The future will depend very much on the performance of these first units in the field. Since operational costs will be very important for these units, high combustion efficiencies and high limestone utilization (in those regions where SO_2 emission control is needed) are important. In both of these areas, improvement is possible.

The development of FBCs for electricity production is proceeding along two paths--the development of AFBC power plants by the Tennessee Valley Authority (TVA) and the development of PFBC plants by DOE and the American Electric Power Company. The TVA is proceeding with the construction of a 20-MW AFBC pilot plant, which will be used to study utility operating methods such as load following, shutdown, and coal feeding. Also, TVA is continuing the design of a 200-MW AFBC power plant. The DOE has tended to concentrate on the development of PFBCs, with major emphasis on hot gas cleanup since this is perceived to be a critical problem area for the commercialization of PFBCs.

During the past year, the transfer of programmatic control of CEN's fossil energy studies from DOE headquarters to Morgantown Energy Technology Center (METC) has been completed. The team at METC has gained a better understanding of the operation of national laboratories; as a result, future interactions between ANL and METC ought to be mutually productive.

The CEN program on FBC is aimed at solving problems, filling information gaps, improving process operability and economics, and reducing environmental impacts. Problems addressed in this program include efficient limestone

utilization, gas cleanup at high temperature and pressure, emission characterization and control, and minimization of the quantity of solid wastes. To assist in the identification of R&D needs, CEN maintains close interaction with industrial developers of FBCs as well as other research organizations. A major effort has been made to review critically the problem areas in PFBC so as to assist METC in the direction of the PFBC developmental effort.

In other divisional work related to coal utilization, studies are under way on materials suitable for the removal of H_2S from coal-generated gas for molten carbonate fuel cells at their operational temperature. Technical assessments and technical management efforts are also being carried out to assist DOE headquarters personnel in coal-related technologies.

B. Limestone Utilization in Fluidized-Bed Combustion

During 1980, activities to elucidate the utilization of limestone and dolomite as sorbents for sulfur in FBC were concentrated in two areas: (1) development of a method for predicting the amount of a given sorbent required to retain effectively the sulfur dioxide produced during the combustion of coal and (2) development of a hydration process for enhancing the extent to which a sorbent can be sulfated. With regard to the latter, increased sulfation would substantially decrease the ancillary costs and the environmental impact of quarrying, transporting, and ultimately disposing of large quantities of sorbent.

1. Sorbent-Utilization Prediction Methodology

A key to the widespread commercialization of fluidized-bed combustor technology is the ability to predict accurately the sorbent feed rate required to retain the coal-derived SO_2 emission within environmental standards. The goal of the present work is to provide a simple, yet reliable, user-oriented prediction methodology. The initial elements of such a prediction methodology have been published in a sourcebook[1] on the utilization of limestone and dolomite as sorbents in atmospheric fluidized-bed combustors. The methodology consists of two models, one to predict the in-bed sulfation and the other to predict attrition performance, along with two standard laboratory tests to determine the sorbent-specific parameters used in the models. The sourcebook also contains the chemical, physical, and morphological properties, as well as the measured values of the parameters, for 29 sorbents selected to reflect (1) the geographic distribution of limestone and dolomite deposits and coal-producing regions and (2) the locations of major thermal power plants in the United States. The models are used as the basis for ranking the 29 sorbents in terms of calcium sulfation and elutriation.

---

[1] D. C. Fee, W. I. Wilson, J. A. Shearer, G. W. Smith, J. F. Lenc, L.-S. Fan, K. M. Myles, and Irving Johnson, Sorbent Utilization Prediction Methodology: Sulfur Control in Fluidized-Bed Combustors, Argonne National Laboratory Report ANL/CEN/FE-80-10 (December 1980).

a. In-Bed Sulfation Model

In the sulfation reaction of limestone sorbents ($CaO + SO_2 + 1/2\ O_2 \rightarrow CaSO_4$), the amount of sorbent required is directly proportional to the concentration of sulfur in the coal feed and inversely proportional to the concentration of calcium in the sorbent feed. The actual Ca/S molar ratio required in a fluidized bed decreases from the stoichiometric value of one as the proportion of SO_2 that must be retained in the bed is reduced below 100%, but increases to the extent that the average utilization of the calcium in the bed is less than 100%. Although the required retention is established by regulation, the average calcium utilization is dependent upon both sorbent-specific and combustor-specific parameters that are difficult to quantify. Limestones from different origins differ significantly in their reactivity with SO_2--both in terms of the initial rate of reaction and the maximum extent to which the calcium oxide can be sulfated to $CaSO_4$. Furthermore, a complex relationship exists between the pore structure developed during calcination and the calcium utilization. For a given pore volume, an optimum pore diameter exists for maximum sulfation. With larger pore diameters, the total surface area decreases; with smaller pore diameters, the pore mouths close before extensive sulfation can occur within a particle. The combustor operational parameters that affect calcium utilization are bed temperature, fluidization gas velocity, bed height, sorbent particle size, CO_2 and SO_2 partial gas pressures, and the fractional volume of the bed occupied by the sorbent.

There have been numerous previous attempts to model the limestone sulfation reaction in a fluidized-bed combustor, but no model adequately reflects the sulfation characteristics of individual limestones. To date, aside from an actual in-combustor evaluation, the sorbent-specific sulfation behavior is best obtained with a thermogravimetric analysis (TGA) of the sulfation process. Accordingly, for the ANL methodology, a standard TGA test was defined. For this standard test, the temperature, SO_2 and CO_2 partial gas pressures, and sorbent particle size are selected, and derived calcium utilizations as functions of the standard-test duration are least-squares fit to obtain an empirical exponential expression that has only two dependent constants.

The combustor-specific parameters that affect calcium sulfation have been combined in a model that reflects the formation and transport of SO_2 in a fluidized bed. A fluidized-bed combustor has three regions--the emulsion or dense phase in the bed, the bubble phase in the bed, and the freeboard above the bed phase. The SO_2 is produced in the emulsion phase by oxidation of the organic and inorganic sulfur compounds in the coal and moves upward at a velocity that slightly exceeds the minimum fluidization velocity, U_{mf}, of the particulate bed materials (i.e., coal, limestone, and ash). The gas in the emulsion phase exchanges with the gas in the bubble phase to an extent dependent on bubble size and the rate at which gas enters the bubble phase, which is $(U - U_{mf})$, where U is the superficial velocity of the gas entering the bed. Thus, after SO_2 forms, it can (1) react with the limestone sorbent, (2) leave the bed via the gas flowing through the emulsion phase, or (3) transfer to the bubble phase and subsequently also leave the bed. The extent of limestone sulfation depends on the average residence time of the

sorbent in the bed which, in turn, is a function of the limestone feed rate. An increase in the feed rate results in a shorter average age of the limestone particles and a smaller extent of sulfation but a greater rate of sulfation. The SO_2 concentration in the off-gas depends on the balance between the rates of limestone sulfation and SO_2 escape from the emulsion phase.

The ANL in-bed sulfation model accounts for the various factors affecting calcium utilization in the following way:

$$\left(\frac{Ca}{S}\right) = \left(\frac{D}{R} - \frac{U\gamma}{Hb(1 - R)(1 - \beta)}\right)^{-1} \qquad (1)$$

where

R = weight fraction of sulfur retained in bed

D = maximum sorbent fractional utilization parameter (determined from TGA)

b = sulfur-capture rate parameter of sorbents (determined from TGA)

H = combustor bed height

$(1 - \beta)$ = fractional volume of bed occupied by sorbent

γ = the ratio of the SO_2 concentration in the emulsion phase to the SO_2 concentration in the bubble phase

For a fluidizing-gas velocity of 2 to 2.5 m/s and an average bed particle diameter of 1000 to 1200 μm, $(1 - \beta)$ is approximately 0.25. Generally, γ is slightly less than unity; when there is uniform gas mixing between the two phases, the ratio equals one. For the gas velocity and particle diameter given above, γ is approximately 0.25 to 0.30. In this model, it is assumed that (1) the fluidized bed consists of an emulsion phase and a bubble phase; (2) the gases and solids in the emulsion phase are uniformly mixed; (3) all of the SO_2 is formed in the emulsion phase; (4) part of the SO_2 can transfer into the bubble phase; (5) the bubble phase moves in plug flow; (6) the dominant mechanism of SO_2 capture in calcined limestone is diffusion within the pores, and SO_2 capture is first order with respect to SO_2 concentration; (7) the standard TGA test accurately simulates the sulfation that occurs in a fluidized bed; and (8) the bulk of SO_2 capture occurs within the fluidized bed even though a significant amount is believed to occur in the splash zone of the freeboard.

Confidence in the predictive capability of the model is established by comparing the model predictions with actual combustor experience. To provide a basis for the comparison, an extensive review of the literature on sorbent performance in AFBCs has been undertaken. Data on experimental variables, sorbent properties, coal properties, and the physical arrangement and operating conditions of combustors have been accumulated into a retrievable data base. Selected combustor-performance data have been extracted from the data base and compared with predicted sorbent performance. Because of problems associated with channeling and slugging found in smaller combustors,

the comparisons are made for large-scale combustors (>45-cm dia), although several smaller combustors are included in the literature review. For each combustor and sorbent selected, the combustor data and the model predictions are given for the same set of operating conditions; an example is shown in Fig. V-1.

In general, the model underpredicts the sulfur retention for a given Ca/S molar ratio in the feed. Possible explanations of this discrepancy are as follows: (1) freeboard sulfation not taken into consideration--sulfur capture in the freeboard region has been reported to be as high as 25% of the total; (2) fines recycle not taken into consideration--fines recycle is known to enhance sulfur capture; and (3) inadequacy of the standard TGA test--the maximum calcium utilization achieved in the combustor is higher

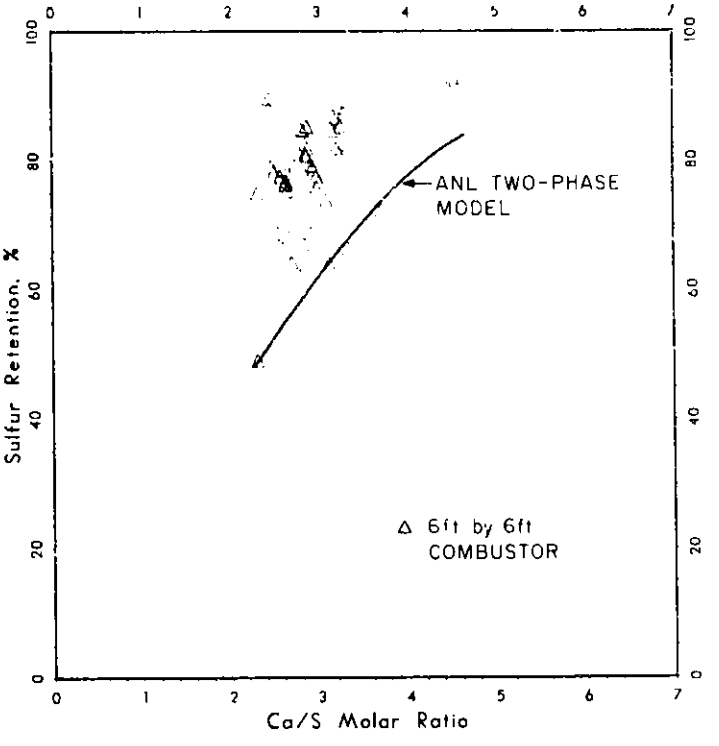

Fig. V-1. Projected and Actual Performance of Sorbent ANL-9202 in Babcock & Wilcox Combustor (1.8 × 1.8 m).

Fluidized Bed Operating Conditions

Temperature: 850°C = 1562°F
Pressure: 101 kPa = 1.0 atm
Fluidizing Velocity: 2.44 m/s = 8.00 ft/s
Bed Height: 1.20 m = 3.93 ft
Coal Feed Rate: 900.0 kg/h = 1982.4 lb/h
Sulfur Content of Coal: 3.60 wt %
Bed Area: 3.34 m^2 = 36.0 ft^2
Sorbent Particle Dia: 1200 μm = 0.0472 in.

than that in the TGA test. The higher utilization in the combustor occurs because the alkali metals present in the coal tend to increase the porosity of the sorbent and because the motion of the particles in a fluidized bed tends to abrade the calcium sulfate surface layer on the sorbent, thereby exposing unreacted calcium oxide.

b. Attrition Model

An attrition model is under development to account for the disintegration of the limestone particles (1) due to grinding during both pneumatic transport to the bed and fluidization in the bed and (2) due to thermal shock and decrepitation during calcination. Because the process of grinding is a complex phenomenon that is affected by hardness, abrasion resistance, impact elasticity, and structural imperfections, a stochastic or probabilistic, rather than a deterministic, approach was selected. The sorbent-specific parameters for the model are determined from a standard attrition test. The test also yields information about particle disintegration during calcination, although no model has yet been developed. Upon being attrited, the small particles become entrained in the fluidizing gas and are elutriated. Since the extent of elutriation depends upon the mass and diameter of the particles and the velocity of the fluidizing gas, small lightweight particles show a greater tendency to be elutriated. An elutriation model has been adapted from several previously reported in the literature.[2-5] Unfortunately, the relationship of attrition and elutriation to sulfation is not completely understood at this time because the ability of a sorbent to capture sulfur is affected by particle size in two somewhat opposing ways. First, for a given total weight of sorbent in the bed, small particles react more rapidly and capture more sulfur; thus, selective elutriation of the small sorbent particles decreases the sulfur-capture ability of the bed. Second, selective elutriation of small particles effectively increases the average residence time of large particles in the bed because fewer of the larger particles are removed through the overflow that maintains the bed height. Thus, the large particles survive to achieve higher utilizations (though lower reactivities) than would occur in the absence of elutriation. A higher feed rate of the sorbent is then required to reduce the average residence time of the large particles to the level at which the desired sulfur capture is achieved.

In further activities with the sorbent-utilization prediction methodology, we will seek to redefine the standard sulfation tests, to rectify the limitation of the attrition/elutriation model, and to expand the methodology handbook to include the effects on sulfur capture of freeboard sulfation, in-bed ash buildup, fines recycle, and nonuniform SO_2 generation.

---

[2] D. Merrick and J. Highly, AIChE Symp. Ser. 70(137), 366 (1974).

[3] L. Austin, K. Shoji, V. Bhatia, V. Jindal, and K. Savage, Ind. Eng. Chem. 15, 187 (1976).

[4] J. Wei, W. Lee, and R. F. Krambech, Chem. Eng. Sci. 32, 1211 (1977).

[5] L. S. Fan and R. C. Strivastava, Chem. Eng. Sci., in press.

2. Hydration-Enhanced Limestone Utilization

Fundamental to the experimental approach of seeking ways to enhance the extent of the sulfation of limestone and dolomite sorbents is the search for alternative ways of enlarging the pore structure of the sorbent. Past efforts have utilized common inorganic salts, but, more recently (see last year's report), it was discovered that hydration and subsequent in-bed dehydration of partially spent sorbents greatly enhances their sulfur-capture capacity. The enhancement appears to result from changes in pore-size distribution created by the expansion of the sorbent during (1) the formation of $Ca(OH)_2$, (2) the dehydration of $Ca(OH)_2$, and (3) the recrystallization of the CaO.

Mechanistically, sulfation of fresh sorbent proceeds until further reaction with the SO_2 from the coal is impeded by the buildup of a $CaSO_4$ reaction surface layer. Subsequent water treatment hydrates some of the residual CaO to form $Ca(OH)_2$, with a resultant expansion that cracks the surface layer. Dehydration of the $Ca(OH)_2$ at temperatures above 800°C then forms CaO having greater porosity, larger average pore diameters, and smaller crystallite size than does untreated CaO. The resultant sorbent has increased gas permeability and surface area and, thus, is susceptible to further sulfation upon exposure to SO_2-containing combustor gas.

The effects of partial hydration on overflow material from an AFBC are shown in a series of photographs presented in Fig. V-2. The limestone used as bed material is Grove limestone (ANL-9501), which has a nominal $CaCO_3$ content of 95%. After passing once through the combustor, the available calcium in the limestone feed has been wholly calcined and partially sulfated to about 22-26% $CaSO_4$, forming a dense surface layer on the particles. The second photograph shows expansion cracks in the surface layer of $CaSO_4$ and resultant polygons of $CaSO_4$, both of which increase the permeability of the particle. In the particle interior, $Ca(OH)_2$ is formed from residual CaO as small crystallites. Because of their large molar volume compared with CaO, the crystallites extrude through the surface layer, as seen in the first and third photographs, thereby causing particle expansion and the observed cracking of the $CaSO_4$ surface layer. Upon subsequent dehydration, the small crystallites of $Ca(OH)_2$, as seen in the fifth photograph, produce a very reactive form of CaO having a large surface area. The pore space produced by the loss of the combined water results in a more permeable system having a favorable pore-size distribution for further sulfation. Except for cracks resulting from particle expansion, the surface layer of $CaSO_4$ maintains its integrity during hydration (as seen in the fourth photograph) and dehydration; furthermore, the integrity of the entire particle is maintained despite successive recrystallizations of the calcium oxide.

A differential thermal analysis of partially sulfated and hydrated limestones was undertaken to identify the chemical species reacted. The principal species of interest were $Ca(OH)_2$, $Mg(OH)_2$, $CaSO_4 \cdot 2H_2O$, and $CaSO_4 \cdot 1/2\ H_2O$. The results indicate (1) that $Mg(OH)_2$ formation starts when $MgCO_3$ concentration exceeds about 32 wt %, (2) that hydration forms $Ca(OH)_2$ preferentially, and (3) that there is little evidence for the formation of $CaSO_4 \cdot 2H_2O$ or $CaSO_4 \cdot 1/2\ H_2O$, even when $CaSO_4$ constituted more than 70% of the spent sorbent.

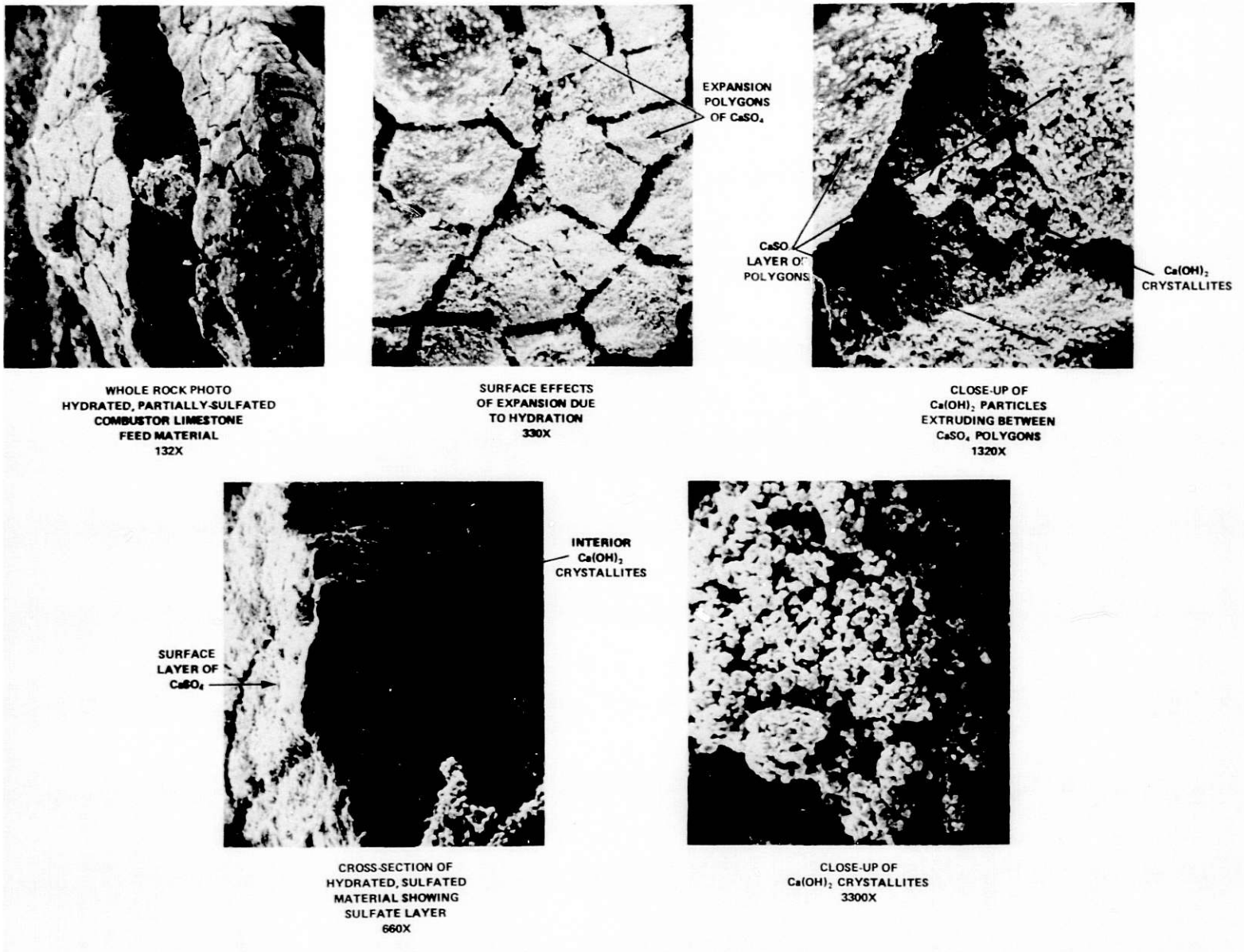

WHOLE ROCK PHOTO
HYDRATED, PARTIALLY-SULFATED
COMBUSTOR LIMESTONE
FEED MATERIAL
132X

SURFACE EFFECTS
OF EXPANSION DUE
TO HYDRATION
330X

CLOSE-UP OF
$Ca(OH)_2$ PARTICLES
EXTRUDING BETWEEN
$CaSO_4$ POLYGONS
1320X

CROSS-SECTION OF
HYDRATED, SULFATED
MATERIAL SHOWING
SULFATE LAYER
660X

CLOSE-UP OF
$Ca(OH)_2$ CRYSTALLITES
3300X

Fig. V-2. Partially Sulfated Limestone Additive from a Fluidized-Bed Combustor Showing Physical Effects of Hydration (Grove Limestone, ANL-9501)

Engineering studies are under way to ascertain the kinetics of the hydration process and to develop methods of utilizing the water in a commercially suitable manner. An approach under consideration is to contact the spent sorbent with steam or steam-air in a fluidized-bed reactor. In this approach, it is desired to recover both the sensible heat of the spent sorbent and the heat of hydration.

A series of experiments was undertaken to determine the effect of process temperature (100 to 300°C) on the hydration rate of various spent sorbents. For each sorbent tested, the initial rate of reaction (first 1/2 h) decreased with increasing temperature; however, the ultimate reaction rates were fairly independent of the temperature. In addition, the initial rates of reaction were found to increase with increased concentration of water vapor up to 12 wt % water; further experiments are under way to test steam containing 30 to 70 wt % water. A relationship is being developed that will correlate both temperature and steam concentration with the rate of hydration.

In further activities related to the hydration process, various designs of hydrators, i.e., fluidized bed, raked bed, rotary drum, and countercurrent flow towers, will be investigated. The objective will be to identify and quantify the parameters critical to optimization of the process. Engineering flowsheets will be prepared that depict the essentials of the various process schemes. Laboratory experiments will be conducted to evaluate the extent of sorbent decrepitation during the hydration process in relation to the levels of prior sulfation and conversion of the available CaO to $Ca(OH)_2$.

C. Flue Gas Cleaning for Pressurized FBCs

1. Removal of Alkali Metal Compounds from Hot Flue Gas

In the industrial application of PFBC to the generation of electricity, a potential problem is "hot corrosion" of the gas turbine (downstream from the fluidized bed) by alkali metal compounds. The hot corrosion is believed to be caused by the deposition of liquid alkali metal sulfates on the turbine components. The alkali metal sulfates are formed by the chemical reaction of gaseous alkali metal chlorides (the chemical form of alkali metals transported by the hot gas) with SO_2 by the reaction:

$$2NaCl(g) + H_2O + SO_2 + 1/2\ O_2 \rightarrow Na_2SO_4(\ell) + 2HCl \qquad (2)$$

This reaction is shifted to the right by the decrease in temperature that occurs as the hot gas passes through the turbine.

To alleviate this corrosion problem, it has been proposed that, before entering the turbine, the hot gas be passed through a granular bed of a material that reacts with or removes gaseous alkali metal chlorides from the gas stream. Earlier studies showed that diatomaceous earth and activated bauxite may be used to remove gaseous NaCl and KCl from a hot gas stream. The gaseous alkali metal chlorides react with diatomaceous earth to form nonvolatile compounds, but are, for the most part, physically adsorbed on the activated bauxite. During the past year, studies have been completed on a method of regenerating activated bauxite, and a method has been developed

for determining adsorption-isotherm and breakthrough data at high temperatures and pressures.

It has been found that most of the NaCl removed from a hot gas stream by activated bauxite can be removed from the activated bauxite by leaching with water (see last year's report). This leaching procedure is successful because most of the gaseous NaCl is physically adsorbed on the activated bauxite and only a small part is chemically bound to it (probably by reaction with the clay impurities in the bauxite). After it is dried, the bauxite can be reused as a high-temperature sorbent for gaseous NaCl. Studies are under way at CEN to test this regeneration concept.

In an experiment of ten cycles of adsorption and water-leaching regeneration, the capture efficiency of the bauxite was not decreased with repeated regeneration, but approximately 2% of the bauxite was converted to fines and was lost during each water-leaching cycle. The rate of the leaching process was studied to determine the best combination of water-to-bauxite weight ratio, temperature, and contact time. The results indicated that, to achieve optimum regeneration, a five-to-one weight ratio of water to bauxite should be used at about 180°C and 1000-kPa pressure (10 atm) for 5 to 10 min. It is believed that the rate of leaching is controlled by the rate of diffusion of NaCl through the internal pores of a bauxite particle when the water-to-bauxite weight ratio is five or more. The total amount of NaCl leached was found to increase in successive cycles at these water-to-bauxite ratios. The data collected in these studies are being used to design a regeneration system.

Previous studies of the removal of gaseous NaCl had been done at 100-kPa pressure (1 atm). During the past year, a new apparatus was placed in operation to measure the sorption characteristics of sorbents at high pressures and temperatures. This experimental apparatus was designed so that sorption-isotherm data and breakthrough data can be obtained under selected conditions of pressure, gas composition, gas flow rate, temperature, and bed characteristics. Knowledge concerning these parameters is needed for the design of a practical system for the cleanup of hot gas. The sorbent bed in the new apparatus is divided into four to six sections by wire mesh so that the extent of penetration of NaCl into the bed can be determined at the end of an experiment. While these experimental data are being collected, various equipment concepts for using granular sorbents for hot gas cleanup will be studied.

2. Development of Na_2SO_4 Dew Point Meter

As indicated above, the hot corrosion of turbine components is believed to be due to the deposition of liquid Na_2SO_4, which is formed when gaseous NaCl and SO_2 react according to reaction 2. In view of the complex nature of the equilibrium relation, knowledge about the gaseous alkali metal content of the gas stream is not sufficient for accurate prediction of whether Na_2SO_4 will form when the flue gas is expanded through the turbine. The concept developed at CEN for a Na_2SO_4 Dew Point Meter involves lowering the temperature of a sample of the gas stream and determining the temperature at which liquid Na_2SO_4 will deposit. Comparison of the Na_2SO_4

dew-point temperature with the gas temperatures expected in the turbine will allow prediction of the sites where Na_2SO_4 will deposit.

Two different methods of detecting a deposit are under study. For the first method, a laser beam is reflected off the test surface, and the quantity of deposit determined by interferometry or ellipsometry. This method has been carefully studied, and the sensitivity and equipment needs evaluated. Both optical techniques (interferometry and ellipsometry) are expected to be capable of measuring the growth rate of deposits as thin as 0.1 μm and of detecting deposits as thin as 0.02 μm. The second method under consideration involves measurement of the electrical conductivity of a deposit. An experimental study is currently under way to determine whether the electrical method will work. In these studies, a conductivity cell was constructed by embedding platinum electrodes in the surface of a high-purity alumina disk. The disk will be placed in a gas stream containing gaseous alkali metal compounds and cooled. From the rate of decrease in electrical resistance of the disk, the rate at which the deposit thickness increases can be estimated. Measurements, at several temperatures, of the rate of thickness growth will allow the dew point temperatures to be estimated.

3. Cyclone Evaluation for Particulate Removal

Particulate loading in the hot flue gas from PFBCs is of concern in all experimental work since particulate matter could cause damaging erosion of gas turbine blades. Recently, two large experimental installations, the EXXON miniplant and the National Coal Board/Coal Utilization Research Laboratory (NCB/CURL) pilot plant, have yielded encouraging results with respect to particulate loadings. The EXXON hot gas cleanup system achieved an outlet gas loading of less than 0.15 g/m^3 (110 ppm). This system consisted of three cyclones in series, designed very simply as ceramic castings inside pressure vessels. The first cyclone was designed for "roughing" to recycle unburned carbon into the fluidized bed and not for high performance. Of most significance was the performance level of the third cyclone--removal of 90% or more of the particles in the size range of 1-2 μm. In tests at CURL, also with a three-cyclone system, loadings were 0.15 g/m^3 (110 ppm) and less, and the mean particle size was less than 2 μm in the outlet gas from the third cyclone. These test results indicate that, at least for certain coal/limestone combinations, adequate turbine lifetimes might be obtained with well-designed cyclones coupled with turbines made somewhat more rugged by the use of blade coatings or claddings. Attaining the particulate emission requirements of the Environmental Protection Agency (EPA) may require additional cleanup, which could be accomplished downstream from the turbine.

Results of literature evaluations and experiments on cyclone performance were collected in a report (in preparation) that presents estimates of the best particulate separation attainable with cyclones in PFBC hot flue gas service, as well as qualitative estimates for alternatives (such as bag filters and electrostatic precipitators) to simple cyclones. The evaluation in

this report allows the particle loadings attainable for full-size cyclones to be estimated and indicates whether alternative or supplemental cleanup steps will be required to obtain particulate loading in the turbine inlet gas at levels currently projected to give adequate turbine lifetimes.

The performance of a full-size cyclone system was calculated for inlet conditions of 870°C (1600°F) and 1000 kPa (10 atm), assuming particulate loading and particle-size distribution similar to those observed in CURL tests (about 10^4 ppm, with mean particle diameter of 35 μm). Based on the results of EXXON's cyclone testing, a three-cyclone system was found to be capable of meeting the most recent turbine-inlet tolerance estimates of General Electric Co. (GE). The three-cyclone system has 1.8-m (6-ft) dia primary and secondary units, each with a 30.5-m/s (100-ft/s) inlet velocity, and a 0.9-m (3-ft) dia tertiary unit with a 45-m/s (150-ft/s) inlet velocity. If twice the particulate loading were present (20,000 ppm), as was assumed in GE's Gas Cleanup Performance Requirement for a Coal-Fired Combined Cycle,[6] a fourth cyclone would have to be added to the system--another 0.9-m-dia unit. Total pressure drops were also predicted for these systems, based on the Shephard and Lapple correlation.[7] Pressure drops were found to be about 41 kPa (6 psi) for the three-unit system and 62 kPa (9 psi) for the four-unit system.

Gas throughputs for units of these diameters (i.e., 0.9 and 1.8 m) would be on the order of 41 kg/s (90 lb/s) for the primary and secondary units, but only 14-16 kg/s (30-35 lb/s) for the tertiary unit. These throughputs would be required for a 300-MW combined-cycle power plant with six parallel trains for hot gas cleanup. Lower throughput requirements would allow smaller units to be used, and particulate removal performance would improve accordingly.

D. Fluidized-Bed Combustion Program Evaluation and Analysis

1. Program Planning Assistance for METC

A PFBC technology assessment is in preparation to assist METC in management of the PFBC development program. In each of several topic areas, a background report is being prepared. Topics covered will include combustor performance, solids feeding and handling, materials behavior, hot gas cleaning, turbine integration, controls and instrumentation, environmental performance, cycle selection, and advanced concept development.

For each topic, the state of the art is being derived from information previously known or available in the literature concerning PFBC technology and other related technologies. This review will include all current projects funded under DOE or other government agencies and any privately funded projects that can be identified, both in the U.S. and foreign countries.

---

[6] PFB Coal Fired Combined-Cycle Development Program, Annual Report July 1978 to June 1979, General Electric Co., Energy Systems Programs Department FE-2359-61 (May 1980).

[7] C. B. Shephard and C. E. Lapple, Ind. Eng. Chem. 32(9), 1246 (1940).

The scope, objectives, costs, and schedules of these efforts will be included where possible. Once this information is compiled, an evaluation of the topic areas will be made that will include such factors as the probability of success of individual projects, crucial or critical considerations in the development effort, information to be gained from the work, and information gaps or shortcomings still remaining. Recommendations for further developmental efforts will then be made, as well as suggestions concerning existing programs (i.e., changes in direction, date of completion, etc.).

Individual topic areas are being assigned on the basis of the expertise and knowledge gained during the course of two PFBC assessment studies made during FY 1980, namely, the International Energy Technology Assessment Program and the PFBC Systems Engineering Effort (see below). This activity is a continuation of last year's effort in which a methodology for carrying out program planning was developed.

2. Instrumentation Needs for FBCs

The state of the art of instrumentation for application to FBC technology has been reported[8] in the past year. Much of the information for this study was gathered in a formal survey in which most domestic and a number of foreign FBC projects were contacted. As part of this survey, each project was mailed forms requesting information on FBC design details, as well as forms for the specification of instrumentation and measurement needs. Returns from the respondents have been consolidated into this report.

This report gives, in the context of the general FBC process, an overview of the major measurements conducted in all FBC units, supplemented by a brief discussion of a number of additional types of measurements now principally conducted in research facilities. In addition, an extended discussion of deficiencies in present instrumentation is presented, with emphasis on the more significant problems. The major areas of deficiency identified in this study include mixed-phase mass-flow metering, entrained particulate monitoring, on-line composition monitoring of both solids and gases, bed-level measurement, and temperature measurement.

3. Project Management Support

At the request of METC, Argonne personnel participated in a review of the hot gas cleanup system proposed for installation in the Curtiss-Wright 13-MWe pilot plant. The purpose of the review was to evaluate small gas turbine (SGT) rig data on hot gas cleaning devices proposed for installation in the pilot plant.

---

[8] C. L. Herzenberg, K. E. Griggs, R. F. Henry, and W. F. Podolski, A Study of Instrumentation Needs for Process Control and Safety in Coal Fluidized-Bed Combustion Systems, Argonne National Laboratory Report ANL/CEN/FE-80-15, in preparation.

4. International Energy Technology Assessment Program

The objective of this DOE-sponsored program is to investigate foreign fossil energy technologies in order to discover technological developments that can be transferred to the United States. Information was collected principally through literature reviews, foreign-travel trip reports of U.S. personnel, and interviews with U.S. travellers to foreign countries and foreign visitors to the United States. Argonne, Oak Ridge National Laboratory (ORNL), and Lawrence Livermore Laboratories (LLL) collaborated on the project under the coordinating direction of LLL. Based upon the information gathered, ANL prepared assessment reports on PFBCs and materials of construction for coal gasification processes; the former report was prepared by CEN and the latter by the Materials Science Division (MSD). This program will continue next year at a lower level of effort.

5. Atmospheric Fluidized-Bed Boiler Installation at ANL

Argonne is planning to replace one or two existing oil/gas boilers in its heating plant with an AFBC unit. CEN provided a statement of work for the procurement of architect/engineering (A/E) services and served on the technical evaluation team which reviewed proposals from A/E firms. In addition, CEN completed a conceptual design for the AFBC boiler installation, which included design criteria, a preliminary description of the layout of the system, and a description of the interactions among the various subsystems.

6. Systems Engineering

The objective of this program was to produce an up-to-date review and evaluation of fluidized-bed combustion technology, both in the United States and elsewhere. This review will be used by DOE in a larger systems engineering effort to compare various advanced fossil fuel technologies according to cost and performance and to assess the adequacy and appropriateness of research and development programs in the various technologies. Atmospheric and pressurized fluidized-bed combustion were dealt with in separate reports, each of which summarized the technical performance, environmental impacts, economics and market factors, and current and planned R&D programs for the FBC technology. These two technologies were evaluated by CEN at the request of the Energy and Environmental Systems Division (EES) of ANL, which is directing the assessment of a large number of energy technologies for DOE.

7. Design of Advanced Fossil Fuel Systems

The Chemical Engineering Division is participating in an ANL program to design advanced fossil fuel systems. As part of this program, performance and cost data will be gathered to compare the following types of electric power plants: conventional pulverized coal with flue gas desulfurization, pressurized fluidized-bed combustion, and gasifier/combined-cycle systems. An A/E firm will design the conventional plant and will complete balance-of-plant

layouts and cost estimates for plants employing the advanced technologies. Separate contractors will provide input to the A/E for the unique components and systems associated with the advanced technologies. CEN is assisting in the selection of the PFBC contractor and the specification of design parameters of the PFBC system and is reviewing the output and monitoring the progress of the contractors and A/E.

E. Sampling and Analysis of Fluidized-Bed Combustion Gases

Hot off-gas streams from fluidized-bed combustors contain polycyclic organic matter (POM) that consists partly of carcinogenic or mutagenic polycyclic aromatic hydrocarbons (PAHs). The present effort consists of (1) a critical review and evaluation of existing protocol for the analysis of PAHs; (2) identification and evaluation of the problems associated with sampling PAHs as well as identifying them with a commercially available gas chromatograph/mass spectrometer; (3) an experimental investigation of the chemical transformations that occur during sampling and tend to alter the data; and (4) development of an instrument that will eliminate the sampling stage of the analysis and will allow real-time chemical analyses of PAHs.

1. Analytical Protocol for PAHs

A major problem associated with the analysis of organic compounds in stack gases is the large number of species (about one hundred) present at ultratrace levels, i.e., 10^{-9} g/m^3. The only analytical technique currently available for the identification and quantification of such species is gas chromatography (GC) combined with a mass spectrometer (MS) and a computer spectra reduction system. The GC separates the complex mixture of compounds, and the MS identifies the mass for each compound. For suitable detection by the MS, at least 10^{-10} g of each species is required. However, only up to 10^{-8} m^3 of sample can be injected into the GC at a time--for an overall sensitivity of the GC/MS analysis of about 10^{-2} g/m^3 (10 μL). Thus, before analysis, the PAHs must be concentrated from large volumes of stack gas by a factor of about 10^6.

In the earliest sampling methods, fly ash particulates were collected on filters; and the vapors were collected with organic solvent impinger systems, e.g., EPA Method 5.[9] The methods had poor efficiencies for vapor collection and recovery, leading to significant distortions of the data. More recently, polymeric adsorbents such as Tenax and XAD-2 have been developed to alleviate this problem. One technique with resins involves a heated filter to volatilize the PAHs from the fly ash and a cooled adsorbent column in tandem to condense and collect the volatile PAHs; the Source Assessment Sampling System (SASS) developed by EPA utilizes this scheme.

The accuracy of an analysis of PAHs sampled on polymeric resins depends not only on the adsorption efficiency of each species, but also on

---

[9] Fed. Regist. 44(233), 69464-69575 (December 3, 1975).

the desorption efficiencies. Generally, those species that are readily adsorbed are the most difficult to desorb and vice versa. Low temperatures, 15 to 50°C, and low flow rates are used to increase adsorption efficiencies. Care must be taken while extracting or thermally desorbing from sorbents so that chemical alterations or fracturing of the PAH species are avoided. Tenax, which is thermally desorbed, has a high affinity for polar PAHs; whereas XAD-2, which is chemically desorbed, has a high affinity for nonpolar compounds. Although the collection efficiencies of both resins are near 100%, major difficulties are encountered in minimizing background contaminations; as a result, Tenax requires prolonged baking and XAD requires multisolvent extraction. Quantitative GC/MS analysis is achieved by proportionating the total integrated ion current of the PAH to that of a deuterium or carbon-13 substituted analogue internal standard of known concentration.

Currently, efforts are being made to develop an acceptable protocol for the quantitative analysis of the PAHs present in off-gas streams. Problem areas will be identified and explored to define the limits of the accuracy and reproducibility of the protocol. An exploratory investigation will be undertaken to evaluate the effects of large quantities of the major components (NO_x, SO_x, CO_x, O_2, and N_2) sweeping through the sampler.

2. On-Line Instrumentation for Monitoring PAHs

The problems associated with the sampling of PAHs can be minimized by the use of on-line instrumentation having sufficient sensitivity to make concentration of samples unnecessary. An additional advantage of on-line instrumentation is that the results are obtained in real time and are not delayed or averaged by the duration of sampling. A survey of methods for on-line analysis of PAHs indicated that potentially successful analytical techniques for direct measurements of aromatic compounds are double (or triple) mass spectroscopy, multiphoton laser ionization mass spectroscopy, and laser-induced fluorescence in a molecular beam.

Mass separation/mass spectral characterization (MS/MS) is an analytical method in which a mass spectrometer is used for separation and another one is used for identification of the components of a mixture. The technique involves (1) ionizing the components of the mixture either by electron impact or by chemical transfer, e.g., $(M + H)^+$, (2) resolving the ionized mixture into individual components by one of the two mass analyzers, and (3) identifying the separated ionized components in the second analyzer. The high sensitivity of MS/MS is achieved by performing the ionization at atmospheric pressure--with the unfortunate consequence of greatly increasing the number of ionization reactions, particularly when water vapor is present, and thus increasing the complexity of species identification.

Very selective ionization of one compound in a mixture can be achieved by resonance multiphoton ionization (MPI), in which the ion fragment distribution may be controlled by laser power and wavelength. In this technique, molecular beams or gas streams are irradiated by the output of a

tunable pulsed laser, and the charged species produced by multiphoton ionization are analyzed by a mass spectrometer. A study of the ion fragmentation patterns as a function of laser power and laser wavelength allows even isomers to be distinguished. The MPI process can produce more gentle ionization at low laser powers and more extensive fragmentation at high laser powers than electron-impact ionization can. This feature is very important for the resolution and identification of polycyclic aromatic compounds. Different wavelengths yield different mass spectra and aid in identification. A tunable UV source can be used as an adjunct to the laser.

Fluorescence is a potential method for on-line measurements, since POMs are inherently fluorescent materials. However, the technique requires (1) prior isolation of individual compounds to eliminate overlapping of excitation and emission wavelengths of different species and (2) low temperatures and pressures to eliminate broadening of bands. Presently, fluorescence analysis is done either in conjunction with gas chromatography or in solid solvent matrices at 70 K. Selective excitation of electronic states of individual POMs in a molecular beam by a tunable laser might reduce band overlapping and broadening.

It is concluded that, at present, no completely satisfactory method exists for the on-line monitoring of PAHs in stack gas. Consequently, the assessment of promising methods will continue.

F. Fossil Fuel Conversion and Utilization

1. Gas Cleanup for Fuel Cell Use

This effort comprises two projects that are a part of the DOE Advanced Environmental Control Technology (AECT) Program. These projects are called "Contaminant/Absorbant Interaction Studies for Hot Gas Cleanup for Fuel Cell Application" and "Process Measurement Control Technology Design for Fuel Cells." Because of the importance of these efforts to the molten carbonate fuel cell program, close coordination is maintained with the Advanced Fuel Cell Program Office in CEN (see Section IV of this report). Molten carbonate fuel cell power plants promise a higher coal pile-to-bus bar conversion efficiency as compared with coal-fired steam plants. An additional two to five percent efficiency can be gained by using a hot-sulfur removal process rather than cold-gas sulfur removal. However, no hot-sulfur removal process currently available will clean the process stream to the low sulfur content required by molten carbonate fuel cells.

The first project mentioned above involves investigation of materials that (1) absorb H_2S at temperatures approximating the molten carbonate fuel cell operating temperature (650°C) and (2) are regenerable. To begin this project, a subcontract has been let with Giner, Inc. to follow up on preliminary thermodynamic and laboratory investigations previously funded by the DOE molten carbonate fuel cell program. In the earlier studies, several promising absorption systems were identified that operate at the desired temperatures and appear to be fully regenerable. During 1981, based on results obtained by Giner, DOE will decide whether to proceed with engineering development of hot gas cleanup or to transfer this effort to the coal-gasification hot gas cleanup program at METC.

The second project consists of a survey of commercial-scale analytical and control instrumentation for interfacing coal gasifiers with molten carbonate fuel cell power plants. Requirements will be established for this instrumentation, and deficiencies of currently available instruments will be identified. A plan will then be prepared for the development of improved instrumentation. This development work will include either nominal improvements of existing equipment (which can be carried out by the instrument manufacturers themselves) or the development of new, state-of-the-art instrumentation, to which ANL can make a definite contribution. The survey and development plan will be completed in 1981, and further work in this area will depend upon the conclusions from this work.

2. Environmental Control for Coal Utilization

The objective of this program, managed by Argonne's Energy and Environmental Systems Division, is to provide guidance to the staff of the DOE Office of Environment in their efforts to ensure that adequate technology is developed for mitigating the environmental impacts of increased coal utilization. The program focuses on control technology for coal-based power and steam generation. It supplies in-depth evaluations of technical, environmental, and economic aspects of the various options available or under development.

The responsibility of CEN in this program comprises technical assessments related to (1) the control of nitrogen oxide (NO_x) emissions from conventional coal-fired boilers, (2) integrated coal gasification/fuel cell power generation, (3) integrated coal gasification/combined-cycle power generation, and (4) solvent-refined coal (SRC)/conventional boiler power generation.

During FY 1980, two subcontractors' reports were issued on integrated coal gasification/combined-cycle power generation,[10,11] and one subcontractor's report was issued on NO_x-control technology for utility boilers.[12] In addition, a draft report on environmental control aspects of SRC production and combustion was revised and is currently being reviewed and edited, and a report on the assessment of combustion modification to achieve NO_x control for coal-fired boilers is being prepared.

3. Technical Management of Synfuel Utilization Project

The Chemical Engineering Division provides technical support to DOE and the Pittsburgh Energy Technology Center (PETC) in the management of a broad alternative-fuels effort whose objective is to ensure the existence of

---

[10] Environmental Control Implications of Generating Electric Power from Coal, Argonne National Laboratory Report ANL/ECT-3, Appendix C (December 1977).

[11] Gasification/Combined-Cycle Power Generation: Environmental Assessment of Alternative Systems, Argonne National Laboratory Report ANL/ECT-7 (November 1978).

[12] Status of Combustion-Modification Technology for Utility-Boiler NO_x Control, Argonne National Laboratory Report ANL/ECT-TM-1 (December 1978).

the fuel technology base required for timely substitution of synfuels for petroleum and natural gas in stationary combustors. Principal substitute fuels, such as coal-derived liquids, will contribute initially to the nation's liquid fuel needs in the mid-1980's; by the year 2000, about three quads* per year of energy may be derived from liquids made from coal.

The management effort has consisted of providing a program plan establishing objectives, reviewing proposals, reviewing the work of contractors, and providing contract procurement information for DOE. The Synfuel Utilization Project is part of the Advanced Research and Technology Development Program managed by PETC in the Fossil Fuel Utilization Division of DOE.

*1 quad = 10^{15} Btu.

VI. MAGNETOHYDRODYNAMICS (MHD) HEAT AND SEED RECOVERY TECHNOLOGY

A. Overview

Open-cycle magnetohydrodynamics (MHD) is a developing technology that promises to substantially improve the electrical efficiency of coal-fired power plants and to reduce their environmental impact. The CEN effort in support of the multidivisional MHD program is directed toward developing the technology required for the components downstream from the MHD channel-diffuser and for processes to recycle the potassium seed material. Potassium salts are added to enhance the electrical conductivity of the combustion gas. The major focus of the CEN effort is an experimental program to determine the effects of seed and slag on the MHD steam bottoming plant (heat and seed recovery system).

Figure VI-1 is a conceptual representation of the gas system downstream from the MHD channel-diffuser. This portion of the gas system is analogous to the steam-generating portion of a conventional power plant, but it must perform the additional functions of separating slag and seed, recovering seed material, preheating primary combustion air to high temperatures, and reducing very high NO_x concentrations to acceptable levels. Moreover, because the combustion gas entering the bottoming plant is fuel-rich and laden with vaporized potassium salts and entrained slag particles, this component of the MHD power plant must operate under conditions that are more highly fouling and more corrosive than in conventional coal-fired power plants.

The overall objective of the Argonne MHD Heat and Seed Recovery Project is to provide the requisite technical data for designing and operating the downstream gas system and the seed-recycle process. The immediate project goals are to support the design and operation of the 20-MW Heat Recovery-Seed Recovery pilot plants being built at the University of Tennessee Space Institute. In cooperation with this project and other DOE contractors, our long-range objective is to provide the technical data base needed to design the 500-MW(t) MHD Engineering Test Facility (ETF), which will be built in the late 1980's to demonstrate the feasibility of an integrated coal-fired MHD power plant.

B. Argonne MHD Process Engineering Laboratory (AMPEL)

AMPEL, constructed by Argonne's Engineering Division, is a versatile facility for testing MHD steam-generator components under prototypic MHD conditions. The facility can supply a mixture of combustion gas, potassium compounds, and coal ash at a rate of 1 kg/s and at temperatures in the range from 2000 K to about 2500 K. The mixture is produced either by combustion of a slurry of fuel oil, coal ash, and K_2SO_4 with air preheated to 1050 K or by the combustion of pulverized coal plus K_2SO_4.

It has been proposed that, to complete combustion in an MHD plant, relatively cool air be injected into the fuel-rich combustion gas immediately downstream from the radiant boiler and upstream from the steam superheater,

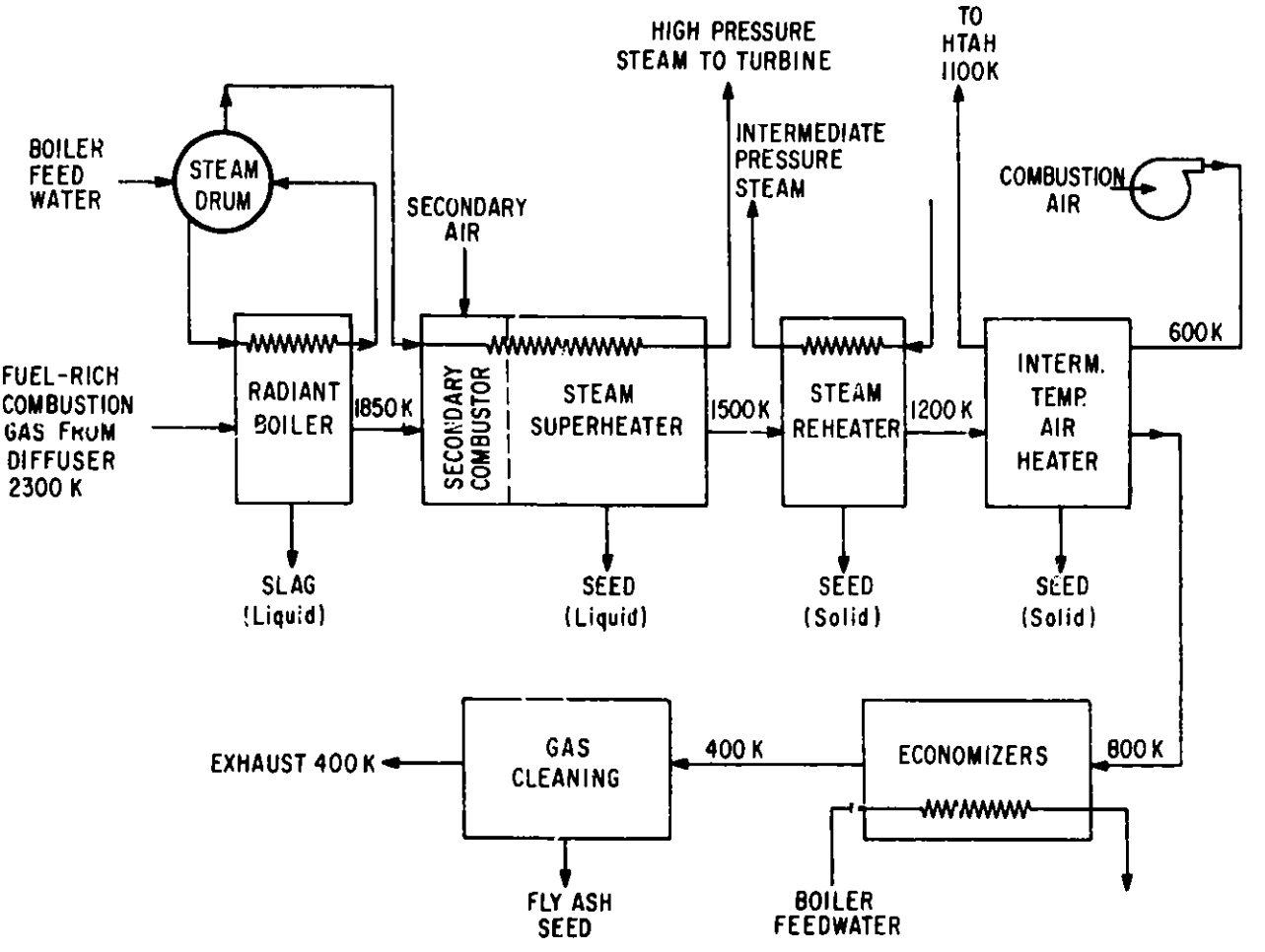

Fig. VI-1. Reference Downstream Gas System for Open-Cycle MHD Power Plant

where the gas temperature would be 1700 to 1900 K (see Fig. VI-1). During 1980, AMPEL was used to obtain experimental data on the formation of NO_x when air is injected into the channel exhaust gases through the secondary combustor. These results were used to verify a chemical kinetics model,[1] which was then used to predict NO_x behavior in large MHD systems. This model, which incorporates chemical reaction kinetics with the radiative and convective heat-transfer rates in radiant boilers of various geometries, employs 29 reactions that are important to the formation and destruction of major species in the combustion gas, including NO_x.

In the MHD steam bottoming plant, the steam and air heaters will be exposed to highly fouling conditions because of the very large amounts of potassium seed in the gas stream. The deposits, which will be primarily K_2SO_4,

[1] A. J. Sistino, Analytical Studies of NO_x Decomposition in the Radiant Boiler of an Open-Cycle MHD Power Plant, Argonne National Laboratory Report ANL/MHD-79-7 (April 1979).

will rapidly accumulate on the heater tubes, and the thickness of the deposits must be controlled to maintain heat-transfer effectiveness and gas flow. The deposit characteristics will depend, to a large extent, on the gas temperature. Consequently, tests are under way in AMPEL to determine the heat-transfer performance in banks of air-cooled tubes exposed to a gas stream that contains potassium seed; this experimental setup is intended to simulate a steam super-heater exposed to seeded combustion gases at various temperatures. One of the AMPEL tests was performed with a tube bank consisting of fifteen 4.2-cm OD vertical tubes (three rows) on 12.2-cm square pitch; the gas temperature entering the tube bank was about 1800 K. After 3 h of operation, the gas-side of the deposit surface that had formed on the vertical tubes reached the melting point of K_2SO_4 (1340 K), and the condensing seed material subsequently flowed off the tubes. Furthermore, the heat-transfer coefficient approached a steady-state value, which was 80% of the coefficient for the clean tubes. These findings indicate that an MHD steam superheater operating under similar conditions (i.e., liquid seed deposit) could perform effectively without periodic mechanical removal of the deposit. At gas temperatures below 1500 K, where the seed deposit will be solid, the accumulating material must be periodically removed to prevent plugging of flow passages and to maintain heat-transfer effectiveness. Of special concern is the temperature range from about 1500 to 1300 K, where entrained liquid seed particles solidify as they deposit on cooled tubes. In Soviet MHD facilities,[2] seed deposits formed in this manner were very difficult to remove by conventional mechanical techniques, e.g., soot blowers.

The radiant boiler, which will be located immediately downstream from the channel-diffuser in an MHD plant, must (1) produce steam by transferring heat from the combustion gas to water-cooled walls, (2) reduce NO_x levels by slow cooling of the gas, and (3) decrease seed losses caused by potassium reacting with the slag. In 1982, the many design problems related to the radiant boiler will be investigated in AMPEL. The radiant-boiler tests will be used to examine the rate of NO_x decomposition, radiant heat transfer from a particulate-laden combustion gas, seed losses by interaction with slag, and corrosion of refractory lining and metal boiler tubes. The final design of the test apparatus, which will be installed in the coal-fired test leg of AMPEL, is under way.

C. Thermochemical Support Studies

In the MHD system, 10 to 30% of the coal slag is expected to be carried downstream from the combustor. This slag is present as entrained particles and vaporized potassium salts in the generator and diffuser, but most of the vapor condenses before it reaches the radiant boiler (2300 K). At temperatures from 2300 K down to 1700 K, the slag reacts with the potassium seed to form potassium silicates and potassium-containing aluminosilicates which are dissolved in the other slag oxides. Some of these silicate particles and a

---

[2] M. A. Styrikovich and I. L. Mostinsky, A Study of the Processes Resulting from the Use of Alkaline Seed in Natural Gas-Fired MHD Facilities, U.S. Department of Energy CONF-770402-8 (1977).

small fraction of the gaseous slag and seed condense on the cooled walls of the generator and diffuser. A portion of the remaining slag and seed condenses on the walls of the other downstream components, and final removal of slag and seed is accomplished in an electrostatic precipitator or bag filter.

During 1980, CEN thermochemical studies included (1) measurements of the thermal diffusion of potassium in potassium silicate, (2) thermodynamic modeling of coal-seed-slag gases and condensates, and (3) examination of deposits formed on cooled tubes in AMPEL. These studies are briefly discussed below.

Potassium Thermal Diffusion in Slag. At high temperatures ($\gtrsim$1000 K), potassium could undergo thermal diffusion through slag films formed on surfaces in the channel, diffuser, and radiant furnace; this diffusion would result in corrosion of the structural materials. In laboratory experiments, homogeneous mixtures of potassium silicate and silica in platinum containers were heated to high temperatures, and then the thermal diffusivity of potassium in silicates was determined. These experiments showed no significant thermal diffusion of potassium after one to two hours at temperatures up to 1800 K and a thermal gradient up to 270 K/cm. Calculations using irreversible thermodynamics suggested that the steady-state distribution of potassium in K_2O-SiO_2 solutions will vary no more than 16% for a temperature range of 1240 to 1500 K.

Potassium Loss to Slag. Recovery of potassium from chemically stable silicates, aluminates, and aluminosilicates dissolved in the slag is very difficult and may not be economically feasible. The MHD80 computer code,[3] with which the equilibrium compositions of the coal-seed-slag gases and condensates can be estimated, was used to estimate potassium loss to slag under expected operating conditions in the MHD system.

According to these calculations, if it is assumed that one-third of the coal ash is carried from the combustor into the channel, then the liquid slag particles entering the boiler will contain about 5% of the total potassium added to the system. As the gas cools in the channel-diffuser, the potassium content in the slag particles will increase to about 6% of the total potassium added to the system. If only the smaller slag particles remain entrained in the gas stream as it leaves the radiant boiler at about 1700 K, the total potassium loss to the slag will increase to 9-10% of the total potassium. The condensation of K_2SO_4 begins just downstream from the radiant boiler, at a temperature of about 1680 $\pm$ 100 K.

Because of the difference in the partial pressures of the minerals in the slag, it separates into two chemically different entities. The slag with components of low partial pressure, alumina and calcia, is more likely to be removed as large particles in the radiant boiler. Of the potassium contained in this slag fraction, approximately 90% is potassium aluminate and potassium aluminosilicate, compounds that are water insoluble. The smaller slag particles of the reacted potassium are present as potassium silicate, which alone is water soluble.

---

[3] P. E. Blackburn, GASCON and MHDGAS: Fortran IV Computer Codes for Calculating Gas and Condensed Phase Compositions in Coal-fired Open-cycle MHD Systems, Argonne National Laboratory Report ANL/MHD-77-4 (December 1977).

In conclusion, this study indicates that the fraction of total potassium captured at equilibrium by the slag will be about 10% if one-third of the slag is carried downstream from the combustor; however, because a portion will be water soluble, only about 6% will be unrecoverable by water washing. As the slag carry-over increases, the fraction of total potassium forming water-insoluble compounds with the slag will increase proportionately.

Characteristics of Seed Deposits. In a recent seed-deposition test at AMPEL, 35 parts K_2SO_4 and 3.2 parts fly ash were added to 100 parts No. 2 fuel oil burned in stoichiometric air (SR* = 1). The seed and fly ash condensed on a vertical air-cooled tube (4-cm OD), which had been placed 2.6 m downstream from the combustor where the gas temperature was 1900 to 2000 K. The tube surface temperature was 700 K, and the fly ash and K_2SO_4 were condensed for 4.5 h. A layer of fly ash and slag was found on the upstream side of the tube, and frozen seed was found below the tube. In later stages of the test, the K_2SO_4 apparently condensed as a liquid on the slag-seed layer after it reached a thickness such that the surface was above the melting point of K_2SO_4 (1342 K). The liquid K_2SO_4 flowed down the tube, leaving an outer film of slag. The layer was observed to consist of two phases: a light-blue phase on the inside and a dark-blue phase on the outside. The light-blue phase was 90% water soluble (i.e., K_2SO_4 and K_2CO_3), and the total layer was 67% water soluble and 33% water insoluble.

The layer was analyzed by electron probe to establish the distribution of potassium, aluminum, sulfur, iron, calcium, and silicon. Since the layer was porous and heterogeneous, quantitative (i.e., stoichiometric) analysis was difficult to make, and analysis of results could only be done qualitatively.

The potassium distribution appeared to be relatively uniform (to ±20%) over the full thickness of the layer (0.43 cm). Sulfur concentration was fairly uniform up to 0.15 cm from the tube surface, indicating that practically all the layer up to this point was K_2SO_4. Calculations showed that some K_2CO_3 should have condensed on the tube, but K_2CO_3 could not be detected because the electron probe is insensitive to carbon. Between 0.15 and 0.29 cm, the potassium sulfate appeared to contain some calcium and aluminum as silicates; potassium aluminosilicate and potassium silicate were probably also present. This area also contained iron, probably as iron oxide since there was no correlation of iron with silicon or sulfur. Between 0.29 and 0.37 cm, there were isolated areas containing sulfur; this finding suggests inclusions of potassium sulfate in a slag matrix. The concentrations of potassium, iron, calcium, silicon, and aluminum were high; thus, this region was mostly slag consisting of potassium-slag compounds such as K_2SiO_3, $KAlSiO_4$, and $KAlO_2$. The region from 0.37 to 0.43 cm was all slag and potassium-slag compounds; no sulfur was found here. The fact that no K_2SO_4 was found in this outer region suggests that the surface temperature may have exceeded the melting point by as much as 100 K, to about 1450 K.

---

*SR is the stoichiometric ratio (oxygen fed to combustion process/oxygen required for combustion of fuel to CO_2, H_2O, SO_2).

Calculations based upon the equilibrium condensation model[3] agreed qualitatively with the probe analysis, with some exceptions. According to the equilibrium calculations, the slag concentration of the layer increased with temperature above 900 K (i.e., >0.12 cm), whereas the increase in slag concentration started at about 0.15 cm according to the probe analysis. Although the probe analysis indicated very little slag in the initial layer, about 10% of this initial deposit was calculated to be slag. Both the probe analysis and the calculated condensation showed a high level of potassium throughout the film, even though potassium sulfate was absent from the outer layer, which was at the highest temperature. The mole fraction of potassium was calculated to be 0.27 in the outer slag layer (from 0.37 to 0.43 cm) and from 0.28 to 0.32 in the layers containing sulfate and carbonate (below 0.37 cm); this finding is consistent with the probe analysis. With the slag distribution determined by electron probe analysis, about 75% of the slag-seed layer was calculated to be K_2SO_4 and K_2CO_3; this finding agrees reasonably well with the above observation that 67% of the deposit was water-soluble potassium compounds.

During the next year, thermochemical studies will be continued on the seed-slag deposits.

D. Seed-Reprocessing Studies

The primary function of the MHD seed-reprocessing system is the conversion of K_2SO_4 to a sulfur-free salt such as K_2CO_3, which is then returned to the primary combustor. The most promising chemical process for this operation involves the high-temperature reduction of the sulfate to sulfide with coal or gasified coal, followed by the conversion of the sulfide to the carbonate. In FY 1980, funding for this work was minimal and will remain so in FY 1981. During 1980, CEN assisted DOE in managing seed-reprocessing studies by industrial firms and in evaluating their results. In these studies, a few semi-commercial processes were examined; and the critical issues were shown to be the large energy usages, especially for the reduction step, and the effect of coal-ash impurities on the processes. In the future, CEN efforts will be directed toward lowering the amounts of coal required for the reduction step.

VII. SOLAR ENERGY

The Chemical Engineering Division's solar energy activities are part of the overall $3 million Applied Solar Energy Program at ANL. The ANL program includes work on collectors (CEN), thermal energy storage (CEN, MSD, ENG, and CT),* and solar system reliability (EES).† The program supports the Presidential goal (1978) of achieving 20 quads of energy production by the year 2000 from solar energy. The CEN activities on solar collector development and thermal energy storage are described below.

A. Solar Collector Development

1. Introduction

A national program to establish solar energy as a practical resource has been under way for six years. A large-scale activity in that program has been solar collector development. Three major types of solar-thermal collectors--flat plate, evacuated tube, and parabolic trough--have emerged in the industry with some federal support; however, DOE is generally withdrawing its support of further collector work.

Results now coming in from federally funded demonstration projects show that, in solar heating and cooling of buildings and in industrial process-heating applications, the flat-plate collector has inadequate performance characteristics, the evacuated-tube collector has too high an initial cost, and the tracking parabolic-trough collector has operation and maintenance problems. As a consequence, the collector manufacturers themselves are seeking viable alternatives to their current designs, alternatives that would combine the lower cost and ease of use of the flat-plate collector with the performance of the evacuated-tube or parabolic-trough collector. A strong candidate has been found in the coupling of an evacuated-tube receiver to a nonimaging concentrating reflector; but, because of low profit margins and evaporating direct government support, small-business manufacturers have not been able to shoulder the cost of personnel and time required to (1) explore properly the theory of nonimaging concentration, (2) choose an appropriate concentrator, and (3) optimize it for an application.

Originally assembled to prove that the "ideal" compound parabolic concentrator (CPC) concept is useful in solar-energy applications, the CEN Solar Energy Group has become the acknowledged leader in nonimaging concentrating collector technology. The group's collector development and commercialization activities include optical design studies, hardware tests and evaluations, and support for standards organizations. As a result of these efforts, the group has become the design clearinghouse for manufacturers and other solar researchers in universities and government laboratories.

---

*Designations of ANL Divisions: CEN = Chemical Engineering Division, MSD = Materials Science Division, ENG = Engineering Division, and CT = Components Technology.

†EES = Energy and Environmental Systems.

First-generation collectors based on the nonimaging optics as developed by ANL are already available commercially. The near-term goal of the CEN collector work is the introduction of second-generation nonimaging collectors that overcome the practical limitations of the available collector materials and ideal optical concentrator designs that were encountered in the first-generation collectors. Achievement of this goal is nearing completion. The long-term goal of the work is a complete transfer of technology to industry. Although some progress toward this goal has been made through intensive interactions with industry, it may prove unattainable because of present federal funding policies and the current economic climate. Because of cutbacks in DOE funds, the collector program is being phased out in FY 1981, with the carry-over funds from FY 1980.

2. FY-80 Work Highlights and Significance

As part of an optical design study, seven first-generation collector designs were reviewed and evaluated. Six of the nonimaging concentrator designs came from industry--Owens-Illinois, General Electric, Energy Design Corp., Sunmaster Corp., American Solar King Corp., and TRISUN--and one came from a joint effort between the University of Chicago and GTE Sylvania. The evaluations showed that all the designs suffer 5-20% optical losses because of the necessary gap between absorber and reflector and that most suffer from the low solar absorptance (about 0.8) typically found in commercial evacuated-tube receivers.

Four second-generation optical designs developed at ANL were studied as a result of the above findings. Two of the designs--the four-facet "gaplossless" collector and its generalization, the multifacet "gaplossless" collector--are modifications of the classic CPC cusp; the modifications result in elimination of optical losses through the absorber-reflector gap at the expense of some angular acceptance. This gaplossless-collector concept originated at ANL and is being patented by DOE. The studies show this trade-off to be advantageous in certain applications. In the third design studied, the problem of low solar absorptance is overcome by making the absorber-reflector system an optical cavity with enhanced absorptance through multiple reflections, an effect first described at ANL.[1] Although this can only be achieved in a system with an optical concentration of less than unity, the study shows that the resulting collector will be advantageous in certain applications. The final design studied was the multifacet gaplossless reflector employed as a secondary concentrator coupled to a conventional focusing parabolic trough. Computer ray-trace calculations show that the secondary reflector/receiver combination can be designed to appear bigger from the edges than from the center of the primary reflector, exactly the property needed to allow relaxation of the accuracy requirements of the primary mirror shape; and, hence, cost for the primary mirrors can be reduced.

As part of the effort on hardware testing and evaluation, the optical/thermal performance of nine collector modules was measured. Three of these were first-generation Argonne prototypes--the ANL 1.5X CPC cusp, the

[1] W. R. McIntire, J. J. O'Gallagher, A. Rabl, and R. Winston, Absorption Enhancement in Solar Collectors by Multiple Reflectors, Solar Energy 24, 323-326 (1980).

ANL 3X CPC, and the ANL 5X CPC--and three were first-generation industrial collectors--the Energy Design 1.3X CPC cusp, the Sunmaster 1.08X CPC, and the Chamberlain 2.6X CPC cusp. The remaining three modules were second-generation prototypes, including an ANL 0.87X enhanced-absorptance design and gaplossless designs by ANL and General Electric. The measurements showed that the CEN Solar Group's computer programs adequately predict the optical performance of all the designs studied so far, and that the gaplossless and enhanced-absorptance designs can indeed recoup the optical losses of the first-generation designs.

A long-term performance test of first- and second-generation nonimaging collectors was initiated to assess the importance of incident-angle modifiers, diffuse sky conditions, and thermal time constants on these collectors as compared to traditional flat-plate collectors.

In addition, the optical properties of the two new absorber materials from the University of Sydney and Optical Coatings Research and a new reflector material from the NHK Corp. were measured. The results indicate that, with some development, these materials would be superior to those now used commercially. Measurement of the thermal performance of three evacuated receiver tubes from the University of Sydney, Philips-Holland, and Energy Design and Analysis was also undertaken, but is not yet completed.

Standards-organizations support has been continued through active participation in working committees. Members of CEN are on the Solar Energy Standard Committee of the American Society of Mechanical Engineers (ASME), on Committee 93R of the American Society of Heating, Refrigeration, and Air Conditioning Engineers (ASHRAE), and on Committee E44 of the American Society for Testing and Materials (ASTM). Each of these committees is developing solar-related standards and is in need of the experience that CEN participation brings.

3. Status and Direction

Studies of second-generation optical designs for solar collectors have been completed and reported.[2] The hardware test and evaluation data are still being analyzed and need to be reported. Review and evaluation of second-generation commercial collector designs will be necessary in the coming year, but at present this activity is unfunded. The task involving secondary concentrator development had to be scaled down when only partial project funding was received from DOE. As a result, only the prototype design study is complete, whereas under the original plans, the fabrication of the prototype would be under way. In addition, the use of nonimaging collectors for the *in situ* generation of steam mentioned in the preceding report in this series had to be dropped. Support is being sought to continue the secondary concentrator task jointly with an industrial partner and to complete the long-term performance tests.

---

[2] W. R. McIntire, *New Reflector Design which Avoids Losses through Gaps between Tubular Absorbers and Reflectors*, Solar Energy *25*, 215-220 (1980).

B. Ice Storage

1. Objectives

The objective of this program is to develop a cost-effective method of passive cooling that uses underground ice formation during winter for year-long cooling needs. This work is an extension of the CEN effort in applying solar technology to the heating and cooling of buildings. This cooling method is passive in that it uses passive refrigeration devices (modified heat pipes) which use no external power and automatically extract heat from a water-filled storage container and reject it to the cold air during the winter. The near-term goal of this program is to determine the feasibility of this passive-cooling method, based on theoretical analyses and experimental measurements. The long-range goal is to develop this cooling system from the research-prototype stage to industrial commercialization and large-scale utilization by the public sector.

2. Accomplishments

The basic elements of this cooling system were presented in last year's report. Since that time, several basic design changes have been made, and considerable progress has been attained in hardware development. A full-size tank was constructed during the winter of 1979-80, and limited operation of full-size heat pipes was attained. These pipes were cylindrical and fabricated from common black-iron pipe. One disadvantage of using cylindrical pipes is the limited surface area available for ice freezing. The obvious solutions are the use of larger diameter pipes or many small pipes, but these measures would result in major cost increases. To obtain large surface areas at a reasonable cost, we have fabricated and tested indoors heat-pipe evaporator and condenser units made from Roll-bond™ panels. These panels are commercially available copper or aluminum sheets with integral fluid channels. They have been used in the refrigeration industry and are now widely used as solar-collector absorber plates.

At the present time, we are also in the process of using Roll-bond™ to fabricate several full-scale heat pipes for use outdoors during this winter. The configuration of the evaporator is that of an insulated plastic cylinder to which four Roll-bond™ heat pipes are attached. Each evaporator unit will have approximately 3 m^2 (32 ft^2) of surface area. The above-ground condenser units are also sheets of Roll-bond™ panels with a corresponding area of 15 m^2 (160 ft^2). These panels can be positioned on the roof or walls of a structure and be reasonably unobtrusive.

Experience obtained this winter will determine the future direction of our work. We intend to monitor the performance of our heat pipes during actual winter conditions and take corrective actions if necessary. In addition, based upon the performance of our tests, we will be able to do a comprehensive economic analysis of the concept.

C. Thermal Energy Storage

Three projects on thermal energy storage are in progress. Two of them were recently initiated (Fall 1980) and represent areas where ANL expertise is being brought to bear on industry-wide problems or on problems where it has not yet been established that a commercial product can be developed. The three projects are "Stratified Storage Measurement and Analysis," started in October 1979; "Testing of Latent Heat Storage Units," started in October 1980; and "Development of Thermal Energy Storage Device Using Cross-Linked High-Density Polyethylene," started in November 1980. A brief description of these projects follows.

1. Stratified Storage Measurement

a. Objectives

Estimates by others have shown that thermal stratification in storage tanks can improve the performance of solar systems by 5-15% compared with that of fully mixed systems. Unfortunately, typical solar systems behave like mixed systems because the designers do not know how to achieve stratification and take advantage of it. Computer models of stratified tanks have been developed by the University of Wisconsin, Boeing Computer Services, University of Alabama, and ANL. Of these, only the COMMIX-SA code developed at ANL provides information useful to tank designers.

The objectives of this ANL project are to measure thermal stratification in thermal storage tanks, analyze the experimental results, and develop a semi-empirical model of stratification. End products of the effort will be (1) experimental data for validation of the COMMIX-SA computer code and (2) guidelines incorporating the semi-empirical model for designers of thermally stratified tanks.

b. Accomplishments

Elementary analysis has shown that modifications of the conventional collection strategy will be necessary to achieve good stratification. Five baffle and diffuser configurations have been tested in a tank similar in size and shape to a domestic water heater. These tests have provided data that indicate directions for improving COMMIX-SA. Results of tests have shown that vertical baffles degrade thermal stratification rather than enhance it. In the absence of vertical baffles, temperatures are nearly constant in any horizontal plane within the tank, except near the inlet and outlet. Most of the mixing in the tank occurs near the inlet and outlet, with little mixing occurring in between. A semi-empirical model of tank performance based on identification of the mixing region is being developed.

2. Testing Latent Heat Storage

a. Objectives

Approximately twelve manufacturers have latent heat storage (LHS) units on the market or nearly ready to be marketed. Although most manufacturers have thoroughly tested their units, there is little agreement as

to the best test methods and format for reporting results. One point of agreement, however, is that the ASHRAE 94-77 test standard was intended primarily for sensible heat storage and has many shortcomings when applied to LHS.

The objectives of this project are (1) to develop a procedure for testing LHS units and (2) to test commercially available LHS units in cooperation with Oak Ridge National Laboratory (ORNL) and report on the results. Results are expected to indicate the industry-wide performance levels of LHS units. Knowledge gained from testing will be used to suggest improvements in existing test standards.

b. Accomplishments

The ASHRAE 94-77 standard has been reviewed and its shortcomings noted. A preliminary procedure for testing an LHS unit based on measuring its heat-exchanger effectiveness is being developed with the aid of a computer analysis of the freezing-melting phenomenon of the storage material. A small LHS unit has been purchased for bench-scale tests to prove the merits of the preliminary test procedure. When the preliminary test procedure has been proven, a final test procedure will be written and published. ORNL will do full-scale testing, using the final test procedure, and results will be published jointly by ANL and ORNL.

3. Development of a Thermal Energy Storage Device Using Cross-Linked High-Density Polyethylene

a. Objective

Cross-linked high-density polyethylene (HDPE) has been developed as an LHS material by Monsanto Corp. and the University of Dayton. In the form of pellets, HDPE changes phase at 130°C, has a latent heat of 193 J/g (46 cal/g), and does not change shape or fuse at temperatures up to 150°C. The objective of this project is to design and build a prototype LHS device using HDPE as a storage medium. Approximately 6,800 kg (15,000 lb) of the HDPE is presently being manufactured and will be freely available for the prototype. Such a storage device can be used for solar-powered air-conditioners ("chillers") and industrial processes requiring heat at temperatures up to 130°C.

b. Accomplishments

Properties of HDPE have been reviewed and chiller characteristics have been evaluated. The prototype LHS unit will be designed to power a 3-ton chiller and will use ethylene glycol, water, or a mixture of the two fluids as a heat-transfer fluid. The container will be an ASME-rated pressure vessel of approximately 2.65-m^3 (700-gal) capacity. Approximately 1,700 kg (3,800 lb) of HDPE will be required.

VIII. FAST REACTOR CHEMISTRY

A. Reactor Fuels Chemistry

The gas-cooled fast reactor (GCFR) program is an incremental program that relies heavily on LMFBR base technology. However, some features, namely, the use of vented fuel pins, roughened cladding, helium coolant, and direct contact between the primary coolant and the steam generator, are unique to the GCFR. Studies are being made to evaluate the effect of GCFR conditions on fuel-pin performance. These studies show that successful utilization of the unique GCFR design features requires an understanding of the complex chemistry and transport phenomena occurring under the large temperature gradients that exist within the uranium-plutonium oxide fuel pin.

The large radial temperature gradients ($\gtrsim$500 K/mm) typical of GCFR mixed-oxide fuel pins will induce substantial oxygen redistribution within the fuel as a result of thermomigration effects. A steady-state oxygen profile will develop when the diffusive flux of oxygen is balanced by the opposing flux arising from the existing temperature gradient. The resulting variation in the local oxygen potential is a significant factor in determining the extent to which fission products (such as cesium and molybdenum) react with each other as well as with the fuel and the cladding. Such reactions can conceivably lead to swelling of the fuel pin and, hence, to potentially detrimental blockage of gas-flow transport paths.

1. Oxygen Solid-State Thermomigration and Its Heat of Transport

It is believed that, under a temperature gradient,[1] solid-state thermomigration is mainly responsible for oxygen as well as actinide redistribution in mixed-oxide fuel. A common assumption is that oxygen in hypostoichiometric mixed-oxide fuel pins migrates via a vacancy mechanism. Since the oxygen self-diffusion coefficient is expected to be several orders of magnitude larger than that of the metal ions, the problem can be reduced to that of oxygen migrating in its own sublattice. In this case,[2] if one makes appropriate choices in defining the generalized thermodynamic driving forces that are responsible for matter fluxes, then one can obtain the following equation for the steady-state vacancy distribution profile:

$$\frac{dx}{dT} = \frac{Q_V^* \cdot \left(1 - \frac{x}{2}\right) x}{\left(1 + \frac{\partial \ln \gamma_V}{\partial \ln C_V}\right) RT^2} \qquad (1)$$

Here, γ_V is the oxygen-vacancy activity coefficient, $x/2 = C_V$ represents the deviation from stoichiometry, Q_V^* is the oxygen-vacancy heat of transport, R is the gas constant, and T is the absolute temperature. The term Q_V^* is a convenient quantity to work with since it isolates the "dynamical" aspect of the heat of transport due to vacancy migration.

---

[1] See e.g., F. A. Nichols, J. Nucl. Mater. 84, 1 (1979) and references therein.

[2] See e.g., R. E. Howard and A. B. Lidiard, Rep. Prog. Phys. 27, 161 (1964).

The heat of transport for oxygen vacancies, Q_V^*, has an important bearing on the local oxygen-to-metal (O/M) ratio. This is particularly true for the approximately stoichiometric condition near both the surface of the fuel element and the interface of the fuel with the fuel blanket. As a result of thermal migration, the local O/M ratio is fairly close to stoichiometry at both locations. A relatively small variation in the value of Q_V^* can lead to a small but significant change in the local oxygen potential. The sensitivity of the local O/M ratio to variation in Q_V^* near the fuel element surface is shown in Fig. VIII-1 (initial O/M = 1.98), wherein a change in Q_V^* from 5 to 20 kcal/mol leads to a change in O/M from 1.992 to 2.000, respectively. Thus, Q_V^* is a quantity of significant interest in determining oxygen redistribution and, consequently, local O/M variation.

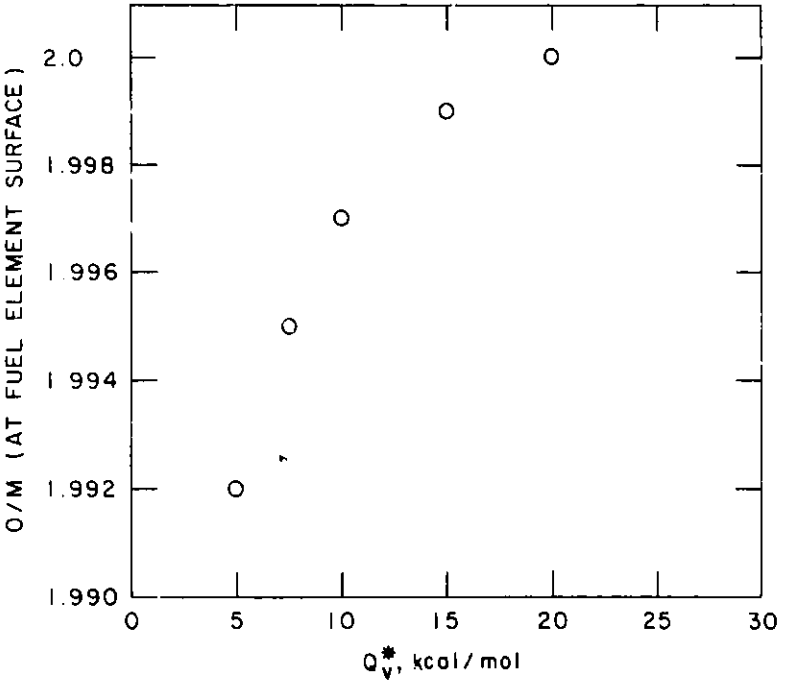

Fig. VIII-1. Sensitivity of O/M Near Fuel Element Surface to Q_V^* (at stoichiometry)

In most experiments in which the heat of transport is measured, the thermodynamic factor $1 + \partial \ln \gamma_V / \partial \ln C_V$ is approximated by unity. In other words, the actual quantity measured has been Q', where

$$Q' = Q_V^* / (1 + \partial \ln \gamma_V / \partial \ln C_V) \qquad (2)$$

An analysis of Q' will involve some understanding of both Q_V^* and the thermodynamic factor $1 + \partial \ln \gamma_V / \partial \ln C_V$. The term Q_V^* is the oxygen-vacancy heat of transport in the limiting case of zero vacancy concentration and governs the magnitude of Q' when the oxygen-vacancy concentration, C_V, is small.

2. Oxygen Heat of Transport at Stoichiometry

Let us consider a single vacancy in a system at a certain temperature T. For this vacancy to jump to a nearest neighbor position, a sufficient local concentration of vibrational energy must exist around the vacancy. This vibrational energy may result from atomic thermal fluctuations in the region surrounding the vacancy. This amount of energy is dissipated and dispersed to the rest of the lattice after the jump, when the vacancy has reached equilibrium with its new surroundings. Thus, this energy precisely represents the migration energy, $E^m_{O_v}$. The contribution to the heat of transport from $E^m_{O_v}$ v(t), where v(t) is the average velocity of this energy flux at time t, can be estimated as follows:

$$Q^*_v = \frac{-2}{a} E^m_{O_v} \int_o^\infty v(t)\, dt$$

$$= \frac{-2}{a} E^m_{O_v} [d(\infty) - d(o)] \qquad (3)$$

If one assumes that the saddle point for the jump is situated halfway between the initial and final stable positions for the vacancy, then d(o) = a/2, where a is the jump distance. The term d(∞) represents the distance from the initial vacancy position to the position where (1) all the energy associated with a successful jump has been transported to and dissipated in the lattice and (2) the vacancy has returned to equilibrium with the surroundings after the jump. If one assumes that all the energy transported (i.e., $E^m_{O_v}$) is dissipated at the final stable site, then d(∞) = a. Thus, we have $Q^*_v = -E^m_{O_v}$. This is in agreement with the earlier analysis of Le Claire,[3] Brinkman,[4] and Allnatt and Rice.[5]

In a real solid at a finite temperature T, the portion of the energy that propagates away from the final stable site decays via anharmonic damping (i.e., phonon-phonon interaction). The extent to which this occurs is characterized by the phonon relaxation time, τ_{ph}, of the material involved. It is expected that, for ionic materials, one can write Q^*_v in the following form:

$$Q^*_v = -\left[\alpha E^m_{O_v} + Q^*_I\left(\omega\tau_{ph}\right)\right] \qquad (4)$$

Here, α is a factor set by the extent to which the effective jump distance differs from a/2, ω is the characteristic Debye frequency (about 10^{13} s^{-1}), $E^m_{O_v}$ is the migration energy of the entity, and Q^*_I represents the contribution to Q^*_v from phonon damping.

---

[3] A. D. Le Claire, Phys. Rev. 93, 344 (1954).

[4] J. A. Brinkman, Phys. Rev. 93, 345 (1954).

[5] A. R. Allnatt and S. A. Rice, J. Chem. Phys. 33, 573 (1960).

Precise values for α and Q_I^* can only be obtained through detailed molecular dynamics simulation and/or experiment. The few computer simulations[3,6,7] that are presently available indicate that $\alpha \approx 1$ (in fact, it ranges from 0.8 to 1.33) and that $Q_I^* \approx \alpha E_{O_V}^m$. As yet, no such simulation is available on materials of the actinide mixed-oxide type (of the fluorite structure) and at the high-temperature regime (about 2000 K) that is of interest to us. However, we believe that the physical picture described above, culminating in Eqs. 3 and 4, is basically correct.

3. Oxygen Heat of Transport at Off-Stoichiometry

It is also important to examine the behavior of Q_V^* away from stoichiometry. Experimental measurements[8] have shown that Q' decreases as the value of x, the deviation from stoichiometry, increases. Although the data possess a fairly wide range of scatter, it is clear from the measurements that Q' decreases with x and vanishes somewhere around an $O/M \sim 1.93$. Figure VIII-2 shows these experimental measurements as a function of the mean Pu valence, $V_{Pu} = \left(4 - \frac{2x}{y}\right)$; based upon this figure, one can say that Q' decreases with decreasing V_{Pu} to a point where it becomes very small near the trivalent state of plutonium. We have chosen to resolve this puzzling phenomenon in terms of the defect thermodynamics of mixed-oxide fuels. Once that has been achieved, only one parameter, Q_V^*, is required to analyze the problem of oxygen thermomigration in mixed-oxide fuel.

The quantity $1 + \partial \ln \gamma_V / \partial \ln C_V$ represents the nonideality of the oxygen vacancies in the mixed-oxide fuel. As such, the deviation from unity of this quantity is a result of complicated chemical interaction and defect complex formation within the mixed oxide. The nature of the oxygen defect structure in (U,Pu) mixed oxide is highly controversial. For example, defect complexes such as $(Pu^{3+})_2 O_V$ and $Pu^{3+} O_V$ have been proposed,[9-14] where O_V is an oxygen vacancy.

Thus, we have proceeded with the following points in mind. Firstly, in calculating oxygen thermomigration in $(U,Pu)O_{2-x}$, we shall retain, to the

---

[6] H. B. Huntington, J. Phys. Chem. Solids 29, 1641 (1968).

[7] H. B. Huntington, M. D. Feit, and D. Lortz, Crystal Lattice Defects 1, 193 (1970).

[8] C. Sari and G. Schumacher, J. Nucl. Mater. 61, 192 (1976).

[9] F. Schmidt, J. Nucl. Mater. 58, 357 (1975).

[10] C. R. A. Catlow, J. Nucl. Mater. 74, 167 (1978).

[11] L. Manes and Hj. Matzke, J. Nucl. Mater. 74, 167 (1978).

[12] D. I. Norris, J. Nucl. Mater. 79, 118 (1979).

[13] D. I. Norris, Proc. Int. Conf. on Fast Breeder Reactor Fuel Performance, March 5-8, 1979, Monterey, California.

[14] D. I. Norris, Proc. Third Europhysics Topical Conf. on Lattice Defects in Ionic Crystal, Sept. 17-21, 1979, University of Kent at Canterburg, U.K.

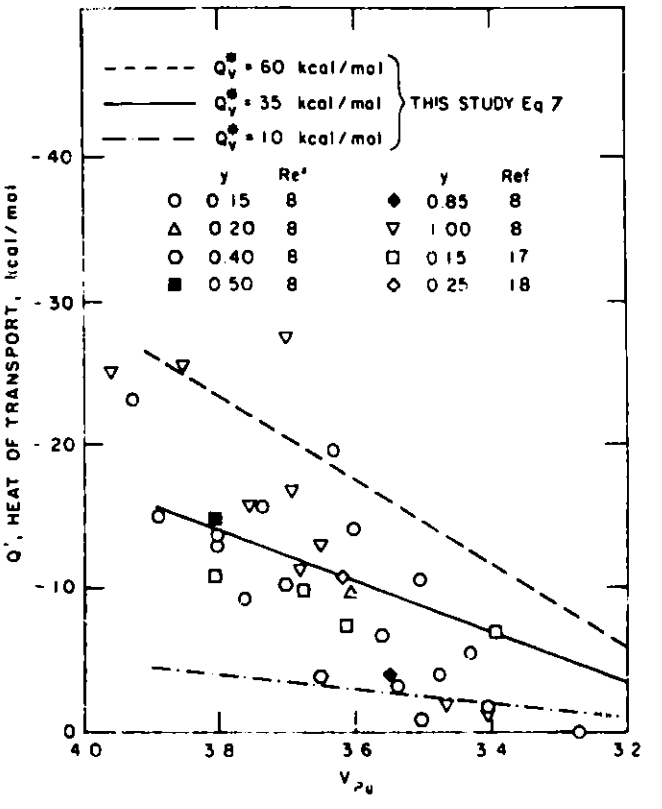

Fig. VIII-2. Effective Heat of Transport of Oxygen Vacancies as Function of Plutonium Valency

extent possible, the simple vacancy/interstitial picture in the oxygen sublattice. Secondly, we have related the thermodynamic factor $1 + \partial \ln \gamma_V / \partial \ln C_V$ to the oxygen partial pressure, P_{O_2}, which is one of the major thermodynamic quantities that has been extensively measured[15] for the mixed oxide.

To obtain the dependence of Q' on stoichiometry, the following two relationships[15-16] were utilized:

$$1 + \frac{\partial \ln \gamma_V}{\partial \ln C_V} = -\frac{1}{2} \frac{\partial \ln P_{O_2}}{\partial \ln C_V} \tag{5}$$

$$\ln P_{O_2} = 4 \ln \frac{y - 2x}{2x} + \ln K \tag{6}$$

[15] C. E. Johnson et al., Chemical Engineering Division Fuels and Materials Chemistry Annual Report, July 1973-June 1974, Argonne National Laboratory Report ANL-8122 (January 1975).

[16] C. E. Johnson and S. W. Tam, in Reactor Development Program Progress Report, August 1980, Argonne National Laboratory Report ANL-RDP-98, p. 5.1 (October 1980).

Here, C_v is the oxygen-vacancy concentration, y is the fractional plutonium concentration, P_{O_2} is the oxygen partial pressure, and K is independent of C_v. Both relationships are reasonably accurate for $x \gtrsim 0.01$ and moderate temperature.

On this basis, one would expect that the experimentally measured Q' (using Eq. 2) varies with V_{Pu} in accordance with

$$Q' = Q_v^* \quad \frac{(V_{Pu} - 3)}{2} \tag{7}$$

The results as described by Eq. 7 are shown in Fig. VIII-2, along with experimental data[8,17,18] in the range of 20-60 kcal/mol for Q_v^*. Based upon Fig. VIII-2, the following observations were made. Equation 7 accounts for the dramatic decrease of Q' with decreasing V_{Pu}. Further, Eq. 7 shows that Q' will vanish around $x = y/2$, a composition at which all Pu^{4+} has been converted to Pu^{3+}. Most of the data are bounded by the lines calculated for $Q_v^* = 10$ and 60 kcal/mol; however, a value for Q_v^* of 35 kcal/mol ($x > 0.01$) seems to reproduce the trend of the data best. Despite the data scatter, which is typical of heat of transport measurements,[18] the decreasing trend and the vanishing of Q' with V_{Pu} represent unmistakable characteristics which are accounted for by Eq. 7 in a natural manner.

In conclusion, we have shown that, when proper account is taken of the thermodynamic factor $1 + \partial \ln \gamma_v / \partial \ln C_v$, the result gives a natural description of the experimental measurements of the decreasing trend of Q' with V_{Pu}. The crucial result of the model is the prediction that Q' will vanish at $V_{Pu} = 3$, which correlates well with the data shown in Fig. VIII-2.

B. High-Temperature Physical Properties Studies for Reactor Safety Analysis

1. Compilation and Extrapolation of Thermophysical Data to Very High Temperatures

In modeling reactor accidents, reactor safety analysts need to know the thermophysical properties of reactor materials (such as coolants, fuels, and structural materials) from room temperature to very high temperatures (about 6000 K).

To provide reliable recommended values of these properties for safety analysts, we assess the available experimental data, fit the data by various methods (e.g., least-squares technique), and perform calculations using thermodynamic relations as well as approximation and extrapolation techniques when necessary. All recommended property values have been examined to ensure thermodynamic consistency. Theoretical consistency with regard to the dominating phenomena is another important criterion in the choice of the mathematical formulation of equations to fit property data. In addition to recommending

---

[17] M. G. Adamson, E. A. Aitken, S. K. Evans, and J. H. Davies, Thermodynamics of Nuclear Materials 1974, Proc. IAEA Symp., Vienna, 1975, p. 39.

[18] A. B. Lidiard, Proc. IAEA Symp. on Thermodynamics, Vienna, July 1965, Vol. II, p. 3.

values of thermophysical properties, we also provide the safety analyst with an estimation of the uncertainty in the recommended values. These uncertainties are determined from experimental uncertainties when provided, from the error in fitting the data, and from the estimated uncertainties in any approximations or extrapolation techniques used in the calculations.

The thermodynamic properties of sodium previously recommended by Padilla[19] have been updated by us. We have determined the thermodynamic properties of sodium (1) for the saturated liquid and vapor and the subcooled liquid from room temperature to the critical point (2509 K) and (2) for the superheated vapor from room temperature to 1600 K. The low temperature for the latter case was necessitated by the limitations of the quasi-chemical model of Golden and Tokar[20] used in these calculations. For saturated sodium, transport properties were also determined.

Our recommended properties of sodium have been documented in an ANL report, Thermophysical Properties of Sodium,[21] which tabulates the recommended values, provides the equations used and the errors, and discusses the methods used to determine the properties. Furthermore, the computerized codes used in the calculation of these properties have been documented.[22] Copies of both reports have been sent to colleagues in the United Kingdom, who will make comparisons with the recommenda ions of sodium properties by scientists in the United Kingdom, France, and the Federal Republic of Germany; in this way, international agreement on the values used for these properties can be reached. A magnetic tape of the property values and the computer codes used to calculate them have been sent to Oak Ridge National Laboratory, where the property values have been included in a data base entitled Safety Analysis Computerized Reactor Data (SACRD).

Experimental data on the thermophysical properties of UO_2 have been reexamined, and preliminary reports on the thermodynamic and transport properties of UO_2[23,24] have been distributed for comments and review by experts in

---

[19] A. Padilla, Jr., Extrapolation of Thermodynamic Properties of Sodium to the Critical Point, Proc. Seventh Symp. on Thermophysical Properties, National Bureau of Standards, Gaithersburg, Maryland, May 10-12, 1977, pp. 887-895.

[20] G. H. Golden and J. V. Tokar, Thermodynamic Properties of Sodium, Argonne National Laboratory Report ANL-6323 (1967).

[21] J. K. Fink and L. Leibowitz, Thermophysical Properties of Sodium, Argonne National Laboratory Report ANL-CEN-RSD-79-1 (May 1979).

[22] J. K. Fink, Computer Codes Used in the Calculation of High-Temperature Thermodynamic Properties of Sodium, Argonne National Laboratory Report ANL-CEN-RSD-79-2 (December 1979).

[23] J. K. Fink, M. G. Chasanov, and L. Leibowitz, Thermodynamic Properties of Uranium Dioxide, Argonne National Laboratory Report ANL-CEN-RSD-80-3 (December 1980).

[24] J. K. Fink, M. G. Chasanov, and L. Leibowitz, Transport Properties of Uranium Dioxide, Argonne National Laboratory Report ANL-CEN-RSD-80-4 (December 1980).

the field prior to formal publication. In these reports, significant changes in the recommended values of thermophysical properties of UO_2 have been made for the enthalpy and heat capacity as well as the thermal conductivity and diffusivity.

Past assessments[25,26] of the experimental data on enthalpy and heat capacity of UO_2 have fit the data to a three-term equation recommended by Kerrisk and Clifton[25] (K-C). The first two terms of this equation represent contributions from phonons and thermal expansion. The third term contains an anomalous contribution, which is not included in the first two terms and which is attributed to Frenkel defects. Recently, Rand et al.[26] used the K-C equation to fit the data to 2670 K and a linear equation above this phase-transition temperature, and Young[27] and Harding et al.[28] suggested that the anomalous contribution is due to an electronic contribution.

During the previous year, we compared the fit of the enthalpy and heat-capacity experimental data to the following mathematical formulations: (1) the K-C equation from 298.15 to 3120 K (the melting point); (2) the K-C equation with an electronic term for the anomalous contribution; (3) the two-equation Rand formulation; and (4) the Rand formulation with an electronic term in the nonlinear equation to represent the anomalous contribution. We found that the data were best fit by the formulation in item 4, with a phase transition at 2670 K as proposed by Rand.[26] In addition to providing the best fit, this formulation is theoretically consistent with thermal-conductivity data.

The thermal-conductivity and thermal-diffusivity data of UO_2 have been analyzed by us to ensure thermodynamic and theoretical consistency with respect to enthalpy, heat capacity, and density. Thermal conductivities were calculated from measured thermal diffusivities, our new heat capacities, and densities based on the data of Christensen.[29] Then, the combined data (measured thermal-conductivity data and thermal-conductivity data calculated from thermal-diffusivity data) were fit using a nonlinear least-squares technique.[30] Various forms of equations, based on different phenomenological assumptions, were tried; and it was found that the data are best fit by a two-term nonlinear equation below 2670 K and a linear equation above the transition temperature.[24] The two terms of the nonlinear equation represent contributions from phonons and electrons.

---

[25] J. F. Kerrisk and D. G. Clifton, Nucl. Tech. 16, 531 (1962).

[26] M. H. Rand, R. J. Ackermann, F. Grønvold, F. L. Oetting, and A. Pattoret, Int. Rev. Hautes, Temp. et Refract. 15, 355 (1978).

[27] R. A. Young, J. Nucl. Mater. 87, 283 (1979).

[28] J. H. Harding, P. Masri, and A. M. Stoneham, J. Nucl. Mater. 92, 73 (1980).

[29] J. A. Christensen, J. Am. Ceram. Soc. 40, 607 (1963).

[30] P. R. Bevington, Data Reduction and Error Analysis for the Physical Sciences, McGraw-Hill, New York, NY (1969).

Previous assessments[31,32] of the thermal conductivity of UO_2 recommended a three-term nonlinear equation whose terms represent contributions from phonons, electrons, and a conduction decrease due to dislocations. We found that, statistically, the data do not justify the inclusion of the dislocation term. In addition, the two-equation formulation recommended by us fits both the thermal-conductivity and thermal-diffusivity data better and is consistent with the theoretical basis of the equations that we derived for enthalpy and heat capacity.

Future plans include (1) completion of the reports on the thermophysical properties of UO_2, (2) inclusion of the recommended thermophysical property values of UO_2 in the data base (SACRD), (3) assessment of available experimental data and recommendation of thermophysical properties of the mixed oxides $(U,Pu)O_2$, and (4) determination of equations to represent the enthalpy and heat capacity of all the alkali metals.

2. Thermodynamic Functions of Fuel-Vapor Species at Very High Temperatures

Thermodynamic functions for fuel-vapor species at high temperatures (up to 6000 K) are needed in the analysis of hypothetical reactor accidents. These functions can be calculated by means of statistical mechanics. The molecular energy levels used in the calculations come from spectroscopic measurements. The thermodynamic functions obtained by this method are believed to be more reliable for vapor-pressure calculations at high temperatures than functions obtained by extrapolation of lower temperature data or by experimental methods that have not been calibrated.

Our program combines an experimental part and a calculational part. The goal of the experimental studies is to obtain spectroscopic data on uranium, plutonium, and thorium oxides, nitrides, and carbides that are required for the calculations. The goals of the calculational studies are (1) to estimate data that are not experimentally available, (2) to estimate uncertainties in various contributions to calculated thermodynamic functions, and (3) to provide a consistent "best estimate" of the thermodynamic functions for fuel-vapor species.

In earlier studies at CEN, the matrix-isolation technique[33] was combined with Fourier-transform infrared spectroscopy[34] to determine the

---

[31] J. C. Weilbacher, High Temperatures-High Pressures 4, 431-438 (1972); J. C. Weilbacher, Measurement of the Thermal Diffusivity of Mixed Uranium and Plutonium Oxides, CEA-R-4572, Centre d'Etudes Nucléaire de Fontenay-aux-Roses, France (1974).

[32] R. Brandt and G. Neuer, J. Nonequilibrium Thermodyn. 1, 3-23 (1976).

[33] B. Meyer, Low Temperature Spectroscopy, American Elsevier, New York (1971).

[34] D. W. Green and G. T. Reedy, in Fourier Transform Infrared Spectroscopy: Applications to Chemical Systems, Vol. 1, J. R. Ferraro and L. J. Basile, Eds., Academic Press, New York (1978).

molecular geometries and to measure the stretching mode frequencies of uranium oxides,[35,36] uranium nitrides,[37] thorium oxides,[38] plutonium oxides,[39] plutonium nitrides,[40] and thorium nitrides.[41] For each observed polyatomic molecule, the molecular geometry, which is an essential parameter for the calculation of thermodynamic functions, was determined by using ^{18}O or ^{15}N substitution.

More recently, the low-frequency vibrational modes of both UO_3 and UO_2 were observed[42] in argon matrices at 14 K. The absence of measured frequencies for these modes was previously a major source of uncertainty[43] in the calculation of the thermodynamic functions of the uranium oxide vapor species. These measurements, together with previous results,[35,36] give all the required vibrational frequencies for both UO_3 and UO_2 either from direct measurement or from calculations that result from the analysis of the measurements.

Examination[44] of the relationship between the available spectroscopic data and the evaluated thermodynamic functions for gaseous uranium, plutonium, and thorium oxides showed the need for revision of some data. New $\Delta H_f^\circ(298.15\ K)$ values that were consistent with spectroscopic data were derived[45] for each of the gaseous oxides. These ΔH_f° values as well as measured spectroscopic data, derived molecular structures, estimated bond lengths, and a model[44] of the electronic structures were used to calculate[46] thermodynamic functions of the gaseous uranium, plutonium, and thorium oxides.

---

[35] S. D. Gabelnick, G. T. Reedy, and M. G. Chasanov, J. Chem. Phys. 58, 4468 (1973).

[36] S. D. Gabelnick, G. T. Reedy, and M. G. Chasanov, J. Chem. Phys. 59, 6397 (1973).

[37] D. W. Green and G. T. Reedy, J. Chem. Phys. 65, 2921 (1976).

[38] S. D. Gabelnick, G. T. Reedy, and M. G. Chasanov, J. Chem. Phys. 60, 1167 (1974).

[39] D. W. Green and G. T. Reedy, J. Chem. Phys. 69, 544 (1978).

[40] D. W. Green and G. T. Reedy, J. Chem. Phys. 69, 552 (1978).

[41] D. W. Green and G. T. Reedy, J. Mol. Spectrosc. 74, 423 (1979).

[42] D. W. Green, G. T. Reedy, and S. D. Gabelnick, J. Chem. Phys. 73, 4207 (1980).

[43] D. W. Green, Calculation of the Thermodynamic Properties of Fuel-Vapor Species from Spectroscopic Data, Argonne National Laboratory Report ANL-CEN-RSD-80-2 (September 1980).

[44] D. W. Green, J. Nucl. Mater. 88, 52 (1980).

[45] D. W. Green, Int. J. Thermophys. 1, 61 (1980).

[46] D. W. Green, Tables of Thermodynamic Functions for Gaseous Thorium, Uranium, and Plutonium Oxides, Argonne National Laboratory Report ANL-CEN-RSD-80-1 (March 1980).

New thermodynamic functions for the condensed phase of uranium dioxide have been derived using the recommended[23] heat capacities for $UO_2(s)$ and $UO_2(\ell)$. A new method of extending the oxygen-potential model for UO_{2-x} is being developed at CEN. Oxygen pressures calculated from this model, together with the thermodynamic functions of the vapor species,[46] allow the calculation of vapor pressures and compositions for the uranium-oxygen system as functions of temperature and condensed-phase composition for $T \leq 6000$ K. Preliminary results[47] indicate that the vapor composition is very sensitive to both temperature and composition of the condensed phase, whereas the total pressure is relatively insensitive to both. Furthermore, the oxygen-to-uranium ratios of the vapor and condensed phases are unequal for $3000 \leq T \leq 6000$ K.

Future plans include (1) the measurement of the bending-mode frequency of ThO_2, (2) inclusion of the new oxygen-potential model in the calculations for the uranium-oxygen system, and (3) extension of the method to the plutonium-oxygen and mixed uranium-plutonium-oxygen systems.

3. Enthalpy of Thoria/Urania Fuels

Enthalpy measurements for thoria/urania fuels are being performed for Westinghouse Electric Corporation's Bettis Atomic Power Laboratory in an induction-heated drop-calorimetric system which was developed to measure the enthalpies of the reactor fuels. This system is capable of operation up to 3500 K, using tungsten as the capsule material. Currently, work is being performed on ThO_2–30 wt % UO_2, ThO_2–15 wt % UO_2, ThO_2–8.36 wt % UO_2, and ThO_2 in the temperature range of 2300 to 3400 K. Published experimental enthalpy data for ThO_2 are available up to 2773 K,[48] and experimental enthalpy data for $(Th_{0.9}U_{0.1})O_2$ are available only to 2270 K.[49]

For these enthalpy experiments, a sample sealed in a tungsten capsule is suspended in an induction coil, and the capsule is heated to the desired temperature. When temperature equilibrium has been reached, the hot capsule is dropped into an adiabatic calorimeter. The temperature rise in the calorimeter is measured with a quartz thermometer. The procedure is repeated with an empty capsule, and the enthalpy of a sample found by the difference between the heat for the full capsule and the empty one.

A series of measurements of the apparent enthalpy was carried out on an empty capsule at temperatures from approximately 2175 to 3400 K. Duplicate runs were found to agree within less than 0.5%. In a standardization series of tests, enthalpy measurements were performed at temperatures between

---

[47] D. W. Green and L. Leibowitz, in Reactor Development Program Progress Report, Argonne National Laboratory Reports ANL-RDP-84, p. 2.51 (June 1979) and ANL-RDP-85, p. 2.25 (July 1979).

[48] M. Hoch and H. G. Johnson, J. Phys. Chem. 65, 1184 (1961).

[49] J. R. Springer, E. A. Eldridge, M. U. Goodyear, T. R. Wright, and J. F. Lagedrost, Fabrication, Characterization and Thermal-Property Measurements of ThO_2–UO_2 Fuel Materials, Battelle Memorial Institute Report BMI-X-10210 (October 1, 1967).

about 2200 and 2800 K for a molybdenum standard reference material (781) which had been obtained from the National Bureau of Standards (NBS). The results agreed with NBS data to within about 1%. The uncertainty in the enthalpy data reported by NBS is about ±1.5% at 2500 K. In addition, standardization enthalpy measurements of UO_2 were made at 2729, 2595, and 2800 K. The results were within -0.45, +0.49, and -0.48%, respectively, with published data.[23] This is considered satisfactory agreement.

Enthalpy measurements have been made on $(Th_{0.7}U_{0.3})O_2$ between 2300 and 3200 K and on ThO_2 between 2500 and 3221 K. The data are shown in Fig. VIII-3 and compared with literature data[48] for ThO_2. Note that a transformation occurs between 2900 and 3000 K; this finding agrees with the prediction of Bredig[50] that disordering of the anion lattice will occur in solids with a fluorite-type structure. Work is continuing on these ThO_2-UO_2 systems and consideration is being given to future work on UO_2-PuO_2 systems.

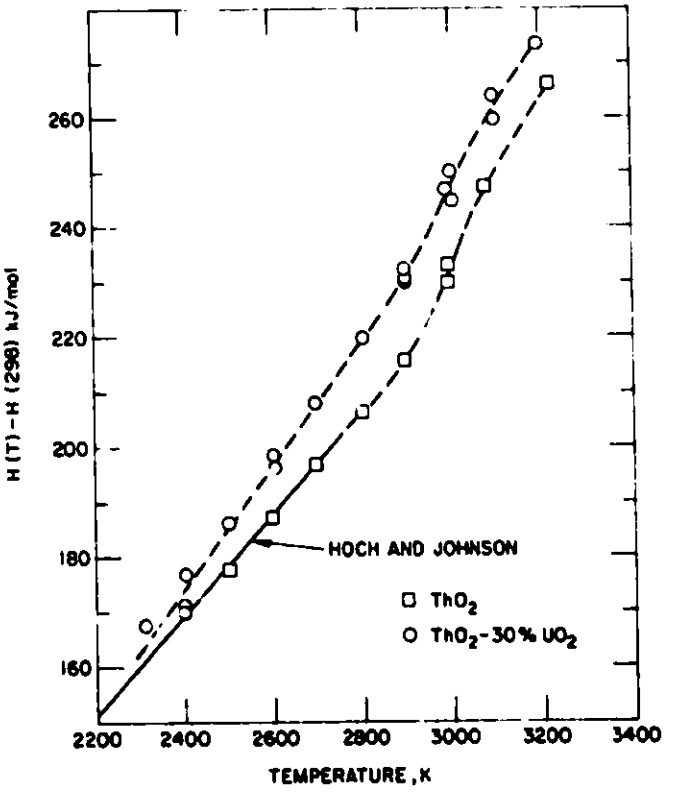

Fig. VIII-3. Enthalpy of ThO_2 and ThO_2-30% UO_2

[50] M. A. Bredig, Coll. Int. sur l'études des transformations crystalline à hautes températures, Odeillo, p. 41 (1971).

C. Sodium Technology

1. Cold-Trap Optimization

Sodium impurities, particularly Na_2O and NaH, are normally controlled by low-temperature precipitation in cold traps. In small- and medium-scale sodium systems such impurities are easily controlled by cold traps; however, in large LMFBR steam generators, hydrogen is introduced into the sodium at a high rate, imposing a significant burden on the cold traps. The hydrogen is produced by normal water-side corrosion of the steam-generator tubes and diffuses through the tubes into the sodium system. The objective of this work is to develop calculational and design methods to maximize the capacity of cold traps for retaining impurities, particularly NaH, while maintaining acceptable performance efficiency.

Cold-trap design optimization can best be achieved by developing a mathematical model for parametric design analysis. Such a model is being developed as part of this work. To develop the model, it was necessary to investigate the precipitation characteristics of NaH and Na_2O impurities. This investigation was done using a simple, small-scale cold trap and a one-dimensional computer model.

The one-dimensional computer model uses experimental data (e.g., temperature profiles, wire-mesh packing density, geometrical dimensions, and impurity concentrations) to calculate the distribution of impurity deposits within the cold trap. The model is based on the assumptions that: (1) no supersaturation is required for nucleation, (2) no homogeneous nucleation occurs, (3) impurity crystal growth is first order and proceeds according to $dm/dt = kA(C - C_e)$, where dm/dt is the rate of mass deposition on the crystal, k is the mass-transfer coefficient, A is the surface area, and C and C_e are the impurity concentration and the equilibrium concentration, respectively.

The results of model calculations were compared with results from impurity precipitation experiments. The impurity precipitation experiments were done using small, simple cold traps that consisted of 19-mm-dia stainless steel tubes, 560 mm long, with thermocouple wells along the center and air cooling on the exterior to establish a temperature gradient along the trap's length. These tubes were packed with stainless steel wire mesh to different densities, which provided extended surface area for impurity nucleation and growth. The impurity concentrations in the sodium entering and leaving the cold traps were measured continuously with on-line oxygen and/or hydrogen meters. Either oxygen or hydrogen, as appropriate, was injected into the upstream sodium to maintain a constant concentration at the cold-trap inlet. As the sodium was cooled, the impurity crystals precipitated along the temperature gradient in the cold trap.

After the experiments, the cold-trap tubes were cut apart in a helium-atmosphere glovebox. Each segment was analyzed for total hydrogen or total Na_2O content, and the impurity mass distributions thus determined were compared with the computer-model predictions.

The results of the experiments with NaH precipitation were in excellent agreement with the model predictions. The agreement was equally good over a wide range of wire-mesh packing densities, ranging from zero (no packing) to 0.47 mg/mm^3. The results of the Na_2O precipitation did not agree as well with predictions as did the NaH data. In one case, with no packing, the model predicted a deposition of 740 mg Na_2O in the trap, whereas only 3.1 mg was found deposited in the post-test analysis. In other cases, the total quantity of impurity found was in approximate agreement with the predicted quantity, but the distributions of the impurity in the trap were different. These differences are thought to be due to two causes: (1) inaccurate or drifting oxygen-meter calibration and (2) poor adhesion of the Na_2O crystals on the stainless steel surfaces.

Based on the results of these small-scale experiments, a more comprehensive two-dimensional computer model is being developed for calculating mass deposits in cold traps. This model will use information gained in the small-scale experiments; this information includes the first-order crystal growth equation, which was proven valid by the experiments, the observed increase in crystal surface area with increased mass of impurity deposition, and the tendency of Na_2O crystals to break away from smooth stainless steel surfaces.

2. Sodium Purification by Distillation

Use of sodium as a heat-transfer fluid in the LMFBR results in some degree of radioactive contamination of the sodium. The severity of this contamination can vary, depending on the circumstances of the reactor operation. In the event that several fuel-element cladding breaches occur and the activity in the sodium becomes too great to allow continued routine operation, it will be necessary to decontaminate the sodium. Sodium from decommissioned reactors may also require decontamination before reuse.

Over the past three years, we have explored several methods for decontaminating sodium. These methods include soluble gettering, electrochemical separation, reaction with various solids (including graphite), and low-pressure distillation. The radioactive species of primary concern in the decontamination studies are ^{137}Cs, fuel particles, and various fuel-coolant reaction products. Fission products of lesser concern include isotopes of barium, iodine, antimony, strontium, and tellurium. Of all the methods considered or tested for the removal of these species from sodium, the most promising appears to be low-pressure distillation.

One exception to this conclusion is removal of cesium from sodium by reaction with graphite. A reticulated vitreous carbon (RVC) trap was tested on EBR-II for control of ^{137}Cs activity in the sodium.[51] This trap was very successful in removing cesium; however, it is specific for cesium and it offers the possibility of introducing carbon-bearing impurities into the sodium.

---

[51] W. H. Olson and W. E. Ruther, in Reactor Development Program Progress Report, March 1977, Argonne National Laboratory Report ANL-RDP-59, p. 1.5 (May 1977).

A computer model was developed and used to calculate the fission-product separation factors that could be expected with the distillation method. The quantities of fission products in sodium are expected to be very low on a mass-fraction basis; therefore, these solutions were assumed to obey Henry's Law, and activity coefficients, when available in the literature, were used in the calculations. Using the computer model, a parametric study was done to determine the best design and operating conditions for maximizing fission-product separation.

Based on the computer-model calculations, a small-scale (102-mm dia) distillation column with total reflux was designed and tested. The column was entirely constructed of Type 304 stainless steel and packed with wire mesh. The testing results obtained with the 102-mm column were given in the preceding report in this series. Based on the success of these earlier tests, a larger (204-mm dia) distillation column was designed and tested. The 204-mm-dia column is composed of three packed sections, each 0.61 m high, as well as a reboiler at the bottom and a condenser at the top. Contaminated sodium is fed between the bottom and middle packed sections, and purified sodium is withdrawn between the middle and top packed sections. A very small stream is withdrawn from the bottom of the reboiler to minimize accumulation of heavy (low vapor pressure) fractions and particulates. A small stream is also withdrawn from the condenser to remove accumulated cesium.

The column has been operated with (1) nonradioactive sodium to determine its thermal performance and (2) radioactive sodium to compare achieved separations with the model calculations. To test the performance of the column with radioactive fission products, 1.2 mCi of ^{137}Cs and 0.34 mCi of ^{133}Ba were added to the sodium. Elemental nonradioactive cesium and barium were also added to help dilute the effect of undesirable surface interactions between the stainless steel and the fission products. Unfortunately, the barium apparently reacted with small amounts of Na_2O dissolved in the sodium and formed small BaO particles that adhered to the system surfaces. The ^{133}Ba thus became unavailable for separation measurements. A good separation of ^{137}Cs was achieved, but it was not possible to measure the precise separation factor because the ^{137}Cs in the purified sodium stream was below the background level and essentially all the cesium that had been added to the system rapidly accumulated in the condenser. This cesium continually recycled in the condenser and was unavailable for measurement of its activity.

The separations achieved in these tests were somewhat better than expected, although quantitative separation factors could not be determined. The separation factor achieved with the small-scale distillation column (given in last year's report) was approximately five times higher than that achieved with the RVC trap tested on EBR-II. The maximum measurable separation factor achieved with the large-scale column was approximately four times the RVC separation results. The concentrated accumulation of cesium in the condenser suggests that this type of separation system may be used not only to purify the contaminated sodium, but also to concentrate the fission products into more easily disposable quantities of sodium waste. Future work will concentrate on measuring the separation factors and comparing them with the model calculations. Other fission products will also be tested.

3. Sodium Waste Technology Program

Operation of LMFBRs has produced in the past, and continues to produce, radioactive sodium and sodium-containing radioactive waste. Disposal of this waste, until two years ago, had been deferred to future years. The primary difficulty of disposal of such waste is the danger of reaction of the sodium metal with moisture or oxygen to cause fires or explosions that might spread contamination. The objective of the program, therefore, is to develop processes and to build facilities at ANL-West that convert sodium and sodium-bearing waste to disposable forms.

During 1979, a literature survey and paper study were conducted to determine the most promising process for handling the waste sodium. The equipment for the selected process consists of a vessel for melting, draining, and evaporating elemental sodium from solid waste components; a storage vessel for accumulating waste sodium; an oxidation calciner for converting elemental sodium to the oxide; and a glass melting furnace for making a simple sodium silicate glass. This process, called the Melt-Drain-Evaporation-Calcination (MEDEC) process, is in the final design stage at ANL-West, and our work is in support of that program. Specific objectives of our work are to develop the oxidation calcining process for sodium and to determine the effectiveness of the evaporation process for removal of sodium from cold traps.

In the calcining process, a rotary-drum reactor is preloaded with a Na_2O bed and heated to 200°C. Elemental sodium is then introduced onto the bed and thoroughly mixed. Oxygen is slowly introduced to convert the sodium into the oxide. This process has been successfully operated on a medium scale, using a standard-size (55-gal) stainless steel drum as a reactor vessel for processing sodium in quantities of up to 2 kg per batch. The process is easily controlled and performs satisfactorily; however, care must be taken to avoid adding oxygen beyond the stoichiometric amount to prevent formation of Na_2O_2, which may react rapidly with subsequent sodium additions. This reaction can raise the bed temperature high enough to cause localized sintering.

A test of the evaporative method for removing sodium from a cold trap was successful. In this test, a small cold trap was loaded with Na_2O until sodium flow was blocked, using the apparatus for monitoring and purifying sodium (AMPS). The cold trap was then inverted and connected to a vacuum system having a drain tank and a sodium-vapor condenser. As the cold trap was heated, most of the sodium drained into the tank; and, on further heating, the residual sodium evaporated from the interior surfaces of the trap and from the oxide deposit. Post-test analysis indicated that less than 0.1% elemental sodium remained in the Na_2O deposits, with most analyses indicating about 0.03% Na. The bare metal surfaces were free of elemental sodium within the detection limit of the method (approximately 1 to 5 μg Na).

The Chemical Engineering Division's future work in the sodium waste technology program will be concentrated on developing methods for determining the end point of sodium evaporation, defining further the operating conditions of the calcining method, developing the low-pressure distillation method for waste-sodium recovery, and making additional tests of the evaporative method for the removal of sodium from cold traps.

IX. NUCLEAR FUEL CYCLE STUDIES

A. Nuclear Waste Management Studies

The Chemical Engineering Division's program on nuclear waste management is focused on high-level waste. During 1980, this CEN effort included investigations of (1) leaching that might occur from waste forms destined for geologic formations as well as the impact resistance of these waste forms, (2) the encapsulation of radioactive waste in a metal matrix, and (3) radionuclide migration from a breached nuclear-waste repository. In addition, geochemical studies are under way on the migration of trace elements in the earth's crust, which is only peripherally related to waste management, and on oil-well logging, for which no connection to waste management is appropriate.

1. Waste Form Characterization

It will be necessary for solidified radioactive waste to meet guidelines that establish the maximum permissible radioactive releases from final waste disposal sites or from accident scenarios. Of concern are releases that would result from (1) contact of the waste form with water and subsequent leaching, (2) mechanical impacts to the waste causing airborne releases and an increase in surface areas available for leaching, and (3) volatilization of waste-form constituents during an accident (high-temperature conditions).

Sensitive analytical techniques must be combined with well-defined experimental measurements and procedures to characterize the potential amount of material release. The analytical procedures must be designed to accommodate the diverse solid waste forms in simulated test environments and to allow results obtained at different laboratories to be compared. Sensitive analytical techniques and analysis methodologies are being developed as part of a national effort to measure the dispersion potential of solid waste forms. Two CEN programs that are part of this effort are described below.

a. Leachate Characterization

The leaching characteristics of solid waste forms are being measured with techniques designed to detect small amounts of radioactive elements transported from the waste. Radioactive species are introduced into the solid waste forms either by neutron activation or by the addition of small (trace-level) quantities of radioactive isotopes. In both cases, the species are detected by their radiations.

An extensive series of leach tests is being performed on three different simulated waste glasses: Battelle Pacific Northwest Laboratory (PNL) glass, designated PNL 76-68, and two Savannah River Laboratory (SRL) glasses, designated SRL frit 211 and modified SRL frit 211. These tests are being done to identify potential problem areas and to establish whether any variations in leach rates are observable for several methods of measuring

leach rates in glass. Additionally, the sensitivity, accuracy, limitations, and applicability of neutron activation analysis* (NAA) are being defined.

In our work to evaluate NAA for leach-rate measurements, we wished to establish whether effects due to neutron activation itself affect the observed elemental release. Consequently, leach tests are being done in deionized water on both neutron-activated and nonactivated waste specimens to allow direct comparison of specimens with different irradiation histories. Different analytical groups (at ANL and Ames Laboratory) analyzed the leachates from the nonactivated specimens for silicon and cesium by conventional solution analyses; the leachates from the neutron-activated specimens were analyzed at ANL by beta and gamma counting and also by conventional solution analyses. Comparison of the analytical results for the PNL 76-68 glass with results obtained by the Materials Characterization Center of PNL was also done. Comparison of the leach-rate data from the many tests done under controlled conditions showed no difference greater than 20% in the leach rates of activated and nonactivated samples. In addition, no significant effects on the leaching process due to neutron activation have been observed to date. It is tentatively concluded that the neutron activation method is a viable analytical method for measuring leach rates of simulated waste glasses.

Table IX-1 lists some elements in a typical waste glass (PNL 76-68) that could be detected by NAA, along with the associated sensitivity limits. In this table, the standard irradiation and radiation-counting conditions are given because the detection data are dependent on the standard conditions selected. No glass network-forming elements such as silicon and boron could be detected by the neutron activation method used. However, a representative group of waste elements, ^{141}Ce, ^{134}Cs, ^{152}Eu, ^{95}Zr, and ^{65}Zn, were measured with NAA at sensitivity levels exceeding those available when conventional spectroscopic detection methods are applied to solutions.

The applicability of NAA to waste forms other than glass has also been studied. Tests done on two alternative crystalline waste forms--supercalcine and SYNROC--indicate that the method can also be used on these materials.

In the above studies, NAA with gamma-ray analyses was found to be a viable method of monitoring the leaching process from solid waste forms. This method has enhanced sensitivity as compared with conventional detection methods and appears to be the only method capable of detecting rare earth elements that are present in low concentrations. To further improve the sensitivity and elemental applicability of NAA, the method can be used in conjunction with different irradiation and radiation-counting conditions and with radiochemical separations.

The type of evaluation procedure mentioned above for the NAA method is also being applied to glass-waste forms containing radioactive tracers. The addition of radioisotopes optimizes the gamma-ray analyses and thereby improves overall sensitivity. The effects, if any, of introducing

---

*Briefly, the neutron activation analysis technique consists of inducing radioactivity in a solid by neutron activation, measuring the quantity of this radioactivity, leaching the solid in an aqueous medium, and measuring the fraction of the radioactivity leached.

Table IX-1. Applicability of NAA to PNL 76-68 Glass

Conditions: PNL 76-68 glass and MCC-1 test conditions[1]
Sample Irradiations: flux, 3×10^{13} n_{th}/cm^2-s; time, 4 h
Counting Time: solid sample, 30 min; leachate, 900 min

Isotope Detected	Sensitivity, µg/mL	Minimum Detectable Normalized Elemental Loss, g/m^2
^{65}Zn	2.5×10^{-3}	3×10^{-3}
^{95}Zr	2×10^{-3}	1×10^{-2}
^{134}Cs	2×10^{-5}	3×10^{-4}
^{141}Ce	4×10^{-4}	4×10^{-3}
^{152}Eu	5×10^{-6}	8×10^{-4}

radioactive tracers into the leaching process will be quantified. In addition, leach rates of elements for which NAA is not applicable can be studied by the tracer method.

In the future, radioactive tracer and NAA techniques will be applied to characterize the volatilization of waste-form constituents under simulated accident conditions.

b. Brittle Fracture Studies

Mechanical impacts to solid wastes might occur during processing, handling, interim storage, and transportation. Standardized impact tests for characterizing the impact resistance of high-level waste forms are needed for technology assessment of alternative waste forms. As a result, a general methodology for characterizing impact fracture of brittle materials is being developed for evaluation of material properties and for use in accident analyses of large-scale waste systems. Because the chief safety concern is dispersibility of radioactive materials in accidents, two practical parameters have been selected for impact-fracture characterization: the total fracture surface area available for leaching and the quantity of fragments within the respirable particle-size range ($\lesssim$10 µm).

[1] D. M. Strachan, R. P. Turcotte, B. O. Barnes, L. A. Bray, and J. H. Westsile, Standard Leach Tests for Nuclear Waste Materials, Materials Research Symposium D--Scientific Basis for Nuclear Waste Management, Boston, MA, November 16-21, 1980.

As reported last year, a preliminary model for the brittle fracture process has been developed. This model is based on the repeated observation that particle-size distributions of small-scale specimens of brittle material (e.g., Pyrex cylinders with dimensions of 38-mm OD by 100 mm long) which have been mechanically impacted by a drop weight can be fitted to a lognormal distribution. Recently, lognormal particle-size distributions were found for vitreous materials, crystalline materials, glass ceramic materials, and even conglomerate brittle materials (e.g., sandstone and nephelene syenite). The granular conglomerates with weakly cemented grains showed some intergranular fracture and were included to examine the versatility of the model.

It was observed that the lognormal particulate distribution is described by three statistical parameters: geometric mean particle size (D_g), geometric standard deviation (σ), and a shape factor related to the surface area-to-volume ratio. In preliminary impact tests, these statistical parameters appeared to be correlated with the impact energy per unit volume of the impacted specimen and to be relatively independent of specimen size and drop-weight velocity.

The applicability of the lognormal fracture model is illustrated by the graphical presentation of particle-size measurements made at PNL for free-fall impact tests of full-scale (2.3 m long by 0.61-m OD) simulated waste-form canisters. Figure IX-1 is a plot of the glass-fragment distribution measured in two full-scale canisters of simulated waste glass. The "before impact" curve characterizes the particle-size distribution of as-fabricated glass in large waste canisters; fracture is primarily due to thermal shock during fabrication. The sieve data reported by PNL show a lognormal distribution up to about 7 mm. The "after impact" curve is the particle-size distribution for a canister dropped in free fall from a height of 7.6 m; these data also appear to have a lognormal distribution. By extrapolation of these data, a respirable particle-size fraction of 0.15 wt % was predicted; this agrees very well with the value of 0.13 wt % independently obtained by sedimentation analysis at PNL. Further, the mass mean diameter (D_g) in Fig. IX-1 is 3.4 mm, which agrees with the mass mean diameter of 3.7 mm obtained at PNL by sieve analysis. The upper line, $P_s(D)$, represents the cumulative surface area of the particulate in the canister. As shown, $P_s(D)$ has a lognormal distribution, with 97% of the total particulate surface area contained in particle sizes <4 mm. Finally, one can estimate from Fig. IX-1 that the effect of the 7.6-m drop was to increase the respirable particle-size fraction by two orders of magnitude. Unfortunately, PNL did not report any sedimentation-analysis results for the as-fabricated glass; consequently, the accuracy of this estimate cannot be confirmed. In summary, these results indicate that our fracture model, which was developed from tests of small-scale waste specimens, may be applicable to full-scale waste forms. Quantitative correlations of the parameters of the fracture model remain to be developed. In addition, methods of predicting accident consequences based on dynamic stress analyses are also being considered.

The results of this work are needed for material and accident evaluations by Savannah River Laboratory, Sandia Laboratory, and the Materials Characterization Center at PNL. To fill the gaps of our brittle fracture

model, additional experimental work must be done, including small-scale impact tests with different materials of various sizes and shapes. Comparisons of drop-weight and free-fall impact tests, including tests of small samples with and without canisters, are planned. Further evaluations of methods of measuring particle size (i.e., sieving, Coulter Counter analysis, BET surface area measurements, and scanning electron microscopy) will also be undertaken. Microscopic size analysis is being done (under a subcontract) by the Ceramic Engineering Department of North Carolina State University.

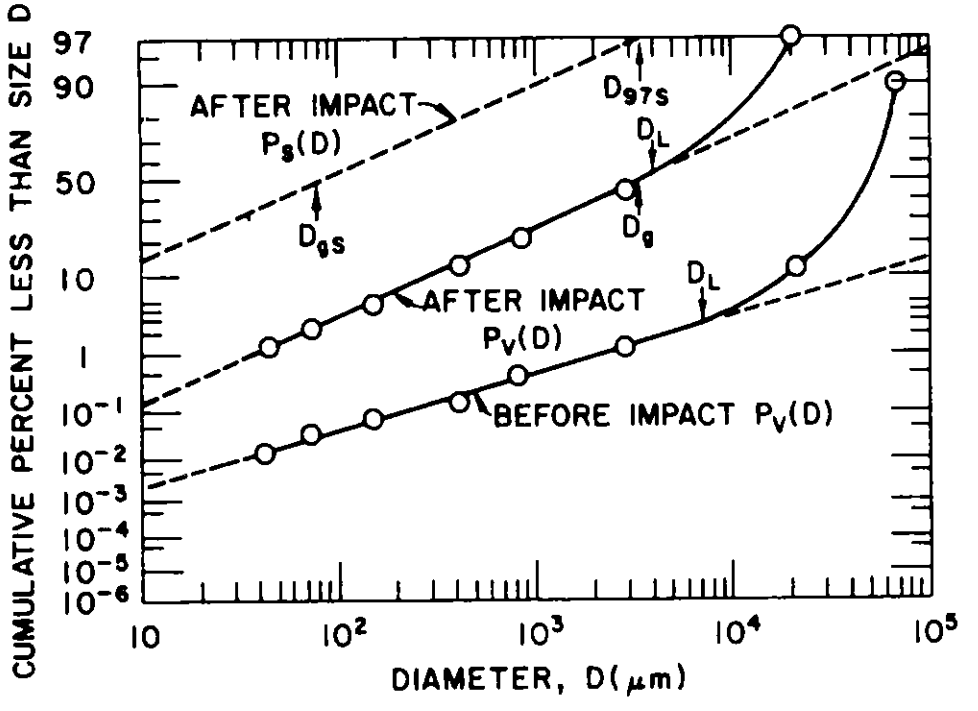

Fig. IX-1. Lognormal Analysis of Particle-Size Data Reported by PNL for 0.61-m-dia Canister of Class (before and after being dropped from 7.6 m onto an unyielding surface). The symbols are defined as follows: D_g is the geometric mean particle size, D_{gs} is the geometric mean of the surface distribution, D_L is the value of D at which the points begin to deviate from lognormal, $P_V(D)$ is the cumulative fraction of material volume as a function of D, $P_S(D)$ is the cumulative fraction of total surface area as a function of D, and D_{97_S} is the value of D for which the cumulative surface is 97% of the total surface area.

2. Metal-Matrix Encapsulation of Waste

Alternative waste forms that offer improved properties or simplified fabrication in comparison with glass monoliths are being developed by DOE-funded programs. Many of the alternative glass and crystalline waste forms are granular materials, which will probably require the use of other materials for consolidation to less dispersible forms. Encapsulation of such waste forms in a corrosion-resistant metal matrix that also has good impact resistance is one alternative that has been proposed. Glass waste made into small glass beads and encapsulated in a lead-alloy matrix is probably the most advanced consolidation concept. The use of glass beads, rather than large glass monoliths, would provide a means of enhancing quality assurance/control; and, if the beads are encapsulated in a lead-alloy matrix, recycle options for waste not satisfying disposal specifications are more easily envisioned. However, these features and the decreased dispersibility risks are gained at the expense of introducing unknown processing complexities absent from the relatively well-studied glass monolith process. Thus, quantification of this decreased dispersibility risk is needed to judge whether further process development is merited.

The Chemical Engineering Division has been assessing the advantages of encapsulating radioactive waste forms in metal matrices, as compared with using monolithic glass waste forms. The activities undertaken in this program over the past year are summarized below.

Impact tests of cylindrical composites (about 5-cm OD by 5 cm long) of glass beads and lead were conducted and the impacted composites examined. Axial impacts were delivered to these composites in two ways--either with a drop-weight impact device or by free-fall drop onto an unyielding surface. These tests showed that fracture of the glass beads occurs due to point contacts of the encapsulated beads, which cause high localized stresses to be formed. Protective envelopes of lead surrounding the composites were found to decrease fracture significantly, with fracture decreasing as the thickness of the envelope was increased. No differences in test results were observable for the drop-weight and free-fall impacts.

Leaching experiments were also performed with the glass beads-lead composites. Leach rates of neutron-activated glass beads encapsulated in a lead-alloy matrix were found to be lower than those for neutron-activated nonencapsulated glass beads. Furthermore, no significant difference in leach rates of impacted and nonimpacted composites was observed. Since impacted composites were known to contain fractured beads, these results imply that penetration of leachant into the interior of composites may be less a problem than previously postulated.

Experiments were performed to examine the compatibility of SRL glass with two lead alloys--"chemical lead" and lead-10 wt % tin. No significant chemical compatibility problems were observed when the mixtures of SRL glass and lead alloys were heated to temperatures below 700°C. However, the SRL glass formulation was found to soften enough at these temperatures to flow between mesh retainers and to float to the surface of the molten lead.

An economic study was conducted to compare the costs of metal-matrix encapsulation of waste with the costs for formation of a borosilicate glass monolith. The four principal waste-solidification methods among those evaluated were: (1) spray calcination of liquid waste followed by melting with crushed glass frit in a continuous glass melter to form a borosilicate glass monolith; (2) direct feed of liquid waste into a glass melter to form a glass monolith; (3) production of glass beads from a liquid-fed continuous glass melter, with the beads then being encapsulated into a lead metal matrix; and (4) spray calcination of liquid waste followed by agglomeration into supercalcine pellets, which are then sintered and encapsulated in a lead metal matrix. It was concluded that the largest single cost of any waste solidification alternative is the cost of the building and support structures. Costs due to equipment were only a small fraction of the total facility cost. Therefore, arguments for the selection of one process over another on the basis of equipment costs alone appear irrelevant. The two metal-matrix processes evaluated (glass beads in lead and supercalcine pellets in lead) had higher annual operating costs (i.e., labor, chemicals, and canisters) than did the glass monolith processes (spray calcination and direct liquid feed), but these costs were relatively small fractions of the annualized capital costs for the entire facility. The direct liquid-fed glass-monolith process had the lowest estimated cost; however, when the uncertainties in the state of this process, in equipment development, and in the cost estimates are included, the conclusion reached is that all processes cost the same within the sensitivity of the analysis. A final report detailing the cost study is being prepared.

The metal-matrix encapsulation program was terminated at the end of FY 1980; the only remaining DOE-sponsored work on metal encapsulation of waste will be a small effort by PNL.

3. Geochemical Studies

Radioactive waste must be disposed of in a fashion that prevents its return to man's environment. Disposal of radioactive waste in geologic formations may offer a practical method of permanently isolating the waste from the biosphere. The Chemical Engineering Division is investigating geologic formations as a barrier to the movement of radioactive waste elements from a breached repository. This work is part of the Waste-Rock Interactions Technology Program (WRIT) managed by PNL through the Office of Nuclear Waste Isolation (ONWI) at Battelle (Columbus, Ohio) for DOE.

Previous results from this CEN work indicated that, although many geologic formations are barriers to the movement of radioactive elements dissolved in groundwater, interactions between the formation rocks and radioactive elements are varied and do not lend themselves to simplified descriptions. As an alternative to studying each possible interaction individually, CEN's geochemistry group has been simulating breached repository conditions in laboratory experiments and then observing the behavior of all radioelements simultaneously.

These laboratory experiments, illustrated in Fig. IX-2, simulate the components of the repository that can affect radioelement behavior (such as the backfill material, canister, thermal field, and radiation field). To identify interactions that control radioelement migration, the results of

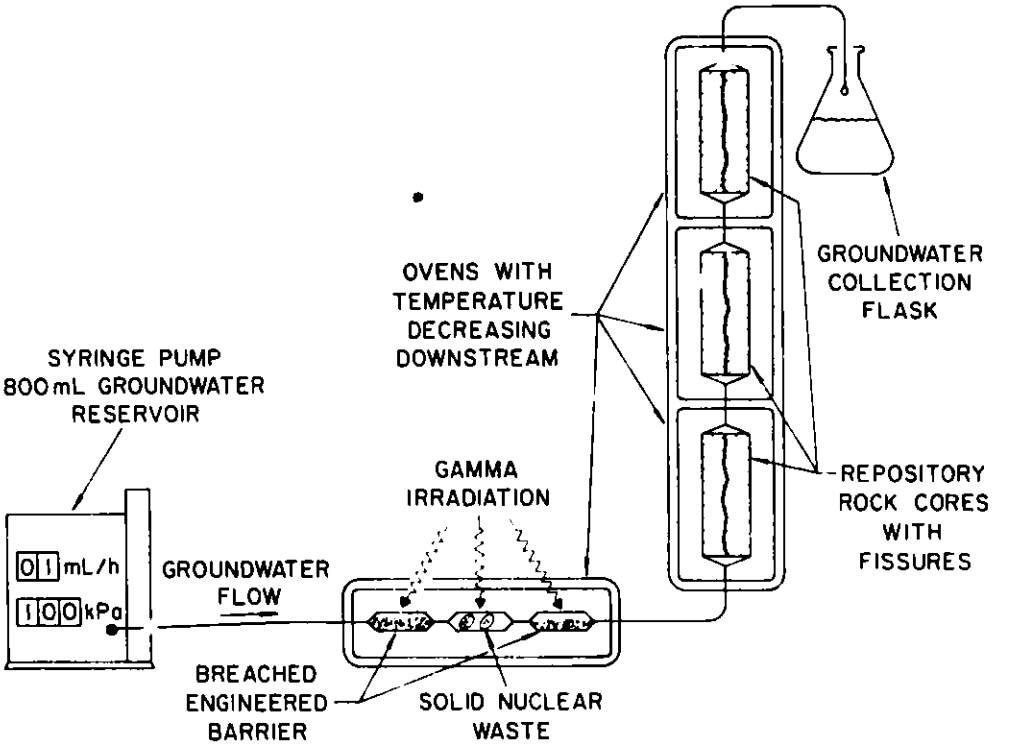

Fig. IX-2. Groundwater Stream Simulation Experiment

these complex simulation experiments are compared with the behavior predicted from simpler experiments. The results of these simulation experiments could be used directly as part of the licensing process of a nuclear-waste repository; we are proposing site-specific tests for projects such as the basalt waste-isolation program and the proposed repository at the Nevada test site.

In the groundwater simulation work over the past year, the migration of Ce, Na, and Cs in granite and granite saprolite was investigated to show the behavior of these elements in a weathering-granite environment (i.e., saprolite). The results indicate that the weathered rock delays transport of these elements relative to the groundwater in a very similar manner to base granite. Hence, the granite weathering that would occur with water intrusion is not expected to affect adversely the barrier property of the granite host rock.

In other geochemical studies, CEN is undertaking (1) an applied program to develop oil-well logging methods and (2) a basic research program (i.e., supported by the Basic Energy Sciences Division of DOE) to investigate the migration of trace elements in the earth's crust.

The goal of the first program is to develop nuclear logging techniques that measure, with good accuracy, the residual-oil level in a depleted oil reservoir. Knowledge of the residual-oil level is important for determining the feasibility of enhanced oil-recovery techniques. Being considered, because of its potential accuracy, is the log-inject-log approach in which a physical or chemical property at various depths in a bore hole is logged, the

reservoir formation is injected with a fluid, and the bore hole is logged again. Differences in the two logs can be attributed to displacement of the natural fluids in the reservoir by the injected fluid. In this work, the nuclear logging methods considered include the use of a pulsed neutron source, a neutron detector, or a gamma detector as the logging tool, and a radiochemical or neutron-absorbing solution as the injected fluid. The program has just been initiated and will require evaluations of current logging methods, numerical analyses of trace elements in reservoir fluids, and laboratory core-flood experiments.

The second program is focused on understanding the mechanisms that underlie the mobilization of trace elements in rocks under natural conditions. Insight into these natural processes can also be used in designing a nuclear-waste repository.

The migration of trace elements caused by the intrusion of a granite monzonite magma into sediments is being studied using a suite of samples collected from the Notch Peak Intrusion in the House Range of western Utah. The effects of heat from the intrusion in an earlier geological era are analogous to the effects of nuclear-decay heat in a waste repository. The effects of the intrusion, which have developed during the millions of years since heating, could be seen in the samples of siltstone and limestone. Measurements at CEN indicate a permeability of 2×10^{-6} darcy for sediments unaffected by intrusion; this permeability is sufficient for sedimentary rock to conduct and transport fluids and trace elements during the metamorphic event (i.e., the intrusion of granite magma). Therefore, it is possible that trace-element migration occurred.

Another project in the basic program centers on understanding the hydraulic properties of massive formations of crystalline rock. Because of their uniformity and compactness, these formations may offer attractive sites for nuclear-waste repositories. The study presently uses cores from the Precambrian granite-rhyolite terrain that extends from the Mississippi River eastward into Ohio. The rock cores, which were obtained from holes drilled by Commonwealth Edison in northern Illinois, are being studied by approximately 20 geoscience groups, a consortium that serves as a model for the National Continental Scientific Drilling Program. Figure IX-3 is a photograph of the core obtained from the 1.3-km (4239-ft) level of drill hole UPH-3 in northern Illinois. In initial studies at CEN, the permeability of pressure-loaded cores will be measured and compared with the gross permeability measured by pressurizing the bore hole. An auxiliary study will be done to determine the composition of the groundwater in the Precambrian structure by rinsing the rock fissures with pure water. Both rock permeability and in situ groundwater composition are important considerations for the siting of a nuclear-waste repository.

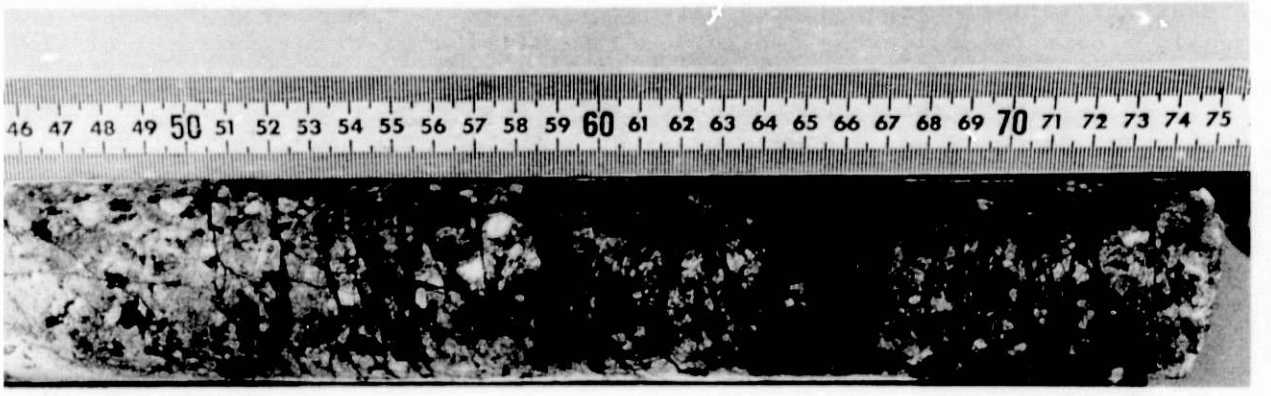

Fig. IX-3. Core from 1.3-km Level of Precambrian Granite-Rhyolite (Northern Illinois). ANL Neg. No. 308-80-494

B. Nuclear Fuel Reprocessing

Work is continuing in the program to develop advanced solvent extraction equipment for aqueous reprocessing of spent fuel from nuclear power reactors. Primary emphasis in our program is on the technology needed to design and operate annular centrifugal contactors. Contactors of various sizes have been built and tested for their mechanical, hydraulic, and mass-transfer characteristics. The near-term objective is to develop a contactor design that can form the basis for construction of a multistage extraction bank for use in ORNL's Integrated Equipment Test Facility. Such a design is almost complete.

The annular centrifugal contactor was first conceived at ANL in 1969, and a prototype unit was built and tested in 1970. This contactor is a modified version of the plant-scale contactor in use at the Savannah River Plant (SRP). In the SRP contactor, aqueous and organic process streams are fed into a mixing chamber beneath a vertically suspended hollow rotor. A mixing paddle attached to an extension of the rotor shaft mixes the phases as the rotor spins, and pumps the mixture upwards into an orifice in the bottom of the rotor. Within the rotor, the organic and aqueous phases are separated under centrifugal force, and the separated phases are then directed by means of circular weirs to the appropriate discharge ports. Multistage countercurrent extraction is achieved by connecting the required number of contactors in series.

In the ANL modification of the SRP contactor, the separate mixing chamber and paddle are eliminated. Instead, the two phases are fed into the top of the annulus between the rotor and the casing and are mixed by the spinning rotor as they flow down the annulus. At the bottom, the resulting dispersion flows inward to the central rotor orifice. Advantages of the ANL design are (1) simpler fabrication, including the use of commercially available components, and (2) potential ease of remote maintenance.

Experience from earlier work with contactors having rotor diameters of 2, 9, and 25 cm was incorporated into the design of an annular centrifugal contactor with a 12-cm-dia rotor, which was tested during the past year. This 12-cm-dia contactor, shown in Fig. IX-4, performed well in mechanical,

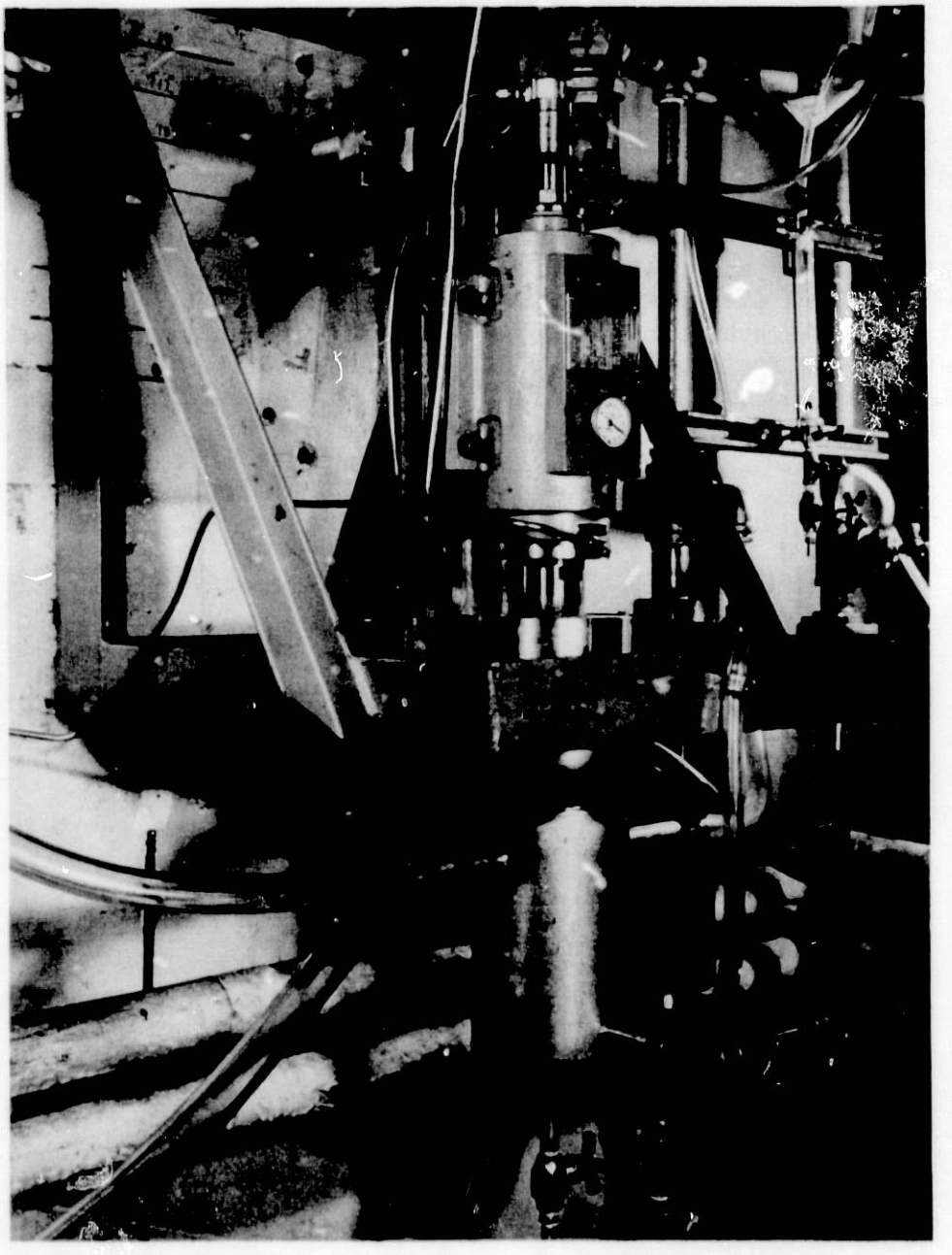

Fig. IX-4. Motorized Spindle and Annular Centrifugal Contactor with a 12-cm-dia Rotor. ANL Neg. No. 308-80-80

hydraulic, and mass-transfer tests. The mechanical tests resulted in an improved understanding of equipment vibration, which will be used in the design of a multistage contactor. The hydraulic tests showed that the unit can operate at its theoretical maximum capacity. Based on these hydraulic tests, several minor changes in contactor design are being recommended to ORNL. The mass-transfer tests showed excellent contactor performance; uranium extraction efficiencies were greater than 98% under normal operating conditions. These tests have demonstrated that the 12-cm-dia contactor will be

capable of meeting the processing requirements of all sections of the 0.5 Mg/day plant to be constructed by ORNL.

A 4-cm-dia contactor was also designed, built, and tested. The rotor for the 4-cm-dia contactor is shown in Fig. IX-5. In this work, the objective was to determine if the 4-cm-dia contactor performed enough like the 12-cm-dia contactor to make it useful in the evaluation of multistage operation in plant-scale equipment. A key problem with the multistage 2-cm-dia contactor (see last year's report) was resistance to inversion from organic-continuous to aqueous-continuous dispersions in the annulus, and this made it unsuitable for evaluating the behavior of larger units. Fortunately, the 4-cm-dia contactor showed low resistance to phase inversion, and thus a multistage unit was designed and built. This multistage contactor should provide us with an insight into the possible operating problems of a multi-stage 12-cm-dia contactor.

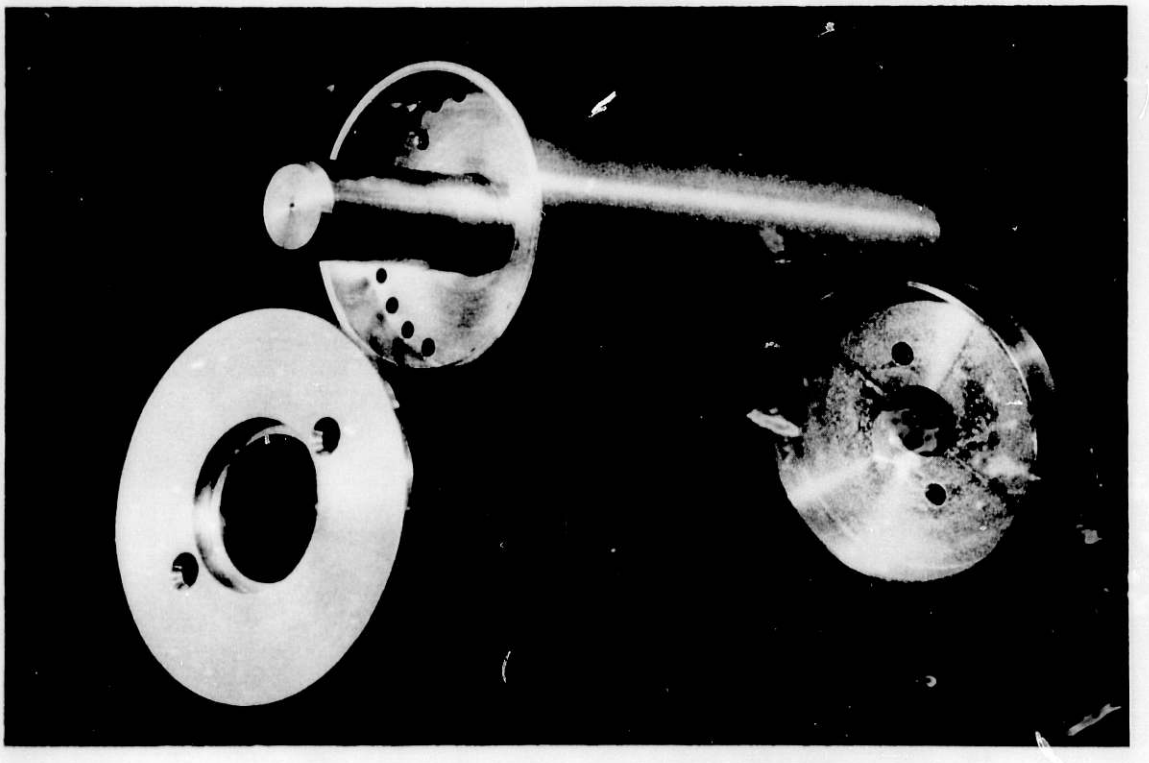

Fig. IX-5. Rotor for 4-cm-dia Contactor.
ANL Neg. No. 308-80-334

The 4-cm-dia contactor will be used to test three other aspects of the annular contactor:

1. Mixing zone operation. This work has only begun, and many useful results are expected in the next year. Eventually, we hope to develop a model for mixing-zone operation that is as useful as the dispersion-band model (see last year's report) has been for understanding the operation of the centrifugal settling zone inside the rotor.

2. The capability to handle three liquid phases. Such flow systems can occur in nuclear fuel reprocessing flowsheets--for example, in the Thorex process for reprocessing thorium fuels. Thus far, only the physical properties of several three-phase thorium systems have been measured.

3. The capability to be used directly in an aqueous process to reclaim scrap mixed-oxide fuel. The feasibility of this concept is being studied by CEN in conjunction with Westinghouse-Hanford. The small size of the unit and its stable operation make it attractive for semiremote operation under computer control, where strict accountability of the fissile metal is required.

In summary, the basic single-stage design for the multistage process contactor has been completed. Future effort will be focused on the potential problems of multistage units, including vibrations, hydraulics, and mass-transfer efficiency. In support of this effort, a detailed model of mixing-zone operation will be developed, and the contactor will be tested with three liquid phases under a variety of operating conditions.

C. LWBR Proof-of-Breeding Analytical Support Project

The Light Water Breeder Reactor (LWBR), now in full operation at Shippingport, Pennsylvania, is the focal point for the national effort to develop technology for breeding in a light water reactor. Breeding in the LWBR will be evaluated after a little more than four years at full power by nondestructively assaying a representative sample of the end-of-life (EOL) fuel rods with an irradiated-fuel assay gauge (IFAG), which is a delayed-neutron device presently being developed by the Bettis Atomic Power Laboratory (BAPL). ANL's role in this program is to provide data which will initially permit calibration and verification of the performance of the BAPL prototype IFAG and, later, will validate the performance of the production IFAG (PIFAG). The data are obtained by destructive physical, chemical, and radiometric analyses of irradiated LWBR fuel rods and fuel-rod segments.

Preparation of samples for analysis requires precision cutting of the fuel rod into segments, pulverization of the fuel, and dissolution of the fuel. Cutting is done by shearing, which simultaneously pulverizes the fuel and largely frees it from the cladding hulls. Required process operations include fuel rod weighing, accurate location of segment boundaries, high fuel recovery, and minimal intersegment cross-contamination. After dissolution of the rod segments, the solutions are analyzed for total uranium and uranium isotope abundances by a mass spectrometric/isotopic dilution method and for selected fission products (^{137}Cs, ^{144}Ce, ^{95}Zr) by radiometric techniques. All of the process work is carried out in the Shielded Cell Facility in the ANL Chemistry Division, using master-slave manipulators.

The program at ANL has three major phases:

1. Processing of irradiated experimental rod sections (GRIP-II segments) in pilot-scale equipment to provide BAPL with calibration and validation data for the IFAG.

2. Design and procurement of full-scale equipment to accommodate four sizes of full-length (about 3-m) EOL rods; this includes equipment for the disposal of scrap and waste generated by the process work.

3. The EOL campaign to provide BAPL with data to "fine-tune" the PIFAG; this campaign is to be followed by final waste treatment and cell cleanout.

With regard to the third phase, the EOL campaign is presently scheduled for CY 1983, and completion of cell cleanout is targeted for the end of CY 1985. The first phase was completed in mid-CY 1980, with formal acceptance of the results by DOE. The second phase includes activities involving the (1) full-scale shear, (2) single-unit (prototype) dissolver, (3) multiple dissolver system, (4) scrap and waste equipment, and (5) computer system. The status of each is described below.

1. Full-Scale Shear (FSS)

In 1979, design and procurement of the FSS were completed. Subsequently, a three-part testing program which will lead to qualification of the FSS was developed. All of this testing will be done with unirradiated materials. The first part, now virtually completed, consisted of cold-shearing studies, using only the shear head-end assembly in mockup. The second part, now about 50% complete, consists of an out-of-cell functional checkout of all shear feed/measurement system components, which will be followed by testing of the FSS assembly. Final testing and qualification will be done with the shear installed in a cell and with all operations performed remotely; installation is scheduled for spring 1981.

For the cold-shearing tests, about 150 dummy rod segments, consisting of ThO_2 pellets loaded into Zircaloy tubes, were assembled. Four sizes of EOL rods were tested: seed (0.78-cm dia), standard blanket (1.45-cm dia), power-flattening blanket (1.34-cm dia), and reflector (2.11-cm dia). The tests demonstrated that the shear has sufficient capacity to cut through all four rod sizes, and it is capable of "double cutting," in which the gas-plenum section is severed from the fuel-bearing section of the rod. The shear has the capability of cutting at speeds up to 100 cm/s (40 in./s), although most testing was done using a slow shear stroke of 2.5 to 5 cm/s (1-2 in./s). The shear blade (type M-42 tool steel) showed only minimal wear after over a total of 2500 cuts; the blade is reversible, and about half of the total cuts were accumulated on each of the cutting edges.

Fuel (thoria) recovery was very high, with mean values ranging from 99.97 to 99.99%. For each rod size, the optimal cut length required to achieve complete dislodgement of the fuel from the individual cut pieces (hulls) and good pulverization was determined to be approximately half the rod diameter. Results of slow-speed shearing suggested that fuel loss per cut and average particle size increase with increasing size of the rod. High-speed shearing does not appear to enhance fuel dislodgement, but does slightly improve fuel pulverization while slightly lowering fuel recovery rates. Furthermore, binding of the shear blade seems to occur from successive high-speed shear strokes. Therefore, slow-speed shearing will be investigated further.

Other shear tests dealt with determining the location of the actual shear plane in order to establish the accuracy of segment length measurements and characterize (and quantify) intersegment cross-contamination. High-speed films made of actual shear strokes were particularly helpful in characterization of the cross-contamination problem. Initial results indicated that, for all rods except the largest, the 2.1-cm-dia reflector rod, the shear cut was quite accurate, with calculated cross-contamination values being about 0.02%. However, in the case of the reflector rod, initial results showed that about 0.27% of the fuel in a typical (26.7 cm long) segment would be transferred to the preceding segment. This level of transfer is presently unacceptable, and means of minimizing this problem are being considered. With minor exceptions, shear performance was found to be satisfactory.

The shear feed/measurement system and associated controls and instrumentation were set up in a mockup area and are undergoing calibration and testing. Some minor rework of the system has been done to improve remote repair and maintenance capabilities. A laser calibration of the feed system was performed to check its ability to position a rod in the shear. Analysis of calibration data showed that the positioning error of the entire system is no greater than 0.050 mm. Backlash in the drive train is on the order of several hundredths of a micrometer, which is considered negligible. Test shearing of full-length dummy (MgO-filled) fuel rods in the mockup area is planned for early in CY 1981.

2. Single-Unit Dissolver (SUD)

The SUD system, which consists of the dissolver, support components, and controls, was installed in a shielded cell (K-3) early in CY 1980 and was essentially fully operational by the year's end. In boilup tests with water and nitric acid, basic operating parameters such as heatup and cooldown times, power settings for heater controllers, and requirements for condenser cooling water flow were established.

A remaining problem is remote maintenance of the heaters. The present design has heaters mounted in an annular space between a tantalum primary vessel and an outer stainless steel shell. Testing of a unit with external heaters has started. Information from the next round of testing will serve as input for the design of the multiple dissolver system.

3. Multiple Dissolver System (MDS)

The MDS will consist of four dissolvers (basically of the SUD design) within an alpha barrier in a shielded cell (M-1). The design and procurement of this MDS is mainly being conducted by the Engineering Division at ANL; the conceptual design for this system was approved in May 1980. During the EOL campaign, the four dissolvers and associated controls and subsystems will be installed in Cell M-1 for the dissolution of 330 fuel-rod segments. Installation of the MDS is presently scheduled for late 1981.

4. Scrap and Waste Equipment

This CEN effort is mainly directed at disposing of the about 2000 L of dissolver solution that will be generated during the EOL campaign; this waste will be disposed of at a storage site away from ANL. The plan is to

convert the material to a solid form by spray calcination. The basic design of the calciner and off-gas system is a modification of the laboratory-scale system designed and built by PNL.[2] It is planned to test a calciner in a mockup area before installing it in a shielded cell. The bulk of the fabrication and installation of calcination equipment in a shielded cell is scheduled for CY 1981.

Design of a waste calcine package that will meet present shipping and storage-site criteria is in progress. Dose rates are being calculated for various designs by using a transport theory code (DOT IV). Individual waste shipments will involve several (55-gal) drums contained in a leased overpack, which will be carried by truck. The present estimate is that about 100 drums may be required to dispose of the calcine alone.

5. Computer System

Experience gained during work with the pilot-scale equipment indicated a strong need for automation of data collection and data processing in order to eliminate the errors associated with manual transcription and hand calculation of numbers. In addition, it was found necessary to impose rigorous control over the operational sequences for the pilot-scale shear and dissolver in order to ensure, via reproducible procedures, that stringent limits of error in the analytical results would be met. Accordingly, it was decided to employ a computer system for use in all EOL operations. During the past year, the functional requirements of the system and its overall architecture were developed. This system will serve the following functions:

1. Automatic collection and storage of all data generated during the EOL campaign, including process history of samples, analytical data, and process control information.

2. Process control of the shear hydraulic system, the air-cooling systems, the water-cooling systems, the dissolvers, the spray calciner for liquid waste, and the off-gas systems.

3. Full automation of the highly repetitive cut/feed cycle of the FSS.

4. Real-time statistical evaluation of data quality.

5. Error analysis of analytical results.

6. Computer production of interim reports, including analytical reports to be forwarded to BAPL, process control reports (internal use), and equipment performance records.

---

[2] M. S. Hanson, D. A. Knox, and D. N. Berger, Design Features of the Laboratory-Scale Radiochemical Immobilization System, Battelle Pacific Northwest Laboratory Report PNL-3027 (May 1980).

Operator control for the shear and dissolver systems will be provided by the use of computer-stored operating procedures made available to operators through cathode ray tube (CRT) terminals at work stations.

This system will consist of four computers and six terminals. The central processing unit, a VAX-11/780,* is being procured and will be installed at CEN by early CY 1981; this computer will be shared with other CEN programs. An intermediate computer, a PDP-11/23,* will be interfaced with the shear, dissolvers, and waste calciner; this computer will be located in ANL's Chemistry Division and used only by the LWBR Proof-of-Breeding Project. Operational control of and data collection from the primary analytical instruments, i.e., the mass spectrometer and the gamma spectrometer, will be interfaced with a small computer (microprocessor) that will collect data and transfer it directly to the VAX-11/780. The PDP-11/23 computer and a number of other hardware items have been procured and are being interfaced with the process systems as they are readied.

The software for use with the PDP-11/23 computer system is also under development. The software includes: (1) a monitoring program which sequentially scans (and processes) some 130 electronic signals from process sensors, (2) an operating program which provides the medium through which the operators interact with the computer and with the several operating systems, and (3) a data management program. Item (1) is essentially done; items (2) and (3) are now being developed. Testing of the integrated system is scheduled for mid-CY 1981.

*Product of Digital Equipment Corp., Maynard, MA.

X. MAGNETIC FUSION ENERGY RESEARCH

A. Introduction

The program on fusion energy research at CEN embodies a family of applied research topics covering a variety of interrelated areas of fusion reactor technology. The CEN work includes (1) systems analysis and engineering experimentation, (2) materials research and development, and (3) neutron dosimetry and damage analysis. The results of this work in recent years have spearheaded important advances in a number of key areas related to first-wall and blanket performance and to fuel-cycle strategies for fusion reactors. These advances were discussed in the previous report in this series.

Over the past year, several significant changes have taken place in the CEN fusion activities. These changes are (1) a redirection of both the engineering experimentation and the materials research to provide greater emphasis on the development of solid rather than liquid tritium-breeder materials; (2) a broader role in major national and international design activities, including studies of a fusion engineering device that has been proposed for construction and operation by the early 1990's; (3) an expansion of the dosimetry and damage analysis project to permit additional emphasis on the development of advanced damage analysis methodology; and (4) increased participation in joint research projects involving other ANL divisions, other laboratories, and industry. These changes have resulted in a discontinuation (presumably temporary) of work on liquid lithium processing and hydrogen isotope permeation. In particular, operation of the Lithium Processing Test Loop has been curtailed pending DOE's decision on its future role in the development of liquid lithium technology.

B. Systems Analysis and Engineering Experimentation

This part of the CEN fusion research effort is focused on processing technology for liquid and solid tritium-breeder materials and on the evaluation of operating criteria, system design concepts, and component performance for tritium-handling facilities.

1. Liquid Breeder Processing Research

On October 5, 1979, the Lithium Processing Test Loop (LPTL), described in a previous report in this series, developed a lithium leak in the electromagnetic (EM) pump channel, which damaged the pump, its surrounding support structure, and the underlying floor pan. A thorough analysis of the causes and consequences of the pump failure was conducted by personnel from CEN and several other ANL divisions. Metallurgical analyses of the elliptical pump channel and adjacent piping revealed that there was a significant buildup of iron crystallites and other solid material in the region of the current-carrying bus bars (region of high magnetic field), which may have resulted in a flow restriction that caused cavitation and erosion of the channel walls. The location of the failure was in a region of high residual stress (due to cold work left over from channel fabrication); this failure is typical of other cold work/stress-related failures encountered in components operated in forced-circulation lithium loops. Another important result was the isolation of crystals of a compound characterized as Li_xCrN_y. Compounds of this type

are believed to be responsible for much of the Fe, Cr, and Ni mass transfer encountered in lithium loops constructed of stainless steel. The importance of nitrogen in the mass-transfer mechanism has long been suspected, but verification of the existence of stable ternary Li-M-N compounds (M = Fe, Cr, Ni) had not heretofore been achieved.

Repairs to the LPTL facility; the design and fabrication of a new EM-pump with a circular, stress-free channel; and refilling of the LPTL with lithium have been completed. However, because of requests for increased emphasis on solid tritium-breeder development by the DOE/Office of Fusion Energy, operation of the LPTL has been temporarily curtailed pending a decision on its future role in the development of liquid-lithium processing technology. The CEN engineering research on solid breeders is discussed later in this section.

Another task in the area of liquid-lithium processing technology, conducted during 1980, involved the measurement of liquidus temperatures in the Li-Pb-Bi system--a potential candidate for breeder blanket applications. Compositions containing 10 and 15 at. % lithium in Pb-Bi (Pb/Bi mole ratio of 0.773) were found to be totally liquid at 131 and 136°C, respectively (see Fig. X-1). Studies are being conducted to determine the Pb/Bi ratio that yields a minimum melting point for lithium fractions of 5 to 20 at. % in the alloy. Assuming that all of the lithium in the alloy is ^{6}Li, compositions in this range would produce relatively high tritium breeding ratios (i.e., >1.2) in a fusion blanket, would require an appreciably thinner breeding zone than pure liquid lithium for the same breeding ratio, would have a melting temperature 30 to 40°C lower than that of lithium itself, and would be much less reactive with air and water than liquid lithium.

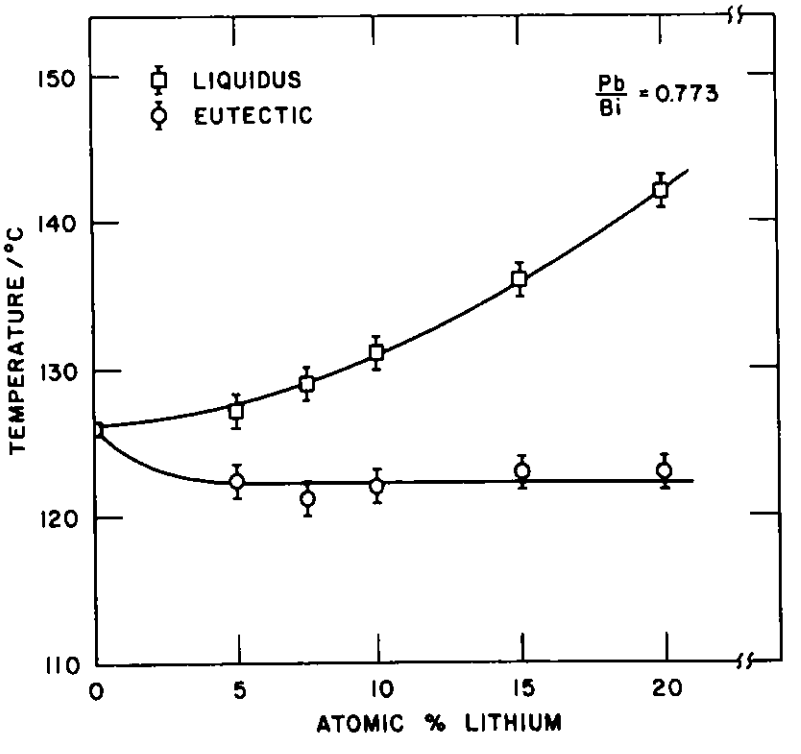

Fig. X-1. Phase Characteristics of Low-Melting Li-Pb-Bi Alloys

2. Tritium Systems Analyses

The design work on fusion-reactor tritium systems has continued during the past year. In this period, CEN personnel participated in several major DOE-sponsored design studies for tokamak fusion reactors, including the STARFIRE Commercial Reactor, the Engineering Test Facility (ETF), and the International Tokamak Reactor (INTOR). STARFIRE is managed by ANL; ETF is managed by Oak Ridge National Laboratory (ORNL); and INTOR is a joint IAEA-sponsored study involving the USA, the European community, the USSR, and Japan.

Major highlights of the work include the following: (1) the establishment of tritium supply guidelines for use in fusion-reactor startup projections (e.g., for ETF, INTOR, STARFIRE); (2) the design of a complete tritium fuel processing facility which incorporates units scheduled for test in the Tritium Systems Test Assembly (TSTA) at Los Alamos National Scientific Laboratory; (3) a parametric analysis of the STARFIRE vacuum system, which resulted in a novel limiter concept that satisfied vacuum, tritium, and neutronic requirements; (4) the design of the STARFIRE solid tritium-breeder blanket for conditions which meet tritium recovery criteria; and (5) the determination of the relative importance of selected physical and chemical parameters on the performance of tritium (spill) cleanup systems through the use of TSOAK-M1 (a reactor-building detritiation simulation code). Design work for the STARFIRE and ETF tritium systems has been completed; but, during the coming year, work on other designs of fusion-reactor tritium systems will continue. A sizable fraction of this work will be directed toward design strategies for tritium removal from solid breeder blankets. Work will also be conducted on INTOR tritium-handling strategies and on tritium-systems studies for a demonstration fusion reactor.

C. Fusion Materials Research and Development

Studies in materials chemistry and compatibility in first-wall and blanket environments for fusion reactors have been in progress at ANL since the early 1970's. Much of the past work has focused on hydrogen dissolution and permeation characteristics of various classes of structural alloys (austenitic steels, nickel-base alloys, refractor alloys, composite materials, and titanium alloys). In recent years, the scope of work was broadened to include other chemistry/compatibility aspects of materials behavior in fusion systems. During 1980, efforts were directed toward studies of (1) hydrogen permeation characteristics of ferritic steels and (2) corrosion of structural alloys by candidate ceramic solid-breeder materials.

In our most recent studies of hydrogen permeation, we have sought to identify alloys with reduced hydrogen permeabilities. An extensive survey was conducted to obtain hydrogen permeation data for pure iron, ferritic alloys, and martensitic alloys; this survey revealed that, when the alloys contained small amounts of aluminum, they generally had lower permeabilities than the aluminum-free alloys. Therefore, experiments were conducted to measure hydrogen permeation rates through three Fe-Cr alloys having varying amounts of aluminum: 16 Cr-0 Al, 18 Cr-2 Al, and 16 Cr-5 Al. The maximum permeation reduction (a factor of 200 lower than pure iron) was obtained with the 18 Cr-2 Al alloy. Comparisons of the data from this study (see

Fig. X-2) showed that the aluminum content required to achieve the maximum resistance to hydrogen permeation for these alloys in oxidizing environments is less than 2 wt % and is probably related to the chromium content in the alloy.

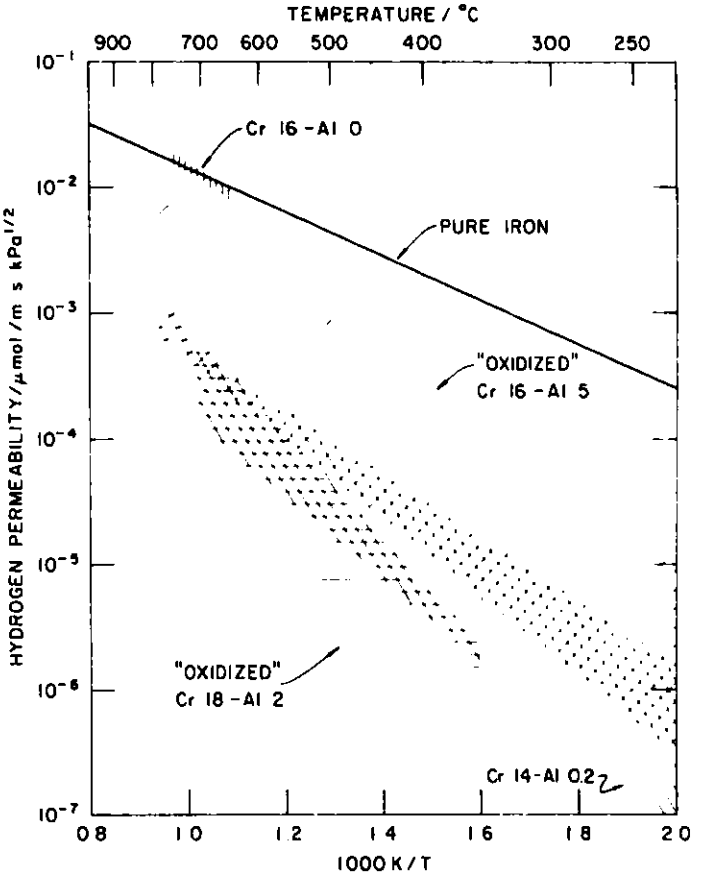

Fig. X-2. Hydrogen Permeabilities of Selected Fe-Cr-Al Alloys in Comparison with Pure Iron

In other studies, measurements of the corrosivity of candidate solid tritium-breeder materials at 600°C have been made using the reaction-couple method. Specimen tabs of four structural alloys--316 stainless steel, Inconel-625, Ti6242, and HT-9--were exposed to Li_2O, $LiAlO_2$, and Li_2SiO_3 platelets. Scanning electron microscopy revealed that corrosion product layers had developed at the alloy/ceramic interface for all couples. These layers contained elements that were present in both the alloy and the ceramic. Of the three candidate breeder materials, Li_2O appeared to be the most corrosive and $LiAlO_2$ the least corrosive at 600°C. Several mixed-oxide reaction products ($Li_xM_yO_z$, M = Ni, Fe, Cr) were identified by X-ray diffraction analysis of the corrosion product layers. At present, quantitative information is being gathered on corrosion rates, layer thickness, and chemical composition of the corrosion products.

In the coming year, the work in fusion materials research will continue to be an important part of CEN's fusion-related activities. However, as a result of some recent changes in programmatic priorities within the DOE/Office of Fusion Energy Program, the work on hydrogen permeation will be reduced so that increased effort can be devoted to newly established tasks pertaining to solid breeder development as discussed below.

D. Solid Breeder-Blanket Technology

As noted earlier, the development of solid tritium-breeder technology is becoming a prominent thrust within the national fusion energy program. With some redirection of existing funds as well as some new funds, a solid tritium-breeder program was mounted at ANL during the past year. This program consisted of two interactive components--one concerned with the engineering aspects of blanket system design and blanket processing and the other concerned with materials behavior (e.g., chemical stability, tritium release characteristics, ease of fabrication, neutronic response, and radiation effects). Both components are briefly described below.

Work in engineering research during the past year included (1) a comprehensive analysis of solid breeder-blanket performance and (2) planning and conceptual design of an experiment to test continuous, in-pile recovery of tritium from a miniaturized solid breeder assembly. Since the physical and chemical data base for potentially viable solid breeders is extremely limited, modeling and extrapolations from known properties of similar materials have been used to make performance predictions. Also, analysis of a variety of tritium recovery methods resulted in the conclusion that the most viable method is continuous, in situ tritium recovery from a stationary compact of solid pellets by means of low-pressure ($\leq$1 atm) helium purging. The results of assessments conducted to date indicate that the most promising breeder materials are lithium-bearing ceramics, e.g., $LiAlO_2$, Li_2ZrO_3, Li_2O, Li_2SiO_3, and Li_2TiO_3.

To provide engineering data for design and modeling activities, a series of in-pile experiments is planned to test in situ tritium recovery. The first experiment, TRIO-01, is currently in the conceptual design stage. The experiment will be directed by ANL, and will also involve participation by ORNL. The current plans for TRIO-01 are to test simultaneously in situ tritium breeding and recovery from one or perhaps two candidate solid breeder materials. The tritium will be removed by a low-pressure purge stream flowing through channels that are formed in a sintered plug of the breeder material encapsulated in a small, tubular assembly. At present, the two leading candidates for breeding materials are $LiAlO_2$ and Li_2ZrO_3. The experimental variables will include assembly configuration, breeder temperature, and neutron fluence.

These engineering experiments are expected to provide input to the materials research program, in which critical fundamental properties of solid breeder materials will be measured. The materials research effort is a new addition to the solid breeder program. The long-term goal of this effort is to develop, for all candidate breeder materials, an accurate and complete thermochemical, thermophysical, and engineering data base that can adequately support activities related to systems design and blanket processing.

Since tritium is expected to leave the breeder bed (via a purge stream) as T_2 or T_2O, data on tritium solubility, phase relationships, and vaporization behavior in solid-breeder systems are essential; hence, our materials work has started with a study of these properties. Thus far, work has begun on the tritium-Li_2O system; as soon as samples of Li_2ZrO_3 and $LiAlO_2$ of high purity are prepared, similar measurements will be made on these systems too.

In the near term, it is expected that a study of the thermodynamics of the various candidate systems and the development of procedures for analyzing tritium and impurities at very low concentrations (e.g., 1-3 ppm) will be the primary focus of the ANL contribution to the national materials program on tritium breeders. The long-term direction of the ANL effort will be dependent upon findings in the materials studies and the engineering irradiation test program.

E. Recent Advances in Neutron Dosimetry and Damage Analysis

The intense radiation fields expected in magnetic fusion reactors can produce severe damage in component materials. The CEN-based Dosimetry and Damage Analysis Project contributes to ongoing studies of radiation damage conducted by ANL and other laboratories. The primary goal is the development of techniques to routinely characterize reactor and accelerator radiation environments in terms of neutron fluence, energy spectrum, and fundamental damage parameters such as nuclear displacements, internal gas production, and transmutation rates. This vital information provides a means of (1) correlating materials effects observed at different facilities and (2) predicting the performance of materials in fusion reactors.

Twelve fusion-related experiments in fission reactors are now in progress at the Oak Ridge Research Reactor (ORR), the High Flux Isotopes Reactor at ORNL, and the Omega West Reactor at Los Alamos National Scientific Laboratory. As an example, tritium breeding in a lithium-containing sample was determined in an experiment conducted jointly by members of ANL and ORNL at the ORR poolside facility. In this experiment, thermocouple wires were subjected to dosimetry analysis and to X-ray and quantitative chemical analysis. The derived tritium breeding rate, based on the data in Fig. X-3, showed that about 17% of the ^6Li was converted to tritium. The results of this analysis also illustrated that the capability exists to adjust neutron energy spectra by considering all known data as well as their errors and covariances; consequently, confident error assignments can be made for all derived damage and transmutation rates.

Accelerator neutron sources are difficult to characterize due to the poor quality of neutron activation data and to flux and spectral gradients close to the source. Recent ANL work has focused on integral neutronic testing of activation data, and an adequate data base has been established with which flux spectra can be routinely determined to ±10-30% accuracy and derived damage rates to ±10%. In addition, dosimetry analyses have been conducted for the 14 MeV Rotating Target Neutron Source (RTNS-II) at Lawrence Livermore Laboratory (LLL) and for the Cyclotron at the University of California at Davis. Detailed flux and spectral gradients were determined

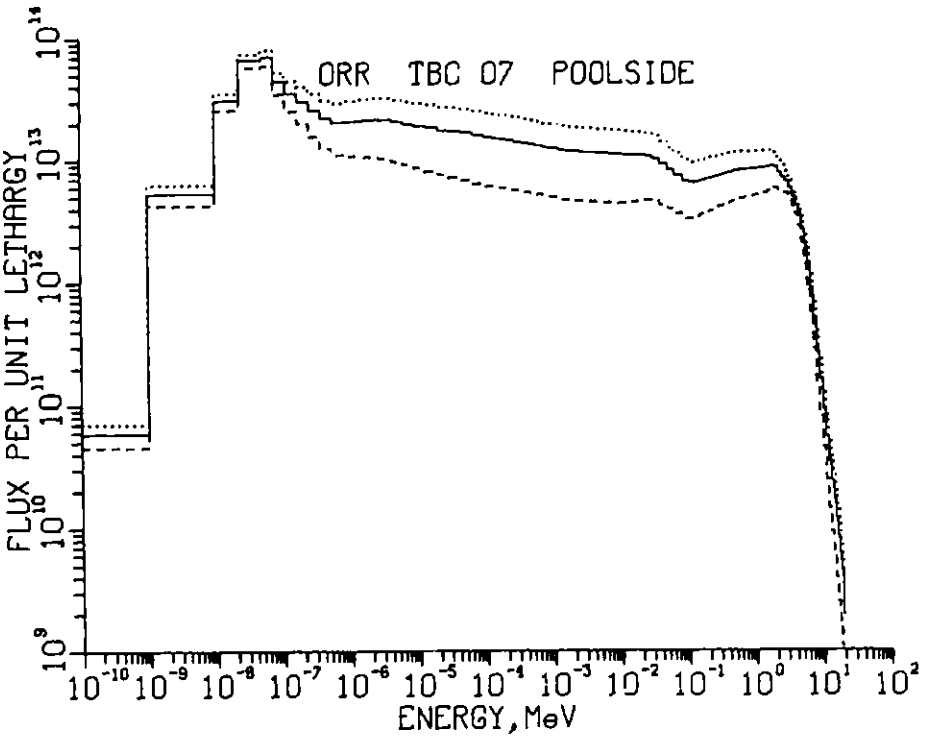

Fig. X-3. Neutron Spectrum Deduced for ORR in Terms of Flux per Unit Lethargy (energy times flux). The dashed and dotted lines represent one standard deviation errors.

throughout the target rooms, which required gamma analysis of hundreds of small samples. One interesting new result is that the thermal flux has been shown to be roughly equal to the flux at the rear wall of RTNS II, whereas the 14 MeV flux increases by a factor of 10^4 as one approaches the source. This previously unmeasured flux is important to experiments conducted far from the source, such as studies of superconducting magnet materials and insulators.

In order that experimenters can utilize neutron exposure data, it is very important to derive fundamental nuclear damage parameters. Extensive data files of damage parameters have thus been computed for 21 elements, including damage parameters for 6 key elements up to 50 MeV obtained from accelerator irradiations. These data files have been made available to the fusion community via the fusion computer service at LLL. The data are currently being revised using newly available nuclear cross sections, and existing computer codes are being upgraded to include the (n,γ) capture reaction and energy-averaged angular effects for elastic scattering.

Future plans include development of key nuclear activation data, especially above 14 MeV where the data base is inadequate. Such data are needed for present-day accelerators as well as for facilities now under development, such as the Fusion Materials Irradiation Test Facility at Hanford Engineering

Development Laboratory and the Intense Pulsed Neutron Source at ANL. Perturbed spectra will be intensively studied using large masses of materials to simulate fusion-reactor neutron conditions. Also, the existing nuclear counting facilities at CEN are now being expanded to handle the increasing demand for precise neutron exposure data for fusion materials studies.

XI. BASIC ENERGY SCIENCE

A. Homogeneous Catalysis

This research is devoted to the elucidation of the reaction pathways whereby homogeneous organometallic catalysts activate small molecules, e.g., CO, and direct their subsequent reactions to specific chemical products. Intimate details connecting the molecular structures of the catalysts, the nature of intermediate species, and the thermochemical parameters of each reaction step are sought by a combination of techniques, including chemical kinetics, and spectral and isotopic studies under high-temperature and high-pressure conditions. The reactions (novel or well-known) that are being investigated often have potential significance for industrial processes of fuel conversion, energy storage, or feedstock manufacture.

1. Experimental and Theoretical Studies of Mechanisms in the Homogeneous Catalytic Activation of Carbon Monoxide

a. Experimental Studies

Our research was originally based on the idea that organo-transition metal compounds capable of thermal generation of a radical or radical pairs might afford an entry into the problem of CO hydrogenation with homogeneous mononuclear catalyst complexes. We had estimated that $HCo(CO)_4$ attack on CO by the radical pair mechanism should be reasonably favorable (thermochemical estimates for this type of reaction are easily made).[1,2] The immediate success[2] of our attempted reactions with $HCo(CO)_4$ and $HMn(CO)_5$ made it possible for the first time to study the reductive transformation of CO with readily characterizable catalysts by the conventional techniques of physical organic chemistry.

We have proposed a mechanism involving only mononuclear intermediates in the $HCo(CO)_4$-catalyzed reaction summarized as follows:

$$HCo(CO)_4 \overset{K}{\rightleftharpoons} (CO)_3Co(CHO)\ (I) \tag{1}$$

$$(CO)_3Co(CHO) + H_2 \underset{k_{-2}}{\overset{k_2}{\rightleftharpoons}} (CO)_3H\ Co(CH_2O)\ (II) \tag{2}$$

$$(CO)_3H\ Co(CH_2O) \xrightarrow[k_3]{\text{fast}} \text{products} \tag{3}$$

---

[1] H. M. Feder and J. Halpern, J. Am. Chem. Soc. 97, 7186 (1975).

[2] J. W. Rathke and H. M. Feder, J. Am. Chem. Soc. 100, 3623 (1978).

Reaction 1 is considered to be a rapid equilibrium. The transition state occurs in reaction 2. This mechanism is consistent[3] with the following observations: First, the products are the same as those we obtained by $HCo(CO)_4$-catalyzed hydrogenation of the formaldehyde precursors, paraformaldehyde and s-trioxane, which likely react via complex (II). Second, the rate law is $d(\Sigma \text{ products})/dt = k_{obs}[HCo(CO)_4]P_{H_2}$, where $k_{obs} = k_2k_3K/(k_{-2} + k_3)$. Third, the activation parameters in 1,4-dioxane solution near 200°C are $\Delta H^* \sim 41$ kcal mol^{-1}, $\Delta S^* \sim 0$ Gibbs mol^{-1}. Fourth, the rates are increased (via changes in ΔS^*) by a factor of ~20 in the following solvent series: heptane < benzene < 1,4-dioxane < 1,4-dioxane + 16% water < 2,2,2-trifluoroethanol. Fifth, the deuterium isotope effect in 1,4-dioxane at 182°C is $k_H/k_D = 0.73$.

Early in these studies, it was recognized that methanol, methyl formate, and ethylene glycol are primary reaction products of the CO hydrogenation reaction. Although there are exceptional circumstances where these materials were essentially the only products observed, in most cases these products are converted to other materials by secondary reactions. These secondary reactions include (a) alcohol homologation, (b) transesterification, (c) methanolysis, (d) alkane cleavage, (e) aldolization, (f) CO_2 formation, and (g) glycerol and 1,2-diol formation.

To determine the formation ratios of the primary reaction products, it is necessary to allow for the secondary reactions. Fortunately, only secondary reactions (a) and (b) are important in the dilute solutions used in our studies. Rate constants and branching ratios for the primary reaction products, tabulated as $f(CH_3OH)$, $f(CH_3O_2CH)$, and $f[C_2H_4(OH)_2]$, are given in Table XI-1 for a range of conditions. The tabulated values are independent of the extent of reaction and depend only on the reaction conditions.

Determination of these branching ratios has enabled us to propose[3,4,5] a mechanism for the product-determining steps,

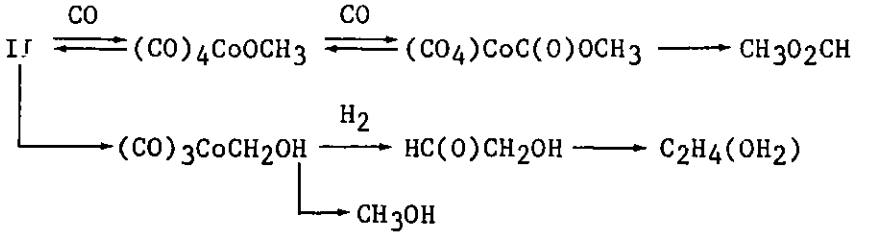

These steps, consistent with the observed variations of the branching ratios with hydrogen and carbon monoxide pressures, use intermediate steps precedented in transition-metal organometallic chemistry.

---

[3] H. M. Feder and J. W. Rathke, Ann. N.Y. Acad. Sci. 333, 45 (1980).

[4] J. W. Rathke and H. M. Feder, Catalysis in Organic Syntheses--1980, W. R. Moser, Ed., Academic Press, N.Y., in press.

[5] H. M. Feder, J. W. Rathke, M. J. Chen, and L. A. Curtiss, Advances in Chemistry Series, American Chemical Society, in press.

Table XI-1. Reaction Parameters for the Cobalt Carbonyl Hydride Catalyzed Hydrogenation of Carbon Monoxide at 182°C

Experiment No.	Conditions	Average $[HCo(CO)_4]$, M	P_{H_2}, atm	P_{CO}, atm	$10^7 \cdot k(2)$ $atm^{-1}s^{-1}$	Percent		
						f(CH_3OH)	f(CH_3O_2CH)	f[$C_2H_4(OH)_2$]
1	a	0.12	96.5	115	2.0	50	25	24
2	a	0.10	192	121	1.7	44	25	33
3	a	0.078	30.2	113	1.8	75	23	2.4
4	a	0.089	100	123	2.0	48	19	33
5	a	0.051	26.5	340	1.9	65	28	7.8
6	b	0.11	102	111	2.7	43	20	35
7	c	0.03	149	149	0.69	72	7.0	22
8	d	0.084	115	115	2.4	52	0	48
9	e	0.081	154	179	2.7	45	26	29
10	e	0.034	97.1	170	2.0	54	24	22
11	e	0.052	161	108	2.0	68	12	20
12	f	0.0025	161	108	6	90	10	0

[a] In 1,4-dioxane solution.

[b] In 1,4-dioxane solution with deuterium used in place of hydrogen.

[c] In 1,4-dioxane solution with 3 PBu_3/Co. The major hydridic species is believed to be $HCo(CO)_3PBu_3$.

[d] In 1,4-dioxane solution containing 8.5M H_2O.

[e] In 2,2,2-trifluoroethanol solution.

[f] At 214°C in 2,2,2-trifluoroethanol solution.

b. Theoretical Studies

Significant support for our proposed mechanism, reactions 1 to 3, has been provided by semi-empirical molecular-orbital calculations.[5] The geometries of the various intermediates were first optimized using the modified extended Hückel theory (MEHT) method described by Anderson, and then the approximate molecular electronic energies at these geometries were determined using MEHT parametrized to give known bond dissociation energies. The most important results of these calculations (uncertainties of ±10 kcal mol^{-1}) are summarized as follows:

(a) The 16-electron formyl cobalt tricarbonyl, $Co(CO)_3(CHO)$, was found to have a nearly planar structure and to be 9 kcal mol^{-1} less stable than $HCo(CO)_4$. This is in agreement with a previous estimate[3] of 16 kcal mol^{-1} based on thermochemical considerations.

(b) The energy of the octahedral complex, $CoH_2(CO)_3(CHO)$, was found to be +52 kcal mol^{-1} relative to $HCo(CO)_4 + H_2$. This complex has the correct stoichiometry to be near the transition state, experimental relative energy +41 kcal mol^{-1}.

(c) The dissociation of formaldehyde from the complex $HCo(CO)_3(CH_2O)$ was calculated to require an energy of 6 kcal mol^{-1}. The thermochemically estimated[3] value was 10 kcal mol^{-1}. The CH_2O ligand is found to form a weak bond to cobalt, with nearly free rotation of the ligand such that the ligand can readily position itself for hydrogen transfer to either carbon or oxygen. The isomeric hydroxycarbene complex, $H(CO)_3Co(=CHOH)$, was found to be less stable than the formaldehyde complex by >60 kcal mol^{-1} and is considered unlikely to play a significant role in the catalytic cycle.

(d) The molecules $(CO)_3CoCH_2OH$ and $(CO)_3CoOCH_3$ have been examined briefly. They form quite energetically from the formaldehyde complex by internal hydrogen transfers. It will require more accurate calculations to determine whether the difference between the two pathways accounts for the observed branching ratio.

2. Ethanol Synthesis

Concerns over the depletion of petroleum reserves early in the next century have spurred renewed interest in using coal and synthesis gas ("syngas," $H_2 + CO$) made from coal as sources of clean transportation fuels and chemical feedstocks. The direct conversion of syngas to ethanol and the "indirect" reaction of syngas with methanol to yield ethanol (homologation) have been studied as possible alternative processes for the production of ethanol. Ethanol is an important solvent, chemical feedstock, and fuel extender and is currently produced from ethylene obtained from petroleum or from feed grains by fermentation.

One homogeneous catalytic system for methanol homologation has been extensively discussed in the literature, the catalyst being $Co_2(CO)_8/HCo(CO)_4$. This system was first reported by I. Wender in the late 1940's. The principal reaction is

$$CH_3OH + 2H_2 + CO \rightarrow C_2H_5OH + H_2O \qquad (4)$$

Because of current economic incentives, the cobalt-catalyzed methanol homologation reaction has been recently reinvestigated with various additives, and several patents have appeared. However, the economic viability of the cobalt-based processes is still in some doubt, the main problems being inadequate conversion, selectivity, and catalyst recovery.

We have discovered[6] a new catalytic system for the homologation of methanol. At temperatures ≥180°C, iron pentacarbonyl was found to catalyze the homologation of methanol to form ethanol in the presence of syngas and a tertiary amine according to the reaction

$$CH_3OH + 2CO + H_2 \longrightarrow CH_3CH_2OH + CO_2 \qquad (5)$$

The only significant side product observed is methane. The iron carbonyl system is efficient in the use of hydrogen in that carbon dioxide, rather than water, is the oxygenated by-product. Also in contrast to the cobalt carbonyl system, propanol and higher alcohols are not found in the product solution. These differences are accounted for by the mechanism of the reaction, which combines precedented steps in an unprecedented sequence. The iron carbonyl system appears to be competitive with the cobalt carbonyl system in rate and selectivity, and may prove to be an attractive process for the homologation of methanol.

The mechanism which we have proposed for this reaction is as follows:

$$Fe(CO)_5 + B + H_2 \rightleftharpoons HFe(CO)_4^- + BH^+ + CO \qquad (6)$$

$$MeOH + CO \overset{[B]}{\rightleftharpoons} MeO_2CH \qquad (7)$$

$$MeO_2CH + B \rightleftharpoons BMe^+ + O_2CH^- \qquad (8)$$

$$BMe^+ + HFe(CO)_4^- \longrightarrow Me(H)Fe(CO)_4^- + B \qquad (9)$$

$$Me(H)Fe(CO)_4^- \longrightarrow \text{Products} \qquad (10)$$

$$O_2CH^- + BH^+ \overset{[Fe]}{\longrightarrow} H_2 + CO_2 + B \qquad (11)$$

where B is the tertiary amine and Me is methyl.

---

[6] M. J. Chen and H. M. Feder, Catalysis in Organic Syntheses--1980, W. R. Moser, Ed., Academic Press, N.Y., in press.

Reactions 6 to 8 are well known and specify the minimum requirements placed upon the amine. In order for these reactions to occur, the amine must have a pK_a of about 10, be relatively sterically unhindered, and chemically stable under the reaction conditions. Trimethylamine and N-methylpiperidine work well. The S_N2 character of reaction 9 is the reason why methanol is converted to ethanol, while ethanol is not converted to propanol. (Very large differences in rates for nucleophilic substitution at methyl vs. ethyl have been observed for S_N2 reactions.) We have demonstrated that reactions 9 and 10 occur by subjecting the salt, $NMe_4^+ HFe(CO)_4^-$, dissolved in a nonreactive medium to similar reaction conditions. The ratio of methane to ethanol was affected by CO pressure, additives, and reaction temperature. Reaction 11 was also demonstrated to occur by subjecting the salt, $HN(Me)_3^+ O_2CH^-$, to the reaction conditions. This reaction is important because it regenerates the amine that is depleted in reaction 6. A cosolvent, 1-methyl-2-pyrrolidinone, which enhances the ability of the iron carbonyl to catalyze reaction 11 and significantly increases the lifetime of the catalyst, has been found.

A conversion rate of 13% per hour with 70% selectivity has been achieved in a batch reactor. Improvements are expected when construction of a continuous reactor (fulfilling more of the requirements of the system) is completed.

Although our discussion of the above reaction sequence implies considerable knowledge of the overall catalytic reaction, we emphasize that many important aspects of this system have not yet been firmly established. For example, the precise nature of reaction 10, which determines the ratio of methane to ethanol, is not yet known. Fortunately, although the system as a whole is complicated by the simultaneous occurrence of many reactions, which add up to a catalytic cycle, we have found that some of the most important steps are amenable to individual study due to the occurrence of stable intermediates which can be prepared and subjected to reaction conditions. The favorable location of these stable intermediates in the catalytic sequence makes it likely that we will be able to generate a clear understanding of the entire system.

B. Thermodynamics

This program embodies experimental and theoretical research on the thermodynamic properties of a wide variety of inorganic and organic materials. Calorimetric, vapor pressure, electrical resistivity, and solubility studies are done. These studies are combined with theoretical calculations in statistical mechanics and quantum mechanics to extend the experimental measurements and to provide a basis for making predictions about unknown systems. Emphasis is placed on gaining a fundamental understanding of the properties of materials significant to science and to numerous technologies (e.g., fission, fusion, energy storage, and waste management).

1. Theory

We are developing fundamental solution theories in order to understand the fundamental properties of solutions, expand our ability to predict solution properties a priori, and facilitate the use of theories in technological applications.

a. Recent Advances in Theories of Molten-Salt Solutions

The thermodynamic properties of multicomponent ionic reciprocal systems for molten salts are derived using the conformal ionic solution (CIS) theory.[7] In such systems, schematized by $A_1^+,\ldots, A_n^+/X_1^-,\ldots, X_p^-$, the Helmholtz free energy of the mixture, A_m, is shown to be a function of the thermodynamic properties of the pure components and the binary subsystems. If a refers to anions and c to cations, one has

$$A_m = RT\left(\sum_a X_a \ln X_a + \sum_c X_c \ln X_c\right) + \sum\sum X_a X_c\, A^\circ_{ca}$$

$$+\sum_c \sum_a \sum_{a'<a} X_a X_{a'} X_c \Gamma(ca,ca') + \sum_a \sum_c \sum_{c'<c} X_a X_c X_{c'} \Gamma(ca,c'a)$$

$$+\sum_a \sum_{a'<a} \sum_c \sum_{c'<c} X_a X_{a'} X_c X_{c'} \frac{[\Delta A^\circ(c,c',a,a')]^2}{2ZRT} \qquad (12)$$

where X_a is the anion fraction, X_c is the cation fraction, A°_{ca} is the Helmholtz free energy of the salt ca, $\Gamma(ca,c'a)$ and $\Gamma(ca,ca')$ are the so-called interaction parameters in the binary system having a common anion and a common cation, respectively. The parameter Z is usually taken to be six, and $\Delta A^\circ(c,c',a,a')$ is the standard Helmholtz exchange free energy accompanying the metathetical reaction:

$$ca(\ell) + c'a'(\ell) \rightleftharpoons c'a(\ell) + ca'(\ell) \qquad (13)$$

Equation 12 should prove useful not only in concentrated solutions but also in dilute solutions, where it could be used to calculate solubility products of minor species in multicomponent solvents and to define ionic association. For example, in a binary solvent referred to as BY-CY, the activity coefficient of AX at infinite dilution (which is directly related to the solubility product of AX) can be derived from Eq. 12.

Ion associations (or preferential solvation) are very likely to occur in dilute reciprocal salt solutions and can be represented by

$$A^+ + X^- \rightleftharpoons (AX)$$

$$AX + A^+ \rightleftharpoons (A_2X)^+ \text{ etc.}, \qquad (14)$$

The energy of formation of such species (e.g., AX) and its dependence on the solvent properties can be calculated from the CIS theory through Eq. 12. The relation derived is shown to be dependent only on the properties of the pure components and the binary subsystems. Thus, one is able to predict a priori the possible existence of such species as well as their stabilities and dependence upon solvent composition and properties.

[7] M.-L. Saboungi, J. Chem. Phys. 73, 5806 (1980).

b. Phase-Diagram Calculations

Computations of phase diagrams of reciprocal and additive ternary systems are conducted to test the validity of the solution theories that we are developing for complex systems, many of which are of interest in technology such as fuel-cell electrolytes and aluminum smelting electrolytes.[8] In our study of cryolite-based phase diagrams, we have calculated the ternary phase diagrams of AlF_3-CaF_2-NaF, AlF_3-CaF_2-LiF, and CaF_2-LiF-NaF. Several conclusions were reached:

1. The use of equivalent mole fractions to represent the thermodynamic properties of mixing of binary subsystems simplifies the mathematical representation.

2. The conformal ionic solution theory leads to a priori phase-diagram predictions that are consistent with reliable thermodynamic information.

3. A controversy surrounding the nature and the extent of the solid solubility of CaF_2 in Na_3AlF_6 has been examined. Based on a careful analysis, we have shown that the CaF_2-Na_3AlF_6 join is not a quasi-binary, and the controversy concerning the different experimental results can be reconciled if one assumes a solid solubility of $NaCaAlF_6$ in Na_3AlF_6. In Fig. XI-1, the calculated phase diagram of the AlF_3-CaF_2-NaF system is shown; for comparison purposes, a section of the CaF_2-Na_3AlF_6 join is given in Fig. XI-2.

Further work is planned on multicomponent (quaternary, quinary, etc.) cryolite-based systems, including systems containing Al_2O_3. Such complex systems are a challenge to our ability to utilize fundamental solution theories.

c. Applications of the Coordination Cluster Theory

The coordination cluster theory[9] is a statistical-mechanical theory for the activity coefficients of a dilute solute in a multicomponent solvent. During the past year, we have deduced relations for slag exchange equilibria,[10] molten salts,[11] and aqueous solutions. In slag exchange equilibria, we used the theory to demonstrate that preferential solvation is the most important factor leading to deviations from the well-known Flood-Grjotheim equation.[12] In molten reciprocal salt systems, the theory permitted us to rationalize the energetics of association of cations and anions in dilute solutions.

---

[8] M.-L. Saboungi, P. L. Lin, P. Cerisier, and A. D. Pelton, Met. Trans. 11B, 493 (1980).

[9] M. Blander, M.-L. Saboungi, and P. Cerisier, Met. Trans. 10B, 613-622 (1979).

[10] M.-L. Saboungi and M. Blander, Can. Met. Quart., in press.

[11] M. Blander and M.-L. Saboungi, Acta Chem. Scand., in press.

[12] H. Flood and K. Grjotheim, J. Iron Steel Inst. (London) 171, 64-70 (1952).

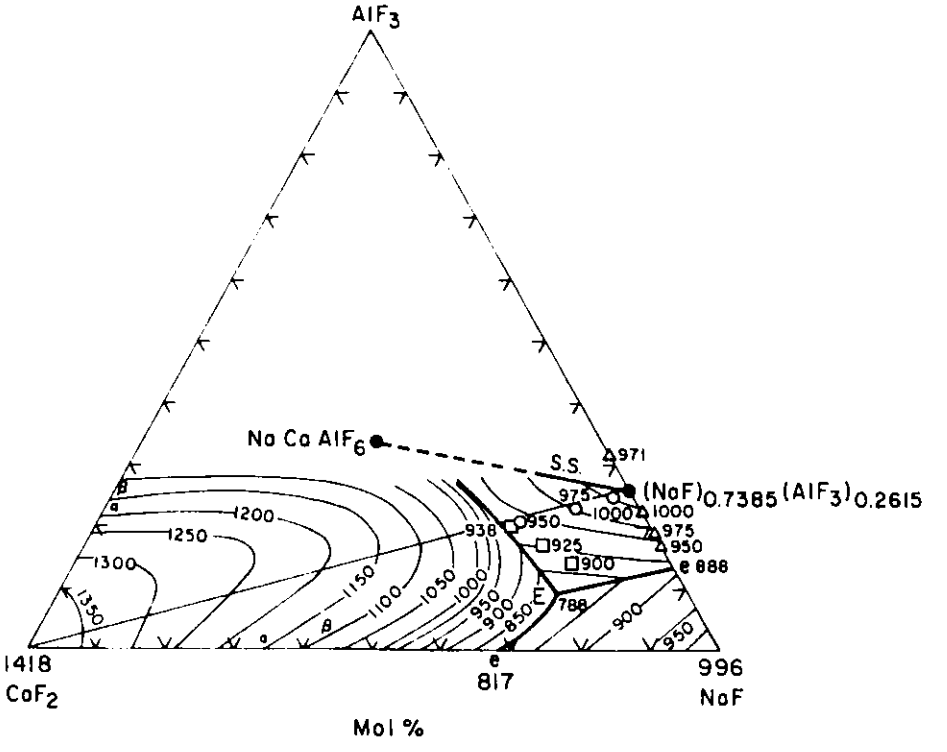

Fig. XI-1. Computer-Generated Phase Diagram for AlF_3-CaF_2-NaF System

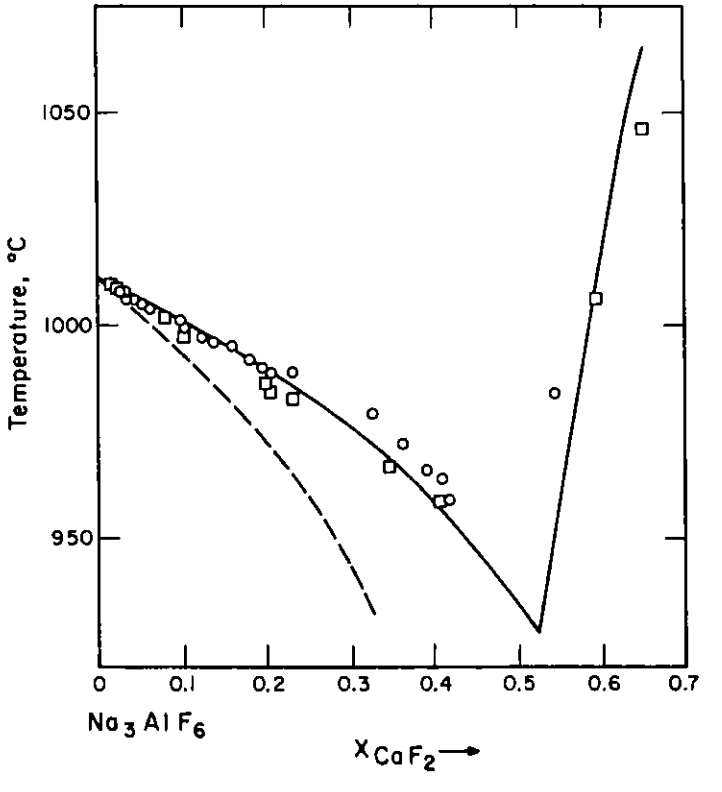

Fig. XI-2. Calculated Phase Diagram of CaF_2-Na_3AlF_6 Join. (The circles and squares represent results of two separate experiments.)

For the dissolution of a salt (CA) in a binary solvent consisting of water (W) and another component (P), e.g., peroxide, dioxane, methyl alcohol, we have considered the formation of the solvated solution species or clusters $C(W_{Y-j}P_j)$ and $A(W_{Z-i}P_i)$ in a solvent of composition (X_W, X_P). For the case in which the coordination numbers of C and A are independent of the species composition (i.e., independent of i and j), one can deduce a relatively simple expression for the activity coefficients of the salt,

$$\frac{1}{\gamma_{CA}} = \left[\sum_{j=0}^{Y} \frac{Y!}{(Y-j)!\,j!} \left(\frac{X_W \gamma_W^{t_C}}{\gamma_{C(W)}^{1/Y}}\right)^{Y-j} \left(\frac{X_P \gamma_P^{t_C}}{\gamma_{C(P)}^{1/Y}}\right)^{j} \exp\left(-\frac{\Delta G_j}{RT}\right)\right]\left[\sum_{i=0}^{Z} \frac{Z!}{(Z-i)!\,i!} \left(\frac{X_W \gamma_W^{t_A}}{\gamma_{A(W)}^{1/Z}}\right)^{Z-i} \left(\frac{X_P \gamma_P^{t_A}}{\gamma_{A(P)}^{1/Z}}\right)^{i} \exp\left(-\frac{\Delta G_i}{RT}\right)\right] \tag{15}$$

where X and γ are the concentrations and activity coefficients of the solvent components, respectively; t is a parameter which can range between 1/Z (or 1/Y) and 1/2; and $\gamma_{C(W)}$, $\gamma_{A(W)}$, $\gamma_{C(P)}$, and $\gamma_{A(P)}$ are single-ion activity coefficients in the pure solvent components which when combined are related to the component activity coefficients by the relations,

$$\gamma_{CA(P)} = \gamma_{C(P)}\gamma_{A(P)}$$
$$\gamma_{CA(W)} = \gamma_{C(W)}\gamma_{A(W)} \tag{16}$$

Because of the appearance of four parameters (three are independent) and only two measurable activity coefficients, an independent measurement (such as nuclear magnetic resonance) is needed in order to use Eq. 15. The term ΔG_i (or ΔG_j) is related to the sum of a Born solvation energy for an anion (or cation) cluster and an "excess free energy of mixing" of W and P molecules in the solvation shells of the anion (or cation) cluster. Since the radii of the clusters are relatively large, the Born energies are relatively small and likely to be essentially independent of i (or j).

No comparisons of Eq. 15 have yet been made with experimental data. However, for a model introduced by Covington and Newman,[13] Eq. 15 reduces to a form exactly equivalent to, but much simpler than, their equation. It is apparent from Eq. 15 that Covington and Newman were able to ignore the

[13] A. K. Covington and K. E. Newman, Thermodynamics of Preferential Solvation of Electrolytes in Binary Solvent Mixtures, Thermodynamic Behavior of Electrolytes in Mixed Solvents, W. F. Furter, Ed., Advances in Chem. Series, American Chemical Society, Washington, D.C. (1976).

concentration-dependent terms, γ_W and γ_P, in analyzing experimental data in solvents with fairly small deviations from ideality because of the smallness of the factors t_A and t_C.

We plan to analyze Eq. 15 and consider experiments that might test its implications. In addition, we will continue to expand the applications of the coordination cluster theory.

2. Alloy Thermodynamics

a. Activity Coefficients for Alloy Systems

To test the range of validity of the coordination cluster theory (CCT), we have measured the activity coefficients for dilute solutions (about 10^{-1} mol %) of lithium in Bi-Pb, Pb-Mg, Bi-Tl, and Bi-Al alloys as a function of solvent composition and temperature. The most extreme case is that for Li-Al-Bi, shown in Fig. XI-3, where the Al-Bi solvent exhibits a

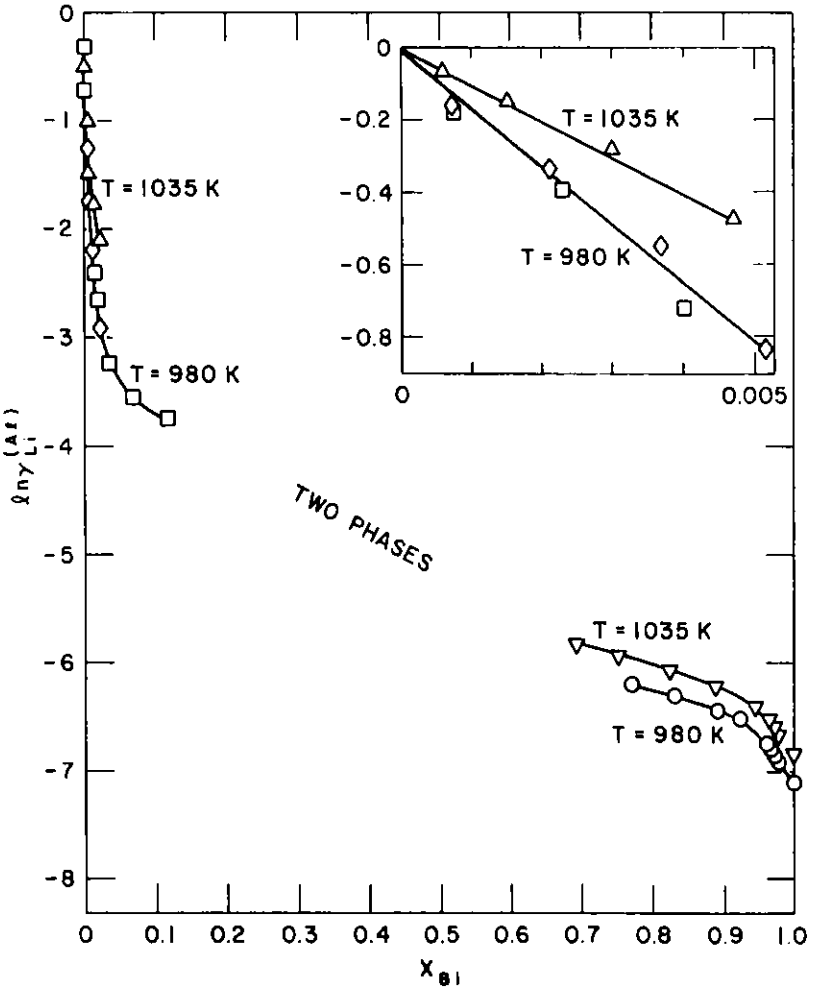

Fig. XI-3. Variations of ln γ_{Li} vs. X_{Bi} in the Li-Al-Bi System at 980 and 1035 K

miscibility gap and has large positive deviations from ideality. For all these systems, the calculations derived with the CCT are in agreement with our precisely measured emf data.

In the future, the scope of this program will be broadened to include studies of ordering in binary alloy systems. The systems that will be studied are those which exhibit a metal-to-nonmetal (MNM) transition at a given composition (i.e., ionic alloys) since the ordering phenomenon is known to occur close to this transition. The MNM transition has been observed in the Li-Bi, Li-Pb, Na-Bi, Na-Pb, and Na-Sn systems. In an effort to gain some information about the ordering phenomenon, our initial work will focus on the Na-Bi system by studying its behavior in dilute solutions. In dilute solution, the magnitude and the temperature dependence of the slope for the activity coefficient of sodium might be related to the attraction (or repulsion) existing between the solute and solvent atoms, which leads to ordering.

b. Binary Alloy Thermodynamics by the Hydrogen Titration Method

The hydrogen titration method (HTM), which was described in the preceding report in this series, continued to be used as a probe for measuring fundamental thermodynamic properties of hydrogen solutions in metals and for the development of generalized models and predictive capability for binary alloy systems. For example, recent HTM work has identified a class of A-B alloys that react with hydrogen to form stable hydrides of the type AB_x. Evaluation of available data has shown that at least three A-B pairs, Ca-Al, Ca-Si, and Mg-Si, show potential as media for hydrogen storage. The first of these systems was recently investigated, and the results are summarized below.

Two intermediate compounds, $CaAl_2$ and $CaAl_4$, exist in the Ca-Al system. Equilibrium hydrogen pressures for mixtures of these compounds are shown in Fig. XI-4 as van't Hoff isopleths. An interesting feature in Fig. XI-4 is that the two closely spaced isopleths at the top intercept the 100- to 1000-kPa pressure band at temperatures that are potentially useful for hydrogen storage. If $CaAl_2$ were chosen as the starting alloy, then the isothermal hydriding would proceed in the sequence $CaAl_2 \rightarrow CaAl_4 \rightarrow Al$ as long as the hydrogen pressure is maintained at a value above the upper isopleth. Conversely, for pressures below those of the lower isopleth, the reverse reaction sequence would occur. Therefore, $CaAl_2$ can serve as a "high-temperature" hydrogen storage medium with an absorptive capacity of 2.1 wt % H, which compares favorably with 1.9 wt % H for FeTi and 1.4 wt % H for $LaNi_5$, two prominent "low-temperature" hydrogen storage media.

In addition to storage information, HTM data for Ca-Al yielded (1) verification of the stoichiometry of the intermediate compounds, (2) calcium activities and the corresponding emf's of $[Ca/Ca^{2+}/Ca\text{-}Al]$ cells, (3) standard free energies of hydriding and formation of $CaAl_2$ and $CaAl_4$, and (4) standard enthalpies of formation of $CaAl_2$ and $CaAl_4$ that are less negative by a factor of two than those listed for these compounds in current thermochemical compilations. Since Ca-Al alloys are under consideration as electrodes

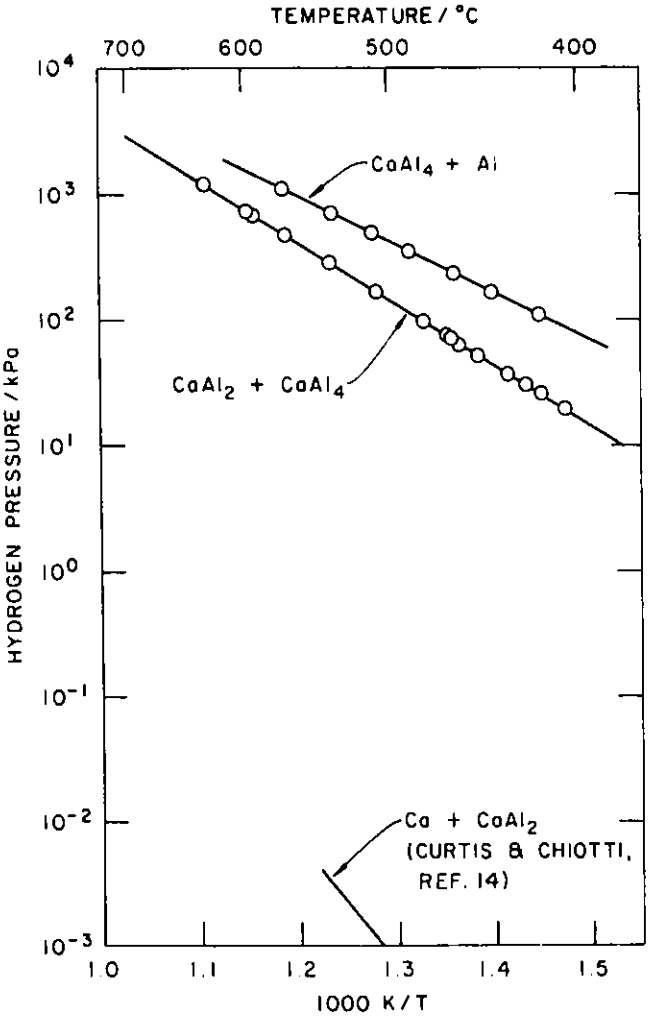

Fig. XI-4. Van't Hoff Isopleths for the Two-Phase Fields of the Ca-Al System

in calcium/metal sulfide batteries, the calcium activity information is especially pertinent.

Recently, HTM studies on Ca-Si were started. One of its intermediate compounds, CaSi, may have excellent potential for storing hydrogen (2.8 wt % H) over the 130-180°C temperature range. Future plans include similar studies on other suitable binary alloy systems, e.g., Mg-Si.

---

[14] R. W. Curtis and P. Chiotti, Thermodynamic Properties of Calcium Hydride, J. Phys. Chem. 67, 1061 (1963).

3. Thermochemistry

The thermochemistry program has as its principal objective the precise and accurate determination of the thermochemical properties of materials of interest in energy-related (e.g., nuclear, coal, hydrogen storage, geothermal) processes and phenomena. The scope of the program also includes the interpretation of the results obtained with a view to predicting the thermodynamic properties of related materials. In the past year, CEN's thermochemistry studies have been concentrated on zeolites, uranium compounds, and metallic sulfides.

a. Thermodynamic Properties of Zeolite Minerals

The thermodynamic properties of zeolites are of interest in the exploitation of the hot-dry-rock geothermal resource. Although the chemical and physical properties of zeolites, both natural and synthetic, have been extensively studied, there have been almost no studies conducted on their basic thermodynamic properties. Hence, we have undertaken a program to determine the thermodynamic properties of selected natural and synthetic zeolites.

Samples of five naturally occurring minerals--analcime, natrolite, mesolite, scolecite, and thomsonite--have been received from W. S. Wise of the University of California at Santa Barbara. Professor Wise is also attempting to prepare some synthetic zeolites with various Al/Si ratios so that the effect of this ratio on the thermodynamic properties can be determined.

To date, the enthalpies of formation of analcime, dehydrated analcime, and natrolite have been determined using hydrofluoric acid reaction calorimetry, and the enthalpy functions of analcime to 625 K have been determined using drop calorimetry. In addition, low-temperature measurements (between 5 and 350 K) of heat capacity have been completed on analcime. For analcime having the composition $Na_{0.96}Al_{0.96}Si_{2.04}O_6 \cdot 1.02H_2O$, the following thermodynamic properties* at 298.15 K were obtained: ΔH_f° = -3304.0 ± 3.3 kJ mol^{-1}, C_p° = 212.15 J K^{-1} mol^{-1}, S° = 227.12 J K^{-1} mol^{-1}, ΔS_f° = -740.5 ± 1.2 J K^{-1} mol^{-1}, and ΔG_f° = -3083.2 ± 3.3 kJ mol^{-1}. The enthalpy increments of analcime between 298.15 K and 625 K are given as a function of temperature by the equation:

$$H_T^\circ - H_{298.15\ K}^\circ = -62490.5 + 241.5099T - 0.250464T^2 + 5.769880 \times 10^{-4}T^2 - 3.218547 \times 10^{-7}T^4 \qquad (17)$$

These measurements allow us to compile a table of the complete thermodynamic properties of analcime between 0 and 625 K.

The enthalpies of formation of dehydrated analcime, $Na_{0.96}Al_{0.96}Si_{2.04}O_6$, and natrolite, $Na_2Al_2Si_3O_{10} \cdot 2H_2O$, were determined to be -2972.3 ± 3.5 kJ mol^{-1} and -7032.0 ± 6.2 kJ mol^{-1}, respectively.

---

*Symbols have their usual thermodynamic meaning.

Our results for the enthalpies of formation of analcime and dehydrated analcime are more negative by 76 and 60 kJ mol^{-1}, respectively, than those reported by Barany.[15] His paper describes the only previous reaction calorimetric study of any zeolite. The results of Barany have been shown[16] to have a significant systematic bias and, hence, agreement between his values and ours would not be expected.

A concern in hot-dry-rock geothermal energy is the plugging of cracks in the native rock between inlet and outlet bore holes, through which water must circulate. A reaction between native feldspar and hot water to produce analcime and quartz is known to proceed at low temperatures; and, because it forms a high-volume product, the reaction could cause the cracks in the rock to become plugged. For the analcime specimen in our study, the reaction would be written as

$$0.96NaAlSi_3O_8(c) + 1.02H_2O(\ell) \rightarrow Na_{0.96}Al_{0.96}Si_{2.04}O_6 \cdot 1.02H_2O(c) + 0.84SiO_2(\alpha) \quad (18)$$

Based on our derived ΔG_f° values for analcime and literature data for the other components of reaction 18, we deduce the equilibrium temperature to be approximately 380 K. At temperatures in excess of 380 K, the formation of analcime is not favored, and plugging of the cracks in the rock would not be a serious problem.

Future work will comprise systematic measurements of low- and high-temperature thermodynamic properties, including the standard enthalpy of formation, of natrolite, mesolite, scolecite, thomsonite, and other zeolites that may play a role in the extraction of geothermal energy.

b. Thermodynamic Properties of Uranium Compounds

Although numerous thermochemical studies of uranium fluorides have been reported in the literature, it appears that the enthalpy of formation, ΔH_f°, of only one of those fluorides, namely, UF_6, has been established with any degree of certainty. In order to rectify this situation, a cooperative program to firmly establish ΔH_f° values for UF_3, UF_4, α- and β-UF_5, and, if possible, U_2F_9 and U_4F_{17} has been established between the CEN thermochemistry group and other groups at the Netherlands Research Foundation (ECN, Petten), the Los Alamos Scientific Laboratory, and the Chemistry Division at Argonne. To date, results have been obtained for α- and β-UF_5, UF_4, and UF_3.

The enthalpy of formation of β-UF_5 has been based on the following calorimetrically measured results ("soln A" denotes $Ce(SO_4)_2 \cdot 41.60H_2SO_4 \cdot 1274.4H_2O$):

---

[15] R. Barany, Bureau of Mines Report of Investigations RI5900, United States Department of the Interior, Bureau of Mines (1962).

[16] B. S. Hemingway and R. A. Robie, J. Res. U. S. Geol. Survey 5(4), 413-429 (July-August 1977).

$$1/2UO_2(c) + \text{soln A} = \text{soln B}, \quad \Delta H = -111.46 \pm 0.60 \text{ kJ mol}^{-1} \tag{19}$$

$$1/2UO_3(c,\gamma) + \text{soln B} = \text{soln C}, \quad \Delta H = -38.27 \pm 0.67 \text{ kJ mol}^{-1} \tag{20}$$

$$5HF(aq) + \text{soln C} = \text{soln D}, \quad \Delta H = -81.32 \pm 0.75 \text{ kJ mol}^{-1} \tag{21}$$

$$\text{soln E} = UF_5(c,\beta) + \text{soln A}, \quad \Delta H = 190.26 \pm 0.51 \text{ kJ mol}^{-1} \tag{22}$$

$$\text{soln D} = \text{soln E} + aq, \quad \Delta H = 1.06 \pm 0.11 \text{ kJ mol}^{-1} \tag{23}$$

Summation of the above reactions gives

$$1/2UO_2(c) + 1/2UO_3(c,\gamma) + 5HF(aq) = UF_5(c,\beta) + 2\ 1/2H_2O(\ell) \tag{24}$$

where $\Delta H = -39.73 \pm 2.55$ kJ mol^{-1}. Combination of this result with critically selected ΔH_f° values for UO_2, γ-UO_3, HF(aq), and $H_2O(\ell)$ gives $\Delta H_f^\circ(UF_5,c,\beta) = -2085.8 \pm 2.1$ kJ mol^{-1}. We have also studied the following reaction:

$$UF_5(c,\alpha) + \text{soln A} = \text{soln E}, \quad \Delta H = -197.83 \pm 1.98 \text{ kJ mol}^{-1} \tag{25}$$

When this result was combined with the result for reaction 22, we obtained

$$UF_5(c,\alpha) = UF_5(c,\beta), \quad \Delta H^\circ(298.15 \text{ K}) = -7.6 \pm 2.0 \text{ kJ mol}^{-1} \tag{26}$$

This enthalpy of transition agrees with the critically selected value of -7.9 kJ mol^{-1}. The enthalpy of formation of β-UF_5 also agrees with the selected value, -2075 ± 17 kJ mol^{-1}, but is clearly more precise.

Experimental work on UF_3 and UF_4 has, essentially, been completed. Solution calorimetric measurements were performed at ECN and fluorine bomb measurements at ANL. There are, unfortunately, disagreements between the ΔH_f° values from the two laboratories; therefore, at this time definitive results cannot be given for UF_3 and UF_4.

In irradiated nuclear fuels, interactions between the fission-produced "noble" metals, Ru, Rh, and Pd, and the fuel yield the exceptionally stable intermetallic phases URu_3, URh_3, and UPd_3. Quantitative, e.g., thermodynamic, data for these alloys are important not only for practical operations such as fuel reprocessing, but also as test cases for theories of chemical bonding which have been invoked to explain their exceptional stabilities. Conventional experimental techniques (e.g., solid-state emf measurements, Knudsen effusion) have proved satisfactory for the determination of ΔH_f° of URu_3 and URh_3, but have been unsuccessful when applied to UPd_3.

We have just concluded a determination of $\Delta H_f^\circ(UPd_3)$ by fluorine bomb calorimetry. This work clearly shows that, thermodynamically, UPd_3 is indeed very stable. The result also lends strong support to the Brewer-Engel theory of chemical bonding, which, inter alia, predicts exceptional stabilities for compounds formed from transition metals only.

We observed that several thermochemical cycles which have $\Delta H_f^\circ(UO_2)$ in common yield ΔH_f° values for various uranium compounds that may be inconsistent with results obtained from other thermochemical cycles. In order to check the currently accepted value for $\Delta H_f^\circ(UO_2)$, we measured the enthalpy of the reaction

$$UO_2(c) + 3F_2(g) = UF_6(c) + O_2(g) \qquad (27)$$

by fluorine bomb calorimetry. Our result for $\Delta H_f^\circ(UO_2)$ agrees exactly with the assessed value. This indicates that the inconsistencies in the thermochemical cycles are not due to an incorrect value for $\Delta H_f^\circ(UO_2)$.

The only planned studies on uranium-containing compounds involve the determination of ΔH_f° of UOF_4 and $AgUF_6$; this work will be carried out in cooperation with J. G. Malm (Chemistry Division of ANL).

c. Thermochemistry of Sulfides

There is a serious lack of reliable thermodynamic data for inorganic sulfides. This situation is rather surprising when one considers the importance of many of these materials in connection with solid-state and high-temperature science, corrosion phenomena, extractive metallurgy, energy storage, and geothermal systems. Thermodynamic data for those sulfides which have been studied--usually by high-temperature vaporization techniques or oxygen bomb calorimetry--frequently suffer from large uncertainties because the vaporization or combustion reactions are difficult to define precisely. This situation is illustrated dramatically by the results that we obtained from a recent literature search. For the 74 sulfides that we surveyed, the mean uncertainty in the ΔH_f° value was about ± 50 kJ mol^{-1}. Uncertainties of this order of magnitude render the data worthless for most practical applications.

The only generally applicable technique for the reliable determination of ΔH_f° values of inorganic sulfides is fluorine bomb calorimetry. We have applied this technique in recent years to the study of As_4S_4 and As_2S_3,[17] Sb_2S_3,[18] MoS_2,[19] US[20] and US_2.[20] Within the past few months, we have extended these studies to include $CuFeS_2$ (chalcopyrite)[21] and K_2S.[21] Each one of these investigations has revealed serious errors in the generally accepted thermochemical values.

---

[17] G. K. Johnson, G. N. Papatheodorou, and C. E. Johnson, J. Chem. Thermodyn. 12, 545 (1980).

[18] G. K. Johnson, in press.

[19] P. A. G. O'Hare, E. Benn, F. Y. Cheng, and G. Kuzmycz, J. Chem. Thermodyn. 2, 797 (1970).

[20] P. A. G. O'Hare, J. L. Settle, H. M. Feder, and W. N. Hubbard, Thermodynamics of Nuclear Materials, 1967, International Atomic Energy Agency, Vienna (1968).

[21] W. V. Steele and G. K. Johnson, unpublished results.

It is proposed, therefore, that fluorine bomb calorimetry be used to establish firm values for a number of selected sulfides of technological importance. The next compounds to be studied will be Al_2S_3 (for which ΔH_f° values of -586, -510, -556, -920, -858, -854, and -799 kJ mol^{-1} have been reported) and WS_2 (for which ΔH_f° values of -201, -301, -230, -255, -285, -280, -255, and -276 kJ mol^{-1} have been reported). Enthalpies of the following combustion reactions will be determined:

$$Al_2S_3(c) + 12F_2(g) = 2AlF_3(c) + 3SF_6(g) \quad (28)$$

$$WS_2(c) + 9F_2(g) = WF_6(g) + 2SF_6(g) \quad (29)$$

and combined with the literature values for ΔH_f° of AlF_3, SF_6, and WF_6 to derive the desired ΔH_f° results.

Both Al_2S_3 and WS_2 are of current technological interest--the former as a potential source (in place of Al_2O_3) of Al and the latter as a possible deleterious product in LiAl/FeS electrochemical cells that employ W as a current collector.

4. Gas-Condensed Phase Equilibria

Gas-condensed phase equilibria in complex multicomponent systems are of primary importance in a number of energy technologies such as magnetohydrodynamics, coal combustion, desulfurization, and coal gasification. The purpose of this work is the development and application of sophisticated computer programs and data bases capable of determining the chemistry of complex multicomponent multiphase systems.

We have performed calculations of the condensation of alkali sulfates in combustion gases and obtained two significant results when the condensation of solutions was taken into account. First, we found that, in comparison with pure Na_2SO_4, Na_2SO_4-K_2SO_4 solutions condense at somewhat higher temperatures, but have a much lower liquidus temperature. Under typical burner conditions, this means that a much larger fraction of the alkali sulfate condenses to corrosive liquids rather than to less corrosive solids. Figure XI-5 illustrates the fraction of alkalis condensed and the pressures of selected species in a typical fuel-oil combustion gas. Second, we found that, in the presence of dolomite (used for desulfurization in fluidized beds) as entrained solids, the possibility of corrosive sulfate liquids, rather than solids, being formed in turbines and in condensers increases dramatically.

Currently, we are improving our computer programs in several ways: (1) by the incorporation of reciprocal molten-salt solution theories that can handle the more complicated solutions that occur in hot corrosion such as the mixture Na^+, K^+, Ca^{2+}, Mg^{2+}/SO_4^{2-}, Cl^-, and CO_3^{2-}; (2) by the modification of the computer codes to use advanced mathematical techniques for minimization of free energies; and (3) by expanding the data base. We plan to use these improvements to further examine the condensation of sulfates from combustion gases relevant to hot corrosion.

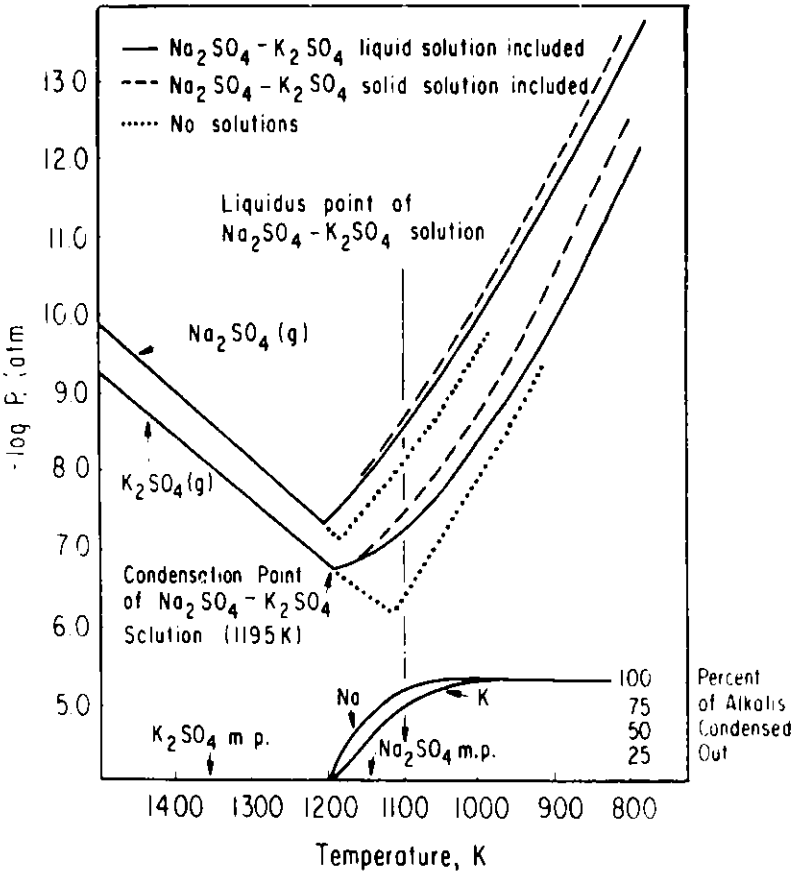

Fig. XI-5. Partial Pressures of Na_2SO_4 and K_2SO_4 in a Typical Fuel Oil Combustion Gas (with and without considering the formation of solutions).

5. Impurity Interactions in Liquid Metals

Electrical resistometry has been used to examine the nature, extent, and rate of metal/nonmetal interactions in liquid metal solutions. These studies have focused on the reaction of nitrogen with selected metallic elements in liquid lithium, since nitrogen is known to play a key role in the compatibility of metals with lithium. The systems under study are Li-Cr-N and Li-Ca-N.

The interactions in the Li-Cr-N system are believed to be critical to an elucidation of the mechanism of corrosion and mass transfer of chromium-containing steels by liquid lithium. During 1980, investigations using scanning electron microscopy and ion microprobe mass analysis, together with sampling and wet chemical analyses, were completed and combined with our prior resistometric data to better elucidate the mechanism of reaction of chromium with nitrogen in liquid lithium. The combined data collected during this series of studies support the proposed formation of Li_9CrN_5 in lithium solutions.

The data indicate that the solubility of the ternary compound is significantly higher than that of chromium metal. This finding could account for the well-known enhancement of dissolutive corrosion and chromium mass transfer in lithium-stainless steel systems observed under conditions of high nitrogen concentrations in the lithium.

Precipitation techniques, involving the formation of nitrides that have much lower solubilities in liquid lithium than does Li_3N, offer a promising method for reducing nitrogen levels in liquid lithium systems. The experimental results on the Li-Ca-N system, obtained to date, indicate that calcium additions may represent an avenue of possible utility in this regard. The Ca-N reaction in liquid lithium has been examined for both high and low nitrogen activities. In the high nitrogen domain ($[N]/[Ca]>>1$), the experimental results indicate that the compound LiCaN forms and precipitates from the melt. The results for $[N]/[Ca]<1$ could not be explained in this way. However, by assuming (1) a finite solubility for LiCaN in lithium and (2) the existence of an equilibrium between LiCaN and Ca_3N_2, it was possible to interpret the $[N]/[Ca]<1$ results. Specifically, the temperature dependence of the data observed at low nitrogen concentrations was found to be consistent with a shift in the LiCaN-Ca_3N_2 equilibrium with temperature. The composite results show that, by carefully adjusting the calcium activity in lithium, it should be possible to control nitrogen levels in the 100 to 1000 wppm range.

C. Environmental Chemistry

1. Overview

In the environmental chemistry program, we are attempting to understand the chemistry of airborne particulate matter, determine the significant mechanisms for the formation of primary (formed at the source) and secondary (formed in the atmosphere) aerosol sulfate and nitrate, and investigate those atmospheric processes that give rise to acid precipitation. To achieve these goals, we are developing sensitive instruments and analytical techniques for characterizing atmospheric aerosols, conducting laboratory experiments to investigate the formation of primary and secondary sulfates and nitrates, and conducting field studies, as necessary, to establish the validity of laboratory results in the atmosphere.

2. Characterization of Atmospheric Aerosols

The Attenuated Total Internal Reflection instrument, the ATR-impactor described briefly in last year's report, has been field-tested for sampling atmospheric aerosol and has been found to be effective even with very short sampling times, i.e., on the order of one minute. This device combines inertial impaction for sample collection with attenuated total internal reflection for analysis, yielding a very sensitive instrument. The sensitivity arises from the use of multiple total internal reflections, at each of which the infrared light is attenuated by infrared-active species present in the particles on the surface of the internal reflection element. In the past year, field tests have been conducted, both in ground-level sampling

and sampling aboard an aircraft provided by Pacific Northwest Laboratory. Tests on the ground at Argonne showed that sampling times as short as one minute are adequate to obtain a sample which produces an infrared spectrum that can be interpreted. Typically, a sample collected in one minute at an air flow rate of 75 L/min covers only about 10% of the surface of the internal reflection element. Thus, individual aerosol particles are collected without interaction with other, possibly different, particles in the same 0.5- to 1.2-μm size fraction. This capability to sample and analyze particles without permitting possible interactions between them should permit analysis of, for example, co-emitted acidic and basic particles from a source.

The capability of the device to sample and analyze the emissions from a single isolated source was evaluated during a week-long series of airborne field experiments. A modified, instrumented DC-3 aircraft was provided by courtesy of Jeremy Hales, Pacific Northwest Laboratory, Richland, WA. The on-board instrumentation included gas analysis instruments (SO_2, O_3) and meteorological instruments (temperature, pressure, altitude). The airborne tests of the ATR-impactor were conducted around a power plant near Centrallia, WA. The upwind air was of marine origin and had a very low loading of aerosol particles. In traverses of the plume between 5 and 20 miles from the stack, sulfate aerosol particles were collected in amounts sufficient to be analyzed by the ATR method. In fact, a sample amount sufficient for analysis was collected in a single traverse of the plume 6 miles from the stack, even though the power-plant plume itself was very clean, being cleaner than the typical urban environment in the northeastern United States. Further studies are planned of the ATR-impactor for sampling of both a strong isolated source and a diffuse urban source of emissions.

The sensitivity of the Fourier-transform infrared (FT-IR) spectroscopic method for condensed-phase nitrate has been extended to the submicrogram level, using the infrared absorption band appearing at 1384 cm^{-1}. Five different series of standard samples were used to calibrate the absorption bands at 840, 1384, and 2430 cm^{-1} for the nitrate ion. The band at 840 cm^{-1} is subject to interferences from other atmospheric condensed-phase species and is, therefore, not used for measuring nitrate in atmospheric samples. The 1384 cm^{-1} band is a very sensitive indicator for nitrate and is useful in detecting amounts of nitrate down to about 0.1 μg. However, its high sensitivity makes the band unsuitable for samples containing more than about 40 μg of nitrate, for which the absorbance at 2430 cm^{-1} is used instead. The nitrate calibration factors have been applied to the analysis of field samples collected in Riverside, CA, in 1974-1975. The quantities of nitrate calculated from the two absorption bands, at 1384 and 2430 cm^{-1}, showed very good agreement over the rather wide range of amounts of nitrate present in those samples. Future work on the FT-IR method will focus on the calibration of the spectra of acidic sulfates and other atmospheric species.

3. Chemistry of Atmospheric Sulfate Formation

Oxygen isotopy is being used to investigate the mechanisms active in the transformation of gaseous sulfur dioxide to particulate sulfuric acid and partially or completely neutralized ammonium sulfate.

At the time we began our study, three views had been advanced concerning the probable formation mechanism of atmospheric aerosol sulfate from SO_2. These views were as follows:

(1) Formation involves the homogeneous oxidation of SO_2 to SO_3 followed by subsequent reaction with atmospheric water to form H_2SO_4, the initial oxidation being light-induced.

(2) Formation involves the conversion of SO_2 to H_2SO_3 and subsequent oxidation to H_2SO_4; the oxidation step proceeding heterogeneously and catalytically, in the absence of light.

(3) Primary sulfate emissions from power plants (as SO_3) are the major source of atmospheric sulfates.

Mechanism (1) was the one most favored by the environmental science community. A small group of scientists believed that the heterogeneous sulfate formation mechanism was important, but the evidence supporting it was sparse. Given the fact that the quantity of SO_3 released from stacks would account for at most 5% of atmospheric aerosol sulfate, the sulfur trioxide mechanism did not occupy a position of high regard.

Against this background, we began our work to determine the relative importance of the homogeneous and heterogeneous mechanisms. We have convincingly shown that the heterogeneous mechanism is important in atmospheric sulfate formation and that, in fact, in some locales (Chicago) and during certain periods of the year (late autumn, winter, and early spring), it is very likely the predominant mechanism.

Having established the prominence of the aqueous oxidation mechanism, we turned our attention to a study of a variety of SO_2 oxidation processes, both homogeneous and heterogeneous in nature, to see if we could reproduce in the laboratory the isotopy observed in the atmospheric sulfates. In this connection, we have examined: (1) Fe^{3+}-catalyzed air oxidation in the aqueous phase; (2) charcoal-catalyzed air oxidation in the aqueous phase; (3) oxidation in an aqueous solution of H_2O_2; (4) homogeneous oxidation in humidified air, induced by a high-voltage spark; (5) homogeneous oxidation in humidified air containing NO_2; (6) homogeneous oxidation in humidified air, induced by gamma irradiation; and (7) oxidation on activated charcoal in humidified air in the absence of liquid water. In all instances, the oxygen isotope ratio of the final sulfate product was lower than that observed for atmospheric sulfates. It is our speculation that the observed oxygen isotopy might be accounted for, at least in part, if the atmospheric sulfate consisted of a product derived from primary sulfate (SO_3). Recent preliminary results based on analysis of flue gas samples supplied by Brookhaven National Laboratory, as well as our own laboratory experiments, seem to support this speculation.

That the formation mechanism of atmospheric sulfate is a complex problem is unquestionable. However, we believe our work has provided some significant insights into the likely formation mechanism(s) and, at the same time, has established an information base which should prove useful in evaluating emission-control strategies. In future work in this area, we will examine the oxygen isotopy of primary sulfate in greater detail.

4. Nitrogen Chemistry

The objective of these studies initially is to determine the vapor-liquid equilibria in the NO_x-H_2O-SO_x-NH_3 system at compositions which might be present in the ambient environment, with particular reference to the compositions involved in acid precipitation and acid deposition. For this purpose, sensitive instruments are being developed for the analysis of the individual nitrogen oxides in a mixture at low overall concentrations. One of the instruments being developed is a chemiluminescent NO_x analyzer. This analyzer is based on the chemiluminescent reaction between NO and O_3. For the measurement of the other nitrogen oxides, the specific oxide is selectively converted to NO and then measured by this method. The instrument has been developed to a stage where it can be used to measure the NO and NO_2 concentrations in air at atmospheric pressure, and is sensitive enough to detect these gases at the levels at which they are usually present in the atmosphere. However, the rate of response to changes in the sample concentration is low, thereby making the instrument difficult to apply to the problem of phase-equilibria determination in its present form. Further development of the instrument will be necessary before it can be applied to static systems at low total pressures, as would be the case in vapor-liquid equilibrium studies. In the meantime, other possible analytical techniques for gas-phase NO_x are being considered, including tunable diode laser infrared spectrophotometry and laser-induced fluorescence spectroscopy. The chemiluminescent instrument will be used in laboratory experiments involving nitrogen chemistry, as well as in field tests to measure ambient NO_x levels.

D. Electrochemistry

This program encompasses fundamental spectroscopic studies of the kinetics and mechanisms of processes occurring at cell electrodes and in electrolytes. Phenomena such as electrocatalysis, electrochemical corrosion, deposition and dissolution, and complexation in molten-salt electrolytes are objects of study. Electrochemical (relaxation and cyclic voltammetry methods), surface analytical (ESCA, AES, SEM),* and spectroscopic (Mössbauer, Raman, UV-visible) tools alone and in combination are employed. Strong emphasis is placed on *in situ* studies employing coupled spectroscopic and electrochemical methods for catalysis and corrosion studies, and on methods for kinetic measurements that are faster than any measured previously. Both model and practical systems are chosen for study. The information gained is expected to lead to an understanding of how the fundamental chemistry of surface and interfacial reactions affects the performance of some practical system.

1. Investigations in Electrocatalysis

Studies are being undertaken to elucidate the factors that determine the rate and mechanism of electroreduction of oxygen on carbon-supported iron phthalocyanine (FePc) electrodes. Spectroscopic and electrochemical techniques, as well as quantum theoretical methods, are employed to obtain correlations between molecular electronic structure and electrocatalytic activity.

---

*ESCA = electron spectroscopy for chemical analysis; AES = Auger electron spectroscopy; and SEM = scanning electron microscopy.

Cyclic voltammetry was used to characterize the electrochemical behavior of FePc films on glassy carbon electrodes in 0.05M H_2SO_4 solution. The films were initially found to catalyze oxygen reduction, but became deactivated on continued cyclic scanning. Activity was restored on standing at open circuit for about one hour, indicating that the deactivation process is probably associated with the slow transport of charge carriers within the p-type semiconductor film electrode. Films prepared by evaporation of a solution containing FePc and organic solvents, as well as by immersion in such a solution, showed significantly higher activity than those prepared by vapor deposition. This difference was found to correlate with the polymorphic form of the films; the former was shown to crystallize in the α-form, while the latter assumed the β-structure. In situ laser Raman spectroscopy of the films indicated coordination of the FePc (through the bridge nitrogen) with water molecules in the solution. The vibrational spectra, however, appear to be independent of potential in the region of 0.4 to -0.9 V vs. Hg/Hg_2SO_4.

Quantum-mechanical calculations were carried out on FePc and its analog, iron porphyrin (FeP), as well as their oxygen adducts. The charge of the iron in both molecules is about 1.4, but the electrons when transferred into the delocalized organic structure are distributed differently. In FeP, with a bridge carbon, this charge is concentrated on the pyrrole rings; whereas, in FePc, it is concentrated on the bridge nitrogen atoms. The electron population of the Fe "d" orbitals also differs in each case. Calculations were made on the structure of the oxygen complexes of FePc and FeP. In the case of the FePc-O_2 complex, oxygen binds side-on to the Fe, with the O-O axis parallel to the FePc plane, i.e., $\overset{\text{O-O}}{\backslash\ /}\ \underset{\text{Fe}}{}$. The electronic ground state of the molecule is a quintet. In the case of the FeP-O_2 complex, oxygen is bound end-on to the Fe, with the Fe-O-O angle equal to 119°, i.e., $\overset{\text{O}}{\text{O}}\!\!\diagup\ 119°$ $\underset{\text{Fe}}{}$. Both quintet and triplet are the low-lying electronic states. The foregoing differences are significant and may be decisive in determining what makes for a good electrocatalyst (FePc) or a mere oxygen carrier (FeP). Experimental evidence on platinum, for example, suggests a side-on configuration for oxygen binding.

The foregoing results indicate some of the salient features of electronic structure that characterize a good oxygen-reduction catalyst. We hope to extend the present studies to other systems and examine the general applicability of the structure-activity correlation found.

2. Studies in Corrosion

Spectroscopic and electrochemical techniques are being applied to the study of anodic corrosion and passivation of metals in aqueous and molten-salt environments. The anodic polarization of Fe, Co, Ni, Cu, Ti, Ta, and Mo in molten LiCl-KCl containing Li_2O were measured at 375 and 450°C. The current-potential curves obtained show characteristic corrosion-passivation behavior that is similar to that found in aqueous systems. In view of the profound difference in the composition and properties of aqueous and molten-salt electrolyte systems, this surprising result is suggestive of a general

law governing the phenomenon of metal passivation. Anodic corrosion rates for the metals in the presence of O^{2-} were significantly less than those in pure LiCl-KCl. Reversibility in the reduction of the oxide films formed was examined by cyclic voltammetry. Oxides of Fe, Co, and Cu appear to be reversibly reducible, while the oxides of Ta, Ti, Ni, and Mo are not. Consequently, use of Fe, Co, and Cu as cathodes for a molten-salt secondary battery is suggested.

Identification of the oxide formed on iron in aqueous neutral and basic solutions is being undertaken using laser Raman spectroscopy. Ex situ spectra showed that, possibly, a mixed oxide and an amorphous film are formed when an iron foil is anodized at 1.9 V vs. SCE in borate buffer solution. Spectra of films formed in phosphate buffer and 6M KOH solutions showed bands that we are attempting to assign to known compounds.

Future plans include studies on the kinetics of film formation and growth and determination of transport properties and their correlation with film composition and structure.

3. Structural Ordering and Complex Ions in Chloraluminate Melts

Molten chloraluminates are an important class of scientifically interesting materials which are used in at least two battery systems and in the new aluminum smelting process developed at Alcoa. The concept of pCl has been developed in such materials for high $AlCl_3$ concentrations (25-70 mol %) to define their basicity. In addition, the solution characteristics have been described in terms of complex ions such as $AlCl_4^-$, $Al_2Cl_7^-$, etc. The purpose of our work is to provide a quantitative thermodynamic and physical basis for the description of the properties of such melts.

We have analyzed the emf measurements of Boxall et al.[22] made at 175°C in a cell:

$$Al/AlCl_3\text{-}NaCl(solid)//NaCl\text{-}AlCl_3/Al \qquad (30)$$

where the mole fraction of $AlCl_3$ was varied from 0.4977 to 0.7000. If the transference number of Na^+ is unity, then the emf is given by

$$E = E_o - (RT/F)\ln(a_{AlCl_3}^{1/3}/a_{NaCl}) \qquad (31)$$

where the activities are for the components in the right-hand half cell, and the left-hand half cell is the reference. Figure XI-6 shows the emf's and the activities of NaCl and $AlCl_3$ calculated from a Gibbs-Duhem integration of the emf's. If pCl is defined as $\frac{3E}{4RT}$ and is zero in a NaCl-saturated melt, then pCl differs little from $-\ln a_{NaCl}$ (about 0.2 difference at $X_{AlCl_3} = 0.7$).

[22] L. G. Boxall, H. L. Jones, and R. A. Osteryoung, J. Electrochem. Soc. 120, 223 (1973).

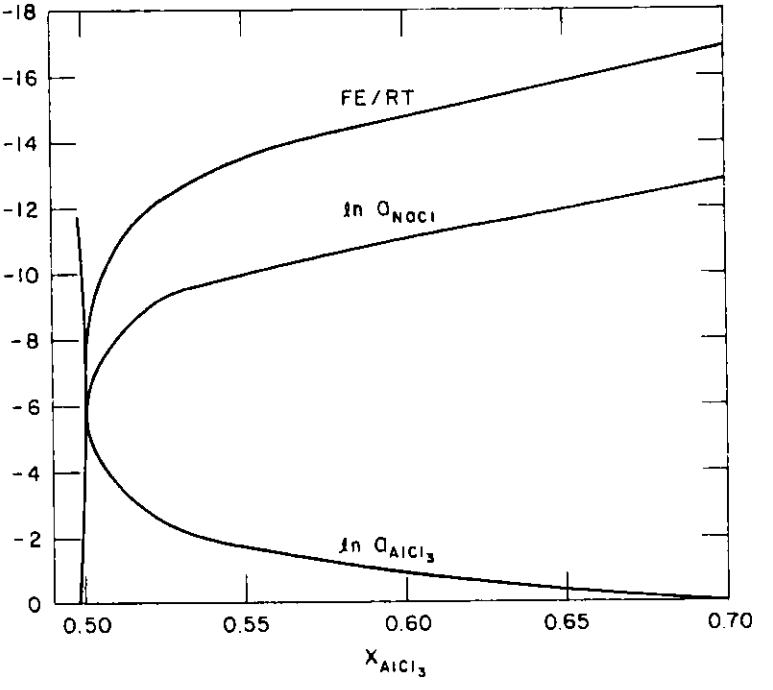

Fig. XI-6. Plots of FE/RT, ln a_{NaCl}, and ln a_{AlCl_3} vs. the Mole Fraction of $AlCl_3$

In this case, pCl appears to have quantitative significance. However, for cases in which the concentration range of the measurements is larger, pCl becomes much less quantitative. For melts where the monovalent chloride concentrations are much higher, the pCl scale is only relative. Our analysis permits one to define the conditions for which the concept of pCl has a quantitative significance.

From our results, we have also calculated the total excess free energy of mixing per mole, which is plotted in Fig. XI-7. The straightness of the curve is indicative of an unusual degree of ordering, such that Na^+ and Al^{3+} are preferred next-nearest neighbors. Such ordering can be understood in terms of the formation of ions such as $AlCl_4^-$ (or $AlCl_n^{3-n}$), as well as in terms of models of solutions analogous to but more sophisticated than the quasi-chemical theory. Comparison with simple theory indicates an unusual degree of ordering near the 50-50 composition.

We hope to examine ordering and complex ions in chloraluminates and will reexamine the use of the concept of pCl in the study of the chemistry of chloraluminate melts. Our examination of literature data indicates that the use of the concept of pCl has led to conclusions inconsistent with an exact thermodynamic analysis.

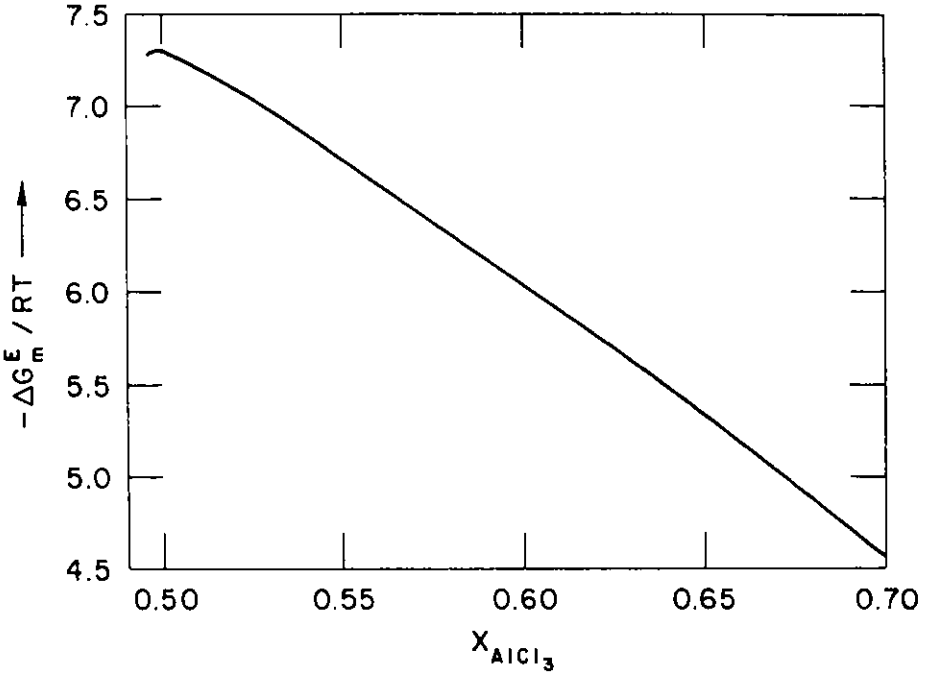

Fig. XI-7. The Excess Free Energy (dimensionless) of Molten NaCl-$AlCl_3$ as a Function of Composition

4. Spectroscopic Investigations of Species in Molten-Salt Electrolytes

The properties of species formed in molten-salt electrolytes are important in understanding the chemistry associated with many high-temperature electrochemical systems, such as metal sulfide-based batteries. Work currently in progress is aimed at using spectroscopic methods to study sulfur dissolution reactions and the structure of the dissolved species in CsCl-$AlCl_3$ melts. Electronic-absorption, resonance-Raman, and ESR (electron spin resonance) spectra were obtained for species formed in solutions containing different S/Al ratios in molten CsCl/$AlCl_3$ (45/55). The results indicated that the S_3^- radical is the predominant sulfur species and that S_3^- tends to form adduct-type molecular ions (e.g., $AlCl_3$:S_3^-) in the melt. In the future, electrochemically generated sulfur, halogen, and iron species in chloraluminate and LiCl-KCl melts will be examined by Raman and absorption spectroscopy.

E. Physical Properties of Salt Vapors

1. Spectroscopic Studies of High-Temperature Molten-Salt Vapors and Vapor Complexes

It is known that the volatility of many metal-halide salts is enhanced by the presence of "acidic gases" (e.g., $AlCl_3$, $FeCl_3$) owing to the

formation of gaseous complexes.[23] Such enhancement may reach factors of up to 10^{14}, making vapor complexes attractive for chemical separations, metallurgical processes, and the development of high-efficiency lamps and lasers.

This CEN program consists of spectroscopic and thermodynamic measurements of a variety of high-temperature inorganic vapors and vapor complexes. The studies are aimed at finding new vapor-phase complexing agents and vapor species and at determining their electronic, vibrational, and structural properties. During the past year, spectrophotometric investigations were conducted on the gas-solid reactions involving $FeCl_2$ and $ErCl_3$ with $AlCl_3$, $GaCl_3$, and $InCl_3$ as carrier gases.

Coherent laser beams were used to excite the vapor complexes formed in $ErCl_3$-ACl_3 (where A = Al, Ga, In) at temperatures between 457 and 1100 K. Scattered light from the high-temperature vapor, stimulated by laser wavelengths near the $^4F_{9/2}$ transition of Er^{3+}, was observed in two spectral regions. The anti-Stokes component was characteristic of the Raman scattering due to $ACl_3(g)$ and $A_2Cl_6(g)$ molecules, whereas the Stokes component was dominated by intense broad bands due to f→f laser-induced fluorescence. Figure XI-8 (bottom) gives an example of the spectral characteristics for the $ErCl_3$-$AlCl_3$ complexes. The temperature and pressure dependence of the laser-induced fluorescence was also investigated for the $^2H_{11/2}$ and $^4S_{3/2}$ states [Fig. XI-8 (top)], using different laser excitation lines. It was concluded that the laser-induced fluorescence proceeded through dissociation of the excited vapor complex and that vibrational equilibration occurred before emission from the Er^*Cl_3 molecule.

Finally, our research has been concentrated on the systematics of structure and bonding for a variety of metal-halide vapor complexes, and a review article outlining these properties has been prepared. In the future, emphasis will be given to completing and analyzing our data base on vapor complexes in the $ErCl_3$-ACl_3 system, as well as in the $FeCl_3$-$CuCl_2$ and GaX_3-Ga systems.

2. Ab Initio Molecular Orbital Calculations of High-Temperature Vapor Complexes

Work has continued on the application of ab initio molecular orbital methods to the study of metal-halide complexes. There has been considerable experimental interest in the complexes present in high-temperature molten-salt vapors, but little theoretical work has been done on them. These theoretical studies are meant to provide information on the bonding, structures, and energetics of metal-halide complexes, which may be difficult to obtain experimentally. During the past year, we have completed work on the complexes $BeF_2 \cdot AlF_3$, $MgF_2 \cdot AlF_3$, and $AlF_3 \cdot BeF_2 \cdot AlF_3$.

---

[23] G. N. Papatheodorou, Proc. of 10th Materials Research Symp. on Characterization of High Temperature Vapors and Gases, J. Hastie, Ed., NBS Special Publication 561, p. 647 (1979).

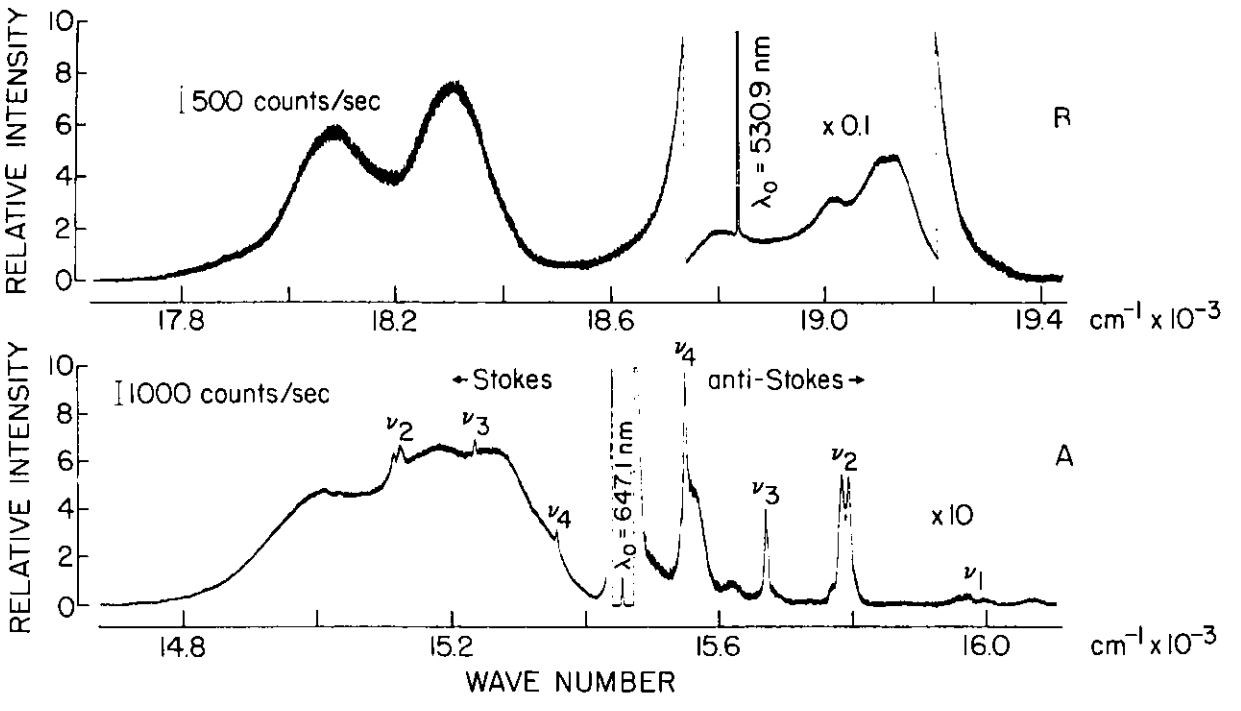

Fig. XI-8. Spectra of Er-Al-Cl Vapor Complexes at 525 K
A. Raman and fluorescence spectra excited with the red 647.1-nm line.
B. Fluorescence spectra of the $^2H_{11/2}$ (about 19000 cm^{-1}) and $^4S_{3/2}$ (about 18200 cm^{-1}) states excited with the green 530.9-nm line.

Corner-, edge-, and face-bridged structures for two 1:1 complexes, $MF_2 \cdot AlF_3$ (where M = Be, Mg), were investigated using an extended basis set. The edge-bridged structure illustrated in Fig. XI-9a was found to be the most stable for both complexes. The face-bridged structure (three fluorines in the bridge) and the corner-bridged structure (one fluorine in the bridge) were only slightly less stable. It was found that the edge-bridged structure may be more accurately described as the ionic complex $AlF_4^- \cdot MF^+$. Calculations of portions of the potential energy surface indicate that it is relatively easy for the cation MF^+ to move about the nearly spherical anion AlF_4^- to form the other two structures.

The 2:1 complex $AlF_3 \cdot BeF_2 \cdot AlF_3$ is the first complex of the type ML_2X_8 that we have studied. We considered six different structures for this complex. The most stable complex was found to have two edge-type bridges, as illustrated in Fig. XI-9b.

These results, along with our previous study of $LiAlF_4$ (see preceding report in this series), indicate that there is a preference for the edge-type bridge (two-fluorine bridge) in metal-halide complexes. Most of the experimental work points towards this type of bridging in the complexes. Another

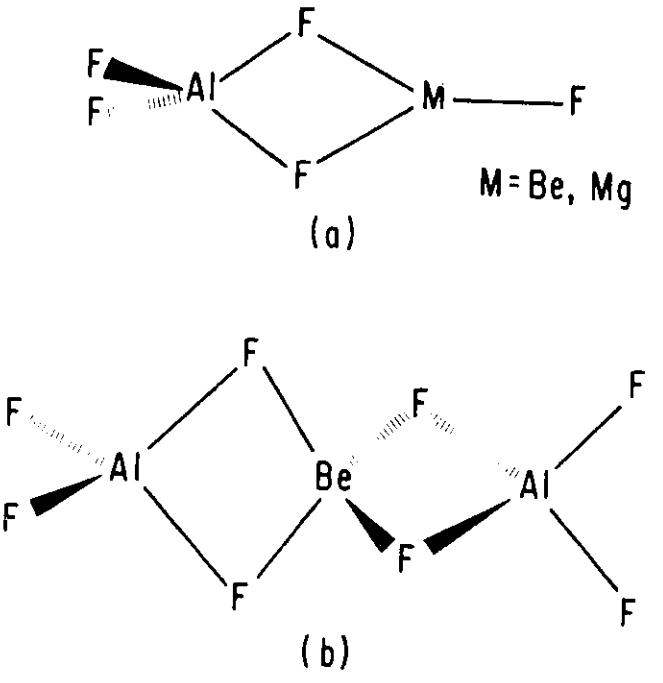

Fig. XI-9. Structures of the Most Stable Forms of $MF_2 \cdot AlF_3$ and $AlF_3 \cdot BeF_2 \cdot AlF_3$

significant finding is that in a 2:1 complex, such as $AlF_3 \cdot BeF_2 \cdot AlF_3$, the bridging preference may be more definite than in 1:1 complexes like $MF_2 \cdot AlF_3$ where, although the edge-type bridge is preferred, there is rather free movement of the cation about the sphere of the anion.

Future work will include further investigation of the coordination in 1:2 complexes such as $BeF_2 \cdot AlF_3 \cdot AlF_3$ and $LiF \cdot BeF_2 \cdot LiF$. Also, work is being initiated on complexes involving LiOH, which may be significant in fuel cell vapors.

3. Dimensional Model for Entropies and Free-Energy Functions

The aim is to simplify considerably the calculation of the nonelectronic entropies and free-energy functions of vapor molecules. Our statistical-mechanical theory[24] indicates that, at a given temperature, differences between entropies or the negative of free-energy functions of molecules of a given stoichiometry (e.g., A_aC_c) are equal to the differences in the term $R \ln [(m_A^a m_C^c)^{3/2} d^{3(a+c-1)}]$, where m is the atomic mass and d is a characteristic size.

[24] D. J. Frurip and M. Blander, J. Chem. Phys. 73, 509–518 (1980).

We examined a series of molecules MX_n, $3 \leq n \leq 6$, and have shown that the data in the JANAF tables are well correlated with our predictions. One of the typically good correlations is for the entropies of MX_3 molecules at 1000 K (see Fig. XI-10). Interestingly, the intercepts for such plots of the entropies at 1000 K for n = 1 to 6 are 20.4, 21.5, 20.0, 20.0, 20.0, and 17.0, respectively. This apparent constancy and comparisons with homonuclear species lend confidence that we can extend our method to calculations for the homonuclear clusters of importance in catalysis and nucleation theory (i.e., 10-50 atoms). We plan to use our correlation and quantum-mechanical calculations of cluster energetics to examine the kinetics of homogeneous nucleation.

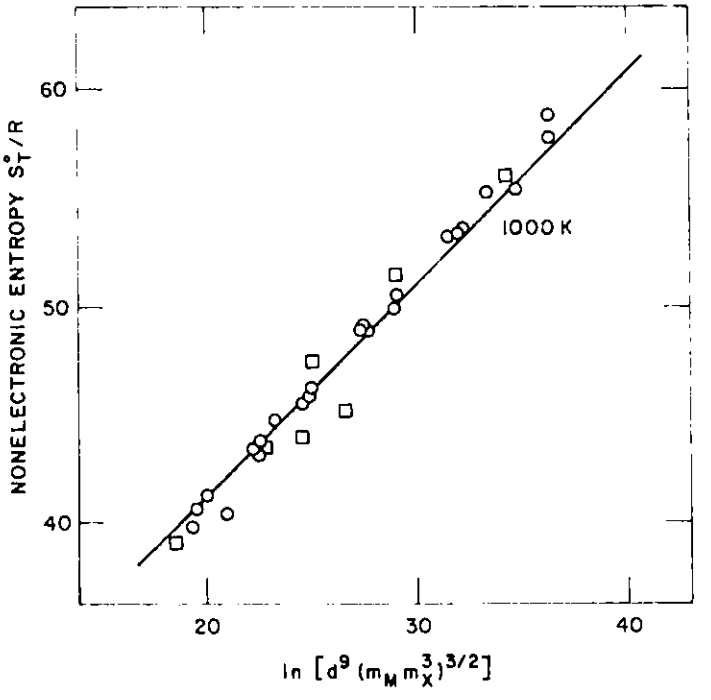

Fig. XI-10. The Nonelectronic Entropy for a Number of $MX_3(g)$ Molecules vs. the Appropriate Logarithmic Term (d is in Å and m is in g mol^{-1}). The square points represent molecules whose spectroscopic parameters (vibrational frequencies, etc.) are, for the most part, estimated. The solid line is a least-squares fit of the circles to a line of unit slope.

XII. ANALYTICAL CHEMISTRY LABORATORY

A. Overview

The Analytical Chemistry Laboratory (ACL) functions as a full-cost-recovery service facility supporting the scientific and engineering programs of ANL. In this capacity, its principal functions are to (1) provide assistance to ANL staff members in solving analytical problems that arise in the course of programmatic activities, (2) perform routine analyses in a way that most effectively uses the Laboratory's resources, and (3) conduct research and development, either independent of or in collaboration with ANL programs, that will assure its capability of performing items (1) and (2) and broaden its analytical capability. Table XII-1 presents a summary of the distribution of service effort of the ACL in FY 1980.

Table XII-1. Summary of ACL Effort in FY 1980

Major Users		% of Total
Chemical Engineering		
Nuclear Waste Management and Fuel Cycle	9.6	
Reactor Safety	1.8	
LWBR Proof of Breeding	8.1	
Electrochemical Programs	10.1	
Coal Programs	5.8	
Advanced Fuel Cell	2.2	63.9
Basic Energy Sciences	7.9	
Dosimetry	2.7	
Fusion Programs	1.7	
Analytical Instrument Development	3.1	
EPRI-EXXON Pu Recycle	1.0	
Others	9.9	
Materials Science		6.7
Biological and Medical Research		6.2
Reactor Analysis and Safety		0.9
Applied Physics		0.8
Chemistry		6.4
Intense Pulsed Neutron Source		1.5
Radiological and Environmental Research		1.3
Energy and Environmental Systems		3.0
Occupational Health and Safety		4.3
Work for Others		2.2
Other ANL Divisions		2.8
		100.0

B. Organic Analysis Facility

The ACL has facilities, located in Building 211 at ANL, for the preparation and analysis of samples requiring the characterization of organic constituents. In this organic analysis facility, a variety of laboratory service equipment has been installed, including a high-capacity ventilation system, laboratory benches with full utilities, four large preparation hoods, and a water purification system. Special consideration has been given to safety in the handling of carcinogenic, toxic, and flammable chemicals. Automated gas and liquid chromatography capabilities are in place. Commercially available gas chromatography/mass spectrometry (GC/MS) instruments are on order, and space for the new instrumentation is being prepared.

As mentioned in previous reports, ACL's Organic Analysis Group is developing a computerized GC/MS system that will perform rapid analysis of complex organic mixtures. This system, which is based on a time-of-flight MS, will provide adequate sensitivity to identify picogram levels of unknown compounds, resolution of multiple-component GC peaks, and significantly lower run time per sample. To date, all components, including a high-speed data collector, have been delivered and checked out. The data collector is being interfaced with the other system components and will be used to test the operability of the GC/MS system.

C. Support to Major R&D Programs

The ACL has continued to play a significant collaborative role in major R&D programs at the Laboratory. A few of the ACL service activities undertaken in the past year are highlighted below.

One of the many CEN users of ACL services is the Proof-of-Breeding (POB) Project, the purpose of which is to determine the extent of breeding in an LWBR (see Section IX.C). In this project, fuel-rod segments, cut with high precision, are dissolved, and samples of the solution are assayed for uranium and selected fission products. Analytical support for the POB Project during the past year has involved studies dealing with (1) problems of statistical analysis of data obtained during the initial shearing, dissolution, and analysis of the fuel-rod segments, (2) cross-contamination of rod segments during the shearing procedure, (3) handling and disposal of the radioactive waste produced during the analytical procedure, and (4) decontamination of the tantalum-lined stainless-steel blend tank used in the analytical effort. In addition, the ACL is assisting in the preparations being undertaken for the POB end-of-life analytical campaign. This effort includes preparation of radiochemical-analysis laboratory space in the Chemistry Division at ANL, development of end-of-life analysis procedures, and acquisition of needed equipment such as an automated thermal ionization mass spectrometer and a γ-spectrometry system.

The Organic Analysis Group is participating in ANL's program to evaluate the environmental effects of high-Btu coal-gasification processes. The ACL service activities include the following: chemical preparation and analysis of samples obtained from process streams and work-space environments at coal-gasification pilot plants, development and evaluation of analytical methods for these samples, and assistance in correlating the biological activity found

in the samples with their chemical characteristics. In October 1980, ACL staff presented papers on this work at the Hanford Life Sciences Symposium on Coal Conversion. It is anticipated that ACL will provide similar services to the newly formed ANL program on alcohol fuels.

As mentioned in Section III of this report, the Office for Electrochemical Project Management (OEPM) undertakes basic and applied research in support of contractor efforts to develop near-term electric-vehicle batteries. Over the past few years, OEPM has been investigating the evolution of arsine and stibine during the charging of lead-acid batteries in electric vehicles. The support for this project provided by ACL has included (1) development of a battery off-gas sampling plan for electric vehicles and garage space at ANL and the Long Island Lighting Co. (Hicksville, NY), (2) analysis of the samples, and (3) interpretation of the analytical results in terms of the operating parameters of the batteries tested. In the later stages, this work was extended to include the evolution and dispersal of hydrogen generated from lead-acid batteries. A detailed report of the results and their significance to established industrial-hygiene exposure limits for arsine and stibine has been prepared.

D. New Capabilities

The ACL is expanding its capabilities in a number of areas. The organic analysis facility cited above is a prominent example. Other examples, of somewhat lesser scope, are given below.

A microanalytical apparatus for determination of hydrogen, oxygen, and nitrogen (HON) by the inert gas fusion technique has been assembled. Through utilization of state-of-the-art pressure measurement equipment, this apparatus is able to determine HON at parts per million levels in most nonvolatile metals and alloys. This capability has been established by the ACL in response to interest expressed by several programs, including the Fusion Power Program and Reactor Safety Program.

In support of a growing involvement by the Occupational Health and Safety Division in the decommissioning of old nuclear facilities, the ACL has obtained instrumentation for the determination of uranium in soil and groundwater samples. This instrumentation measures the fluorescence of uranium produced by a pulsed nitrogen laser after a delay time sufficient to permit the fluorescence of common interferences to decay away and is able to determine as little as 200 picograms of uranium in a sample.

In support of a program in ANL's Applied Physics Division, the ACL has prepared isotopic standards that can be used for very accurate isotopic measurements of lithium. With these standards and the technique of isotopic dilution mass spectrometry, very accurate lithium assays can be obtained.

An Inductively Coupled Plasma-Atomic Emission Spectrometer (ICP-AES), which will provide the Laboratory with rapid and accurate multielement analytical capability, is being procured. The system will consist of the following components: an ICP source, a polychromator for the simultaneous determination of 20 to 30 elements, a scanning monochromator for the sequential analysis of 40 to 60 elements, and a computer to control operation and to collect and

process data as required in order to obtain quantitative determinations. It is anticipated that this instrumentation will have broad application for programs needing accurate multielement determinations. Support for procurement of this instrument is being provided by several forward-looking programs.

E. Future Plans

The ACL will continue to provide analytical support to the Laboratory's scientific and engineering programs. Special attention will be given to the establishment of collaborative relationships with new and ongoing programs and to the development of mechanisms for meeting the special needs of these programs.

XIII. COMPUTER APPLICATIONS

The Computer Applications Group assists CEN staff members in many aspects of computer-related activities, including (1) laboratory data acquisition and control, (2) computer modeling and simulation studies, (3) post-test analysis of experimental results, (4) data-base development and management, and (5) advisory and consulting services.

A. Accomplishments

The major growth in the application of computer technology to research within CEN continues to be in the area of laboratory automation, i.e., data acquisition, instrument control, and data reduction. Reduced costs of mini- and microcomputers have made it highly desirable to automate experimental procedures; moreover, the capabilities and flexibility of these computer systems have proved to be essential for the sophisticated testing, as well as simulation and parametric studies, being conducted in many of CEN's programs. Indeed, much modern instrumentation is packaged with either microprocessors, calculators, or computer-analysis systems of one variety or another.

In the past year, efforts were continued on the development of computer systems (see last year's report) for projects involving the testing of cells and batteries, experiments on high-temperature physical properties, and instrumentation for the Analytical Chemistry Laboratory. In addition, computer systems have been procured for projects involving battery components technology, proof-of-breeding (see Section IX.C.5 of this report), nuclide migration, and fuel cells. Computer programs for these systems are in various stages of development. The total software effort provided through the Computer Applications Group is currently nine man years.

B. Present and Future Plans

Most of the computer systems used for the above CEN programs are members of the PDP-11 family of processors. Although these systems differ in size and scope, their common characteristics include 16-bit word architecture and limitation to 124 K words of total memory and to individual program sizes not exceeding 32 K words. As more numerous and sophisticated demands have been placed on these systems, their limitations have become increasingly apparent. Careful consideration of these limitations has led to the conclusion that the present and future needs of CEN's programs would be best met by the acquisition of a 32-bit minicomputer system that is capable of running (1) a virtual-memory operating system, supporting several megabytes of physical memory, and (2) multi-megabyte programs. As a result, a VAX 11/780 computer facility (Digital Equipment Corp.) has been procured and is presently being installed. This facility will allow most of the smaller minicomputer systems in CEN, as well as some of the newer analytical instruments, to be linked to it via a communications network and will allow for data analysis requiring resources beyond those of the individual minicomputer systems. Furthermore, this centralized computing facility will provide a rapid-response, time-sharing environment for computer-program development; will reduce the need for duplicating

expensive peripheral equipment such as large disks, line printers, tape drives, and plotting devices; and will allow improvements to be made in CEN's word processing equipment.

The new VAX facility will complement the ANL Central Computing Facility (CCF) and will be supported by the Applied Mathematics Division's Friendly Neighborhood Computer (FNC) project. Connection of the VAX facility to the CCF will enable (1) remote job entry to the more generalized facilities of the CCF (thereby allowing for replacement of CEN's Remote Access Data Station with superior equipment) and (2) local performance of the real-time tasks for which VAX will be tailored. Capacity of the system not otherwise being used can be devoted to the running of local batch jobs. Batch jobs involving processing of experimental data stored on the system will be especially appropriate.

Installation of an intelligent port-selector system will be coordinated with the above real-time computing facility. This system will allow terminals throughout the division to be direct-wired to the computer systems of choice through a computer switch. From a terminal in his office, an individual would thus be able to gain access to laboratory computer systems, the VAX system, or the CCF without the use of dial-up modems.

XIV. ADDENDUM.

CHEMICAL ENGINEERING DIVISION PUBLICATIONS--1980

A. Open-Literature Publications

J. P. Ackerman
Advanced Fuel Cell Programs in the United States
Extended Abstracts 31st Meeting Int. Soc. Electrochem., Venice, Italy, September 24, 1980, p. 759 (1980)

R. J. Ackermann and M. Tetenbaum
High Temperature Thermodynamic Properties of the Thorium-Oxygen System
High Temp. Sci. 13, 99 (1980)

R. J. Ackermann and M. Tetenbaum
High Temperature Vaporization Behavior of Oxygen Deficient Thoria
Thermodynamics of Nuclear Materials (Proc. Symp. Jülich, W. Germany, 1979) Vol. 1, IAEA, Vienna, Austria, pp. 29-43 (1980)

C. C. Baker, A. Bolon, R. Clemmer, K. Evans, Jr., J. Jung, D. Smith, L. Turner, T. Blue, J. DeVeaux, D. Driemeyer, J. Metzger, G. Miley, and W. Tetley
Fusion Reaction Technology Impact of Alternate Fusion Fuels
Proc. Eighth Symp. on Engineering Problems of Fusion Research, San Francisco, CA, November 13-16, 1979, IEEE Pub. No. 79CH1441-5 NPS, p. 861 (1980)

C. W. Bale, A. D. Pelton, P. L. Lin, J. Melancon, M. L. Saboungi, and M. Blander
Calculation of Phase Equilibria in the Carbonate Fuel Cell
Extended Abstracts Electrochem. Soc. Meeting, Hollywood, FL, October 5-10, 1980, Vol. 80-2, pp. 357-358 (1980)

G. Bandyopadhyay and T. M. Galvin
Development of Ceramic-Coated Positive Current Collectors for Li-Al/Molten LiCl-KCl/FeS_2 Batteries
Extended Abstracts Electrochem. Soc. Meeting, Hollywood, FL, October 5-10, 1980, Vol. 80-2, pp. 305-306 (1980)

D. L. Barney, R. K. Steunenberg, and A. A. Chilenskas
Recent Progress in Lithium/Iron Sulfide Battery Development
Proc. 15th Intersoc. Energy Conversion Eng. Conf., Seattle, WA, August 18-22, 1980, pp. 198-204 (1980)

L. Bartholme, E. C. Gay, and H. Shimotake
Cycle Life and Performance Evaluation of Positive Current Collectors in LiAl/FeS Cells
Extended Abstracts Electrochem. Soc. Meeting, Hollywood, FL, October 5-10, 1980, Vol. 80-2, pp. 298-302 (1980)

J. K. Bates, L. J. Jardine, and M. Krumpelt
A Nonaqueous Reprocessing Method for Thorium-Based Fuels
ACS Symposium Series, No. 117, Actinide Separations, p. 207 (1980)

R. W. Berg, N. J. Bjerrium, G. N. Papatheodorou, and S. Von Winbush
Resonance Raman Spectra of S_3^- in Molten Salts
Inorg. Nucl. Chem. Lett. 16, 201-204 (1980)

R. W. Berg and G. N. Papatheodorou
Vapor Complexes of Erbium(III) Chloride with Aluminum(III), Gallium(III), and Indium(III) Chlorides
Inorg. Chim. Acta 45, L211-L213 (1980)

P. E. Blackburn and C. E. Johnson
Thermochemistry of Seed and Slag Vaporization and Condensation in Coal-Fired MHD
Proc. AIAA 13th Fluid and Plasma Dynamics Conf., Snowmass, CO, July 14-16, 1980, AIAA-80-1344 (1980)

M. Blander, L. H. Fuchs, C. Horowitz, and R. Land
Primordial Refractory Metal Particles in the Allende Meteorite
Geochim. Cosmochim. Acta 44, 217-223 (1979)

M. Blander and M. L. Saboungi
The Coordination Cluster Theory: Application to Ternary Reciprocal Molten Salt Systems
Acta Chem. Scand. Ser. A 34, 671-676 (1980)

J. A. Bonar, C. R. Kennedy, and R. B. Swaroop
Coal-Ash Slag Attack and Corrosion of Refractories
Am. Ceram. Soc. Bull. 59(4), 473-478 (1980)

S. R. Breon and P. A. Finn
Compatibility of Solid Ceramic Breeder Materials with ADIP Program Alloys
Alloy Development for Irradiation Performance Quarterly Progress Report, October, 1980, U.S. Dept. of Energy Report DOE/ER-004514, p. 195 (December 1980)

A. A. Chilenskas and D. L. Barney
Planning for Commercialization of Lithium/Metal Sulfide Batteries
Foote Prints, Vol. 43, No. 1 (1980)

R. G. Clemmer, R. W. Peterman, D. L. Smith, and V. A. Maroni
Analytical and Experimental Studies of Solid Breeding Materials
Special Purpose Materials Annual Progress Report, U.S. Dept. of Energy Report DOE/ER-0048/1, p. 1 (April 1980)

R. L. Cole
Stratified Storage Measurement and Analysis
Proc. Annual DOE Active Solar Heating and Cooling Contractors' Review Meeting, Lake Tahoe, NV, March 26-28, 1980, U.S. Dept. of Energy Document CONF-800340, p. 11-11 (June 1980)

M. Collares-Pereira and A. Rabl
Simple Procedure for Predicting Long-Term Average Performance of Non-Concentrating and of Concentrating Solar Collectors
Sol. Energy 23, 235-253 (1979)

L. A. Curtiss and D. J. Frurip
Ab Initio Molecular Orbital Calculations on Beryllium and Magnesium Atom Reactions with Water
Chem. Phys. Lett. 75(1), 69-74 (October 1980)

L. A. Curtiss, D. J. Frurip, and M. Blander
Thermodynamic Parameters for the Dimer and Evidence for Higher Polymers in Water Vapor
Water and Steam--Their Properties and Current Industrial Applications, J. Straub and K. Scheffler, Eds., pp. 521-527 (1980)

J. H. DeVan, H. R. Ihle, C. F. Knights, H. R. Konvicka, V. A. Maroni, S. Nasu, J. D. Navratil, and E. Roth
Chemical Aspects of Controlled Nuclear Fusion
At. Energy Rev. 18(2), 553-574 (1980)

M. M. Farahat, A. A. Chilenskas, and D. L. Barney
Heat Generation in Lithium/Iron Sulfide Cells
Extended Abstracts Electrochem. Soc. Meeting, Hollywood, FL, October 5-10, 1980, Vol. 80-2, pp. 234-236 (1980)

H. M. Feder and J. W. Rathke
Hydrogenation of Carbon Monoxide and Related Molecules
Ann. N. Y. Acad. Sci. 333, 45-57 (February 1980)

P. A. Finn, R. G. Clemmer, D. R. Armstrong, N. E. Parker, and L. Bova
The Reactions of Li-Pb Alloys with Water
Trans. Am. Nucl. Soc. 34, 55 (1980)

P. A. Finn, R. G. Clemmer, V. A. Maroni, and C. Dillow
Tritium Handling and Vacuum Considerations for the STARFIRE Commercial Tokamak Reactor
Proc. Eighth Symp. on Engineering Problems of Fusion Research, San Francisco, CA, November 13-16, 1979, IEEE Pub. No. 79CH1441-5 NPS, p. 1638 (1980)

P. A. Finn, R. G. Clemmer, B. Misra, and V. A. Maroni
ETF Interim Design Description Document, Sec. 6
Oak Ridge/Fusion Engineering Device Design Center publication, pp. 40-46 (July 1980)

A. K. Fischer and D. R. Vissers
Agglomeration in Li-Al Alloy Electrodes
Extended Abstracts Electrochem. Soc. Meeting, Hollywood, FL, October 5-10, 1980, Vol. 80-2, pp. 240-242 (1980)

A. K. Fischer and D. R. Vissers
Estimation of Entropy for Thermal Management of Li-Al/FeS_x Cells
Extended Abstracts Electrochem. Soc. Meeting, St. Louis, MO, May 11-16, 1980, Vol. 80-1, pp. 80-82 (1980)

A. K. Fischer and C. E. Johnson
Method of Foaming a Liquid Metal
U.S. Patent 4,183,744 (January 15, 1980)

K. F. Flynn, L. J. Jardine, and M. J. Steindler
Resistance of High-Level Waste Materials to Dissolution in Aqueous Media
Scientific Basis for Nuclear Waste Management, Vol. 2, C. J. M. Northrup, Jr., Ed., Sandia National Laboratories, Albuquerque, NM, pp. 103-108 (1980)

D. R. Fredrickson, G. K. Johnson, and P. A. G. O'Hare
Cesium Chromate, Cs_2CrO_4: High-Temperature Enthalpy Increments and Other Thermodynamic Properties
J. Chem. Thermodyn. 12, 801-805 (1980)

D. J. Frurip and M. Blander
A Dimensional Model for the Calculation of Thermodynamic Properties of Gaseous Molecules and Ions
J. Chem. Phys. 73, 509-518 (1980)

D. J. Frurip, L. A. Curtiss, and M. Blander
Vapor Phase Association in Acetic and Trifluoroacetic Acids: Thermal Conductivity Measurements and Molecular Orbital Calculations
J. Am. Chem. Soc. 102, 2610-2616 (1980)

L. H. Fuchs and M. Blander
Refractory Metal Particles in Refractory Inclusions in the Allende Meteorite
Proc. Eleventh Lunar and Planetary Science Conf., Houston, TX, March 17-21, 1980, Vol. 2, pp. 929-944 (1980)

E. C. Gay, W. E. Miller, and F. J. Martino
Optimization Studies of Lithium/Iron Sulfide Cells for Electric Vehicle Applications
Proc. 15th Intersoc. Energy Conversion Eng. Conf., Seattle, WA, August 18-22, 1980, pp. 211-217 (1980)

Y. Gohar and V. A. Maroni
Impact of Module Size on the Tritium Breeding and Energy Conversion Experiments in an ETF/INTOR Reactor
Trans. Am. Nucl. Soc. 34, 51-52 (1980)

D. W. Green
Relationship Between Spectroscopic Data and Thermodynamic Functions: Applications to Uranium, Plutonium, and Thorium Oxide Vapor Species
J. Nucl. Mater. 88, 51-63 (1980)

D. W. Green
Standard Enthalpies of Formation of Gaseous Thorium, Uranium, and Plutonium Oxides
Int. J. Thermophys. 1(1), 61-71 (1980)

D. W. Green, G. T. Reedy, and S. B. Gabelnick
Infrared Spectra of Matrix-Isolated Uranium Oxides: III. Low-Frequency Modes
J. Chem. Phys. 73(9), 4207-4216 (November 1980)

L. R. Greenwood
Review of Fusion Dosimetry
Proc. Third ASTM-EURATOM Symp. on Reactor Dosimetry, Ispra, Italy, EUR-6813, p. 58 (1980)

L. R. Greenwood
Review of Source Characterization for Fusion Materials Irradiations
Proc. Symp. on Neutron Cross-Sections from 10-50 MeV, Brookhaven National Laboratory, May 12-14, 1980, BNL-NCS-51245, p. 75 (1980)

L. R. Greenwood
Status of Current, Routine Dosimetry at Existing Irradiation Facilities
Proc. Third ASTM-EURATOM Symp. on Reactor Dosimetry, Ispra, Italy, EUR-6813, p. 257 (1980)

L. R. Greenwood
The Status of Neutron Dosimetry and Damage Analysis for the Fusion Materials Program
Proc. Int. Conf. on Nuclear Cross-Sections for Technology, Knoxville, TN, NBS-SP594, p. 812 (1980)

L. R. Greenwood
Uncertainties and Covariances of Spectra Derived from Integral Measurements
Proc. Third ASTM-EURATOM Symp. on Reactor Dosimetry, Ispra, Italy, EUR-6813, p. 693 (1980)

J. E. Herceg and J. P. Ackerman
Molten Carbonate Fuel Cell Overview
Abstracts National Fuel Cell Seminar, San Diego, CA, July 14-16, 1980, pp. 143-147 (1980)

F. Hornstra
Peak Power Measurements at the National Battery Test Laboratory
Electric and Hybrid Vehicle Program Quarterly Report (April, May, June 1980), U.S. Dept. of Energy Report DOE/CS-0026-11, pp. 14-15 (August 1980)

F. Hornstra
Simulated Driving Profiles in the Testing of Near-Term Batteries at ANL
Electric and Hybrid Vehicle Program Quarterly Report (January, February, March 1980), U.S. Dept. of Energy Report DOE/CS-0026-10, pp. 14-16 (May 1980)

F. Hornstra, E. Berrill, P. Cannon, D. Corp, D. Fredrickson, M. Genge, C. Swoboda, and N. P. Yao
Test Results of Computer Generated Simulated Driving Profiles Applied to Near-Term Batteries
Proc. 30th Annual Conf. IEEE Vehicular Technology Soc. (Convergence 80), Dearborn, MI, September 15-17, 1980, Paper No. C-4-2, New York (1980)

F. Hornstra, E. Berrill, P. Cannon, D. Corp, D. Fredrickson, V. Kremesec, W. Lark, C. Swoboda, and C. Webster
Results of Simulated Driving Profiles in the Testing of Near-Term Electric Vehicle Batteries
Proc. EVC Expo '80 Conf., St. Louis, MO, May 20-22, 1980, Paper EVC No. 8034 (1980)

F. Hornstra, P. Cannon, C. Christianson, V. Kremesec, and N. P. Yao
Some Effects of Regenerative Braking on Lead-Acid, Nickel/Iron and Nickel/Zinc Batteries
Extended Abstracts Electrochem. Soc. Meeting, St. Louis, MO, May 11-16, 1980, Vol. 80-1, pp. 12-14 (1980)

E. P. Horwitz, G. W. Mason, C. A. A. Bloomquist, R. A. Leonard, and G. J. Bernstein
The Extraction of DBP and MBP from Actinides: Application to the Recovery of Actinides from TBP-Sodium Carbonate Scrub Solutions
ACS Symposium Series, No. 117, Actinide Separations, pp. 475-496 (1980)

G. K. Johnson and K. H. Gayer
The Enthalpies of Solution and Formation of Cs_2CO_3
J. Chem. Thermodyn. 12(7), 705-708 (1980)

G. K. Johnson, G. N. Papatheodorou, and C. E. Johnson
The Enthalpies of Formation and High-Temperature Thermodynamics Functions of As_4S_4 and As_2S_3
J. Chem. Thermodyn. 12(6), 545-557 (1980)

G. K. Johnson, R. G. Pennell, K. Kim, and W. N. Hubbard
Thermochemistry of Rare-Earth Trifluorides: I. Fluorine Bomb Calorimetric Determination of the Enthalpies of Formation of LaF_3, PrF_3, NdF_3, GdF_3, DyF_3, HoF_3, and ErF_3
J. Chem. Thermodyn. 12(2), 125-136 (1980)

T. D. Kaun, P. F. Eshman, and W. E. Miller
New Approach to Electrode Current Collection for LiAl/Iron Sulfide Cells
Proc. 15th Intersoc. Energy Conversion Eng. Conf., Seattle, WA, August 18-22, 1980, pp. 218-233 (1980)

T. D. Kaun, W. E. Miller, L. Redey, and J. D. Arntzen
Designing Capacity Stability for LiAl/FeS Multiplate Cells
Extended Abstracts Electrochem. Soc. Meeting, Hollywood, FL, October 5-10, 1980, Vol. 80-2, pp. 202-205 (1980)

R. Keller
Energy Conservation in an Optimized Electrochemical Process
Electrochim. Acta 25, 303-307 (1980)

K. Kinoshita and G. H. Kucera
Predicting the Compressive Strength of $LiAlO_2$/Molten Carbonate Structures
Extended Abstracts Electrochem. Soc. Meeting, Hollywood, FL, October 5-10, 1980, Vol. 80-2, pp. 368-369 (1980)

F. R. Kirchner, J. O. Hutchens, P. C. Brennan, D. A. Hangen, H. E. Kubitschek, D. M. Buchholz, R. Kumar, K. M. Myles, and W. P. Norris
Pulmonary Toxicology of Respirable Particles, "Mammalian Responses to Exposure to the Total Diluted Effluent from Fluidized-Bed Combustion of Coal"
Proc. 19th Annual Hartford Life Sciences Symp., Richland, WA, October 22-24, 1979, pp. 29-46 (September 1980)

J. Klinger, N. P. Yao, and G. M. Cook
Simplified Computer Modeling of Battery Behavior Under Various Load Profiles
Extended Abstracts Electrochem. Soc. Meeting, St. Louis, MO, May 11-16, 1980, Vol. 80-1, pp. 9-11 (1980)

D. W. Kneff, H. Farrar, L. R. Greenwood, and M. W. Guinan
Characterization of the Be(d,n) Neutron Field by Passive Dosimetry Techniques
Symp. on Cross-Sections from 10-50 MeV, Brookhaven National Laboratory, May 12-14, 1980, BNL-NCS-51245, p. 113 (1980)

G. H. Kucera
DTA Study of $LiAlO_2$ Polymorphic Transformations
Extended Abstracts Electrochem. Soc. Meeting, Hollywood, FL, October 5-10, 1980, Vol. 80-2, pp. 365-367 (1980)

R. H. Land, V. A. Maroni, and M. Minkoff
An Analysis of Experimental Air-Detritiation Data Using TSOAK-M1
Proc. ANS Symp. on Tritium Technology in Fission, Fusion, and Isotopic Applications, Dayton, OH, April 29-May 1, 1980, U.S. Dept. of Energy Document CONF-800427, pp. 381-386 (1980)

S. H. D. Lee and I. Johnson
Removal of Gaseous Alkali Metal Compounds from Hot Flue Gas by Particulate Sorbents
J. Eng. for Power Trans. 102(2), 397-402 (April 1980)

S. H. D. Lee, I. Johnson, and J. Fischer
Volatility of Selected Minor and Trace Elements in the Low-Temperature Ash of an Illinois Herrin No. 6 Coal
Fuel 59, 816-819 (1980)

R. A. Leonard, G. J. Bernstein, A. A. Ziegler, and R. H. Pelto
Annular Centrifugal Contactors for Solvent Extraction
Sep. Sci. Technol. 15(4). 925-943 (1980)

R. A. Leonard, R. H. Pelto, A. A. Ziegler, and G. J. Bernstein
Flow Over Circular Weirs in a Centrifugal Field
Can. J. Chem. Eng. 58, 531-534 (1980)

M. B. Liu, G. M. Cook, and N. P. Yao
Galvanostatic Polarization of Zinc Micro-Anode in KOH Electrolytes
Extended Abstracts Electrochem. Soc. Meeting, St. Louis, MO, May 11-16, 1980, Vol. 80-1, pp. 1252-1254 (1980)

M. B. Liu, Y. Yamazaki, G. M. Cook, and N. P. Yao
Current Distribution in Porous Zinc Electrodes: I. Experimental
Extended Abstracts Electrochem. Soc. Meeting, Hollywood, FL, October 5-10, 1980, Vol. 80-2, pp. 253-255 (1980)

R. O. Loutfy, G. M. Cook, and N. P. Yao
Saving Energy by the Electrochemical Production of Aluminum via a Sulfide Route
Extended Abstracts Electrochem. Soc. Meeting, St. Louis, MO, May 11-16, 1980, Vol. 80-1, pp. 1019-1022 (1980)

F. J. Martino, E. C. Gay, and W. E. Moore
Status Cells: A Demonstration of LiAl/FeS Cell Performance Reproducibility, Energy Retention and Extended Lifetime
Extended Abstracts Electrochem. Soc. Meeting, Hollywood, FL, October 5-10, 1980, Vol. 80-2, pp. 294-297 (1980)

F. J. Martino, E. C. Gay, and H. Shimotake
Cycle Life Studies of LiAl/FeS Cells Using BN Felt Separators
Proc. 15th Intersoc. Energy Conversion Eng. Conf., Seattle, WA, August 18-22, 1980, pp. 205-210 (1980)

W. R. McIntire
Elimination of the Optical Losses Due to Gaps Between Absorbers and Their Reflectors
Proc. 1980 Annual Meeting Am. Section/Int. Sol. Energy Soc., Phoenix, AZ, June 1980, pp. 600-604 (1980)

W. R. McIntire
New Reflector Design Which Avoids Losses Through Gaps Between Tubular Absorbers and Reflectors
Sol. Energy 25, 215-220 (1980)

W. R. McIntire
Optimization of Stationary Non-imaging Reflectors for Tubular Evacuated Receivers Aligned North-South
Sol. Energy 24, 167-175 (1980)

W. R. McIntire
Secondary Concentration for Linear Focusing Systems: A Novel Approach
Appl. Opt. 19, 3036-3037 (September 1980)

W. R. McIntire
Stationary Concentrators for Tubular Evacuated Receivers: Optimization and Comparison of Reflector Designs
Proc. 1980 Annual Meeting Am. Section/Int. Sol. Energy Soc., Phoenix, AZ, June 1980, pp. 505-509 (1980)

J. W. Meadows, R. J. Armani, E. L. Callis, and A. M. Essling
Half-Life of ^{230}Th
Phys. Rev. C 22(2), 750-754 (August 1980)

W. J. Mecham, L. J. Jardine, R. H. Pelto, and M. J. Steindler
Characterization of Impact Fracture of Brittle Solid Waste Forms
Scientific Basis for Nuclear Waste Management, Vol. 2, C. J. M. Northrup, Jr., Ed., Sandia National Laboratories, Albuquerque, NM, pp. 307-314 (1980)

J. H. Meisenhelder and A. A. Siczek
An Infrared Study of Zirconium Retention in 30% Tributyl Phosphate/n-Dodecane
Radiochim. Acta 27(4), 223 (1980)

C. A. Melendres
Interfacial Behavior of Carbon Supported Iron Phthalocyanine: A Laser Raman Spectroelectrochemical Study
Extended Abstracts Electrochem. Soc. Meeting, St. Louis, MO, May 11-16, 1980, Vol. 80-1, pp. 1169-1171 (1980)

C. A. Melendres
Mössbauer and Raman Spectra of Carbon-Supported Iron Phthalocyanine
J. Phys. Chem. 84, 1936-1939 (1980)

J. F. Miller
Near-Term EV Battery R&D Progress
Electric and Hybrid Vehicle Program Quarterly Report (July, August, September 1980), U.S. Dept. of Energy Report DOE/CS-0026-12, pp. 11-14 (November 1980)

B. Misra, R. G. Clemmer, and D. L. Smith
Influence of Blanket Design Options Upon Tritium Inventories in Solid Breeders
Trans. Am. Nucl. Soc. 34, 50 (1980)

C. D. Morgan, D. Bowers, R. Clemmer, Y. Gohar, and B. Engholm
Conceptual Design of a Tritium Breeding Blanket for INTOR
Georgia Institute of Technology Report INTOR/ENG/80-11 (October 1980)

Z. Nagy
On the Theory of the Potential and Voltage Step Relaxation Techniques for the Investigation of Fast Electrode Reactions
Electrochim. Acta 25, 575-581 (1980)

Z. Nagy
Relaxation Techniques for the Measurement of the Kinetics of Fast Electrode Reactions in Molten Salts
Extended Abstracts Electrochem. Soc. Meeting, Hollywood, FL, October 5-10, 1980, Vol. 80-2, pp. 1612-1614 (1980)

Z. Nagy, J. L. Settle, J. Padova, and M. Blander
Complexing of Al^{3+} in Alkali Halide Melts
Extended Abstracts Electrochem. Soc. Meeting, St. Louis, MO, May 11-16, 1980, Vol. 80-1, pp. 93-95 (1980)

J. J. O'Gallagher, A. Rabl, R. Winston, and W. R. McIntire
Absorption Enhancement in Solar Collectors by Multiple Reflections
Sol. Energy 24, 323-326 (1980)

P. A. G. O'Hare
A Summary of the Symposium
Thermodynamics of Nuclear Materials (Proc. Symp. Jülich, W. Germany, 1979) Vol. II., IAEA, Vienna, Austria, p. 383 (1980)

P. A. G. O'Hare, H. E. Flotow, and H. R. Hoekstra
Heat Capacity (5-350 K) and Recommended Thermodynamic Properties of Barium Uranate ($BaUO_4$) to 1100 K
J. Chem. Thermodyn. 12, 1003 (1980)

H. Ohno and H. Shimotake
Determination of Effective Conductivity of Porous Ceramic Separators Containing Molten LiCl-KCl/FeS Cells
Extended Abstracts Electrochem. Soc. Meeting, Hollywood, FL, October 5-10, 1980, Vol. 80-2, pp. 215-219 (1980)

G. N. Papatheodorou and R. W. Berg
Laser-Induced Fluorescence of High Temperature Vapor Complexes of $ErCl_3$ with $AlCl_3$, $GaCl_3$, and $InCl_3$
Chem. Phys. Lett. 75, 483-487 (1980)

G. N. Papatheodorou and O. J. Kleppa
Enthalpies of Mixing of Binary Liquid Mixtures: $CdCl_2$-AgCl, $MnCl_2$-AgCl, $FeCl_2$-AgCl, and $CoCl_2$-AgCl
J. Chem. Thermodyn. 12, 807-808 (1980)

R. D. Pierce, G. H. Kucera, J. W. Sim, J. L. Smith, and R. B. Poeppel
Development and Testing of Electrolyte Structures
Abstracts National Fuel Cell Seminar, San Diego, CA, July 14-16, 1980, pp. 176-178 (1980)

P. L. Radloff N. Papatheodorou
High-Tempe..ure Raman Spectroscopic Studies of Indium Halide Vapors and Molten Salts: InX, InX_2, InX_3, and $InAlX_4$ (X=Cl, Br)
J. Chem. Phys. 72(2), 992-1000 (January 1980)

L. Redey, S. Higuchi, T. D. Kaun, F. J. Martino, and D. R. Vissers
Electrode Potential Relaxation in High Temperature LiAl/FeS Engineering Cells
Extended Abstracts Lithium Battery Symp., Electrochem. Soc. Meeting, Hollywood, FL, October 5-10, 1980, Vol. 80-2, pp. 220-223 (1980)

L. Redey and D. R. Vissers
Design and Development of Micro-Reference Electrodes for the Lithium/Metal-Sulphide Cell System
Materials for Advanced Batteries, D. W. Murphy, J. Broadhead, and B. C. H. Steele, Eds., Plenum Publ. Corp., New York, pp. 205-209 (1980)

L. E. Ross, S. K. Preto, N. C. Otto, C. C. Sy, and M. F. Roche
Calcium/Iron Disulfide Secondary Cells
Proc. 15th Intersoc. Energy Conversion Eng. Conf., Seattle, WA, August 18-22, 1980, pp. 581-585 (1980)

M. L. Saboungi
Calculation of Thermodynamic Properties of Multicomponent Ionic Reciprocal Systems
J. Chem. Phys. 73(11), 5800-5806 (1980)

M. L. Saboungi and M. Blander
Advances in Theories of Molten Salt Solutions
Extended Abstracts Electrochem. Soc. Meeting, Hollywood, FL, October 5-10, 1980, Vol. 80-2, pp. 1585-1586 (1980)

M. L. Saboungi, P. L. Lin, P. Cerisier, and A. D. Pelton
Computer Analysis of the Phase Diagrams and Thermodynamic Properties of Cryolite Based Systems: I. The AlF_3-LiF-NaF System
Metall. Trans. 11B, 493-501 (September 1980)

J. Shearer, I. Johnson, and C. Turner
The Effects of $CaCl_2$ on Limestone Sulfation in Fluidized-Bed Coal Combustion
Thermochim. Acta 35, 105-109 (1980)

J. A. Shearer, I. Johnson, and C. B. Turner
Interaction of NaCl with Limestones During Calcination
Am. Ceram. Soc. Bull. 59(5), 521-528 (May 1980)

J. A. Shearer, G. W. Smith, D. S. Moulton, E. B. Smyk, K. M. Myles, W. M. Swift, and I. Johnson
Hydration Process for Reactivating Spent Limestone and Dolomite Sorbents for Reuse in Fluidized-Bed Coal Combustion
Proc. Sixth Int. Fluidized-Bed Conf., Atlanta, GA, April 1980, pp. 1015-1027 (1980)

J. A. Shearer, G. W. Smith, K. M. Myles, and I. Johnson
Hydration Enhanced Sulfation of Limestone and Dolomite in the Fluidized-Bed Combustion of Coal
APCA J. 30(6), 684-688 (June 1980)

J. A. Shearer, G. W. Smith, K. Myles, and I. Johnson
Hydration of "Spent" Limestone and Dolomite to Enhance Sulfation in Fluidized-Bed Combustion
Proc. 15th Intersoc. Energy Conversion Eng. Conf., Seattle, WA, August 18-22, 1980, pp. 78-82 (1980)

A. A. Siczek and J. H. Meisenhelder
Zirconium Retention in 30% Tributyl Phosphate/n-Dodecane
Radiochim. Acta 27(4), 217 (1980)

A. A. Siczek, J. H. Meisenhelder, G. J. Bernstein, and M. J. Steindler
Solvent Extraction Studies in Miniature Centrifugal Contactors
Radiochim. Acta 27, 51-60 (1980)

J. W. Sim
Fabrication of Porous Sintered Structures from β-$LiAlO_2$
Extended Abstracts Electrochem. Soc. Meeting, Hollywood, FL, October 5-10, 1980, Vol. 80-2, pp. 372-374 (1980)

J. W. Sim, R. N. Singh, and K. Kinoshita
Testing of Sintered $LiAlO_2$ Structures in Molten Carbonate Fuel Cells
J. Electrochem. Soc. 127(8), 1766-1768 (1980)

J. A. Smaga and J. E. Battles
Evaluation of Nickel Positive Electrode Components in Li-Al/FeS Cells
Extended Abstracts Electrochem. Soc. Meeting, Hollywood, FL, October 5-10, 1980, Vol. 80-2, pp. 199-201 (1980)

D. L. Smith, R. G. Clemmer, and J. W. Davis
Assessment of Solid Breeding Blanket Options for Commercial Tokamak Reactors
Proc. Eighth Symp. on Engineering Problems of Fusion Research, San Francisco, CA, November 13-16, 1979, IEEE Pub. No. 79CH1441-5 NPS, p. 433 (1980)

E. B. Smyk, W. M. Swift, W. F. Podolski, K. M. Myles, and I. Johnson
Methods of Improving Limestone Utilization in Fluidized-Bed Combustion
Proc. 15th Intersoc. Energy Conversion Eng. Conf., Seattle WA, August 18-22, 1980, pp. 62-66 (1980)

B. Srinivasan and K. F. Flynn
Kr and Ze Isotopes from Spontaneous Fission of ^{248}Cm and ^{250}Cf: Comparison with Noble Gases in Carbonaceous Chondrites
Earth Planet. Sci. Lett. 47, 235-242 (1980)

W. M. Stacey, Jr., C. M. Flanagan, G. L. Kulcinski, J. A. Schmidt, T. E. Shannon, J. K. Griffith, T. G. Brown, R. G. Clemmer, et al.
U.S. INTOR, The U.S. Contribution to the International Tokamak Reactor Phase-1 Workshop
Georgia Institute of Technology Report INTOR/80-1 (June 1980)

R. B. Swaroop, J. E. Battles, and R. Hamilton
Development and Evaluation of BN Felt as Separator Material
Proc. Sixth Interam. Conf. on Materials Technology, San Francisco, CA, August 1980, pp. 67-71 (1980)

R. B. Swaroop, J. A. Smaga, and J. E. Battles
Developmant and Evaluation of Materials for High Temperature Lithium/Sulfur Rechargeable Batteries
Proc. Solar Energy Storage Workshop, Panjab University, Chandigarhb, India (1980)

D. K. Sze, R. G. Clemmer, and E. T. Cheng
LiPb, A Novel Material for Fusion Applications
Univ. of Wisconsin Report UWFDM-378 (October 1980)

M. Tetenbaum, W. A. Shinn, and C. E. Johnson
Compatibility Studies of Thorium-Based Metal Fuels with Candidate Cladding Alloys
Trans. Am. Nucl. Soc. 34, 211 (1980)

Z. Tomczuk, K. E. Anderson, D. R. Vissers, and M. F. Roche
Evaluation of High Temperature LiAl/TiS_2 Cells
J. Electrochem. Soc. 127(9), 1882-1885 (September 1980)

Z. Tomczuk, M. F. Roche, and D. R. Vissers
Phase Relationships in Positive Electrodes of High Temperature Lithium-Aluminum/Iron Sulfide Cells
Extended Abstracts Electrochem. Soc. Meeting, Hollywood, FL, October 5-10, 1980, Vol. 80-2, pp. 209-211 (1980)

D. Townly, J. Winnick, and H. Huang
Mixed Potential Analysis of Sulfation of Molten Carbonate Fuel Cell
J. Electrochem. Soc. 127(5), 1104-1106 (1980)

E. H. Van Deventer and V. A. Maroni
Hydrogen Permeation Characteristics of Some Austenitic and Nickel-Base Alloys
J. Nucl. Mater. 92, 103-111 (1980)

E. H. Van Deventer, J. R. Weston, R. W. Peterman, R. G. Clemmer, E. Veleckis, and V. A. Maroni
A Review of Fusion-Related Experimentation on Blanket Tritium Processing and Hydrogen Isotope Migration at Argonne National Laboratory
Proc. ANS Symp. on Tritium Technology in Fission, Fusion, and Isotopic Applications, Dayton, OH, April 29-May 1, 1980, U.S. Dept. of Energy Document CONF-800427, pp. 144-149 (1980)

R. Varma, G. M. Cook, and N. P. Yao
Monitoring Stibine and Arsine in Lead-Acid Battery Charge Gas and in Ambient Air: Development and Testing of a Field Kit
Extended Abstracts Electrochem. Soc. Meeting, St. Louis, MO, May 11-16, 1980, Vol. 80-1, pp. 15-17 (1980)

R. Varma, G. M. Cook, and N. P. Yao
Stibine/Arsine Emission from Lead-Acid Batteries
Second U.S. Dept. of Energy Environmental Control Symp., Reston, VA, March 17-19, 1980, U.S. Dept. of Energy Report CONF-800334/2, pp. 709-719 (June 1980)

R. Varma, C. A. Melendres, and N. P. Yao
In Situ Identification of Surface Phases on Lead Electrodes by Laser Raman Spectroscopy
J. Electrochem. Soc. 127(6), 1416-1418 (1980)

E. Veleckis
Thermodynamic Investigation of the Li-Al and Li-Pb Systems by the Hydrogen Titration Method
J. Less-Common Met. 73, 49-60 (1980)

E. Veleckis, R. M. Yonco, and V. A. Maroni
The Current Status of Fusion Reactor Blanket Thermodynamics
Thermodynamics of Nuclear Materials (Proc. Symp. Jülich, W. Germany, 1979), Vol. II, IAEA, Vienna, Austria, p. 3 (1980)

D. R. Vissers
Lithium-Aluminum/Iron Sulphide Batteries
Materials for Advanced Batteries, D. W. Murphy, J. Broadhead, and B. C. H. Steele, Eds., Plenum Publ. Corp., New York, pp. 47-90 (1980)

W. H. webster, Jr., and N. P. Yao
Progress and Forecast in Electric Vehicle Batteries
Proc. 30th Annual Conf. IEEE Vehicular Technology Soc. (Convergence 80), Dearborn, MI, September 15-17, 1980, Paper No. C-2-5, New York (1980)

W. I. Wilson, R. B. Snyder, and I. Johnson
The Use of Oil Shale for SO_2 Emission Control in Atmospheric-Pressure Fluidized-Bed Coal Combustors
Ind. Eng. Chem. Process Des. Dev. 19, 47-51 (January 1980)

N. P. Yao, C. C. Christianson, R. C. Elliott, T. S. Lee, and J. F. Miller
DOE's Near-Term Electric-Vehicle Battery Program: Status of Improved Lead-Acid, Nickel/Iron and Nickel/Zinc Battery Developments
Proc. EVC Expo '80 Conf., St. Louis, MO, May 20-22, 1980, Paper EVC No. 8029 (1980)

N. P. Yao, C. C. Christianson, F. Hornstra, W. DeLuca, G. M. Cook, J. F. Miller, T. Lee, J. Rajan, and J. Barghusen
Near-Term Batteries
Third Annual Report to Congress for FY 1979, Electric and Hybrid Vehicle Program, U.S. Dept. of Energy Report DOE/CS-0130, pp. 60-68 (January 1980)

N. P. Yao and J. F. T. Miller
Nickel/Zinc Battery: A Promising Candidate for Electric Vehicle Propulsion
Lead-Zinc-Tin '80, J. M. Cigar, T. S. Mackey, and T. J. O'Keefe, Eds., The Metallurgical Society of AIME, Warrendale, PA, pp. 871-884 (1980)

B. Papers Accepted for Publication in Open Literature

C. C. Baker, M. A. Abdou, C. D. Boley, J. N. Brooks, R. G. Clemmer, D. A. Ehst, K. Evans, Jr., P. A. Finn, R. E. Fuja, Y. Gohar, J. Jung, W. J. Kann, R. F. Mattas, B. Misra, et al.
STARFIRE, a Commercial Tokamak Power Plant Design
Accepted for publication in Nucl. Eng. Des.

J. Bates, M. Ader, J. Meisenhelder, W. Shinn, B. S. Tani, and M. Krumpelt
Phase Relations in the Thorium-Cadmium System
Accepted for publication in J. Less-Common Met.

J. K. Bates, L. J. Jardine, K. F. Flynn, and M. J. Steindler
The Application of Neutron Activation Analysis to Leach Rate Studies
Accepted for publication in Proc. Leachability of Radioactive Solids Conf., December 9-12, 1980, Gatlinburg, TN

P. E. Blackburn and C. E. Johnson
Thermochemistry of Seed and Slag Vaporization and Condensation in Coal-Fired MHD
Accepted for publication in J. Energy

M. Blander and M. L. Saboungi
The Coordination Cluster Theory of Solutions
Proc. Carl Wagner Commemorative Symp. on Metallurgical Thermodynamics and Electrochemisty, AIME Society

M. Blander and M. L. Saboungi
On the pCl Concept in the Chloraluminate Melts
Accepted for publication in Proc. Third Int. Symp. on Molten Salts of the Electrochem. Soc.

W. F. Calaway
The Reaction of Chromium with Lithium Nitride in Liquid Lithium
Accepted for publication in Proc. Second Int. Conf. on Liquid Metal Technology in Energy Production, Richland, WA, April 20-23, 1980

W. F. Calaway, J. R. Weston, E. H. Van Deventer, and V. A. Maroni
On-Line Impurity Monitors as Applied to a Study of Cold Trapping in Liquid Lithium
Accepted for publication in Proc. Second Int. Conf. on Liquid Metal Technology in Energy Production, Richland, WA, April 20-23, 1980

M. J. Chen and H. M. Feder
Mechanism of a New Process for Methanol Homologation
Accepted for publication in Proc. Eighth Conf. on Catalysis in Organic Synthesis, New Orleans, LA, June 2-4, 1980

L. A. Curtiss, D. J. Frurip, C. Horowitz, and M. Blander
Characterization of Association in Pyridine Vapor by Measurement of Thermal Conductivity
Accepted for publication in Proc. 16th Int. Thermal Conductivity Conf., Chicago, IL, November 1979

M. M. Farahat, A. A. Chilenskas, and D. L. Barney
Heat Generation in Lithium/Iron Sulfide Cells
Accepted for publication in Proc. Lithium Battery Symp., Electrochem. Soc. Meeting, Hollywood, FL, October 5-10, 1980

H. M. Feder, J. W. Rathke, M. J. Chen, and L. A. Curtiss
Experimental and Theoretical Studies of Mechanisms in the Homogeneous Catalytic Activation of Carbon Monoxide
Accepted for publication in Proc. Symp. on the Catalytic Hydrogenation of Carbon Monoxide at the 180th ACS National Meeting, Las Vegas, NV, August 1980

D. C. Fee and C. E. Johnson
Cesium Thermomigration and Reaction in Nuclear Fuels
Accepted for publication in J. Nucl. Mater.

D. C. Fee and C. E. Johnson
Cesium-Uranium-Oxygen Chemistry in Uranium-Plutonium Oxide Fast Reactor Fuel Pins
Accepted for publication in J. Nucl. Mater.

D. C. Fee and C. E. Johnson
Fuel-Cladding Chemical Interaction in Uranium-Plutonium Oxide Fast Reactor Fuel Pins
Accepted for publication in J. Nucl. Mater.

A. K. Fischer, W. R. Lehman, and D. R. Vissers
Agglomeration in Li-Al Alloy Electrodes
Accepted for publication in Proc. Lithium Battery Symp., Electrochem. Soc. Meeting, Hollywood, FL, October 5-10, 1980

H. E. Flotow and P. A. G. O'Hare
Thermodynamics of the Lanthanide Trifluorides: IV. The Heat Capacities of Gadolinium Trifluoride, GdF_3, Lutetium Trifluoride, LuF_3, and Yttrium Trifluoride, YF_3, from 5 to 350 K
J. Chem. Phys., in press

H. E. Flotow, P. A. G. O'Hare, and J. Boerio-Goates
Heat Capacity from 5 to 350 K and Thermodynamic Properties of Cesium Nitrate to 725 K
J. Chem. Thermodyn., in press

H. E. Flotow and M. Tetenbaum
Heat Capacity and Thermodynamic Functions of β-$^{242}Pu_2O_3$ from 8 to 350 K: Contributions to the Excess Entropy
Accepted for publication in J. Chem. Phys.

D. J. Frurip, L. A. Curtiss, and M. Blander
Thermal Conductivity Measurements and Molecular Association in a Series of Alcohol Vapors: Methanol, Ethanol, Isopropanol, and tert-Butanol
Accepted for publication in Int. J. Thermophys.

D. J. Frurip, L. A. Curtiss, and M. Blander
Thermal Conductivity Measurements and Molecular Association in Ethanol Vapor
Accepted for publication in Proc. 16th Int. Thermal Conductivity Conf., Chicago, IL, November 1979

E. C. Gay, W. E. Miller, V. M. Kolba, and H. Shimotake
Lithium/Iron Sulfide Cell Development for Electric-Vehicle Propulsion
Accepted for publication in Proc. 29th Power Sources Conf., Atlantic City, NJ, June 10-13, 1980, publ. by Electrochem. Soc.

E. C. Gay, W. E. Miller, and F. J. Martino
Use of Multiple Regression Analysis to Develop Equations for Predicting LiAl/Iron Sulfide Cell Performance
Accepted for publication in J. Appl. Electrochem.

B. D. Holt, R. Kumar, and P. T. Cunningham
Oxygen-18 Study of the Aqueous-Phase Oxidation of Sulfur Dioxide
Accepted for publication in Atmos. Environ.

G. K. Johnson
The Enthalpy of Formation of FeF_3 by Fluorine Bomb Calorimetry
Accepted for publication in J. Chem. Thermodyn.

G. K. Johnson and E. H. P. Cordfunke
The Enthalpies of Formation of Uranium Mononitride and α- and β-Uranium Sesquinitride by Fluorine Bomb Calorimetry
Accepted for publication in J. Chem. Thermodyn.

G. K. Johnson, G. N. Papatheodorou, and C. E. Johnson
The Enthalpies of Formation of $SbF_5(\ell)$ and $Sb_2S_3(c)$ and the High-Temperature Thermodynamic Functions of $Sb_2S_3(c)$ and $Sb_2S_3(\ell)$
Accepted for publication in J. Chem. Thermodyn.

G. K. Johnson and W. V. Steele
The Standard Enthalpy of Formation of Uranium Dioxide by Fluorine Bomb Calorimetry
Accepted for publication in J. Chem. Thermodyn.

T. D. Kaun, W. E. Miller, L. Redey, and J. D. Arntzen
Designing Stable Capacity for LiAl/FeS Multiplate Cells
Accepted for publication in Proc. Lithium Battery Symp., Electrochem. Soc. Meeting, Hollywood, FL, October 5-10, 1980

K. Y. Kim, G. K. Johnson, C. E. Johnson, E. H. Appelman, P. A. G. O'Hare, and B. A. Phillips
Thermodynamic Properties of Tricesium Chromium(V) Tetroxide (Cs_3CrO_4)
J. Chem. Thermodyn., in press

K. Y. Kim, G. K. Johnson, P. A. G. O'Hare, and B. A. Phillips
Standard Enthalpy of Formation at 298.15 K of Cs_4CrO_4
J. Chem. Thermodyn., in press

M. A. Kirk, R. C. Birtcher, T. H. Blewitt, L. R. Greenwood, R. J. Popek, and R. R. Heinrich
Measurments of Neutron Spectra and Fluxes at Spallation Neutron Sources and their Application to Radiation Effects Research
Accepted for publication in J. Nucl. Mater.

R. A. Leonard, G. J. Bernstein, R. H. Pelto, and A. A. Ziegler
Liquid-Liquid Dispersion in Turbulent Couette Flow
Accepted for publication in AIChE J.

M. B. Liu, G. Cook, and N. P. Yao
Passivation of Zinc Anodes in KOH Electrolytes
Accepted for publication in J. Electrochem. Soc.

V. A. Maroni
First Wall, Blanket, and Shield Engineering for Magnetically Confined Fusion Power Reactors
Accepted for publication in Proc. of Fourth ANS Topical Meeting on the Technology of Controlled Nuclear Fusion, King of Prussia, PA, October 14-17, 1980

C. A. Melendres and F. A. Cafasso
Electrochemical and In Situ Laser Raman Spectroscopy Studies on Carbon-Supported Iron-Phthalocyanine Electrodes
Accepted for publication in J. Electrochem. Soc.

Z. Nagy
Comparison of Computer Curve-Fitting and Graphical Data Evaluations of the Galvanostatic Double Pulse Relaxation Technique for the Measurement of Kinetics of Electrode Reactions
Accepted for publication by J. Electrochem. Soc.

Z. Nagy
Comparison of Computer Curve-Fitting and Graphical Data Evaluations of the Galvanostatic Relaxation Technique for the Measurements of Kinetics of Electrode Reactions
Accepted for publication in Electrochim. Acta

H. Ohno and H. Shimotake
Determination of Effective Conductivity of Porous Ceramic Separators of LiAl/LiCl-KCl/FeS Cells
Accepted for publication in Proc. Lithium Battery Symp., Electrochem. Soc. Meeting, Hollywood, FL, October 5-10, 1980

G N. Papatheodorou
Spectroscopy Structure and Bonding of High-Temperature Metal-Halide Vapor Complexes
Accepted for publication as a chapter in Current Topics in Material Sciences, E. Kaldis, Ed., North-Holland Publishing Co. (New York, 1981)

G. N. Papatheodorou
Structure and Thermodynamics of Molten Salts
Accepted for publication as a chapter in A Treatise of Electrochemistry, Vol. IV, J. O. Bockris, B. E. Conway, and E. Yaeger, Eds., Plenum Press (New York, 1981)

G. N. Papatheodorou, J. Meisenhelder, and R. O. Loutfy
Vapor Complexes of Fe(II) Chloride with Aluminum Chloride
Accepted for publication in J. Inorg. Nucl. Chem.

L. Redey, S. Higuchi, T. D. Kaun, F. J. Martino, and D. R. Vissers
Electrode Potential Relaxation in High-Temperature Li-Al/FeS Engineering Cells
Accepted for publication in Proc. Lithium Battery Symp., Electrochem. Soc. Meeting, Hollywood, FL, October 5-10, 1980

M. L. Saboungi and M. Blander
Advances in Theories of Molten Salt Solutions
Accepted for publication in Proc. Third Int. Symp. on Molten Salts of the Electrochem. Soc.

M. L. Saboungi and M. Blander
Theoretical Studies of Slag Exchange Equilibria
Accepted for publication in Can. Metall. Q.

M. L. Saboungi, J. Marr, and S. Spineto
Activity Coefficients of Lithium Dilute in Binary Alloys: Measurements and Calculations
Proc. Carl Wagner Commemorative Symp. on Metallurgical Thermodynamics and Electrochemistry, AIME Society

J. R. Selman and M. L. Saboungi
Electrochemistry of Sulfur in Halide Melts
Accepted for publication in The Sulfur Electrode in Non-Aqueous Media, R. P. Fisher, Ed., New York, Academic Press

J. A. Smaga and J. E. Battles
Evaluation of Nickel for Positive Electrode Components in Li-Al/FeS Cells
Accepted for publication in Proc. Lithium Battery Symp., Electrochem. Soc. Meeting, Hollywood, FL, October 5-10, 1980

D. L. Smith, R. H. Lee, and R. M. Yonco
Investigation of Nonmetallic Element Interactions in Vanadium-Alloy/Lithium Systems
Accepted for publication in Proc. Second Int. Conf. on Liquid Metal Technology in Energy Production, Richland, WA, April 20-24, 1980

W. V. Steele, P. A. G. O'Hare, and E. H. Appelman
The Standard Enthalpies of Formation of Cesium Fluoroxysulfate ($CsSO_4F$) and Cesium Peroxydisulfate ($Cs_2S_2O_8$)
Accepted for publication in J. Inorg. Chem.

S. Sudar, S. Zivi, and A. A. Chilenskas
Electric Utility Storage System Utilizing the Lithium-Iron Sulfide Battery
Accepted for publication in Proc. Am. Power Conf., Chicago, IL, April 21-22, 1980

R. B. Swaroop and J. E. Battles
Development of BN Felt for Li-Al/MS_x Battery
Accepted for publication in J. Electrochem. Soc.

M. Tetenbaum
Transport of Fuel and Fission Products from Failed Mixed-Oxide Fuel Pins by Flowing Sodium in LMFBRs
Accepted for publication by Electric Power Research Institute (EPRI)

Z. Tomczuk, S. K. Preto, and M. F. Roche
Reaction of FeS Electrodes in LiCl-KCl Electrolyte
Accepted for publication in J. Electrochem. Soc.

Z. Tomczuk, M. F. Roche, and D. R. Vissers
Phase Relationships in Positive Electrodes of High Temperature Lithium Aluminum/Iron Sulfide Cells
Accepted for publication in Proc. Lithium Battery Symp., Electrochem. Soc. Meeting, Hollywood, FL, October 5-10, 1980

R. Varma, G. M. Cook, and N. P. Yao
Anodization and Sulfation of Tetrabasicleadsulfate in Sulfuric Acid: In-Situ Monitoring of Electrode Surface Phases by Laser Raman Scattering
Accepted for publication in J. Electrochem. Soc.

J. R. Weston, W. F. Calaway, R. M. Yonco, and V. A. Maroni
Recent Advances in Lithium Processing Technology at the Argonne National Laboratory
Accepted for publication in Proc. Second Int. Conf. on Liquid Metal Technology in Energy Production, Richland, WA, April 20-24, 1980

G. Wijbenga and G. K. Johnson
The Enthalpy of Formation of Palladium(II) Hexafluoropalladate(IV), $Pd(PdF_6)$, by PF_3 Reduction Calorimetry
Accepted for publication in J. Chem. Thermodyn.

Y. Yamazaki and N. P. Yao
Current Distributions in Soluble Battery Electrodes:
I. Theoretical
Accepted for publication in J. Electrochem. Soc.

Y. Yamazaki and N. P. Yao
Current Distributions in Soluble Battery Electrodes:
II. Experimental
Accepted for publication in J. Electrochem. Soc.

N. P. Yao
Advanced Secondary Batteries: Their Application, Status, and Market--A Review
Accepted for publication in J. Power Sources

N. P. Yao
Heat Transfer Modeling and Thermal Management of Batteries
Accepted for publication in AIChE Symp. Ser., Tutorial Lectures in Electrochemical Engineering and Science

N. P. Yao, C. C. Christianson, R. C. Elliott, and J. F. Miller
Status of Nickel/Zinc and Nickel/Iron Battery Technology for Electric Vehicle Applications
Accepted for publication in Proc. 29th Power Source Conf., Atlantic City, NJ, June 10-13, 1980, publ. by Electrochem. Soc.

N. P. Yao, C. C. Christianson, and T. Lee
Improved Lead-Acid Batteries--The Promising Candidate for Near-Term Electric Vehicles
Accepted for publication in Proc. 29th Power Source Conf., Atlantic City, NJ, June 10-13, 1980, publ. by Electrochem. Soc.

C. ANL Reports

J. D. Arntzen, V. M. Kolba, W. E. Miller, and E. C. Gay
Fifty Cell Test Facility
ANL-80-50

D. L. Barney, R. K. Steunenberg, A. A. Chilenskas, E. C. Gay, J. E. Battles, F. Hornstra, W. E. Miller, D. R. Vissers, M. F. Roche, H. Shimotake, R. Hudson, B. A. Askew, and S. Sudar
High-Performance Batteries for Electric-Vehicle Propulsion and Stationary Energy Storage, Progress Report for the Period October 1978-September 1979
ANL-79-94

D. L. Barney, R. K. Steunenberg, A. A. Chilenskas, E. C. Gay, J. E. Battles, F. Hornstra, W. E. Miller, D. R. Vissers, M. F. Roche, H. Shimotake, R. Hudson, B. A. Askew, and S. Sudar
Development of Advanced Batteries at Argonne National Laboratory: Summary Report for 1979
ANL-80-32

D. L. Barney, R. K. Steunenberg, A. A. Chilenskas, E. C. Gay, J. E. Battles, W. E. Miller, D. R. Vissers, H. Shimotake
Lithium/Iron Sulfide Batteries for Electric-Vehicle Propulsion and Other Applications, Progress Report for October 1979-March 1980
ANL-80-49

A. P. Brown and G. M. Cook
The Electrorefining of Copper From a Cuprous Ion Complexing Electrolyte: I. Initial Evaluation of Potential for Energy Savings
ANL/OEPM-78-6

A. P. Brown, R. O. Loutfy, and G. M. Cook
The Electrorefining of Copper from a Cuprous Ion Complexing Electrolyte: II. Experimental Comparison of Possible Alternative Electrolytes and Preliminary Cost Engineering Analysis
ANL/OEPM-80-2

L. Burris, D. S. Webster, D. L. Barney, F. A. Cafasso, and M. J. Steindler
Chemical Engineering Division Research Highlights 1979
ANL-80-66

A. A. Chilenskas, J. C. Schaefer, W. L. Towle, and D. L. Barney
A Preliminary Estimate of the Manufacturing Cost for Lithium/Metal Sulfide Cells for Stationary and Mobile Applications
ANL-79-59

H. Diamond, C. S. Sabau, E. P. Horwitz, G. F. Vandegrift, and G. W. Mason
Di-n-amyl-n-amylphosphonate and Tricaprylmethylammonium Nitrate as Potential Extractants for Reprocessing Th-U Fuels
ANL-79-85

D. C. Fee, W. Ira Wilson, J. A. Shearer, G. W. Smith, J. F. Lenc, L. S. Fan, K. M. Myles, and I. Johnson
Sorbent Utilization Prediction Methodology: Sulfur Control in Fluidized-Bed Combustors
ANL/CEN/FE-80-10

J. K. Fink and L. Leibowitz
Thermophysical Properties of Sodium
ANL-CEN-RSD-79-1

D. G. Graczyk, G. Bandyopadhyay, S. M. Gehl, J. P. Hughes, and H. T. Goodspeed
A Laser Microsampling Method for Determination of Retained Fission Gas in Irradiated Nuclear Fuels
ANL-79-86

D. W. Green
Tables of Thermodynamic Functions for Gaseous Thorium, Uranium, and Plutonium Oxides
ANL-CEN-RSD-80-1

J. E. Helt
Evaluation of Alkali Metal Sulfate Dew Point Measurement for Detection of Hot Corrosion Conditions in PFBC Flue Gas
ANL/CEN/FE-80-12

K. J. Jensen and W. E. Streets
Methods of Chemical Analysis Used to Characterize Battery Materials
ANL-80-41

I. Johnson, J. F. Lenc, J. A. Shearer, G. W. Smith, W. M. Swift, F. G. Teats, C. B. Turner, and A. A. Jonke
Support Studies in Fluidized-Bed Combustion, Quarterly Report, April-June 1979
ANL/CEN/FE-79-8

I. Johnson, D. S. Moulton, F. F. Nunes, E. B. Smyk, W. M. Swift, F. G. Teats, and A. A. Jonke
Regeneration of Sulfated Limestone from FBCs, Quarterly Report, April-June 1979
ANL/CEN/FE-79-9

I. Johnson, D. S. Moulton, F. F. Nunes, W. M. Swift, F. G. Teats, and A. A. Jonke
Regeneration of Sulfated Limestone from FBCs, Annual Report, October 1978-September 1979
ANL/CEN/FE-79-13

I. Johnson, K. M. Myles, W. M. Swift, S. H. D. Lee, J. A. Shearer, A. A. Siczek, F. G. Teats, W. I. Wilson, W. A. Boyd, E. B. Smyk, and C. B. Turner
Support Studies in Fluidized-Bed Combustion, Annual Report, October 1978-September 1979
ANL/CEN/FE-79-14

I. Johnson, K. M. Myles, J. F. Lenc, J. A. Shearer, G. W. Smith, O. K. Chopra, F. G. Teats, F. F. Nunes, C. B. Turner, W. I. Wilson, and A. A. Jonke
Investigation of Limestone Sulfation Enhancement Agents and Their Corrosion Rates in FBCs, Annual Report, October 1978-September 1979
ANL/CEN/FE-79-15

I. Johnson, W. F. Podolski, R. F. Henry, J. E. Hanway, K. E. Griggs, E. L. Carls, and A. A. Jonke
Fluidized-Bed Combustion Process Evaluation and Program Support, Quarterly Report, October-December 1979
ANL/CEN/FE-80-1

I. Johnson, W. F. Podolski, K. M. Myles, K. E. Griggs, A. A. Siczek, W. W. Managan, R. W. Doering, J. J. Eichholz, N. M. O'Fallon, C. L. Herzenberg, and A. A. Jonke
Sampling and Instrumentation for Fluidized-Bed Combustion, Annual Report, October 1978-September 1979
ANL/CEN/FE-80-2

I. Johnson, W. M. Swift, S. H. D. Lee, and A. A. Jonke
Alkali Metal Vapor Removal from Pressurized Fluidized-Bed Combustor Flue Gas, Quarterly Report, October-December 1979
ANL/CEN/FE-80-4

I. Johnson, W. M. Swift, and S. H. D. Lee
Alkali Metal Vapor Removal from Pressurized Fluidized-Bed Combustor Flue Gas, Quarterly Report, January-March 1980
ANL/CEN/FE-80-5

I. Johnson, W. M. Swift, S. H. D. Lee, and W. A. Boyd
Alkali Metal Vapor Removal from Pressurized Fluidized-Bed Combustor Flue Gas, Quarterly Report, April-June 1980
ANL/CEN/FE-80-6

I. Johnson, K. M. Myles, and A. A. Siczek
Sampling and Analysis of Hydrocarbons in Combustion Gases, Quarterly Report, April-June 1980
ANL/CEN/FE-80-11

I. Johnson, W. M. Swift, and S. H. D. Lee
Alkali Metal Vapor Removal from Pressurized Fluidized-Bed Combustor Flue Gas
ANL/CEN/FE-80-16

K. Kinoshita
Critical Survey on Electrode Aging in Molten Carbonate Fuel Cells
ANL-79-55

V. M. Kolba, J. E. Battles, J. D. Geller, and K. Gentry
Failure Analysis of Mark IA Lithium/Iron Sulfide Battery
ANL-80-44

R. H. Land, V. A. Maroni, and M. Minkoff
TSOAK-M1: A Computer Code to Determine Tritium Reaction/Adsorption/Release Parameters from Experimental Results of Air-Detritiation Tests
ANL-79-82

S. H. D. Lee, W. M. Swift, and I. Johnson
Diatomaceous Earth and Activated Bauxite Used as Granular Sorbents for the Removal of Sodium Chloride Vapor from Hot Flue Gas
ANL/CEN/FE-79-18

R. A. Leonard, G. J. Bernstein, and A. A. Ziegler
Development of a 25-cm Annular Centrifugal Contactor
ANL-80-15

R. A. Leonard
Prediction of Hydraulic Performance in Annular Centrifugal Contactors
ANL-80-57

M. B. Liu, G. M. Cook, and N. P. Yao
Galvanostatic Polarization of Zinc Microanodes in KOH Electrolytes
ANL/OEPM-80-1

S. Majumdar
Analysis of an Internally Pressurized Prismatic Cell Can
ANL-80-30

C. C. McPheeters and D. J. Raue
Sodium Hydride Precipitation in Sodium Cold Traps
ANL-79-101

C. C. McPheeters, S. B. Skladzien, and D. J. Raue
Experiments on Cold-Trap Regeneration by NaH Decomposition
ANL-79-100

B. Misra and J. F. Davis
Cryogenic Distillation: A Fuel Enrichment System for Near-Term Tokamak-Type D-T Fusion Reactors
ANL-78-96

D. S. Moulton and F. F. Nunes
Limestone Sorbent Regeneration in Externally Fired Rotary Kilns
ANL/CEN/FE-79-12

C. M. Ono, R. Kumar, and J. K. Fink
TRANS4: A Computer Code Calculation of Solid Fuel Penetration of a Concrete Barrier
ANL-80-63

R. D. Pierce, P. A Finn, K. Kinoshita, G. H. Kucera, R. B. Poeppel, J. W. Sim, and R. N. Singh
Advanced Fuel Cell Development, Progress Report for January-March 1979
ANL-79-51

R. D. Pierce, P A. Finn, K. Kinoshita, G. H. Kucera, R. B. Poeppel, R. N. Singh, and J. W. Sim
Advanced Fuel Cell Development, Progress Report for April-June 1979
ANL-79-84

R. D. Pierce, K. Kinoshita, G. H. Kucera, R. B. Poeppel, J. W. Sim, and R. N. Singh
Advanced Fuel Cell Development, Progress Report for July-September 1979
ANL-79-110

R. D. Pierce, G. H. Kucera, D. S. Kupperman, R. B. Poeppel, J. W. Sim, R. N. Singh, and J. L. Smith
Advanced Fuel Cell Development, Progress Report for October-December 1979
ANL-80-33

R. D. Pierce, R. M. Arons, A. V. Fraioli, G. H. Kucera, R. B. Poeppel, J. W. Sim, and J. L. Smith
Advanced Fuel Cell Development, Progress Report for January-March 1980
ANL-80-67

M. Petrick and T. R. Johnson
MHD Heat and Seed Recovery Technology Project--Seventh Quarterly Report: July-September 1979
ANL/MHD-79-16

M. Petrick and T. R. Johnson
MHD Heat and Seed Recovery Technology Project--Eighth Quarterly Report: October-December 1979
ANL/MHD-80-1

M. G. Seitz, P. G. Rickert, R. A. Couture, J. Williams, N. Meldgin, S. M. Fried, A. M. Friedman, and M. J. Steindler
Studies of Nuclear Waste Migration in Geologic Media, Annual Report, October 1978-September 1979
ANL-80-36

M. J. Steindler, M. Ader, R. E. Barletta, J. K. Bates, C. H. Bean, G. J. Bernstein, R. A. Couture, K. F. Flynn, T. J. Gerding, L. J. Jardine, D. K. Kroeck, M. Krumpelt, B. J. Kullen, R. A. Leonard, W. J. Mecham, J. H. Meisenhelder, K. M. Myles, R. H. Pelto, B. B. Saunders, W. B. Seefeldt, M. G. Seitz, A. A. Siczek, L. E. Trevorrow, S. Vogler, A. A. Ziegler, D. S. Webster, and L. Burris
Chemical Engineering Division Fuel Cycle Programs, Quarterly Progress Report, April-June 1978
ANL-78-76

M. J. Steindler, M. Ader, R. E. Barletta, J. K. Bates, C. H. Bean, G. J. Bernstein, R. A. Couture, K. F. Flynn, T. J. Gerding, L. J. Jardine, D. K. Kroeck, M. Krumpelt, B. J. Kullen, R. A. Leonard, W. J. Mecham, J. H. Meisenhelder, K. M. Myles, R. H. Pelto, B. B. Saunders, W. B. Seefeldt, M. G. Seitz, A. A. Siczek, L. E. Trevorrow, S. Vogler, J. Williams, A. A. Ziegler, D. S. Webster, and L. Burris
Chemical Engineering Division Fuel Cycle Programs, Quarterly Progress Report, July-September 1978
ANL-79-6

M. J. Steindler, M. Ader, R. E. Barletta, J. K. Bates, C. H. Bean, R. A. Couture, E. D. Creamer, K. F. Flynn, T. J. Gerding, L. J. Jardine, D. K. Kroeck, M. Krumpelt, B. J. Kullen, O. C. Linhart, W. J. Mecham, K. M. Myles, R. H. Pelto, B. B. Saunders, W. B. Seefeldt, M. G. Seitz, L. E. Trevorrow, S. Vogler, and J. Williams
Chemical Engineering Division Fuel Cycle Programs, Quarterly Progress Report, October-December 1978
ANL-79-29

M. J. Steindler, M. Ader, R. E. Barletta, J. K. Bates, C. H. Bean, R. A. Couture, E. D. Creamer, K. F. Flynn, T. J. Gerding, L. J. Jardine, D. K. Kroeck, M. Krumpelt, W. J. Mecham, J. H. Meisenhelder, K. M. Myles, R. H. Pelto, M. G. Seitz, S. Vogler, and J. Williams
Chemical Engineering Division Fuel Cycle Programs, Quarterly Progress Report, January-March 1979
ANL-79-45

M. J. Steindler, M. Ader, R. E. Barletta, J. K. Bates, C. H. Bean, R. A. Couture, K. F. Flynn, T. J. Gerding, L. J. Jardine, D. K. Kroeck, M. Krumpelt, W. J. Mecham, J. H. Meisenhelder, K. M. Myles, R. H. Pelto, M. G. Seitz, S. Vogler, and J. Williams
Chemical Engineering Division Fuel Cycle Programs, Quarterly Progress Report, April-June 1979
ANL-79-99

M. J. Steindler, R. A. Couture, K. F. Flynn, L. J. Jardine, W. J. Mecham, R. H. Pelto, M. G. Seitz, and J. Williams
Chemical Engineering Division Fuel Cycle Programs, Quarterly Progress Report, July-September 1979
ANL-79-109

M. J. Steindler, J. K. Bates, R. A. Couture, K. F. Flynn, T. J. Gerding, L. J. Jardine, W. J. Mecham, R. H. Pelto, and M. G. Seitz
Chemical Engineering Division Fuel Cycle Programs, Quarterly Progress Report, October-December 1979
ANL-80-61

M. J. Steindler, G. J. Bernstein, R. A. Leonard, J. H. Meisenhelder, R. H. Pelto, A. A. Siczek, and A. A. Ziegler
Chemical Engineering Division Fuel Cycle Applied Technology, Quarterly Progress Report, October-December 1978
ANL-80-77

M. J. Steindler, G. J. Bernstein, R. A. Leonard, J. H. Meisenhelder, R. H. Pelto, A. A. Siczek, and A. A. Ziegler
Chemical Engineering Division Fuel Cycle Applied Technology, Quarterly Progress Report, January-March 1979
ANL-80-79

M. J. Steindler, G. J. Bernstein, R. A. Leonard, R. H. Pelto, A. A. Ziegler, D. S. Webster, and L. Burris
Chemical Engineering Division Fuel Cycle Applied Technology, Quarterly Progress Report, April-June 1979
ANL-80-81

M. J. Steindler, G. J. Bernstein, R. A. Leonard, and A. A. Ziegler
Chemical Engineering Division Fuel Cycle Applied Technology, Quarterly Progress Report, July-September 1979
ANL-80-82

M. J. Steindler, G. J. Bernstein, R. A. Leonard, A. A. Ziegler, D. S. Webster, and L. Burris
Chemical Engineering Division Fuel Cycle Applied Technology, Quarterly Progress Report, October-December 1979
ANL-80-83

W. M. Swift, J. C. Montagna, G. W. Smith, E. B. Smyk
Process Costs and Flowsheets, Bed Defluidization Characteristics, Stone Reactivity Changes and Attrition Losses for a Regenerative Fluidized-Bed Combustion Process
ANL/CEN/FE-78-14

R. Varma, G. M. Cook, and N. P. Yao
Monitoring Stibine and Arsine in Lead-Acid Battery Charge Gas and in Ambient Air: Development and Testing of a Field Kit
ANL/OEPM-78-4

J. E. Young, S. H. Wong, J. E. Johnson, N. Sikand, and A. A. Jonke
Laboratory Support for In Situ Gasification--Reaction Kinetics Annual Report, October 1977-September 1978
ANL/CEN/FE-79-4

S. M. Zivi, H. Kacinskas, I. Pollack, A. A. Chilenskas, D. L. Barney, W. Grieve, B. L. McFarland, S. Sudar, E. Goldstein, and E. Adler
Reference Design of 100 MW-h Lithium/Iron Sulfide Battery System for Utility Load Leveling
ANL-80-19

S. M. Zivi, H. Kacinskas, I. Pollack, A. A. Chilenskas, W. Grieve, B. L. McFarland, and S. Sudar
Conceptual Designs for Utility Load-Leveling Battery with Li/FeS Cells
ANL-80-20

D. Papers Presented at Scientific Meetings

M. Abdou, J. Brooks, R. Mattas, R. Clemmer, P. Finn, D. Smith, B. Misra, et al.
A Limiter/Vacuum System for Plasma Purity Control and Exhaust in Tokamaks
Presented at Fourth ANS Topical Meeting on the Technology of Controlled Nuclear Fusion, King of Prussia, PA, October 14-17, 1980

J. P. Ackerman
Molten Carbonate Fuel Cell Programs in the United States Electrochemical Systems: Batteries & Fuel Cells
Presented at Brazilian Government Agencies, Fortaleza, Brazil, March 2-6, 1980

J. L. Anderson, W. R. Wilkes, and V. A. Maroni
The Development of Tritium Technology for the United States Magnetic Fusion Energy Program
Presented at Eighth Int. Conf. on Plasma Physics and Controlled Fusion Research, Brussels, Belgium, July 1-10, 1980

G. Bandyopadhyay and T. M. Galvin
Out-of-Cell Investigation of Sintering and Creep Behavior of Li-Al Electrode Compositions for Li-Al/FeS Battery Cells
Presented at Fall Meeting of the Electronics Division of Am. Ceram. Soc., San Francisco, CA, October 26-29, 1980

G. Bandyopadhyay, T. M. Galvin, and J. T. Dusek
Stability of Electrically Conducting Ceramic Coatings in Molten LiCl-KCl and Sulfide Environments
Presented at Fourth Annual Conf. on Composites and Advanced Materials, Ceramic-Metal Systems Division, Am. Ceram. Soc., Cocoa Beach, FL, January 20-24, 1980

J. E. Battles, E. C. Gay, R. K. Steunenberg, and D. L. Barney
Development of High-Temperature Secondary LiAl/FeS Batteries at ANL
Presented at First National Seminar on Electrochemical Systems: Batteries and Fuel Cells, Federal University of Ceara, Brazil, March 2-6, 1980

J. E. Battles and J. A. Smaga
Materials Requirements for High Temperature Advanced Secondary Batteries
Presented at Energy-Sources Tech. Conf. & Exhibition, Am. Soc. of Mech. Eng., New Orleans, LA, February 3-7, 1980

A. P. Brown, G. M. Cook, R. O. Loutfy, and N. P. Yao
The Electrorefining of Copper from a Cuprous Ion Stabilizing Electrolyte
Presented at Energy Conservation Measures in Electrowinning and Electrorefining Symp., 109th AIME Meeting, Las Vegas, NV, February 25-28, 1980

W. L. Buck, H. S. Huang, and B. Hubble
Fluidized Bed Combustion Development--An Overview
Presented at Second U.S. Dept. of Energy Environmental Control Symp., Reston, VA, March 17-19, 1980

E. L. Callis, A. E. Essling, G. T. Reedy, and R. J. Meyer
Absolute Li Isotope Ratio Measurements
Presented at 28th Annual Conf. on Mass Spectrometry and Allied Topics, New York, NY, May 25-30, 1980

A. A. Chilenskas
The Impact of Lithium on the Cost and Availability of Lithium-Aluminum/Iron Sulfide Batteries
Presented at Materials and Processes Congress, Am. Soc. Met., Cleveland, OH, October 28-30, 1980

A. A. Chilenskas, R. K. Steunenberg, and D. L. Barney
Lithium/Iron Sulfide Batteries for Advanced Vehicle Propulsion
Presented at Electric and Hybrid Vehicle Advanced Technology Seminar, Pasadena, CA, December 8 and 9, 1980

O. K. Chopra, G. W. Smith, J. F. Lenc, J. A. Shearer, K. M. Myles, and I. Johnson
Effects of Salt Treatment of Limestone on Sulfation and on the Corrosion Behavior of Materials in AFBC Systems
Presented at Sixth Int. Fluidized-Bed Conf., Atlanta, GA, April 9-11, 1980

C. C. Christianson
Electric Vehicles--Status and Prospects
Presented at Michigan Energy Management Institute, Detroit, MI, August 15, 1980

R. G. Clemmer
The Development of Tritium Breeding Blankets for D-T-Burning Fusion Reactors
Presented at Fourth ANS Topical Meeting on the Technology of Controlled Nuclear Fusion, King of Prussia, PA, October 14-17, 1980

R. L. Cole
Conservation and Solar Energy and Residential Solar Heating
Presented to Home Builders Institute, Summit, IL, June 21, 1980

R. L. Cole
Solar Energy
Presented at Illinois Valley College in Oglesby, IL, April 22, 1980

R. A. Couture, M. G. Seitz, and M. J. Steindler
Transport of Cs^+ and Na^+ through Kaolinite in Aqueous Solutions at Elevated Temperatures
Presented at Am. Nucl. Soc., San Francisco, CA, August 24-29, 1980

L. A. Curtiss and D. J. Frurip
Ab Initio Molecular Orbital Studies of Beryllium and Magnesium Atom Reactions with Water
Presented at Seventh Can. Symp. on Theoretical Chemistry, Banff, Canada, June 15-20, 1980

P. A. Finn, R. G. Clemmer, and V. A. Maroni
Tritium Handling Considerations for ETF and STARFIRE
Presented at Fourth ANS Topical Meeting on the Technology of Controlled Nuclear Fusion, King of Prussia, PA, October 14-17, 1980

D. J. Frurip
Homogeneous Nucleation in Metal Vapors: Experiments and Kinetic Modeling
Presented at Chemistry Division, Argonne National Laboratory, March 1980

D. J. Frurip and M. Blander
A Dimensional Analysis of Some Thermodynamic Properties
Presented at 73rd Annual Meeting of the AIChE, Symp. on Thermodynamics, Chicago, IL, November 16-20, 1980

D. J. Frurip and M. Blander
Prediction of the Thermodynamic Properties of Gaseous Hydroxides and Sulfates
Presented at Gordon Research Conf. in High Temperature Chemistry, Plymouth, NH, August 4-8, 1980

A. J. Gorski
Long-Term Ice Storage for Cooling Applications Using Passive Freezing Techniques
Presented at the Passive Cooling Systems for Buildings course at the Energy Technology Center, University of Wisconsin Extension, Madison, WI, July 28-29, 1980

D. G. Graczyk
Laser-Microsampling for Retained Fission Gas in Irradiated Nuclear Fuel
Presented at Joliet Chapter Meeting of American Chemical Society, Joliet, IL, December 15, 1980

D. W. Green, G. T. Reedy, and S. D. Gabelnick
Far-Infrared Spectra of Matrix-Isolated Uranium Oxides
Presented at 35th Annual Symp. on Molecular Spectroscopy, Columbus, OH, June 16-20, 1980

D. W. Green, G. T. Reedy, and S. D. Gabelnick
Uranium Oxides: Low-Frequency Vibrations
Presented (Poster Session) at Gordon Research Conf. in High Temperature Chemistry, Plymouth, NH, August 4-8, 1980

L. R. Greenwood
Use of Uncertainty Data in Neutron Dosimetry
Presented at Workshop on Evaluation Methods and Procedures, DOE, Brookhaven National Laboratory, September 22-25, 1980

F. Hornstra and N. P. Yao
Fixed Point Normalization of Battery Test Data
Presented at DOE/EPRI Workshop on Statistical Techniques and Microprocessors on Battery Research, Rockville, MD, November 6-7, 1980

C. C. Hsu, R. O. Loutfy, M. Krumpelt, and N. P. Yao
High Temperature Chemistry of Alumina + Carbon + Sulfur
Presented at Gordon Research Conf. in High Temperature Chemistry, Plymouth, NH, August 4-8, 1980

W. N. Hubbard
The Enthalpy of Hydriding of $LaNi_{(5-x)}Al_x$
Presented at Seminar of National Research Council of Canada, Ottawa, Canada, October 3, 1980

W. N. Hubbard and P. A. Connick
The Enthalpy of Hydriding of $LaNi_{(5-x)}Al_x$
Presented at 35th Annual Calorimetry Conference, Eufala, AL, August 19-21, 1980

L. J. Jardine
Metal Matrices
Presented at Second Annual Argonne Workshop, Comparative Leaching Behavior of Radioactive Waste Forms--Argonne National Laboratory, Argonne, IL, September 3-4, 1980

A. Jirka, S. Bourne, and M. Peak
Mass and Mutagenicity Balances in Chemical Fractionations
Presented at 20th Hanford Life Sciences Symp., Coal Conversion and the Environment: Chemical, Biomedical, and Ecological Considerations, U.S. DOE and Battelle Memorial Institute, Pacific Northwest Laboratories, Richland, WA, October 19-23, 1980

C. E. Johnson
Irradiation Behavior of Mixed-Oxide Sphere-Pac Fuels
Presented at Seminar at Chemical Technology Division, ORNL, Oak Ridge, TN, September 10, 1980

C. E. Johnson
Thermodynamic and Thermophysical Properties of Candidate Solid Breeder Materials
Presented at DOE/OFE Materials and Radiations Effects Branch Workshop on Solid Breeder Materials, Germantown, MD, July 17-18, 1980

C. E. Johnson and D. C. Fee
Oxygen Getter Coatings for Fission Reactor Fuel Pins
Presented at Int. Conf. on Metallurgical Coatings, San Diego, CA, April 21-25, 1980

C. E. Johnson, S. W. Tam, P. E. Blackburn, and D. C. Fee
Fuel Chemistry Impact on Vented Fuel Pin Design
Presented at GCFR Tech. Review, San Diego, CA, June 4-6, 1980

G. K. Johnson, P. A. G. O'Hare, H. E. Flotow, and W. S. Wise
Thermodynamic Properties of Analcime
Presented at 35th Annual Calorimetry Conf., Eufaula, AL, August 19, 1980

I. Johnson
Fluidized-Bed Combustion
Presented at U. of Akron, Dept. of Chem. Eng. Seminar Series, Akron, OH, September 25, 1980

I. Johnson
Sorbent Utilization, Enhancement and Regeneration
Presented at DOE/WVU Conf. on Fluidized-Bed Combustion System Design and Operation, Morgantown, WV, October 27-29, 1980

S. Johnson, P. Cunningham, and R. Kumar
Chemical Characterization of Atmospheric Aerosol Using Attenuated Total Internal Reflection (ATR) Infrared Spectroscopy
Presented at 89th AIChE National Meeting, Portland, OR, August 17-20, 1980

S. A. Johnson, R. Kumar, and P. T. Cunningham
Infrared Attenuated Total Internal Reflection Spectroscopy--A Method for Chemical Characterization of Plume Aerosol During a Single Traverse
Presented at Second Symposium on Environmental Analytical Chemistry, U.S. DOE and Brigham Young University, Provo, UT, June 18-20, 1980

S. H. D. Lee, W. Swift, and I. Johnson
Activated Bauxite and Diatomaceous Earth Used as Granular Sorbents for the Removal of Alkali Vapors from Simulated Hot Flue Gas of PFBCs
Presented at Sixth Int. Conf. on Fluidized-Bed Combustion, Atlanta, GA, April 9-11, 1980

S. H. D. Lee, W. M. Swift, and I. Johnson
Regeneration of Activated Bauxite Used as a Granular Sorbent for Removing Gaseous Alkali Metal Compounds from Hot Flue Gas
Presented at 25th Int. Gas Turbine Conf., New Orleans, LA, March 10-13, 1980

C. D. Livengood, H. S. Huang, and P. S. Farber
Presented at the 73rd Air Pollution Control Association Annual Meeting, Montreal, Canada, June 22-27, 1980

V. A. Maroni, R. G. Clemmer, and J. R. Weston
A Status Report on Development of Breeder Blanket Technology for D-T Fusion Reactors
Presented at the 73rd Annual Meeting of AIChE, Chicago, IL, November 16-20, 1980

C. C. McPheeters and D. J. Raue
Analysis of Cold Trap Performance Behavior of Hydrogen
Presented at PNC/DOE Specialists' Meeting on Cold Trap Optimization, O-arai Engineering Center, Mito, Japan, January 21-24, 1980

C. C. McPheeters and D. J. Raue
Cold Trap Modeling and Experiments on NaH Precipitation
Presented at Second Int. Conf. on Liquid Metal Technol. in Energy Production, Richland, WA, April 20-24, 1980

C. C. McPheeters and D. J. Raue
Experiments on Cold Trap Regeneration by NaH Decomposition
Presented at PNC/DOE Specialists' Meeting on Cold Trap Optimization, O-arai Engineering Center, Mito, Japan, January 21-24, 1980

B. Misra, C. C. McPheeters, and R. D. Wolson
Fission-Product Removal from Sodium by Distillation
Presented at Second Int. Conf. on Liquid Metal Technology in Energy Production, Richland, WA, April 20-24, 1980

G. D. Morgan, P. B. Stones, D. L. Smith, H. C. Stevens, Y. Gohar, and B. Misra
First-Wall/Blanket Design for the STARFIRE Tokamak Reactor
Presented at Fourth ANS Topical Meeting on the Technology of Controlled Nuclear Fusion, King of Prussia, PA, ber 14-17, 1980

D. S. Moul[illegible], E. B. Smyk, and J. A. Shearer
Hydration Process for Enhanced Calcium Utilization in Fluidized-Bed Combustion
Presented at Chem. and Phys. of Coal Utilization, West Virginia University, Morgantown, WV, June 2-4, 1980

P. A. G. O'Hare, G. K. Johnson, J. H. Malar, G. Wijbenga, E. H. P. Cordfunke, and P. G. Eller
Recent Thermochemical Studies of Fluorides of Lower-Valent Uranium
Presented at Sixth Int. Conf. on Thermodyn., Merseburg, German Democratic Republic, August 25-29, 1980

G. N. Papatheodorou
High Temperature Metal Halide Vapor Complexes
Presented at the Danish Chemical Society, H. C. Ørsted Institut, University of Copenhagen, Denmark, October 9, 1980

G. N. Papatheodorou
Metal Halide Vapor Complexation: Spectroscopy and Structure
Presented at the Institutt for Uorganisk Kjemi, Universitet i Trondheium, Trondheium, Norway, June 23, 1980

G. N. Papatheodorou
Raman Spectroscopy: Molten Salts and Vapors
Presented at the Conf. on Ionic Liquids, Dead Sea, Israel, April 7-12, 1980

R. D. Pierce
Fuel Cells for Energy Production
Presented at Southeast/Southwest Regional ACS Meeting, New Orleans, LA, December 10-12, 1980

J. W. Rathke and H. M. Feder
Mechanism of the Homogeneous Hydrogenation of Carbon Monoxide to Methanol
Presented at Eighth Conf. of the Organic Reaction Catalysis Society, New Orleans, LA, June 2-4, 1980

G. T. Reedy and D. W. Green
Low-Noise Far-Infrared FT-IR Spectra of Matrix-Isolated Species
Presented at the 1980 Pittsburgh Conf. on Analytical Chemistry and Applied Spectroscopy, Atlantic City, NJ, March 1980

M. L. Saboungi and M. Blander
The Calculation of Phase Diagrams of Ionic Systems From Fundamental Solution Theories
Presented at 73rd Annual AIChE Meeting, Symp. on Thermodynamics, Chicago, IL, November 16-20, 1980

M. L. Saboungi and M. Blander
Review of Recent Advances in Theories of Ionic and Metallic Systems
Presented at CALPHAD IX, La Sapiniere, Quebec, May 25-29, 1980

W. W. Schertz
Conservation and Solar Energy
Presented at the home Builders Institute, Summit, IL, May 1980

W. W. Schertz
Solar Energy
Presented a seminar at Joliet Junior College, Joliet, IL, January 17 and February 21, 1980

M. G. Seitz
Stream-Simulation Experiments for Waste Repository Investigations
Presented at Waste Rock Interaction Technology Program Information Meeting, Battelle Northwest Laboratories, Seattle, WA, October 13-15, 1980

M. G. Seitz, R. A. Couture, J. Williams, N. Meldgin, and M. J. Steindler
Transport of Radionuclides in Geologic Media
Presented at Waste Isolation Safety Assessment Program, Tasky, Third Contractor Information Meeting, Pacific Northwest Laboratory, Richland, WA, October 14-17, 1980

M. G. Seitz and M. J. Steindler
Influence of Waste Solid on Nuclide Dispersal
Presented at Workshop on Alternate Nucl. Waste Forms and Interactions in Geologic Media, Oak Ridge National Laboratory, Gatlinburg, TN, May 13-15, 1980

A. C. Sheth and T. R. Johnson
Environmental Aspects of Seed Reprocessing in Coal-Fired, Open-Cycle Magnetohydrodynamic Systems
Presented at 89th National AIChE Meeting, Portland, OR, August 17-20, 1980

H. Shimotake
Recent Battery Development in Japan
Presented at Gould Laboratories, Rolling Meadows, IL, July 22, 1980

J. W. Sim, R. N. Singh, and K. Kinoshita
Fabrication, Characterization and Testing of Sintered $LiAlO_2$ Structures for Use in Molten Carbonate Fuel Cells
Presented at Molten Carbonate Fuel Cell Workshop, Washington, DC, March 10, 1980

D. L. Smith and R. G. Clemmer
Ceramic Breeding Materials for Commercial Fusion Reactors
Presented at Am. Ceram. Soc. Annual Meeting, Chicago, IL, April 28-30, 1980

D. L. Smith, R. G. Clemmer, V. Z. Jankus, and J. Rest
Analysis of In-Situ Tritium Recovery from Fusion Reactor Blankets
Presented at Fourth ANS Topical Meeting on the Technology of Controlled Nuclear Fusion, King of Prussia, PA, October 14-17, 1980

D. L. Smith, R. F. Mattas, R. G. Clemmer, and J. W. Davis
First-Wall/Blanket Materials Selection for STARFIRE Tokamak Reactor
Presented at Fourth ANS Topical Meeting on the Technology of Controlled Nuclear Fusion, King of Prussia, PA, October 14-17, 1980

J. L. Smith
Results of Cell Testing of Recently Developed Molten Carbonate Fuel Cell Components
Presented at EPRI Molten Carbonate Fuel Cell Workshop, Danbury, CT, October 11, 1980

W. V. Steele and R. M. Clay
The Enthalpy of Combustion of a Copper Complex: The Standard Enthalpy of Formation of Dinitrato (1,4,8,11-Tetrazacyclotetradecane) Copper(II)
Presented at 35th Annual Calorimetry Conf., Eufaula, AL, August 19, 1980

M. J. Steindler and W. B. Seefeldt
A Method for Estimating the Challenge to an Air Cleaning System Resulting from an Accidental Explosive Event
Presented at 16th DOE Nuclear Air Cleaning Conf., San Diego, CA, October 20-23, 1980

C. Swoboda, F. Hornstra, and N. P. Yao
The Use of Microprocessors in Battery Testing
Presented at DOE/EPRI Workshop on Statistical Techniques and Microprocessors in Battery Research, Rockville, MD, November 6-7, 1980

S. W. Tam and H. D. Shih
Applications of Diagonal-Dominant Approximation in the Determination of Surface Structure by LEED
Presented at the IBM Thomas J. Watson Research Centre, Yorktown Heights, NY, June 19, 1980

M. Tetenbaum
Oxygen Potentials Above the Plutonium Sesquioxide Phase at 2250°K
Presented (Poster Session) at Gordon Research Conf. in High Temperature Chemistry, Plymouth, NH, August 4-8, 1980

M. A. Wahlgren and K. A. Orlandini
Some Systematic Aspects of the Behaviors of $^{239,240}Pu$, ^{232}Th and ^{238}U in Selected North American Lakes
Presented at Workshop on Recent Advances in Environmental Chemistry of Transuranic Elements, Savannah River Ecology Laboratory, Augusta, GA, April 1-2, 1980

M. A. Wahlgren, K. A. Orlandini, D. M. Nelson, and R. P. Larsen
Oxidation State Characteristics of $^{239,240}Pu$ in Selected North American Freshwaters
Presented at Workshop on Recent Advances in Environmental Chemistry of Transuranic Elements, Savannah River Ecology Laboratory, Augusta, GA, April 1-2, 1980

I. O. Winsch, N. M. Levitz, and J. E. Parks
LWBR Proof-of-Breeding Analytical Support Project
Presented at Proc. of the Remote Technology Division of ANS, Las Vegas, NV, June 1980

R. D. Wolson and C. C. McPheeters
Methods of Sodium Waste Disposal
Presented at Second Int. Conf. on Liquid Metal Technology in Energy Production, Richland, WA, April 20-24, 1980

N. P. Yao
Advanced Batteries for Electric Vehicles
Presented at Joliet Chapter, Illinois Soc. of Professional Engineers, Inc., Joliet, IL, February 27, 1980

N. P. Yao
Advanced Batteries for Electric Vehicles
Presented at SAE Fox Valley Chapter, Aurora, IL, April 23, 1980

N. P. Yao
Advanced Battery Technologies - Where Are They Now?
Presented at Industrial Chemical Session--Modern Engineering and Technology Seminar, Chinese Institute of Engineers, Taipei, Taiwan, July 7-25, 1980

N. P. Yao
Advanced Secondary Batteries for Applications to Electric Vehicles and Electric Utility Load-Leveling
Presented at Lecture--University of Frankfurt, Germany, May 12, 1980

N. P. Yao
U.S. Electric Vehicle Program
Presented at EVE-80, South Australian Government, Adelaide, South Australia, August 25-29, 1980

J. E. Young
National Fuels Processing Overview
Presented at National Fuel Cell Seminar, San Diego, CA, July 14-16, 1980